Ecosystem functions of tidal marsh soils of the Elbe estuary

Dissertation

zur Erlangung des Doktorgrades der Naturwissenschaften

an der Fakultät für Mathematik, Informatik und Naturwissenschaften

Fachbereich Geowissenschaften

der Universität Hamburg

vorgelegt von

Kerstin Hansen

aus Hamburg

Hamburg, 2015

Tag der Disputation: 10.07.2015

Folgende Gutachter empfehlen die Annahme der Dissertation:

Prof. Dr. Eva-Maria Pfeiffer

Prof. Dr. Annette Eschenbach

Contents

Summary

Tidal marshes form a dynamic transition zone between periodically flooded tidal flats and terrestrial ecosystems. Marsh soils are an important component of these wetland ecosystems, providing valuable ecosystem functions like the storage of organic carbon (OC) and the retention of trace metals. The areal extent of tidal marshes at the Elbe estuary and elsewhere is declining and these coastal habitats are threatened by anthropogenic interference and climate change. Therefore, the capacity of tidal marsh soils to provide these ecosystem functions is reduced.

Soils of tidal marshes play an important role in regional carbon cycles since they have the capacity to store considerable amounts of OC. In the first part of this study, soil organic carbon (SOC) pools were determined in tidal marshes along the salinity and elevation gradients of the Elbe estuary. For this purpose, tidal marsh soils were investigated along elevation transects reaching from low to high marshes and in five study sites comprising three salinity zones (oligo-, meso-, and polyhaline zone). SOC concentrations, bulk density, and soil texture were analyzed in all soil horizons down to 100 cm soil depth. The amount of initial allochthonous OC was derived from the OC content in fresh sediments. The deviation of the recent OC content in the soils from the initial content was interpreted as autochthonous accumulation or mineralization by microorganisms. $\delta^{13}C$ values were used to validate this approach. Finally, the SOC stocks of the estuarine marsh soils were estimated by up-scaling the results of the respective study sites to the area of the different marsh zones.

The results of this study indicate an indirect influence of salinity and elevation on the SOC distribution and storage of the investigated marsh soils. Young, low marshes of the study sites seem to be predominantly influences by allochthonous OC deposition whereas the older, high marshes show autochthonous OC accumulation in the topsoils (0 – 30 cm) and mineralization in the subsoils (30 – 70 cm). Consequently, topsoil SOC pools increased with increasing elevation, but SOC pools did not significantly differ in the whole profile (0 – 100 cm). These results suggest that elevation is one factor influencing the SOC pools of tidal marshes. However, salinity seems to be an even stronger influencing factor reducing the above-ground biomass and, accordingly, the autochthonous OC input as well as the allochthonous input by enhanced mineralization of OC along the course of the estuary. SOC pools of the whole profile depth decreased significantly with increasing salinity from 25.0 kg m^{-2} in the oligohaline zone to 9.7 kg m^{-2} in the polyhaline zone. Even though the areal extent of the investigated salinity zones was similar, the oligohaline zone contributed most to the SOC storage of the tidal marshes. The SOC stock within 100 cm soil depth decreased from 0.62 Tg (1 Tg = 10^{12} g) in the oligohaline zone to 0.18 Tg in the

polyhaline zone. An upstream shift of the salinity zones by sea level rise could, therefore, lead to a reduction of the SOC storage of the estuarine marshes.

In the second part of this study, the potential decomposability of the SOC pools was determined. For this purpose, an incubation experiment on selected soil samples was carried out. Topsoil and subsoil samples from the respective salinity zones and elevation classes were incubated for five month under aerobic and anaerobic conditions, to determine factors influencing SOC turnover in the investigated marshes. The quantity and quality of soil organic matter had a major impact on the SOC turnover of the investigated samples. Higher turnover in topsoil samples which were provided with a bigger amount of labile organic substances from the vegetation than subsoil samples, in which big amounts of labile organic matter were most likely already decomposed, support this conclusion. Furthermore, the availability of oxygen was found to be one important factor for SOC turnover. Under aerobic conditions, significantly higher total carbon turnover of 6.3 % SOC in comparison to 4.7 % under anaerobic conditions were found during the incubation time, which represents a reduction of carbon turnover in the order of 25 % in topsoil samples. Subsoil samples did not show differences between aerobic and anaerobic incubation, since subsoil samples of the polyhaline zone had comparatively high total SOC turnover, most probably due to anaerobic sulfate reduction. However, a general difference in SOC decomposability between salinity zones or elevation classes explaining the differences in SOC pools could not be found. These results suggest that processes like tidal inundation or the influence of salt water on the microbial activity, which could not be reproduced in this laboratory experiment, might be more important for in-situ SOC decomposition.

The third part of this thesis addresses the retention function of tidal marsh soils. Trace metal concentrations in soils (i.e. Cd, Hg, Pb, Zn, and As) were compared with those in suspended sediments to account for temporal changes in trace metal input as well as mobilization processes. In total, the investigated marsh soils had low contamination levels, since trace metal concentrations around geogenic background values were dominant in the study sites. Trace metal concentrations were strongly correlated with the fine grain size fraction $< 20\,\mu m$ and SOC concentrations. High pH values in all study sites suggest a high retention capacity of the investigated soils. Concentrations and pools of all investigated metals decreased strongly along the salinity gradient of the estuary. Tidal mixing was suggested to be an important process influencing the trace metal distribution in the study area. Along the elevation gradient trace metal pools increased with increasing height. This finding was attributed to the increasing marsh age along the elevation transect and the decreasing metal input over the last decades, resulting in lower contamination of low marshes which have high sedimentation and accretion rates.

Consequently, low contaminated, young marshes could be distinguished from older high marsh profiles, the latter showing topsoil trace metal peaks from times of heavy pollution of the Elbe river. Trace metal stocks accounted for a considerable proportion of the total trace metal load discharged to the estuary since 1985, indicating a potential threat for the estuarine ecosystems in case of erosion and re-suspension of these soils.

Altogether, this thesis provides a first evaluation of two important ecosystem functions of tidal marsh soils at the Elbe estuary, shows the contribution of these soils in geochemical processes like carbon cycling and trace metal retention, and gives indications on their future development in the face of predicted sea level rise and anthropogenic interference. Nevertheless, further research on in-situ processes is strongly recommended, so that these ecosystem functions can better be accounted for when developing sustainable management strategies for tidal marshes.

x

Zusammenfassung

Tidemarschen bilden eine dynamische Übergangszone zwischen regelmäßig überfluteten Wattflächen und terrestrischen Ökosystemen. Marschböden stellen einen wichtigen Bestandteil dieser Feuchtgebiete dar, da sie wertvolle Ökosystemfunktionen bereitstellen, wie die Speicherung von organischem Kohlenstoff und die Retention von Schadstoffen. Sowohl am Elbe Ästuar wie auch anderswo, geht die flächenhafte Ausdehnung der Tidemarschen zurück. Diese Küstenökosysteme sind außerdem durch anthropogene Eingriffe und den Klimawandel bedroht. Die Kapazität der Marschböden diese Ökosystemfunktionen bereitzustellen ist somit begrenzt.

Marschböden spielen eine wichtige Rolle im regionalen Kohlenstoffkreislauf, da sie das Potential haben beträchtliche Mengen an organischen Kohlenstoff zu speichern. Im ersten Teil dieser Untersuchung, wurden die organischen Bodenkohlenstoff-Pools entlang der Salinitäts- und Höhengradienten des Elbe Ästuars ermittelt. Hierzu wurden Marschböden entlang von Höhentransekten von der unteren in die obere Marsch und in fünf Untersuchungsgebieten, die drei Salinitätszonen (oligo-, meso- und polyhaline Zone) umfassten, untersucht. Organische Kohlenstoffgehalte, Bodendichte und Korngrößenzusammensetzung wurden in allen Horizonten bis in 100 cm Bodentiefe analysiert. Der Ausgangsgehalt an allochthonem organischem Kohlenstoff wurde aus dem organischen Kohlenstoffgehalt von frischen Sedimenten abgeleitet. Die Abweichung des rezenten organischen Kohlenstoffgehalts der Böden vom Ausgangsgehalt wurde als autochthone Anreicherung oder Mineralisation durch Mikroorganismen interpretiert. $\delta^{13}C$ Werte wurden verwendet um diese Methode zu validieren. Schließlich wurde der organische Bodenkohlenstoff-Vorrat der ästuarinen Marschböden abgeschätzt, indem die Ergebnisse der jeweiligen Untersuchungsgebiete auf die Fläche der verschiedenen Marschzonen übertragen wurden.

Die Ergebnisse dieser Untersuchung weisen auf einen indirekten Einfluss von Salinität und Höhenlage auf die Kohlenstoffverteilung und –speicherung in den untersuchten Böden hin. In den Untersuchungsgebieten scheinen junge, niedrig gelegene Marschen hauptsächlich durch allochthone Kohlenstoffablagerungen geprägt zu sein, während ältere, höher gelegene Marschen autochthone Anreicherung von organischem Kohlenstoff in den Oberböden (0 – 30 cm) und Mineralisation in den Unterböden (30 – 70 cm) zeigen. Infolgedessen nahmen die organischen Kohlenstoff-Pools der Oberböden mit zunehmender Höhenlage zu, unterschieden sich aber nicht wenn die gesamte Profiltiefe betrachtet wurde. Somit wurde die Höhenlage als ein Faktor identifiziert, der die Bodenkohlenstoff-Pools der Tidemarschen beeinflusst. Salinität scheint jedoch ein noch stärkerer Einflussfaktor zu sein, da sie sowohl die oberirdische Biomasse und

somit den autochthonen Eintrag von organischem Kohlenstoff als auch den allochthonen Eintrag durch Mineralisation von organischem Kohlenstoff im Verlauf des Ästuars reduziert. Organische Bodenkohlenstoff-Pools der gesamten Profiltiefe zeigten eine signifikante Abnahme von 25.0 kg m^{-2} in der oligohalinen Zone auf 9.7 kg m^{-2} in der polyhalinen Zone. Obwohl die flächenhafte Ausdehnung der untersuchten Salinitätszonen ähnlich war, trug die oligohaline Zone am stärksten zur Speicherung von organischem Kohlenstoff in den Marschen bei. Der organische Bodenkohlenstoff-Vorrat innerhalb von 100 cm Bodentiefe ging von 0.62 Tg (1 Tg = 10^{12} g) in der oligohalinen Zone auf 0.18 Tg in der polyhalinen Zone zurück. Eine durch den Meeresspiegelanstieg verursachte Verschiebung der Salinitätszonen flussaufwärts könnte daher zu einer Reduktion der Kohlenstoffspeicherung der ästuarinen Marschböden führen.

Im zweiten Teil dieser Studie, wurde die potentielle Umsetzbarkeit der organischen Bodenkohlenstoff-Pools bestimmt. Zu diesem Zweck wurde ein Inkubationsexperiment mit einigen ausgewählten Bodenproben durchgeführt. Oberboden- und Unterbodenproben der jeweiligen Salinitätszonen und Höhenstufen wurden über fünf Monate unter aeroben und anaeroben Bedingungen inkubiert, um Einflussfaktoren des Kohlenstoffumsatzes der untersuchten Marschen zu bestimmen. Die Quantität und Qualität der organischen Substanz hatte einen bedeutenden Einfluss auf den Bodenkohlenstoffumsatz der untersuchten Proben. Ein größerer Kohlenstoffumsatz in Oberbodenproben, die mit einer größeren Menge an labiler organischer Substanz durch die Vegetation versorgt werden, als in Unterbodenproben, in denen große Mengen der labilen organischen Substanz höchstwahrscheinlich bereits abgebaut waren, unterstützen diese Schlussfolgerung. Außerdem wurde Sauerstoffverfügbarkeit als ein weiterer wichtiger Faktor für den Umsatz von organischem Bodenkohlenstoff ermittelt. In Oberbodenproben wurde unter aeroben Bedingungen ein signifikant höherer Kohlenstoffumsatz von 6.3 % organischem Bodenkohlenstoff während des Inkubationszeitraums bestimmt, im Vergleich zu 4.7 % unter anaeroben Bedingungen. Dies stellt eine Reduktion des Kohlenstoff-umsatzes um 25 % dar. Unterbodenproben zeigten keine Unterschiede zwischen aerober und anaerober Inkubation, da Unterbodenproben der polyhalinen Zone einen vergleichsweise hohen Kohlenstoffumsatz aufwiesen, was höchstwahrscheinlich auf anaerobe Sulfatreduktion zurückzuführen ist. Dennoch konnte ein genereller Unterschied der Umsetzbarkeit von organischem Bodenkohlenstoff zwischen Salinitätszonen oder Höhenstufen nicht festgestellt werden. Diese Ergebnisse deuten darauf hin, dass Prozesse die im Rahmen dieses Inkubationsexperiments nicht reproduziert werden konnten, wie Überflutungen oder der Einfluss von Salzwasser auf die mikrobielle Aktivität, für den in-situ Abbau an organischem Kohlenstoff von größerer Bedeutung sein könnten.

Der dritte Teil dieser Arbeit beschäftigt sich mit der Retentionsfunktion der Marschböden. Spurenmetallkonzentrationen der Böden (Cd, Hg, Pb, Zn und As) wurden mit denen in schwebstoffbürtigen Sedimenten verglichen, um zeitliche Veränderungen des Spurenmetall-eintrags sowie Mobilisierungsprozesse berücksichtigen zu können. Insgesamt wiesen die untersuchten Marschböden ein geringes Belastungsniveau auf, da Spurenmetallkonzentrationen im Bereich der geogenen Hintergrundgehalte in den Untersuchungsgebieten vorherrschten. Spurenmetallkonzentrationen korrelierten stark mit der Korngrößenfraktion $< 20 \mu m$ und den organischen Kohlenstoffkonzentrationen. Hohe pH Werte in allen Untersuchungsgebieten legen eine hohe Retentionskapazität der untersuchten Böden nahe. Konzentrationen und Pools aller untersuchten Metalle nahmen entlang des ästuarinen Salinitätsgradienten stark ab. Als ein wichtiger Prozess, der die Verteilung von Spurenmetallen im Untersuchungsraum beeinflusst, wurde die Vermischung durch den Gezeitenstrom herausgestellt. Entlang des Höhengradienten nahmen die Spurenmetall-Pools mit zunehmender Höhe zu. Dieses Ergebnis wurde dem zunehmenden Alter der Marsch entlang des Höhentransekts und einer Abnahme der Metalleinträge in den letzten Jahrzehnten zugeordnet, was eine geringere Belastung der unteren Marsch zur Folge hat, die wiederum durch hohe Sedimentations- und Auflandungsraten geprägt ist. Folglich, konnten gering belastete, junge Marschprofile von älteren, höher gelegenen Marschprofilen unterschieden werden, die Spurenmetall-Peaks aus Zeiten stärkster Schadstoffbelastung der Elbe im Oberboden aufwiesen. Die Spurenmetallvorräte machten einen beträchtlichen Anteil an der gesamten Spurenmetallfracht aus, die seit 1985 ins Ästuar eingetragen wurde. Im Falle von Erosion und Re-Suspension der Böden könnte also von den Böden eine potentielle Gefahr für die ästuarinen Ökosysteme ausgehen.

Insgesamt bietet die vorliegende Doktorarbeit also eine erste Einschätzung zweier wichtiger Ökosystemfunktion der Marschböden des Elbe Ästuars, zeigt die Beteiligung dieser Böden an geochemischen Prozessen wie dem Kohlenstoffkreislauf und der Retention von Spurenmetallen und gibt Hinweise auf deren zukünftige Entwicklung angesichts eines steigenden Meeresspiegels und anthropogener Beeinflussungen. Nichtsdestotrotz werden weitere Untersuchungen zu den in-situ Prozessen dringend empfohlen, so dass diese Ökosystemfunktionen noch besser im Rahmen von nachhaltigen Managementstrategien für Tidemarschen berücksichtigt werden können.

List of Figures

List of Tables

List of Abbreviations & Symbols

AD	Anno domini
Bd	Bulk density
BG	Geogenic background
BP	Before presence
CO_2e	Carbon dioxide equivalent
d	Day
dw	Dry weight
DIC	Dissolved inorganic carbon
EC	Electrical conductivity
ff20	Fine grain size fraction < 20 µm
KA5	German key on soil survey (Ad-hoc-AG Boden, 2005)
MHW	Mean high water level
n	Size of a statistical sample
p	Probability value (in statistical significance testing)
Pg	Petagram (= 10^{15} g)
PSU	Practical Salinity Unit (dimensionless)
r_s	Spearman's correlation coefficient
SD	Standard deviation
SedOCP	Sediment organic carbon pool, equivalent to the initial, allochthonous carbon pool
SIC	Soil inorganic carbon
SOC	Soil organic carbon
SOCP	Soil organic carbon pool (the subscripts 30 and 100 refer to a soil depth of 30 cm and 100 cm, respectively)
SOM	Soil organic matter
t	Metric ton (= 10^6 g)
TEA	Terminal electron acceptor
Tg	Teragram (= 10^{12} g)
VPDB	Vienna Pee Dee Belemnite
WRB	World Reference Base for Soil Resources (FAO, 2006)

Soil color

bn	Brown
gr	Grey
oc	Ocher
sw	Black

Soil texture

Ls2	Slightly sandy loam
Lt2	Slightly clayey loam
Lt3	Medium clayey loam
Lu	Silty loam
Slu	Silty-loamy sand
Su3	Medium silty sand
Tu3	Medium silty clay
Uls	Sandy-loamy silt
Us	Sandy silt
Ut2	Slightly clayey silt
Ut3	Medium clayey silt
Ut4	Very clayey silt

List of Definitions

Ah   Mineral topsoil horizon with accumulation of organic matter (< 15 % SOM according to Ad-hoc-AG Boden (2005)).

Allochthonous OC   Organic carbon originating from remote sources introduced by tidal inundation.

Autochthonous OC   Organic carbon originating from plant biomass present within the investigated marshes.

C production   Microbial carbon production as CO_2-C and CH_4-C in mg C g^{-1}dw.

C turnover   Proportion of organic carbon consumed by microorganisms in % of pre-incubation TOC content.

Contamination level   Level of trace metal concentrations in soils (in comparison to geogenic background values), from which a potential risk for the environment can be derived.

Estuary   River mouth; Transition zone between river and sea, characterized by tidal currents, a salinity gradient, and transport of material loads from upstream as well as downstream areas (Schaefer, 2003).

fAh   Buried Ah horizon, in which the original horizon development is interrupted (Ad-hoc-AG Boden, 2005).

Go   Mineral horizon with groundwater influence showing oxidation features due to temporal water saturation (Ad-hoc-AG Boden, 2005).

Gr   Mineral horizon with groundwater influence showing reduction features due to permanent water saturation (Ad-hoc-AG Boden, 2005).

GWP   The global warming potential is an emission metric that integrates the radiative forcing of a substance over a chosen time horizon relative to that of CO_2 (IPCC, 2013).

Heavy metals   E.g. elements with a density > 4.6 g cm^3 (Bahadir et al., 2000). According to Duffus (2002), the term 'heavy metal' is used very inconsistently in scientific literature, referring to density, atomic weight, atomic number, chemical properties, or toxicity of an element and should, therefore, be avoided.

High marsh   Tidal marshes with an elevation > 35 cm above MHW.

Low marsh   Tidal marshes with an elevation between 0 and 35 cm above MHW.

Mesohaline zone: River section with a salinity ranging from 5 to 18 ‰.

Oligohaline zone: River section with a salinity ranging from 0.5 to 5 ‰.

Polyhaline zone: River section with a salinity ranging from 18 to 30 ‰.

Trace metals: The term 'trace metal' includes both essential and non-essential metals and metalloids occurring at low (trace) concentrations in the environment according to Rainbow (2006). In this study, all investigated elements (Cd, Hg, Pb, Zn, and As) are referred to as trace metals.

xx

1 Introduction & Objectives

Tidal marshes of the Elbe estuary are valuable wetland ecosystems providing important ecosystem functions. Marsh soils are important components of these highly dynamic ecosystems, which are constantly influenced by inundation, sedimentation and erosion. In spite of, or even because of these influences, tidal marsh soils perform various ecosystem functions, including the regulation of biogeochemical cycles. However, tidal marshes are threatened by human interference at the Elbe estuary (Boehlich and Strotmann, 2008) and around the world (Gedan et al., 2009). To estimate the extent of ecosystem functioning of marsh soils is, therefore, of overarching interest in the context of climate change and anthropogenic interference. Through this study, a deeper understanding of the ecosystem functions of estuarine marsh soils shall be established.

The central subjects of this thesis are the ecosystem functions of the tidal marsh soils and their interactions with the abiotic and biotic processes of the Elbe estuary. Two soil functions shall be investigated in detail: the function of estuarine marsh soils as sources or sinks for carbon and their retention function for trace metals.

Wetlands in general represent the largest component of the terrestrial biological carbon pool (Chmura et al., 2003). Nevertheless, the contribution of estuarine marsh soils, particularly brackish and freshwater marsh soils, in carbon storage is relatively unknown. For the local carbon budgets a number of processes are relevant, of which sedimentation and erosion, mineralization and methanogenesis, and accumulation of autochthonous and allochthonous organic carbon (OC) prominently act on the actual carbon pools. The processes are strongly modified by the local water and gas exchange which are controlled by topographic height in relation to tidal water level and plant composition (Megonigal et al., 2004; Van der Nat and Middelburg, 2000).

The regional carbon dynamics of the soils of the study region have not been investigated so far. Most studies dealing with soil organic carbon (SOC) pools in marshes were conducted in North America (e.g. Blum, 1993; Craft, 2007; Elsey-Quirk et al., 2011; Loomis and Craft, 2010; Więski et al., 2010). Much less is known about the SOC pools of central European estuaries which may significantly differ in both their biotic and abiotic conditions (Spohn and Giani, 2012). Because of temporal flooding of tidal marshes, the deposition of allochthonous OC associated with suspended sediments plays an important role for the SOC pools of these soils (Middelburg et al., 1997; Tobias and Neubauer, 2009). To the author's knowledge, a quantification of the different

OC sources (autochthonous vs. allochthonous OC) has not been done before, even though it is of particular interest in the context of carbon cycling in tidal marsh soils. Therefore, this study aims to identify the sources and distribution of SOC and the factors influencing the SOC pools of tidal marshes of the Elbe estuary.

To evaluate the carbon storage function of the estuarine marsh soils, the following hypotheses are examined:

1)   OC in sediments represents the initial allochthonous proportion of SOC in marsh soils and it can be used to quantify this proportion in the investigated soils.

2)   The OC distribution is determined by allochthonous OC input in the low marshes and by autochthonous OC input and increased mineralization in the high marshes.

3)   SOC pools decrease with increasing salinity and elevation due to alterations in OC input and decomposition.

Furthermore, SOC turnover is an essential process for the carbon dynamics of tidal marsh soils, which is of particular importance with regard to climate change and sea level rise (Morrissey et al., 2014). Carbon turnover can be influenced by the availability of oxygen which is altered by tidal inundation and water table depth in tidal marsh soils (Megonigal et al., 2004). Moreover, the quantity and quality of soil organic matter (SOM) is an important parameter for the decomposability of SOC (Neubauer et al., 2013). Laboratory incubations are a useful tool to determine the influence of environmental factors and soil characteristics (like C quality) on carbon turnover (Subke et al., 2009; Sutton-Grier et al., 2011).

Regarding the potential decomposability of SOC, the following hypotheses are examined:

4)   C turnover is higher under aerobic conditions which are prevailing in high marshes than under anaerobic conditions common in low marshes, resulting in a different ratio of the investigated greenhouse gases carbon dioxide (CO_2) and methane (CH_4).

5)   Environmental factors like salinity and elevation determine C decomposability as they influence SOC quantity and quality.

6)   The decomposability of C differs between soil depths due to deposition of labile organic substances on the soil surface.

The implications of the potential C turnover for the ability of regional marsh soils to act as a source or sink for carbon will be critically examined with regard to anthropogenic influences.

In addition to their ability to cycle carbon, marsh soils have the potential to filter and buffer pollutants. Pollutants, which are emitted from industries or cities in the catchment of rivers, are transported downstream predominantly adsorbed to suspended particles (Netzband et al., 2002). These substances are deposited on and accumulate in marsh soils, where they can remain for decades or even centuries. In the river Elbe, strongest pollution appeared from the early 1970s to 1990s (IKSE, 2010; Müller, 1996; Prange, 1997). Pollutants discharged in the Elbe consist of a mixture of organic and inorganic substances including heavy metals and the metalloid arsenic (BfG, 2008; Heise et al., 2005; Stachel and Lüschow, 1996), hereafter collectively referred to as trace metals (compare Rainbow, 2006). The analysis of trace metal distribution in soils is, therefore, a useful way to estimate the retention function of these soils.

The hypotheses regarding the evaluation of trace metal contents are:

7) Trace metal pools of tidal marsh soils are decreasing with increasing salinity and elevation due to differences in inundation, sediment deposition, and soil characteristics.

8) Grain size distribution, SOC content, and soil pH are major factors affecting trace metal concentrations in the investigated soils, due to their influence on metal retention and mobilization.

9) The retention function of marsh soils results in long-term storage of trace metals and increases the contamination level of the sites for decades.

10) The vertical distribution of trace metals can, therefore, be used for an estimation of the deposition time of specific horizons and as a proxy for the sedimentation dynamics at the investigated sites.

This study aims to provide a first estimate on the before mentioned ecosystem functions, which can be used as a basis for future studies.

2 Background

2.1 Ecosystem functions of tidal marsh soils

The capacity of ecosystems to provide goods and services, due to complex interactions between biotic and abiotic components of the respective ecosystems, is defined as ecosystem functions (De Groot et al., 2002). Ecosystem functions can be grouped in four classes as regulation functions, habitat functions, production functions, and information functions. When these functions are valued according to their benefits for humans, they are referred to as ecosystem services (De Groot et al., 2002; MEA, 2003). For a sustainable management of ecosystems, a better understanding of ecosystem functions and services is essential to minimize trade-offs, optimize synergies, and promote the resilience of ecosystems (Bennett et al., 2009).

Wetlands, such as tidal marshes, provide valuable ecosystem functions and services (Barbier et al., 2011; Gren et al., 1994). They are important habitats and nursery grounds for specialized plants and animals (Craig and Crowder, 2000; Stiller, 2009). Being involved in different biogeochemical cycles, they act as sources and sinks for nutrients, filters for pollutants, and are part of the global carbon cycle (Müller, 2013; Weiss, 2013). They stabilize water flows and play a key role in coastal protection against storm surges and sea-level rise (Butzeck et al., 2015; Müller, 2013; Temmerman et al., 2013). Finally, they are used for agricultural production through grazing livestock and for human recreation (Barbier et al., 2011). Soils play a major role in these and other processes taking place in the estuarine marshes, as they hold a key position in this ecosystem connecting water and substance fluxes. Two typical functions of tidal marsh soils of the Elbe estuary are their ability to act as a source or sink for organic carbon and to filter pollutants.

2.2 Marsh soils as part of the regional carbon cycle

2.2.1 Organic carbon sources and pools

Understanding the function of tidal marsh soils for carbon cycling requires the quantification of SOC pools and the identification of its influencing factors. Although tidal marshes cover only small areas in Europe (1758 km² according to Dijkema (1990)), marsh soils play an important role in the regional carbon cycle (e.g. Beaumont et al., 2014; Burden et al., 2013; Olsen et al., 2011). In general, SOC pools are controlled by a number of carbon fluxes, including biomass production, mineralization and leaching (Figure 1). These processes in turn are influenced by several biotic

and abiotic factors, like microbial decomposition, soil moisture, soil texture, and the local climate. Depending on the interplay between these factors, tidal marshes can act both as sources (Odum, 2000; Valiela et al., 2000) and sinks (Chmura et al., 2003; Poffenbarger et al., 2011) for carbon.

Beside autochthonous OC input, allochthonous OC plays an important role for the SOC pools in marsh soils (Tobias and Neubauer, 2009). Carbon, from planktonic or terrestrial sources associated with fine-grained mineral particles, was found to be an important component of marsh soils (Ember et al., 1987; Middelburg et al., 1997; Neubauer, 2008). Sedimentation seems to be especially important in low marshes near creeks, whereas in high marshes the autochthonous carbon input of the plant cover is more important (Ember et al., 1987; Middelburg et al., 1997; Spohn et al., 2013; Spohn and Giani, 2012). Marshes are widely recognized as highly productive ecosystems (e.g. Mitsch and Gosselink, 1993; Odum, 1988) and, thus, above- and below-ground biomass production is an important autochthonous SOC source (e.g. Blum, 1993; Elsey-Quirk et al., 2011; Nyman et al., 2006). The amount and quality of litter as well as plant roots depend on plant species composition and influence the accumulation of OC (Valéry et al., 2004).

In estuarine marshes, flooding and salinity gradients are the major drivers for vegetation zonation (Engels and Jensen, 2009), ecosystem functioning (Więski et al., 2010), and SOC dynamics (Craft, 2007; Pfeiffer, 1998). Regular inundations and high soil moisture lead to anaerobic conditions of at least the subsoil and, consequently, to reduced OC decomposition (see chapter 2.2.2), especially in low marshes (Hemminga and Buth, 1991). Carbon turnover in salt marsh soils was found to be slower compared to other terrestrial environments caused by limited oxygen availability (Olsen et al., 2011). Within tidal marshes, SOC contents usually increase with increasing elevation (Chmura et al., 2003; Hulisz et al., 2013; Spohn et al., 2013; Spohn and Giani, 2012), while SOC accumulation and C burial by mineral sediments is of higher importance in low marshes (Callaway et al., 1996; Chmura et al., 2003; Elsey-Quirk et al., 2011). The export and redistribution of organic matter by the tides from low to high marsh zones (Bouchard and Lefeuvre, 2000) could also influence the SOC pools along an elevational gradient. With increasing salinity, SOC concentrations of estuarine marshes were found to decrease (Craft, 2007; Loomis and Craft, 2010; Morrissey et al., 2014). Likewise, standing crop biomass, above-ground carbon stocks, and SOC stocks and accumulation are lower in salt marshes compared to tidal freshwater and brackish marshes (Craft, 2007; Więski et al., 2010). The decreasing SOC contents can also be attributed to higher root decomposition with increasing salinity (Craft, 2007).

In general, soils form the largest terrestrial carbon pool, containing 1395 Pg to 1576 Pg (1 Pg = 10^{15} g) in 1 m soil depth globally (Batjes, 1996; Eswaran et al., 1993; Jobbágy and Jackson, 2000;

Post et al., 1982). Of this carbon pool a significant part of 513 Pg is stored in wetland soils (Bridgham et al., 2006). In a global estimation of carbon sequestration in tidal, saline wetlands Chmura et al. (2003) calculated a carbon storage of 0.43 Pg within 50 cm soil depth for salt marsh soils. The small area covered by tidal marshes, which form a narrow transition zone often restricted landwards by dikes or seawalls, explains the comparatively small global SOC storage. Furthermore, the majority of studies considered a maximum of 30 cm soil depth, even though deeper samples are necessary to be able to evaluate the role of marsh soils within the regional carbon cycle. As the SOC content of tidal marshes is varying with depth, depending on C input and mineralization, an estimation of the stored carbon for a soil depth of 50 cm or 100 cm based on data from surface samples (see attempt of Chmura et al., 2003) may lead to a considerable misjudgment.
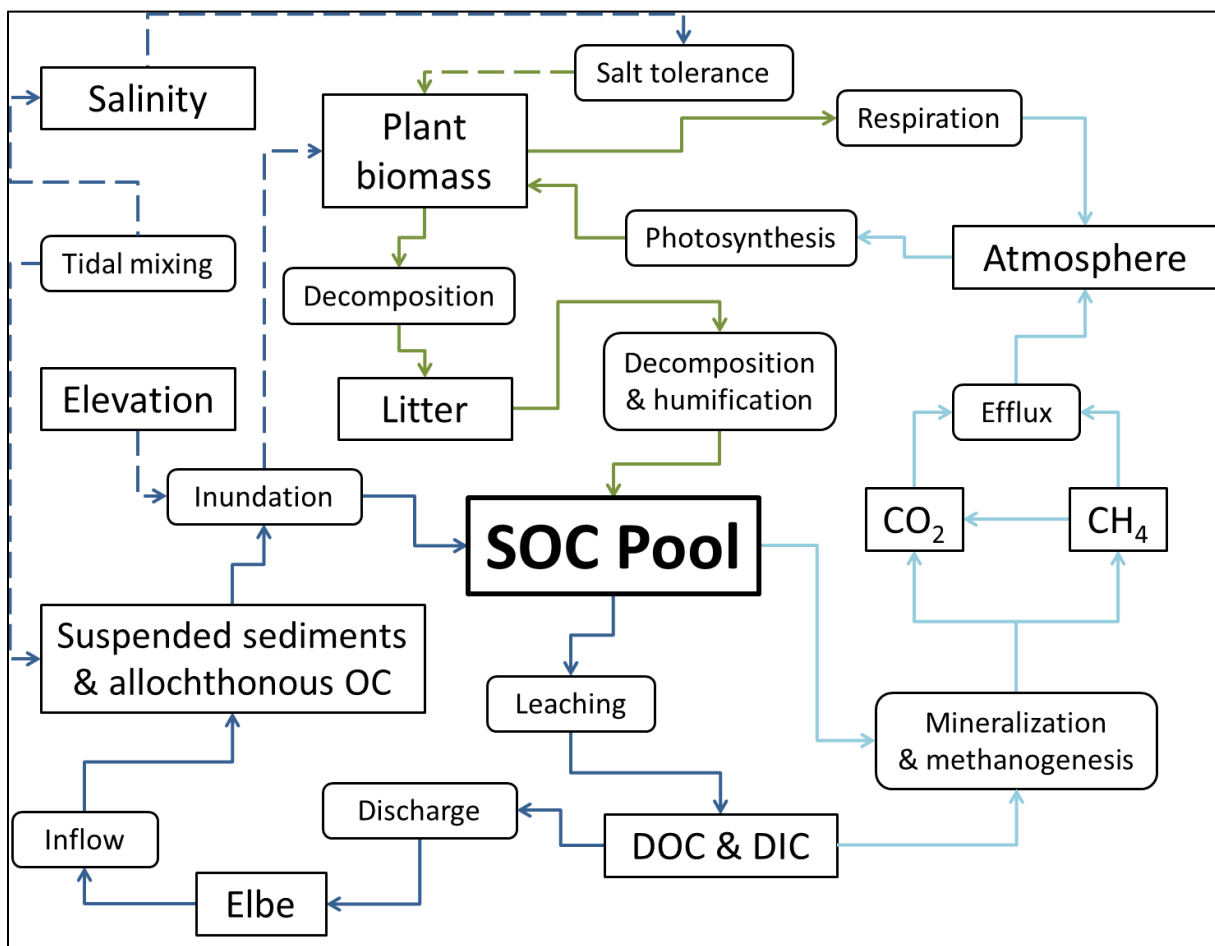
Figure 1: Compilation of important parameters and processes influencing soil organic carbon pools (SOC pool) in tidal marsh soils. Colored arrows denote different flows and influences. Influencing factors related to flooding (dark blue), plant biomass (green), and atmosphere (light blue) are representative for tidal marshes, but not exhaustive.
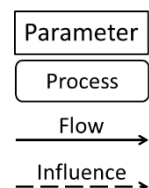
2.2.2 Organic carbon turnover

Decomposition of SOM affects the amount of OC stored in tidal marsh soils, causing emissions of greenhouse gases like carbon dioxide (CO_2) and methane (CH_4). CO_2 emissions resulting from soil respiration is a major natural pathway for release of organic carbon from terrestrial ecosystems to the atmosphere (Ryan and Law, 2005). In marshes, however, soils are often anaerobic due to regular inundations (Mitsch and Gosselink, 1993). Therefore, anaerobic decomposition including CH_4 cycling is another significant process affecting C turnover in theses wetland soils (Whalen, 2005). In tidal marsh soils, both processes can play an important role, depending on elevation and inundation of the sites (Figure 1).

Mineralization of SOM to inorganic compounds like CO_2 is the last step in a sequence of decomposition reactions. SOM decomposition is most rapid when oxygen is available and acts as the terminal electron acceptor (TEA) (Mitsch and Gosselink, 1993). Under aerobic conditions, simple organic compounds are oxidized completely to CO_2 (Megonigal et al., 2004). But even under anaerobic conditions, microbial respiration was found to be the dominant pathway of SOC loss in tidal wetlands (Chambers et al., 2013). However, other metabolic pathways are used for decomposition of organic matter in anaerobic soils. The most important methanogenic pathways are hydrogenotrophic methanogenesis, where H_2 is used as an electron donor and CH_4 and H_2O are produced, and acetoclastic methanogenesis, where acetate is the substrate which is split into CO_2 and CH_4 (see compilations of Garcia et al., 2000; Lai, 2009; Le Mer and Roger, 2001; Megonigal et al., 2004; Whalen, 2005). Typically, methanogenesis occurs when redox potentials range from 250 mv to 350 mv (Mitsch and Gosselink, 1993). Such low redox potentials exist due to reduction of other available TEAs like NO_3^-, Mn^{4+}, Fe^{3+}, or SO_4^{2-} (Megonigal et al., 2004). Methanogenesis is usually inhibited as long as these alternative TEAs are available, because of competition between different microbial communities for substrates. Bacteria reducing these TEAs are able to use substrates more effectively than methanogens, leading to thermodynamic inhibition of methanogenesis (Yao and Conrad, 1999). Competition between sulphate reducing bacteria and methanogens is considered to be a major factor for methane inhibition in marine soils (Tobias and Neubauer, 2009). Thus, CH_4 emissions are often negligible in polyhaline salt marshes with a constant sulfate resupply by tidal inundation (Bartlett et al., 1987; Poffenbarger et al., 2011). In these habitats, methanogenesis is restricted to microenvironments depleted in sulfate, where substrates are available to methanogens (King and Wiebe, 1980) or non-competitive substrates are used by methanogens (Oremland and Polcin, 1982). In contrast to salt marshes, CH_4 production of freshwater marshes was found to be controlled mainly by water

table, soil temperature, and autochthonous C input (Pfeiffer, 1994; Van der Nat and Middelburg, 2000).

In addition to its direct effect on decomposition of SOM, the availability of oxygen has an indirect influence on the actual greenhouse gas emissions of a soil. A considerable part of the produced CH_4 (60 % to more than 90 %) can be reoxidised by methanotrophs in the aerobic zone of wetland soils (Le Mer and Roger, 2001; Pfeiffer, 1994). This is an important process, as the global warming potential (GWP) of CH_4 is 28-fold higher than that of CO_2 (radiative forcing integrated over a 100-year time horizon, according to the IPCC (2013)). The oxidation of CH_4 in topsoils reduces emissions of this highly effective greenhouse gas, mainly controlled by the local water table and oxygen transport by plant roots into the anaerobic soil zone (Megonigal et al., 2004; Sutton-Grier and Megonigal, 2011; Van der Nat and Middelburg, 2000). On the other hand, plants can facilitate CH_4 transport to the atmosphere via functioning as a bypass for CH_4 through the aerobic zone (Chanton and Whiting, 1995). CH_4 venting through aerenchymatic tissue of the reed species *Phragmites australis* is very efficient (Van der Nat and Middelburg, 2000). Thus, CH_4 emissions of tidal marshes along the Elbe estuary might be strongly affected by this process, since large areas of the brackish zone are dominated by dense reed vegetation (see chapter 3.4.1).

Recently, interest in C dynamics of tidal marshes increased, as sea level rise could lead to water table changes and saltwater intrusions into freshwater marshes which could, in turn, alter SOM mineralization and the greenhouse gas balance of these sites (Chambers et al., 2013; Morrissey et al., 2014; Neubauer, 2013; Neubauer et al., 2013; Weston et al., 2014; Weston et al., 2011). However, the results of these studies are ambiguous. While some studies indicate stimulated microbial decomposition and SOC loss due to saltwater intrusion (Chambers et al., 2013; Morrissey et al., 2014; Weston et al., 2011), Neubauer et al. (2013) suggest reduced rates of soil CO_2 and CH_4 production due to long-term saltwater exposure. Anthropogenic disturbances and marsh loss are further factors causing changes in greenhouse gas fluxes resulting in a positive feedback to global warming (Chmura et al., 2011). In summary, the particular importance of tidal marsh soils and their function as part of the C cycle becomes evident. Nevertheless, the decomposability of SOM along salinity and elevation gradients is not consistently clarified and the aforementioned processes could be different in European mineral marshes.

Another important factor influencing the decomposability of SOM is the C quality of the substrates. SOM is composed of a complex mixture of biopolymers, such as carbohydrates, lignin, and hemicellulose, which differ in their recalcitrance against microbial decomposition (e.g.

Megonigal et al., 2004). In general, SOM is subdivided into three conceptual pools (Von Lützow et al., 2008). The active pool is composed of labile OM (e.g. fresh plant residues and root exudates) that can be decomposed rapidly. The intermediate pool is stabilized (e.g. by biogenic aggregation of OM) resulting in longer turnover times. In the passive or stabile pool, OM is further stabilized (e.g. by occlusion in clay microstructures or formation of organo-mineral associations) leading to very long turnover times of centuries to millennia (Kögel-Knabner et al., 2008; Von Lützow et al., 2008). As a result of their different degradability, these pools contribute differently to the emission of greenhouse gases to the atmosphere.

2.3 Marsh soils as sinks for trace metals

2.3.1 Factors influencing trace metal retention and mobilization

The retention and mobilization of trace metals in marsh soils depends on several abiotic and biotic factors. Important processes influencing metal concentrations in these soils are adsorption and desorption, precipitation and dissolution, as well as complexation and decomplexation (Du Laing et al., 2009c). These processes will be described subsequently.

Metal concentrations of marsh soils are resulting from the input bound to suspended particles and from their adsorption to clay minerals, organic substances, and Fe/Mn (hydr)oxides (Blume and Brümmer, 1991). Soils which are rich in these components provide a high cation exchange capacity (CEC) and have a particular potential to bind metals (Christiansen et al., 2002; Evans, 1989). In marsh soils, especially clay and organic matter contents reduce the uptake of trace metals by plants (Du Laing et al., 2009d). The grain size fraction < 20 µm has been found to be of special importance for metal retention (Ackermann et al., 1983). In addition to the sorption on particle surfaces, complexation of trace metals with particulate organic matter, in the form of litter or high molecular weight compounds, can reduce the metal solubility (Du Laing et al., 2006; Kabata-Pendias, 2011). Furthermore, redox processes play an important role in metal precipitation in marsh soils exposed to tidal flooding (Du Laing et al., 2009c). Metal mobility can be reduced by formation of insoluble metal sulfide precipitates under anaerobic conditions and by co-precipitation to Fe/Mn (hydr)oxides under aerobic conditions (Du Laing et al., 2008a; Du Laing et al., 2009a; Du Laing et al., 2009b). Finally, co-precipitation to carbonates can be an important factor in calcareous marsh soils which are common in tidal floodplains.

On the other hand, several processes can lead to mobilization of trace metals. Changing redox conditions due to fluctuations of the water table can be considered as an important mobilization process in tidal marsh soils (Du Laing et al., 2008a; Du Laing et al., 2009a; Frohne et al., 2011; Shaheen et al., 2014). This process can lead to dissolution of metal-containing precipitates in the oxic-anoxic interface. In the course of reduction and oxidation processes, the respective consumption or release of protons can, in turn, affect soil pH (Du Laing et al., 2009c). When pH drops below a certain threshold, metals may become mobilized, depending on the metal species (e.g. Cadmium (Cd) < 6, Zinc (Zn) < 5.5, Lead (Pb), and Mercury (Hg) < 4, see Blume and Brümmer (1991)). Metal cations can be released from the surfaces of sorbents at low pH, due to the reduction of negative surface charges (Du Laing et al., 2009c; Frohne et al., 2011). Many soils of tidal marshes are well buffered against pH changes due to their high carbonate content (Du Laing et al., 2009c). Decalcification might, however, lead to mobilization of trace metals precipitated with carbonates and those bound to particle surfaces as a result of cation exchange with Ca^{2+} (Christensen, 1984; Laxen, 1985).

Furthermore, a distinct salinity gradient and spatio-temporal variations in salinity caused by tidal flooding can influence mobilization processes in estuarine marsh soils (Du Laing et al., 2009c). Salinity can affect metal mobility in two ways (Acosta et al., 2011; Paalman et al., 1994): i) Increased ion concentrations in the brackish zone lead to a growing competition for sorption sites between exchangeable cations resulting in a release of metals. ii) Soluble chloro-metal complexes can be formed as salinity increases resulting in decreased adsorption of metals. Especially the sorption of Cd was found to decrease strongly in the presence of seawater (Andresen, 1996; Du Laing et al., 2008b; Gerringa et al., 2001; Paalman et al., 1994). In comparison to Cd, the adsorption of other trace metals like Pb or Zn are less affected by increased salinity (Gerth et al., 1981; Salomons, 1980).

Besides abiotic processes, biotic processes promote metal availability in marsh soils. Dissolved organic matter, in the form of low to medium weight organic acids, can form soluble metal complexes (Alvim Ferraz and Lourenço, 2000; Du Laing et al., 2009c; Kabata-Pendias, 2011), so that organic matter can cause both metal retention as well as mobilization. Additionally, microorganisms may affect the mobility of metals by decomposition of organic matter and catalysis of various redox reactions (Du Laing et al., 2009c; Megonigal et al., 2004). But also vascular plants can contribute to metal mobilization by root oxidation of the anoxic horizons or by excretion of root exudates (Du Laing et al., 2009c). At the respective sites, the combination and interaction of all these processes determine the mobilization capacity and retention function of the individual marsh soils (Figure 2).
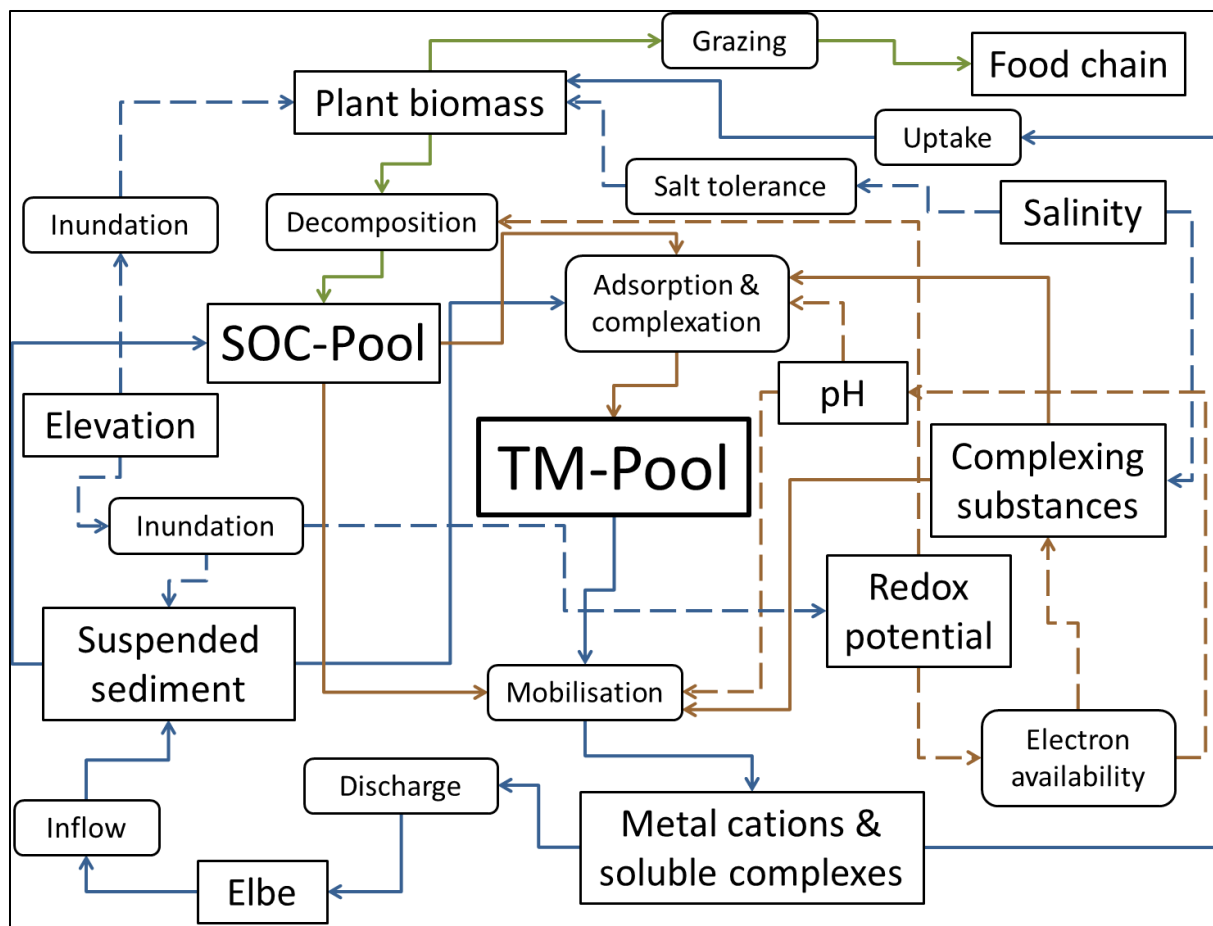
Figure 2: Compilation of important parameters and processes influencing trace metal pools (TM-Pool) in tidal marsh soils. Colored arrows denote different flows and influences. Influencing factors related to flooding (blue), plant biomass (green), and soil forming processes (brown) are representative for tidal marshes, but not exhaustive.
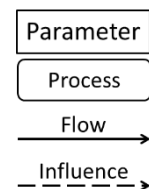
2.3.2 Contamination of the river Elbe, its sediments, and soils

The river Elbe has been one of the most polluted rivers in Germany for decades. Beside organic pollutants like pesticides, inorganic pollutants like trace metals play an important role in the anthropogenic contamination of the Elbe. Major sources for these metals are mining and smelting, chemical industry, municipal sewage, but also natural, geogenic processes in the catchment area (Förstner et al., 2004; Kowalik et al., 2003; Netzband et al., 2002). Pollution was most severe from the early 1970s to the early 1990s (IKSE, 2010; Müller, 1996). Water quality mainly improved with the abandonment of the industrial plants after the German reunification in 1990 and the construction of sewage treatment plants along the course of the river (BfG, 2008; Netzband et al., 2002). Sewage disposal was reduced drastically, which resulted in a decline of 96 % for Hg and more than 99 % for Cd discharge in the catchment areas between 1994 and

2008 (IKSE, 2010). Due to this reduction, trace metal loads in the suspended sediments along the course of the river decreased considerably, but stabilized from the end of the 1990s onwards (BfG, 2008).

In contrast to sediments, contamination of estuarine marsh soils has not been in the focus of many recent studies. In a study of Andresen (1996), a considerable trace metal pollution of tidal marsh soils in the Elbe estuary including Cd, Zn, Pb, and As was found. The determined metal concentrations exceeded the geogenic background values estimated for estuarine sediments of the Elbe strongly (Gröngröft et al., 1998). Maximum trace metal concentrations were up to 16.7 times the background values of Cd (3.7 times for Pb, 4.0 times for As, 8.9 times for Zn). Some of the substances found in this study have a high toxicity for animals or plants. In the EU Water Framework Directive, 33 substances, including Cd, Hg, and Pb, were defined as priority substances representing substances of risk for the aquatic environment (EU WFD, 2008). Due to their hazardous nature and accumulation potential, the contamination of rivers by these substances has to be reduced stepwise by stopping the anthropogenic input (BSU and HPA, 2011; Heise et al., 2005). However, contaminated layers in soils and sediments can be preserved over time as a legacy from the past (Förstner et al., 2004; Netzband et al., 2002; Prange, 1997). Consequently, erosion and re-suspension of sediments enhanced by anthropogenic interferences like dredging, represents a potential threat for the management objectives of the Water Framework Directive (EU WFD, 2000).

The actual concentration of trace metals in the estuarine marsh soils depend on input as well as mobilization of metals at the respective sites. Along the salinity gradient, mobilization increases due to an increase of salinity as explained in chapter 2.3.1. Moreover, salinity can be used as a proxy for the suspended sediment concentration. Highest sediment deposition rates were found in mesohaline marshes of the Elbe estuary (Butzeck et al., 2015). Therefore, differences in deposition of metals attached to fine-grained suspended particles and fixation due to variation in turbidity and texture (Heise et al., 2005; Salomons, 1980) can be expected along the course of the estuary (compare Figure 7). A major process affecting trace metal concentrations along the salinity gradient is the so-called tidal mixing (Gröngröft et al., 1998; Müller and Förstner, 1975; Salomons and Mook, 1977). Due to mixing of high contaminated fluvial and low contaminated marine sediments in the estuary, metal concentrations decrease with increasing salinity towards the estuarine mouth.

Along the elevation gradient, local variability of the water table influences the accumulation and dynamics of trace metals (Du Laing et al., 2009a). Especially, redox sensitive processes affect

metal mobilization due to topography and resulting inundation frequency and duration of tidal marshes (compare chapter 2.3.1). Furthermore, the marsh elevation can have an influence on litter input and SOC pools as well as on suspended sediment input by inundation, as described in chapter 6.1. Since trace metals are mainly attached to these soil components, topography was found to affect metal pollution of tidal marsh and floodplain soils as a result of differences in texture and organic matter content (Chen and Torres, 2012; Rinklebe et al., 2007).

3 Study area

3.1 The Elbe estuary

The river Elbe extends over 1094 km and is one of the longest rivers in Central Europe (IKSE, 2005). The Elbe originates in the Krkonoše Mountains in the northern Czech Republic and reaches the North Sea at river kilometer 727 (km 0 = national border Germany – Czech Republic) (IKSE, 2005). The Elbe estuary stretches over 141 km downstream of a weir at Geesthacht. The area is characterized by an Atlantic climate with annual average precipitation of 719 mm to 905 mm and temperature of 9.0 °C to 9.6 °C (DWD, 2013). The well-mixed, macro-tidal estuary has a long residence time and a mean tidal range of 3 m at its mouth near Cuxhaven and 3.5 m in Hamburg (IKSE, 2005; Middelburg and Herman, 2007). Within the funnel shaped estuary the water level depends on a combination of the river discharge of the Middle Elbe and the tidal water level of the North Sea as well as the predominant wind direction and strength. By mixing of river and sea water (tidal mixing) a brackish zone with increasing salinity towards the North Sea is established. This zone is shifting ca 15 to 20 km upstream and downstream, depending on the strength of the river discharge and the tides (Kausch, 1996). Caused by the tidal currents, big amounts of suspended matter are transported back and forth, which accumulate to a distinct zone of maximum turbidity within the area of the brackish zone between the confluence of the rivers Schwinge and Elbe, and the town Brunsbüttel (Bergemann, 2004a; Middelburg and Herman, 2007).

3.2 Landscape formation

Rapid climatic changes during the Pleistocene shaped the northwest European landscape and its river systems (Gibbard et al., 1988). These processes were controlled by climate induced alterations of the hydrological balance between ice and water (Streif, 1993). A major part of the precipitation was bound in glaciers during cold stages, which led to a global sea-level fall and a regression of the coastline. The area of today's Elbe estuary was covered by ice in the Elsterian and Saalian glaciations (Streif, 1996). The actual course of the lower Elbe was shaped by melt water of the ice sheets at the end of the Saalian ice age.

During the Weichselian glaciation (115000 – 10000 years BP), the ice did not exceed the Elbe (Streif, 1996) and the sea-level was continuously more than 40 m below the present level (Streif,

1993). With the thawing Permafrost at the Weichselian Late Glacial and early Holocene (ca 13000 – 9000 years BP), the characteristic braided rivers of the glacial periods joint single glacial valleys. The "Elbe Urstromtal" was one of these glacial valleys which formed a channel running in northwestern direction that is still visible as a basin on the seafloor of today's North Sea (Figge, 1980).

The rising sea-level in the postglacial period led to the formation of the present coastal landscape, including islands, tidal flats, marshes, and estuaries (Hoffmann, 2004; Streif, 1993). The Pleistocene landscape was covered by Holocene coastal sediments during several transgression phases that were interrupted by regression phases in which peat formation and soil development took place (Figure 3). By these processes, a complex sediment body was built up that reaches around 100 km upstream within the estuaries where it is intermeshed with fluvial sediments. When the sea level rise slowed down considerably (ca. 2000 years BP), the Elbe began to meander (Hoffmann, 1992), which is visible through buried channels cutting through the Holocene layers and formation of inversion ridges where the surrounding soil subsided (Janetzko, 1977).
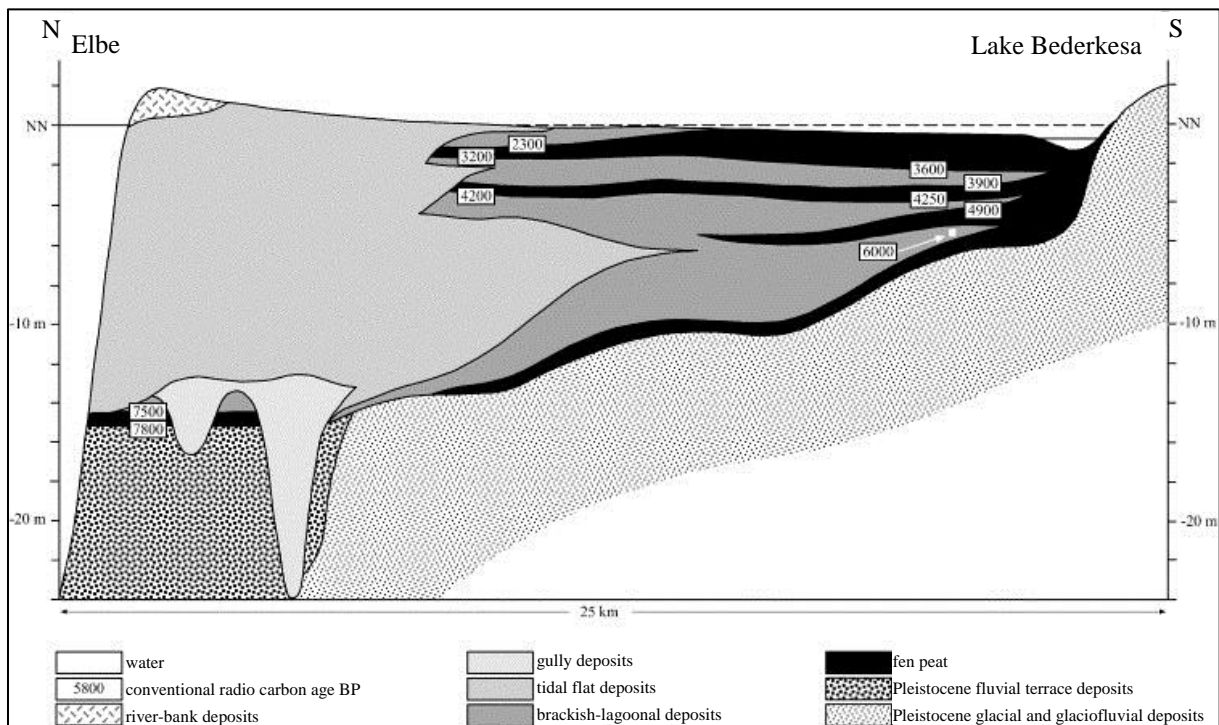
Figure 3: Geology of glacial and postglacial deposits at the Elbe estuary. Deposition age is given in years BP (Streif, 2004).

The marshes of the Elbe estuary were first colonized at the same time period around 2000 years BP (Meier, 1996). In the first centuries AD, people used natural levees along the Elbe and inversion ridges for settlement areas, as widespread peatlands covered the low-lying areas, which made settling and cultivation of land difficult. Approximately 100 years AD, the first artificial dwelling mounds were raised, providing a certain protection from storm surges (Streif, 1996). At this time, people did not yet shape the landscape on a large scale by dike construction or draining (Meier, 1996).

3.3 Anthropogenic changes

3.3.1 Coastal protection

In the second half of the 11th century AD, coastal inhabitants started to protect their properties by building dikes (Meier, 1996). At the beginning, only cultivated land was impoldered, followed by gradually closing the reaches resulting in a contiguous dike parallel to the coast line. A systematic colonization of the coastal lowlands was carried out by Dutch settlers in the 12th century (e.g. 1140 in the Haseldorfer Marsch) (Grüttner, 1992). The constructed polders were drained by a network of ditches parallel to the river and artificial creeks perpendicular to the river. To maintain the drainage system, the ditches were regularly excavated and the material was deposed on the interjacent beds. This procedure led to a strong alteration of the landscape with elevated beds and small ditches which is still maintained in the managed areas of the Elbe estuary today and is visible decades after abandonment of agricultural use (e.g. in the unmanaged part of Dieksanderkoog).

Diking at the Elbe estuary was affected by many setbacks (Großkopf, 1992). Low summer dikes were continuously raised and improved to stable winter dikes since the Middle Ages and tidal flats were embanked for land reclamation. These attempts were often destroyed quickly by severe storm surges during the last 800 years leading to sea incursions into the hinterlands (Bazelmans et al., 2012; Boehlich and Strotmann, 2008). As a result of surface level subsidence through drainage and oxidation of the soils, sea incursions had devastating effects on the settled lowlands (Hoffmann, 2004). Dikes had to be removed and were reconstructed further inland as a consequence of these storm surges and changes in the course of the Elbe (Großkopf, 1992). Nevertheless, a trend towards regulating the river and reducing the dike line proceeded to date. The canalization of the lower Elbe led to a decreasing retention capacity of the marshes followed by increasing tidal ranges and substantial damages during storm surges (Meier, 1996; Reise, 2005).

Today's dike line was established after the storm surge of 1962. Between 1962 and 1978 the dikes along the estuary were modernized and elevated. Large areas including Nordkehdingen (ca 50 km²) and Krautsand (ca 26 km²) were embanked (Figure 4), leaving only relatively small floodplain areas like Asseler Sand (Großkopf, 1992). Since 1900, the floodplain areas of the Elbe estuary decreased by 50 % on the northern bank and 74 % on the southern bank (Boehlich and Strotmann, 2008). An inland relocation of the dikes could be beneficial for both, coastal and nature protection. Valuable ecosystem functions like water retention, carbon and nutrient cycling, and the filtering and buffering of pollutants (see chapter 2.1) as well as the protection of large cities like Hamburg could be improved. Even though this issue has been discussed for many years, it still remains unsolved.
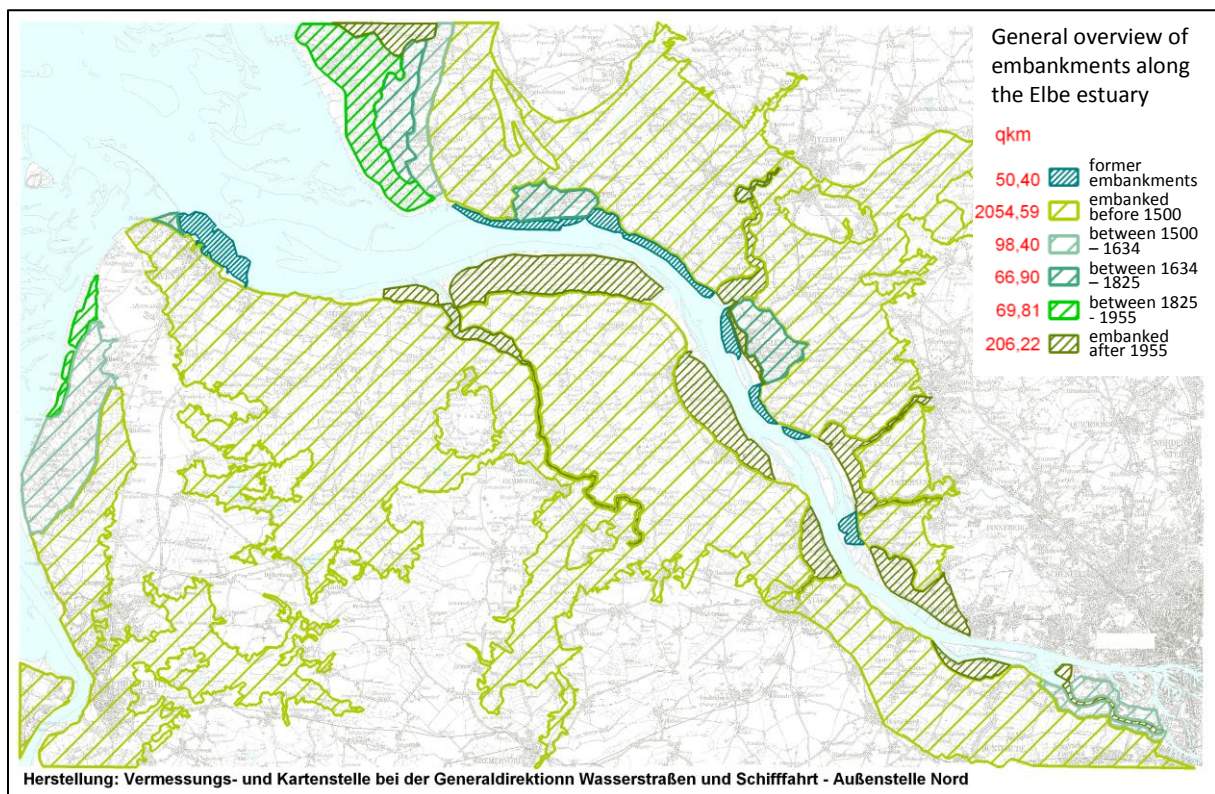
Figure 4: Coastal protection along the Elbe estuary. Extent of impolders (in km⁻²) and period of dike construction are illustrated by shaded areas (by courtesy of WSD Nord).

3.3.2   River-engineering measures

A further anthropogenic influence of the Elbe estuary started with the industrialization in the 19th century. To permit steamboats and, later, container vessels to reach the harbor of Hamburg, the Elbe waterway was dredged eight times, increasing the depth from originally 3 to 4 m at the beginning of the 19th century to approximately 15 m chart datum in 1999 (Kerner, 2007). Yet another deepening of the estuary to more than 17 m is currently discussed. The deepening and

canalization of the waterway led to drastic changes in the morphology of the riverbed (Schirmer, 1994). Sea water streaming in with the rising tide does not lose its energy while passing by barriers like islands, shoal areas, and Meanders. The flood water can flow in unobstructed and reaches further upstream areas. Major changes due to the extensions of the Elbe waterway are an increase in the tidal amplitude and storm surge water levels (Roberz, 2003), an increase of "Tidal Pumping" (Boehlich and Strotmann, 2008), and an upstream shift of the brackish zone (Bergemann, 2004a). These changes in hydrology alter the adjacent tidal marshes and their soils. Lower low water levels lead to increased draining of the marshes, whereas enhanced currents cause increased erosion along the banks (Reise, 2005). Furthermore, an increase in residence time leads to an accumulation of the fine-grained suspended matter within the freshwater part of the estuary (Kerner, 2007). Due to this effect, degradable organic carbon from upstream regions is remineralized already in the freshwater zone and does not reach the brackish zone. Besides organic carbon, the suspended matter contains pollutants that are accumulated in the estuary and its marshes during its decelerated downstream transport (Schirmer, 1994).

3.3.3   Climate change

Central European rivers are strongly influenced by the climatic conditions of their catchment areas (Schirmer, 1996). The climate itself is influenced by human activities, like burning of fossil fuels, which leads to an accumulation of long-lived greenhouse gases in the atmosphere (IPCC, 2013). Therefore, the human induced radiative forcing since industrialization is an important process for current and future climate change. Expected consequences for the Elbe estuary are reduced summer precipitation and increased winter precipitation in the catchment area followed by higher variability of the freshwater discharge to the estuary (Schirmer and Schuchardt, 1993), and a rising sea-level of 40 – 80 cm until 2100 in the German Bight (Gönnert et al., 2009) and more frequent heavy storm events followed by an increase of the high water level within the estuary. These processes may result in erosion and redistribution of sediments (Kirwan and Megonigal, 2013) and will directly influence tidal marshes, which have to be able to keep pace with sea level rise to persist (Butzeck et al., 2015; Müller, 2013). As marshes of the investigation area are restricted by dikes, they will not be able to grow laterally in the inland direction, which could lead to a loss of the high marsh zone (Butzeck et al., 2015; Gedan et al., 2009). The marsh soils could be influenced by salt water intrusion in the freshwater part of the estuary, a general increase in groundwater levels, and an increase in mineralization processes due to higher average temperatures (Schirmer, 1996; Schirmer and Schuchardt, 1993). Climate change could lead to

instability of the estuary and its marshes, as it is already limited in its ability to adapt to such changes due to the abovementioned river engineering and coastal protection measures (Kirwan and Megonigal, 2013; Schirmer, 1996).

3.4   Study sites

3.4.1   Site description

Today, the predominant part of the estuarine marsh is protected from flooding by dikes (Figure 5) and is intensively used for agricultural production. This study focuses on the remaining area between the dikes and the river, which is regularly flooded by normal tides or episodically flooded by storm tides.

The study was conducted in five sites comprising the different salinity zones of the estuary (Figure 5, Table 1). Sites 1 (Haseldorfer Marsch) and 2 (Asseler Sand) are located in the oligohaline zone (0.5 to 5 ‰), sites 3 (Böschrücken) and 4 (Neufelder Vorland) in the mesohaline zone (5 to 18 ‰), and site 5 (Dieksanderkoog) in the polyhaline zone (> 18 ‰). These zones are consistent with the marsh types described in (Butzeck et al., 2015), which were classified according to species composition as tidal freshwater, brackish, and salt marsh. All sites in the oligo- and mesohaline zone are nature reserves, however, partly grazed by sheep or cattle, or annually mowed. In the unmanaged parts of sites 1 to 4 the vegetation is dominated by *Phragmites australis*. Site 5 is situated in the Schleswig-Holstein Wadden Sea National Park and is covered by typical salt marsh vegetation. This site is also partly grazed by sheep. The un-grazed part of site 5 is dominated by *Elymus athericus*.

In this study all marshes that are currently used for agricultural production as pasture or meadow are referred to as managed. All other marshes are referred to as unmanaged marshes.
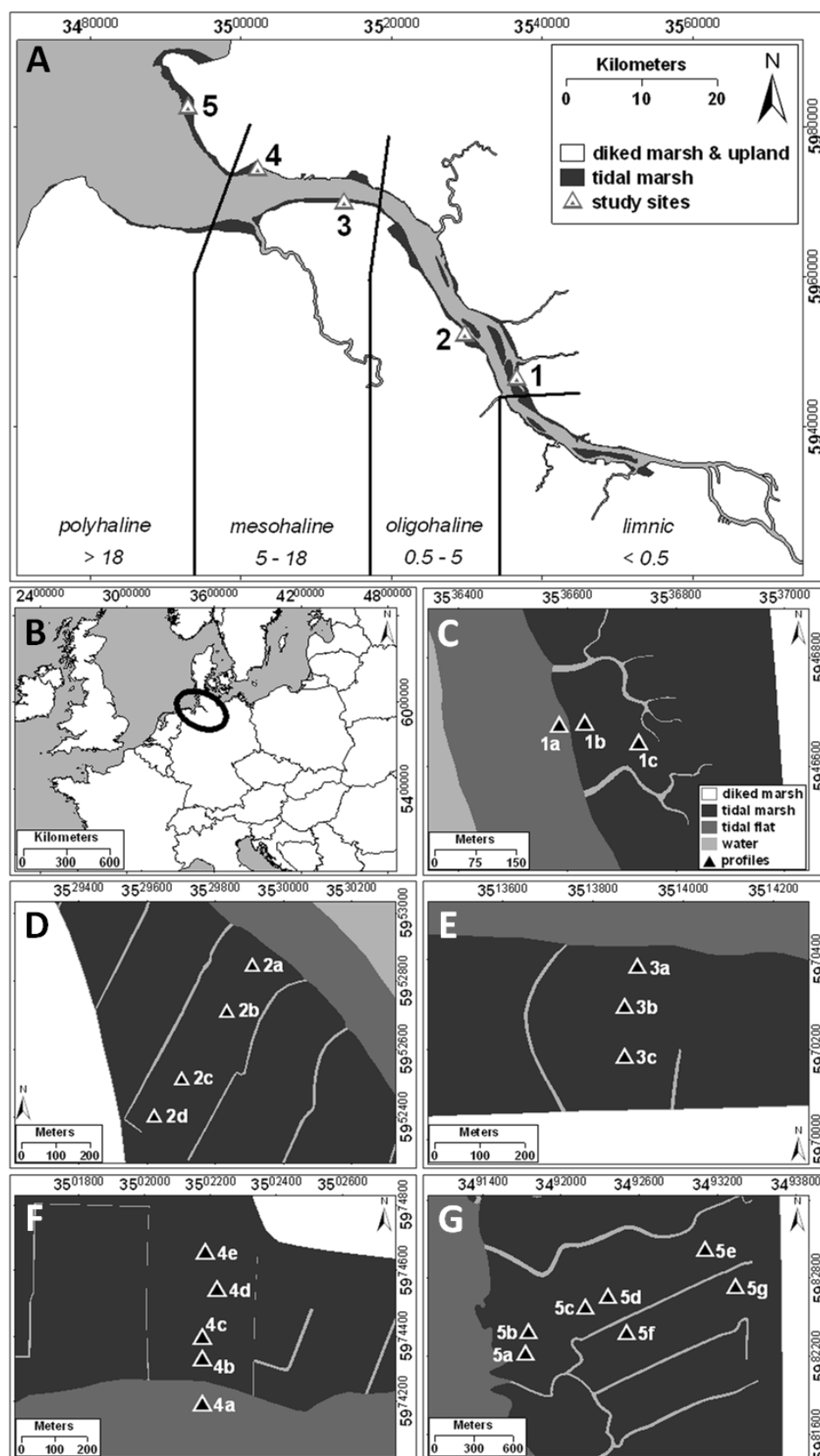
Figure 5: Location of the study sites along the Elbe estuary. (A) Overview of the study area (1 Haseldorfer Marsch, 2 Asseler Sand, 3 Böschrücken, 4 Neufelder Vorland, 5 Dieksanderkoog). The salinity zones of the estuary (in ‰ according to Stiller, 2009) are indicated by italic numbers; (B) Location of the Elbe estuary in Northern Germany; (C – G) Location of the investigated soil profiles along transects from marsh edge to the dike within each study site. Profiles are denoted by combination of site numbers and lowercase letters.

All study sites are typical floodplain areas of the Elbe estuary. The study sites 1, 4, and 5 on the northern bank of the estuary were chosen in cooperation with PhD students of the graduate school ESTRADE (Butzeck, 2014; Müller, 2013; Weiss, 2013). Common sites allowed mutual assistance with field work, exchange of data, and joint publishing of results (Butzeck et al., 2015; Hansen et al., in prep.). This interdisciplinary research approach fulfills the aim of ESTRADE to interconnect researchers across disciplines. The study sites 2 and 3 on the southern bank have been studied within the scope of the Collaborative Research Centre 327 "Tide-Elbe" (e.g. Andresen, 1996; Duve, 1999) and other research projects of the Institute of Soil Science (e.g. Pfeiffer, 1998). Therefore, extensive datasets are available on element budgets and greenhouse gas production.

Haseldorfer Marsch

Study site 1 (Figure 5 C) is located at a lateral branch of the Elbe in the nature reserve "Haseldorfer Binnenelbe mit Elbvorland" within the administrative district Pinneberg (53°39'00"N, 9°33'15"E; River km 656). The site is sheltered by an island (Bishorster Sand, Auberg-Drommel) and covered almost completely with reed bed composed of *Phragmites australis*, associated with *Typha angustifolia* and *Caltha palustris* in the lowest areas. In comparison with the other study sites, the investigated part of the Haseldorfer Marsch was of low altitude and had a shallow water table (Table 1). The mean high water level (MHW) was 1.73 m above NN (WSD-Nord, 2013) and the tidal range was 3.0 m (BSH, 2009). The measured salinity of the groundwater ranged from 0.63 to 1.12 (in Practical Salinity Units (PSU), see chapter 4.1; Table 1).

Asseler Sand

Study site 2 (Figure 5 D) is also located at a lateral branch of the Elbe. The so called "Schwarztonnensander Nebenelbe" is separating the former inland island Asseler Sand and the island Schwarztonnensand. The nature reserve "Asseler Sand" is located in the administrative district Stade (53°42'15"N, 9°26'60"E; River km 666). The investigated part consisted of pasture grazed by cattle and a bordering reed bed dominated by *P. australis*. The marsh was higher elevated than site 1, even in the reed zone (Table 1). MHW and tidal range were 1.6 m above NN and 3.0 m, respectively (BSH, 2009; WSD-Nord, 2013), and the salinity ranged from 0.74 to 1.16 in the groundwater.

Böschrücken

Study site 3 (Figure 5 E) is located in the nature reserve "Außendeich Nordkehdingen II" also within the administrative district Stade (53°51'45"N, 9°12'35"E; River km 691). "Böschrücken" is the name of a sandbank situated in front of the investigated marsh area. A part of the investigated site was mowed for nature conservation purposes in 2010 and the cut grass was removed from the site (Ludwig, pers. comm.). Annual mowing prevents the marsh to be covered by the highly productive species *P. australis*, which is restricted to a narrow reed zone, similar to site 2. Also, the absolute altitude of site 3 was similar to site 2, whereas the height above MHW was slightly higher (Table 1), as MHW was only at 1.49 m above NN and the tidal range was 2.8 m (BSH, 2009; WSD-Nord, 2013). The groundwater table was very deep during field work in summer and the salinity ranged from 1.76 to 4.86.

Neufelder Vorland

Study site 4 (Figure 5 F) is located in the floodplain area of the polders "Neufelder Koog", "Marner Neunkoog", and "Westerkoog" in the administrative district Dithmarschen (53°54'00"N, 9°01'55"E; River km 702). It is the only investigation site that is not explicitly protected as a nature reserve, but merely as a bird sanctuary. The site was partly managed by non-intensive sheep grazing near the dike. An extensive area was unmanaged and consisted of a narrow *Bolboschoenus maritimus* zone, followed by a *P. australis* zone which was associated with *Anthriscus sylvestris* and *Elymus athericus* in the higher parts. The marsh was generally of low elevation (Table 1) and had a MHW and tidal range of 1.49 m above NN and 2.8 m, respectively (BSH, 2009; WSD-Nord, 2013). The groundwater salinity ranged from 4.32 to 7.91.

Dieksanderkoog

Study site 5 (Figure 5 F) is part of the Schleswig-Holstein Wadden Sea National Park in the administrative district Dithmarschen (53°58'25"N, 8°52'55"E; River km 725). The floodplain area in front of the polder "Dieksanderkoog" differed from all other study sites in the distribution of land use zones and its vegetation. The investigated site was divided by a creek into an unmanaged part and a managed part grazed by sheep, both situated perpendicular to the dike, whereas the other sites had land use zones parallel to the dike. Grazing was abandoned in the unmanaged part in 1992 (Stock et al., 2005). Since then, the native invasive species *E. athericus* is

spreading over this part of the marsh. The managed part was dominated by *Puccinellia maritima* associated with *Spartina anglica* and *Aster tripolium* in the low salt marsh and *P. maritima* associated with *Festuca rubra* in the high salt marsh. Surface elevation was only slightly higher compared to site 4 (Table 1). MHW was 1.52 m above NN (WSD-Nord, 2013) and the tidal range was 3.0 m (BSH, 2009). The salinity of the groundwater ranged from 5.21 to 20.93.

3.4.2 Soils of the study sites

Marsh soils of the study sites were formed by recent marine and fluviatile sediments and were classified as "Rohmarschen" and "Kalkmarschen" according to the German key on soil survey KA5 (Ad-hoc-AG Boden, 2005) and as Tidalic Fluvisols according to WRB (FAO, 2006) (see Table 1 for detailed classification). The semiterrestrial marshes developed from tidal flats by constant sedimentation of suspended particles. When the surface elevation exceeded MHW a vegetation cover established and soil forming processes like structure formation, aeration, salt removal, and decalcification occurred (Giani and Landt, 2000). The investigated marsh soils were strongly affected by the predominant hydrological conditions of the study sites, showing distinct horizons with oxidation and reduction features in the order Ah/Go/Gr (compare Ad-hoc-AG Boden (2005) and Abbreviation List). Differences in elevation and inundation led to a certain variability in horizon thickness and characteristics in the investigated profiles (Table 2 - Table 4). The variability of tidal marsh soils of the Elbe estuary will be presented below on the basis of three characteristic examples.

Profile 4b (Table 2) represents a typical soil of the studied low marshes (compare chapter 4.4). The investigated low marsh soils usually had Go-Ah/Go/Gor/Gr horizons, similar to the displayed profile. Where the groundwater table was very shallow, the soils lacked distinct Ah horizons, but showed only Go/Gr horizons (e.g. site 1 compare Table A 1). In this case reduction properties began in merely a few centimeters depth. The investigated low marsh profiles represent an early succession step in soil development with thionic properties and a coherent soil structure.

Profile 2d represents a soil of the studied high marshes (Table 3). High marsh soils typically showed a distinct well-structured Ah horizon. The deep groundwater tables resulted in an increased proportion of oxic properties in comparison to the low marsh soils. These properties indicate a proceeded soil development. In the presented profile 2d, no fluvic properties were

apparent. Nevertheless, the soils of this site can be classified as Tidalic Fluvisols, since the fluvic origin can be assumed due to the location in the floodplain area.

In contrast, fluvic properties were evident in many other high marsh profiles like profile 4e (Table 4). The dynamic conditions of the study sites become apparent in the respective soils as seasonal layers. Sandy layers (light-colored) were deposited during storm surges in the winter season, whereas loamy layers (brown) represent periods of decelerated flow velocities during the summer season. Furthermore, some profiles show buried Ah horizons (fAh) that indicate former topsoil horizons covered by tidal sediments. The latter can develop naturally during calm periods without storm surges or by anthropogenic deposition of material removed from ditches for maintenance of the drainage system.

Table 1: Characteristics of the study sites. The table comprises abiotic parameters, land use classes, and soil types of the investigated plots.

Name	River km	Profile No.	Land use	Height above NN, m	Height above MHW, m	Water table depth, cm	Salinity[a]	Soil type (KA5)	Soil type (WRB)
Haseldorfer Marsch	656	1a	unmanaged	1.44	-0.29	10	0.63	Rohmarsch	Tidalic Fluvisol (Thionic, Calcaric, Humic)
		1b	unmanaged	1.86	0.13	25	1.12	Rohmarsch	Tidalic Fluvisol (Thionic, Calcaric, Humic)
		1c	unmanaged	1.83	0.10	10	0.84	Rohmarsch	Tidalic Fluvisol (Thionic, Calcaric, Humic)
Asseler Sand	666	2a	unmanaged	2.09	0.49	20	1.12	Rohmarsch	Tidalic Fluvisol (Thionic, Calcaric, Humic)
		2b	pasture (cattle)	2.78	1.18	160	0.74	Kalkmarsch	Tidalic Fluvisol (Calcaric, Humic)
		2c	pasture (cattle)	2.68	1.08	nd	0.78	Kalkmarsch	Tidalic Fluvisol (Calcaric, Humic)
		2d	pasture (cattle)	2.35	0.75	140	1.16	Kalkmarsch	Tidalic Fluvisol (Calcaric, Humic)
Böschrücken	691	3a	unmanaged	1.63	0.14	80	4.86	Rohmarsch	Tidalic Fluvisol (Thionic, Calcaric)
		3b	meadow	2.60	1.11	196	1.76	Kalkmarsch	Tidalic Fluvisol (Calcaric, Humic)
		3c	meadow	2.35	0.86	175	4.24	Rohmarsch	Tidalic Fluvisol (Calcaric, Humic)
Neufelder Vorland	702	4a	unmanaged	1.45	-0.04	40	4.32	Rohmarsch	Tidalic Fluvisol (Thionic, Calcaric, Humic)
		4b	unmanaged	1.63	0.14	45	6.73	Rohmarsch	Tidalic Fluvisol (Thionic, Calcaric, Humic)
		4c	unmanaged	1.80	0.31	28	7.91	Rohmarsch	Tidalic Fluvisol (Thionic, Calcaric, Humic)
		4d	unmanaged	1.94	0.45	110	4.97	Kalkmarsch	Tidalic Fluvisol (Calcaric, Humic)
		4e	pasture (sheep)	1.86	0.37	85	6.26	Rohmarsch	Tidalic Fluvisol (Thionic, Calcaric, Humic)
Dieksanderkoog	725	5a	pasture (sheep)	1.56	0.04	46	18.25	Rohmarsch	Tidalic Fluvisol (Thionic, Calcaric)
		5b	pasture (sheep)	1.64	0.12	18	20.93	Rohmarsch	Tidalic Fluvisol (Thionic, Calcaric)
		5c	pasture (sheep)	1.76	0.24	80	17.11	Rohmarsch	Tidalic Fluvisol (Thionic, Calcaric)
		5d	pasture (sheep)	1.86	0.34	77	5.21	Rohmarsch	Tidalic Fluvisol (Calcaric, Humic)
		5e	pasture (sheep)	2.08	0.56	65	18.5	Rohmarsch	Tidalic Fluvisol (Calcaric, Humic)
		5f	unmanaged	1.86	0.34	63	10.65	Kalkmarsch	Tidalic Fluvisol (Calcaric)
		5g	unmanaged	2.15	0.63	55	19.43	Kalkmarsch	Tidalic Fluvisol (Calcaric, Humic)

[a] Salinity in groundwater (in PSU)
nd = not determined

Table 2: Profile description of a typical low marsh profile. Soil horizons, texture, and color are indicated according to KA5 (Ad-hoc-AG Boden, 2005) and soil types according to KA5 and WRB (FAO, 2006). Abbreviations are explained in the abbreviations and definitions lists.
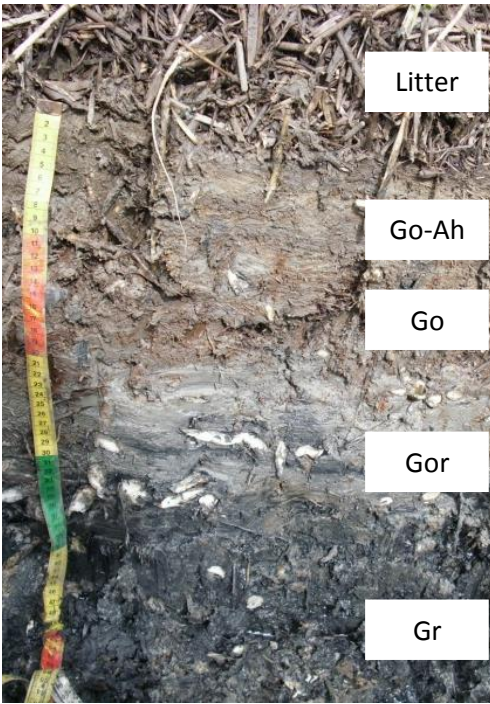
Profile 4b	*Geographic coordinates:* 53°53'59.6" N, 009°01'54.9" E		*Soil type*	
			KA5: Rohmarsch	
			WRB: Tidalic Fluvisol (Thionic, Calcaric, Humic)	
Salinity zone: mesohaline	*Groundwater level:* 45 cm			
Elevation class: low marsh	*Groundwater salinity, PSU:* 6.73			
	Groundwater pH: 6.9			

Soil depth cm	Horizon	Texture	Color	Water content %	Bulk density g cm^3	Special features
0-10	Go-Ah	Ut2	ocbn	58.03	1.00	
10-20	Go	Ut3	ocbn	54.94	1.00	rhizomes & sand lenses
20-34	Gor	Ut2	gr	45.88	0.59	rhizomes
34-45	Gr	Ut4	sw	54.48	0.92	rhizomes & plant fibers
45-70	Gr*	Us	sw	*n.d.*	1.08	water saturated
70-100	Gr*	Su3	sw	*n.d.*	1.10	water saturated

Litter
Go-Ah
Go
Gor
Gr

samples of Gr horizon between 45 and 100 cm soil depth were drilled, due to the shallow water table

Table 3: Profile description of a typical high marsh profile. Soil horizons, texture, and color are indicated according to KA5 (Ad-hoc-AG Boden, 2005) and soil types according to KA5 and WRB (FAO, 2006). Abbreviations are explained in the abbreviations and definitions lists.
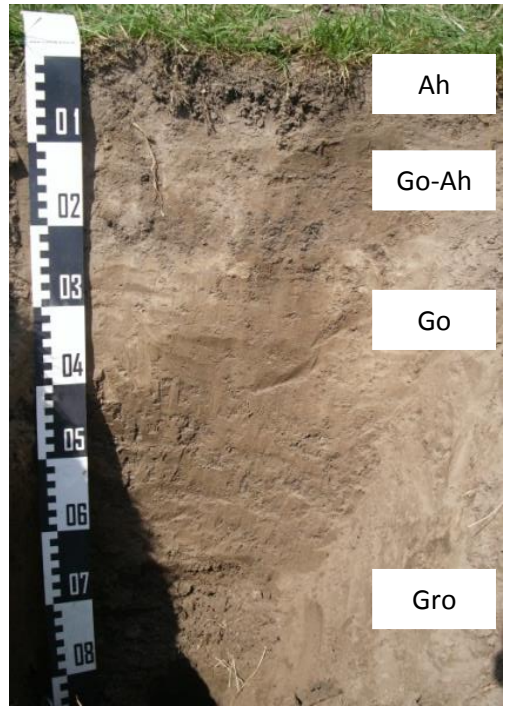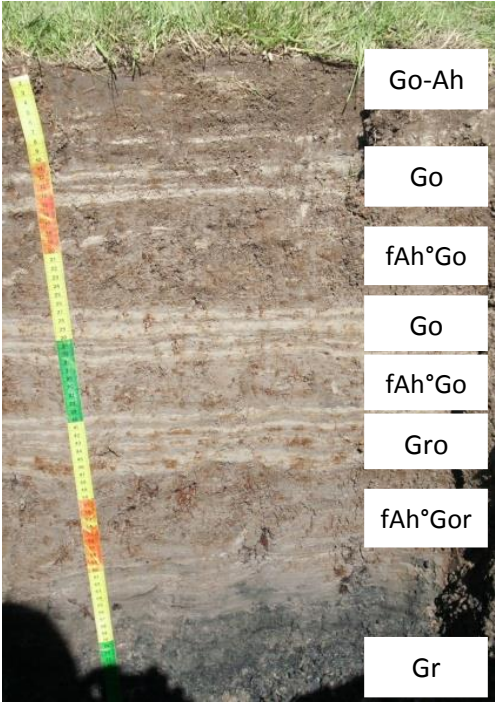
Profile 2d	*Geographic coordinates:* 53°42'07.3" N, 009°26'50.7" E						*Soil type*
							KA5: Kalkmarsch
							WRB: Tidalic Fluvisol (Calcaric, Humic)
Salinity zone: oligohaline	*Groundwater level:* 140 cm						
Elevation class: high marsh	*Groundwater salinity, PSU:* 1.16						
	Groundwater pH: 7.7						

Soil depth	Horizon	Texture	Color	Water content	Bulk density	Special features
cm				%	g cm^3	
0-5	Ah	Tu3	bn	26.21	0.93	fine roots
5-20	Go-Ah	Lt2	ocbn	26.90	1.07	
20-50	Go	Lt3	oc	30.01	1.25	
50-85	Gro	Ls2	groc	40.21	1.43	
85-140	Gor*	Slu	ocgr	*n.d.*	1.27	
140-150	Gr*	Lu	grsw	*n.d.*	1.21	water saturated

Gor and Gr horizon not shown

Table 4: Profile description of a marsh profile with buried topsoil horizons and storm tide layers. Soil horizons, texture, and color are indicated according to KA5 (Ad-hoc-AG Boden, 2005) and soil types according to KA5 and WRB (FAO, 2006). Abbreviations are explained in the abbreviations and definitions lists.

Profile 4e		Geographic coordinates: 53°54'10.1" N, 009°01'55.5" E					Soil type	
Salinity zone: mesohaline		Groundwater level: 85 cm					KA5:	Rohmarsch
Elevation class: high marsh		Groundwater salinity, PSU: 6.26						
		Groundwater pH: 6.8					WRB:	Tidalic Fluvisol (Thionic, Calcaric, Humic)

Soil depth	Horizon	Texture	Color	Water content	Bulk density	Special features	
cm				%	g cm^3		
0-6	Go-Ah	Tu3	bn	45.50	0.73	fine roots	
6-15	Go	Ut4	ocbn	47.07	0.89	sandy layers	
15-26	fAh°Go	Tu3	bn	54.05	0.94	mottles	
26-33	Go	Lu	oc	55.39	1.06	sandy layers	
33-40	fAh°Go	Tu3	bn	57.70	0.98	mottles	
40-49	Go	Uls	groc	n.d.	1.23	sandy layers & mottles	
49-63	fAh°Gor	Tu3	ocgr	66.56	0.83	plant fibers	
63-80	Gr	Tu3	grsw	69.54	0.76		
80-100	Gr*	Tu3	sw	n.d.	0.81	water saturated	

* samples of Gr horizon between 80 and 100 cm soil depth were drilled

4 Material & Methods

4.1 Field methods and sample preparation

In 2010 and 2012, soil profiles ($n = 22$) were surveyed along an onshore-offshore transect spanning from the marsh edge to the dike within each study site (Figure 6). The number of profiles in each site depends on the size of the respective marsh, with a minimum of three profiles in the smallest sites 1 and 3 and a maximum of seven profiles in the largest site 5. The profiles were situated in two different elevational marsh zones (low and high marsh) representing different inundation conditions. A pit was excavated to the depth of the groundwater table and all soil horizons were sampled and characterized according to the German key on soil survey (Ad-hoc-AG Boden, 2005). Supplemental samples from the deeper, water saturated horizons were collected by drilling with a 10 cm-Edelman auger. All samples were homogenized, air dried at room temperature and sieved at 2-mm mesh size. Of each bulk sample, a subsample was finely ground with a vibratory disk mill for subsequent carbon and metal analysis. Additionally, undisturbed soil samples were taken from the respective horizons using 100 cm³ soil cores for analysis of bulk density and volumetric water content. Salinity was determined by measuring electrical conductivity (EC) in the groundwater with a conductivity meter (portable multi-parameter instrument pH/Cond 340i, WTW GmbH, Weilheim, Germany) and converting to salinity using the Practical Salinity Scale according to Bergemann (2005).

To evaluate the influence of autochthonous carbon input on the SOC pools of the tidal marshes, above-ground biomass data (kindly provided by C. Butzeck) were analyzed. Biomass was harvested from 0.25 m² plots ($n = 37$) in the unmanaged marsh zones of sites 1, 4, and 5. The positions of the biomass plots and soil profiles were not identical but comparable (see Butzeck et al., 2015). Biomass was collected at the end of the growing season in September 2010 (summer) representing peak-biomass and in February 2011 (winter) representing the amount of organic matter that will likely be incorporated into the soil in the following growing season. The lower parts of the biomass (up to 50 cm) were washed with tab water to eliminate adherent sediment particles. To determine the dry weight in kg m⁻², biomass was dried in pre-weighted perforated plastic bags for three days at 60 °C (see Butzeck et al., 2015).

To determine the initial allochthonous OC input to the sites for the time of fresh sedimentation, unpublished data from a sediment quality survey was included, which took place at the Elbe estuary in 1994 and 1995 (Miehlich et al., 1997). 141 samples originating from the uppermost 10 cm to 20 cm of the Elbe river sediments were sampled with a Van-Veen-grab from a ship.
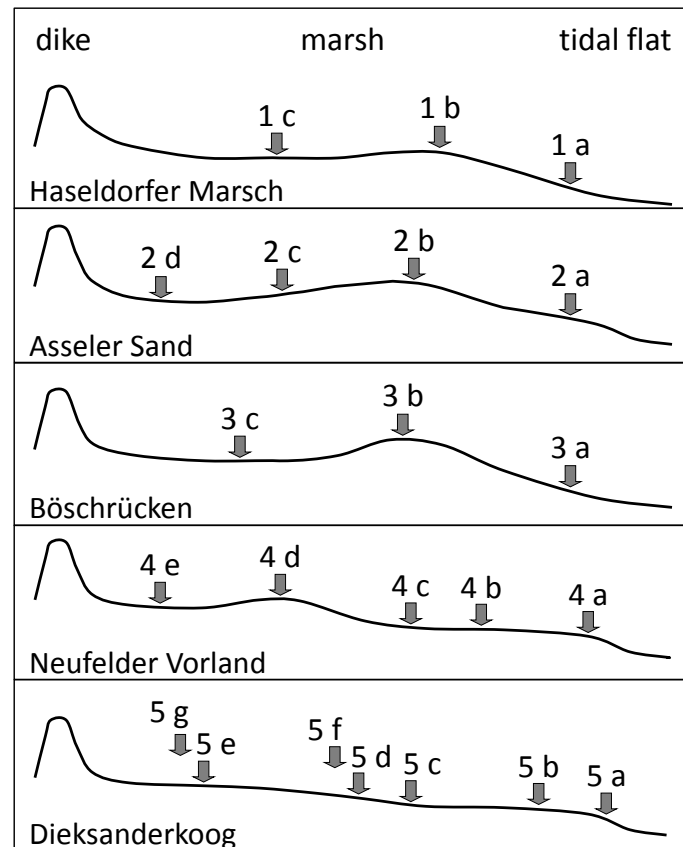
Figure 6: Order of soil profiles along transects from the marsh edge to the dike in each study site. The profiles 5 f and 5 g were situated in the unmanaged zone of study site 5 at the same distance from the dike as the profiles 5 d and 5 e in the managed zone, respectively. The elevation differences between sites and profiles are illustrated simplified and do not present reality exactly. Precise elevation data for each profile are presented in Table 1.

4.2 Soil analysis

4.2.1 Bulk density

Bulk density (Bd) is an essential parameter to determine the amount of carbon and trace metals actually stored in a specific soil volume. Bd was calculated from the weight of the oven dried core samples (105 °C until constant weight), for horizons above the groundwater level. Since the fluidity of horizons below the groundwater level made the collection of undisturbed samples impossible, for these layers Bd was calculated from particle density (measured with AccuPyc II 1340 Helium Pyknometer, Micromeritics GmbH, Aachen, Germany) and water content assuming complete water saturation.

4.2.2   Grain size distribution

Soil texture represents an essential physical parameter, influencing SOC and trace metal retention of soils. Furthermore, the estimation of the allochthonous OC input by sedimentation requires the content of fine grained particles (see chapter 4.5.2). For texture analysis, the samples were digested with H_2O_2 to destroy organic matter when TOC content was > 1 % and with HCl to destroy carbonates when $CaCO_3$ content was > 2 %. The sand fractions were determined by dry sieving at four mesh sizes (630, 200, 125, 63 µm). Silt fractions and clay were measured by sedimentation analysis using the Köhn pipette method according to DIN ISO 11277 (2002) (Sedimat 4-12, UGT GmbH, Müncheberg, Germany).

4.2.3   pH

The reactivity of soils is an essential chemical parameter, influencing element mobility, solubility of carbonates, and the microbial community. The pH is the negative common logarithm of the hydronium ion activity in a solution and can be used as a measure for the acidity or alkalinity of soils. Soil pH was measured in a 1:2.5 soil/water and soil/$CaCl_2$ solution, respectively. For this purpose, 10 g air dried soil was mixed with 25 ml of distilled water or 0.01 n $CaCl_2$ solution. The resulting soil solution was subsequently mixed and pH was measured after one hour with a pH meter (MP 230, Mettler-Toledo GmbH, Gießen, Germany). The precision of the measurement was 0.1 pH units. As adsorbed H^+ ions are displaced from surface charges by $CaCl_2$, the pH measured in the soil/$CaCl_2$ solution is approximately 0.5 pH units lower in comparison to the soil/water solution.

4.2.4   Carbon

Total carbon (TC) and nitrogen (TN) was measured by dry combustion on an elemental analyzer (Vario MAX CNS, ELEMENTAR Analysensysteme GmbH, Hanau, Germany) according to DIN ISO 10694 (1996). The detection limit (DL) was 0.01 % C and N, respectively. From CO_2 evolution after acidification of the samples, the amount of total inorganic carbon (TIC) was determined. Samples collected in 2010 were mixed with ca 40 % H_3PO_4 in closed glass bottles. The mixture was incubated at 80 °C over night and CO_2 was measured at a gas chromatograph (GC) (GC-14B, Shimadzu Corporation, Kyōto, Japan) the day after. For samples collected in 2012, TIC was measured following in-situ HCl acidification procedure using an elemental

analyzer (Vario MAX Cube, ELEMENTAR Analysensysteme GmbH, Hanau, Germany). The concentration of total organic carbon (TOC) was calculated by subtraction of TIC from TC.

4.2.5 $^{13}C/^{12}C$ isotope ratios

To validate the abovementioned differentiation of allochthonous and autochthonous OC input, $^{13}C/^{12}C$ isotope ratios of organic carbon where used (compare e.g. Spohn et al., 2013). For this purpose, 16 samples from three profiles of site 5 (5a, 5d, and 5g) were chosen that differed in elevation and inundation frequency. These soil samples were compared with biomass samples and sediment samples ($n = 3$, respectively). $\delta^{13}C$ values were measured with an isotope-ratio mass spectrometer (Delta V, Thermo Scientific, Dreieich, Germany) coupled to an elemental analyzer (Flash 2000, Thermo Scientific, Dreieich, Germany). Prior to the analysis of isotope ratios of OC, inorganic carbon was removed from the samples by treatment with 40 % phosphoric acid. The measurement range of the replicates was generally less than ± 0.3 ‰. Ratios were expressed as $\delta^{13}C$ values relative to VPDB (Vienna Pee Dee Belemnite) using the external standard IVA soil 33802153 (-27.46 ‰ vs. VPDB).

4.2.6   Aqua regia extraction

For analysis of trace metal contents, the field moist soil samples were divided into two portions. One half was dried, sieved, and ground as described above. The other half was sieved wet at 20 µm mesh size, freeze dried and ground according to Ackermann et al. (1983). Both portions were dried at 105 °C before weighting exactly 1.5000 g of the respective samples into teflon digestion vessels. Metals were extracted with aqua regia (13.4 ml HCl 30 % supra-pur and 3.5 ml HNO_3 65 % supra-pur) under pressure in a microwave (MarsXPress, CEM GmbH, Kamp-Lintfort, Germany) according to DIN ISO 11466 (1997). After a heating phase of 10 minutes, the samples were kept at 160 °C for 15 minutes, followed by a cooling phase of another 10 minutes. Afterwards, the extract was diluted with double distilled water and filled up to a total volume of 50 ml.

By aqua regia extraction mineral and organic compounds are destroyed and bound elements dissolved. The geogenic metals are digested only partly depending on the mineral composition of the sample (Blume et al., 2011). Consequently, the method does not represent the total metal content, but the so called quasi-total metal content. It can be used to estimate the amount of

metals which can be mobilized by long-term natural or anthropogenic changes (e.g. soil acidification, organic matter decomposition, changing redox conditions).

4.2.7 Element analysis

Metal contents (Cd, Hg, Pb, and Zn) of the total sample and the fine fraction < 20 μm (ff20) were analyzed by atom adsorption spectrometry (AAS). Arsenic (As) concentrations were only measured in the ff20. Flame AAS (280FS AA, Varian Inc., Walnut Creek, USA) was used to measure the elements Zn (DL = 0.4 mg kg^{-1}) and Pb (DL = 4.0 mg kg^{-1}). The elements Cd (DL = 2.5 μg kg^{-1}) and As (DL = 40.0 μg kg^{-1}) were measured by AAS with GTA-120 Zeeman graphite tube atomizer (280Z AA, Varian Inc., Walnut Creek, USA). Hg (DL = 5.0 μg kg^{-1}) was measured with a Flow Injection Mercury System (FIAS 100, PerkinElmer Inc., Waltham, USA) after staining with potassium permanganate. To ensure the quality of extractions and measurements, two blanks and replicates per extraction series as well as element standards were routinely included.

4.3 Incubation experiment on carbon turnover

4.3.1 Soil sampling and sample preparation

To estimate the potential turnover of labile and intermediate organic carbon in the study sites, an incubation experiment was conducted. In April 2012 fresh bulk samples from selected plots in the low and high marsh zone at all study sites were collected. At each plot topsoil samples from the first 10 cm and subsoil samples from approximately 50 cm soil depths were collected with an auger.

Fresh samples were stored at 5 °C until further processing within four weeks. For determination of soil respiration samples were incubated under aerobic conditions. Prior to incubation living roots were hand-picked from the soil. The samples were homogenized and brought to a water content of 40 % – 60 % of the maximum water-holding capacity. Finally, 50 g – 100 g of the prepared sample (3 replicates) were filled in 250 ml serum bottles which were closed gas tight using butyl rubber stoppers and kept at a constant temperature of 22 °C in the dark for five month.

For determination of methanogenesis, soil samples were kept under anaerobic conditions during sample preparation within an oxygen-free glove-box constantly flushed with N_2 (99.8 % pure N_2 gas). Roots were hand-picked, soil samples were homogenized, and 50 g – 100 g (3 replicates) were filled in 250 ml serum bottles at actual water content. After closing the bottles the headspace was thrice exchanged with N_2 to ensure anaerobic conditions.

4.3.2 Gas measurements

During the incubation time, headspace gas samples were analyzed for CO_2 and CH_4 concentration in regular intervals (once a week). Prior to each gas sample collection, the internal pressure within the serum bottles was determined with a manometer. Afterwards, 200 μl of the headspace gas was collected with a syringe via a septum. The concentration of CO_2 and CH_4 was measured using a GC (7890A, Agilent Technologies, Santa Clara, USA). The gas sample was injected into the GCs carrier gas (27 ml helium min^{-1}) and the respective components of the gaseous mixture were separated with a Porapak-Q-column (2 mm ID, 1.8 m length). The gases were measured with a thermal conductivity detector (TCD) for CO_2 and a flame ionization detector (FID) for CH_4. Before and after each measurement day, three standard gases (Table 5) were analyzed to ensure measurement accuracy. Additionally, standard 1 was measured after each 20th sample.

Table 5: Standard gases for GC measurements. The nominal and actual concentrations of the respective gases are indicated in ppm.

Standard	CO_2, ppm		CH_4, ppm	
	nominal	actual	nominal	actual
1	10,000	10,210	200	203.5
2			10,000	10,000
3	100,000	100,300	100,000	101,300

To avoid reduction or even inhibition of CO_2 production resulting from high concentration stress of aerobic microorganisms, the headspace was exchanged when CO_2 concentration exceeded 3 % (Knoblauch et al., 2013). To do so, aerobic samples were flushed with synthetic air (80 % N_2 and 20 % O_2) and subsequently measured at the GC during the course of the day.

After finishing the experiment, TC, TN, TIC and pH were determined in the respective subsamples as described in chapters 4.2.3 and 4.2.4.

4.4 External data

The height above mean high water level (MHW) of each profile was derived from topographic height measurements along nearby transects from the years 2008 to 2011 and from MHW data (WSD-Nord, 2013). Measured inundation frequency and duration of the sites 1, 4, and 5 from Butzeck et al. (2015) correlated strongly with the elevation data of WSD Nord (r_s = -0.946 and -0.986, p < 0.001, respectively). Therefore, the height above MHW can be used as an indicator for the inundation frequency of the sites. Finally, elevation was used to divide the marshes in two elevation classes and accordingly inundation types. In this study, tidal marshes up to 35 cm above MHW were classified as low marsh and marshes above 35 cm as high marsh.

Spatiotemporal alterations of metal concentrations in suspended sediments were evaluated using data from two automated sampling stations along the Elbe estuary (FGG Elbe, 2014). Sediment samples were collected in slurry tanks over the course of one month from 1988 onwards. Subsequently, the samples were sieved at 20 μm mesh size as described in chapter 4.2.6 and trace metals were extracted under pressure with HNO_3/H_2O_2 in a microwave (Bergemann, pers. comm.). Since metal concentrations vary with headwater discharge (BfG, 2008), showing higher concentrations in winter than in summer, the data set was split into winter (November to April) and summer season (May to October). The mean values of the winter season were further used for comparison with metal concentrations in marsh soils, as sediment deposition in the study sites was also highest in the winter season (Butzeck et al., 2015).

4.5 Data analysis and calculations

4.5.1 Calculation of SOC and trace metal pools

The soil organic carbon pool (*SOCP*) was calculated as the product of *TOC*, *Bd*, and thickness (*T*) of the respective soil horizons (*h*) in kg C m^{-2}:

$$SOCP = \sum TOC_h \times Bd_h \times T_h \qquad \text{(Eq. 1)}$$

The total soil organic carbon pools of each profile were calculated as the sum of SOCP of each horizon to 30 cm (SOCP$_{30}$) and 100 cm (SOCP$_{100}$) soil depth, respectively. For the calculation, a homogeneous SOC distribution within each horizon was assumed. Likewise, trace metal pools were calculated in g m^{-2} from the respective total trace metal concentrations. The calculation could only be implemented for Cd, Hg, Pb, and Zn, since As was measured solely in the ff20.

4.5.2 Differentiation of autochthonous and allochthonous SOC

The amount of OC present in today's soils is the result of allochthonous input, autochthonous accumulation, and microbial mineralization. To determine the degree of in-situ OC accumulation and mineralization in the recent marsh soils of the study sites, the initial allochthonous OC content at the time of sedimentation has to be known. To calculate this initial OC content, data from the abovementioned sediment quality survey (Miehlich et al., 1997) was used. Here a general relation between grain size distribution and OC content was found for fresh estuarine sediments. The mean OC content of pure sand was lowest with 0.14 % ± 0.08 % and that of harbor sediments with > 85 % silt and clay content was highest with 8.5 %. For all sediment samples, Spearman's correlation coefficient between grain size properties and OC was largest for the proportion of fine grained particles < 20 μm (r_s = 0.920, p < 0.001, n = 121). However, due to the mixing of particles from two different sources (fluviatile and marine, see Gröngröft et al., 1998) and mineralization (Abril et al., 2002; Amann et al., 2012) the ratio between the OC content and the amount of the fine fraction (ff20) changed along the course of the estuary (Figure 7). An exponential model (Eq. 2) was used to calculate the TOC to ff20 ratio (y) for all study sites (x).

$$y = 0.05045 + 4.42404E^{17} \times e^{(-0.06913\,x)} \qquad \text{(Eq. 2)}$$
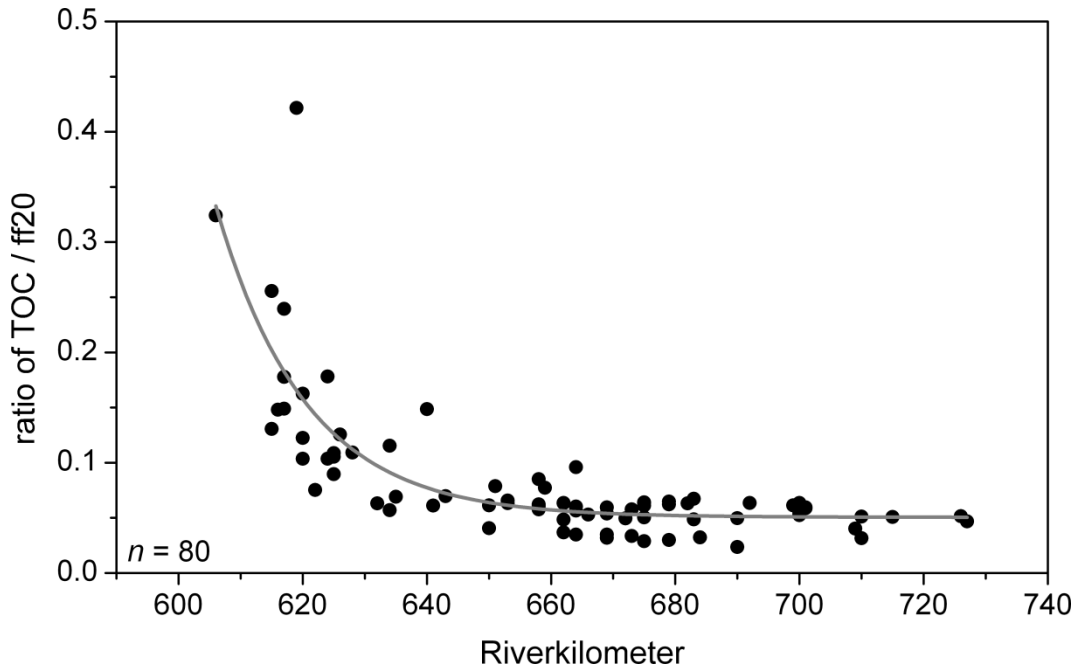
Figure 7: TOC/ff20 ratio of sediments of the Elbe estuary. The distribution of the displayed ratio was fitted by an exponential curve (Eq. 2).

The calculation of the initial allochthonous OC content of the soils of the five study sites is based on the assumption that the TOC to ff20 ratio is equal in fresh sediments and soils at the moment of deposition. Furthermore, the method is only valid in case that this ratio does not considerably change over time. The allochthonous OC content (*SedOC*) was calculated for all soil horizons, using the TOC to ff20 ratio of the respective sites and the *ff20* content of the respective horizons (Eq.3).

$$SedOC = y \times ff20_h \qquad \text{(Eq. 3)}$$

The calculation of the allochthonous organic carbon pools (SedOCP) was done in the same way as described for SOC pools (see Eq. 1) and is referred to as $SedOCP_{30}$ for the upper 30 cm soil depth and $SedOCP_{100}$ for the whole profile of 100 cm soil depth. The differentiation of autochthonous and allochthonous SOC is based on a comparison between SedOC and SOC content in soils. The vertical OC distribution in the investigated profiles and the OC pools were compared (see chapter 5.3.2 and 5.3.3). A difference between the recent SOCP and the initial SedOCP > 0 kg m^{-2} was interpreted as net autochthonous OC accumulation since sedimentation and a difference < 0 kg m^{-2} as depletion caused by microbial mineralization within a given soil depth. In case differences were close to 0 kg m^{-2} ($\pm$ 10 %) the initial allochthonous OC was most probably preserved or accumulation and mineralization processes reached a similar range.

4.5.3 Calculation of CO_2 and CH_4 production and estimation of potential carbon turnover

CO_2 and CH_4 concentration of the produced gas in the headspace ($Conc_{gas}$) was calculated in mg C g^{-1} dry weight (dw) using Henry's law:

$$Conc_{gas} = \frac{C_{gas} \times V_{headspace} \times M_{gas}}{V_M \times m_{sample}} \qquad \text{(Eq. 4)}$$

where C_{gas} is the concentration of gas measured in the headspace in ppm, $V_{headspace}$ is the headspace volume in l, M_{gas} is the molar mass of the respective gas in mg mol^{-1}, V_M is the molar volume in l mol^{-1}, and m_{sample} is the dry mass of the soil sample in g.

In addition to the gas in the headspace, a part of the produced gases is assumed to be dissolved in the soil solution. The total C production is the sum of the headspace C concentration and the dissolved proportion. To calculate the amount of dissolved inorganic carbon (DIC) in the solution, the carbonate system has to be accounted for.

$$DIC = K_H \times p_{CO_2} \times (1 + \frac{K_{H_2CO_3}}{[H^+]} + \frac{K_{H_2CO_3} \times K_{HCO_3^-}}{[H^+]^2}) \times V_{H_2O} \times M_{CO_2} / m_{sample} \qquad \text{(Eq. 5)}$$

The amount of DIC was calculated using the law of mass action (Eq. 5). DIC is given in mg g^{-1} dw, partial pressure of CO_2 (p_{CO2}) in atm, Henry constant (K_H) and first and second dissociation constant K_1 (K_{H2CO3}) and K_2 (K_{HCO3}) in mol l^{-1} atm^{-1}, the hydrogen ion activity [H^+] as 10^{-pH}, the volume of soil solution (V_{H2O}) in l, the molar mass of CO_2 (M_{CO2}) in g mol^{-1}, and soil sample mass (m_{sample}) in g dw. The partial pressure of CO_2 was calculated by multiplication of the measured concentration of CO_2 in the headspace and the internal pressure within the bottles. The hydrogen ion activity was derived from the pH after incubation in each replicate. The applied constants K_H, K_1, and K_2 were calculated according to Plummer and Busenberg (1982) as a function of temperature:

$$logK = A + B \times T + \frac{C}{T} + D \times logT + \frac{E}{T^2} \qquad \text{(Eq. 6)}$$

where T is the incubation temperature in K. The constants A to E (Eq. 6, Table 6) were computed empirically by regression analysis (Plummer and Busenberg, 1982).

Table 6: Constants for calculation of K_H, K_1, and K_2 as a function of temperature. $LogK$ was calculated according to Plummer and Busenberg (1982) using equation 6.

	A	B	C	D	E
$logK_H$	108.3865	0.01985076	-6919.53	-40.4515	669365.0
$logK_1$	-356.3094	-0.06091964	21834.37	126.8339	-1684915.0
$logK_2$	-107.8871	-0.03252849	5151.79	38.9256	-563713.9

The solubility of CH_4 depends mainly on pressure and temperature and to a minor extent on salinity. $CH_{4(aq)}$ in mg g^{-1} dw was calculated by equation 7:

$$CH_{4_{(aq)}} = \frac{\beta}{R \times T} \times C_{CH_4} \times P \times V_{H_2O} \times M_{CH_4} / m_{sample}$$ (Eq. 7)

where β is the Bunsen solubility coefficient in ml CH_4 ml^{-1} H_2O, R is the universal gas constant in l kPa K^{-1} mol^{-1}, T is the incubation temperature in K, C_{CH4} is the concentration of headspace CH_4 in ppm, P is the internal pressure in kPa, V_{H2O} is the volume of soil solution in l, M_{CH4} is the molar mass of CH_4 in g mol^{-1}, and m_{sample} is the soil sample mass in g dw. β was calculated according to Yamamoto et al. (1976):

$$ln\beta = A_1 + A_2 \times \left(\frac{100}{T}\right) + A_3 \times \ln\left(\frac{T}{100}\right) + S[B_1 + B_2 \times \left(\frac{T}{100}\right) + B_3 \times \left(\frac{T}{100}\right)^2]$$ (Eq. 8)

where T is the temperature in K, S is salinity in ‰, and A_1 to B_3 are constants (Table 7).

Table 7: Constants for calculation of the Bunsen solubility coefficient β. β was calculated according to Yamamoto et al. (1976) using equation 8.

A_1	A_2	A_3	B_1	B_2	B_3
-67,1962	99.1624	27.9015	-0.072909	0.041674	-0.0064603

The rates of CO_2 and CH_4 production were calculated from the change of gas concentration in the headspace over time in mg C g^{-1} dw d^{-1}. Due to flushing of aerobic incubations, the calculated gas production rates fluctuated strongly, yielding not trustable rates directly after flushing (compare chapter 6.2.3.2). For that reason, the first post-flushing values were replaced by the mean of the previous and subsequent mineralization rates. From these averaged rates, the cumulative aerobic CO_2 production was calculated. It was assumed that CO_2 was removed completely from the headspace, but DIC concentration was not affected by flushing, as CO_2 diffusion in water is particularly slow (Ramnarine et al., 2012). Thus, DIC was assumed to stay constant at the first post-flushing measurement and regain equilibrium with the new microbial CO_2 production until the subsequent measurement in the following week. In anaerobic

incubations, these problems did not occur, so that rates could be calculated directly from the measured concentrations.

To account for influencing factors apart from C content, production rates were normalized to pre-incubation SOC concentrations and are given in mg C g^{-1} SOC d^{-1}. The pre-incubation SOC content was calculated by adding the amount of C produced during the incubation to the post-incubation TOC value. Finally, the potential decomposability of the soil was estimated from the total C loss compared to pre-incubation SOC concentrations and is given in %.

For interpretation of the GWP of the investigated samples, the CO_2 equivalent (CO_2e) was calculated. For this purpose, the measured CH_4 production was multiplied by a factor of 28 accounting for the stronger radiative forcing in comparison with CO_2 (IPCC, 2013). This value was added to the anaerobic CO_2 production to yield the total CO_2e.

4.5.4 Classification of contamination levels

To evaluate the contamination level of soils different approaches were used. Geogenic background values have been estimated for sediments of the Elbe estuary (Gröngröft et al., 1998). A comparison of the measured concentrations with background values was carried out by calculation of enrichment factors (measured concentration divided by background value) according to Gröngröft et al. (1998). Additionally, the ARGE Elbe classification system was used to assess contamination level of the investigated soil samples (Stachel and Lüschow, 1996). The classification is based on natural background values of Elbe sediments. These background values were comparable to those of Gröngröft et al. (1998) except for As which was considerably lower. Seven pollution classes were distinguished by ARGE Elbe (1996), of which class I represents background values (Table A 14). Class II represents target values which should not be exceeded. However, these target values have the character of orientation values and do not contain ecotoxicological implications. To evaluate the environmental risk coming from polluted soils, ecotoxicological values according to BfG (2008) were determined. Five classes from natural background values to a very high degree of toxicity were distinguished (Table A 14). Class D indicates target values that can be regarded as nonhazardous. Since some of the investigated marshes are used for agricultural production (see chapter 3.4.1), an evaluation according to the German Ordnance on soil protection and contaminated sites (BBodSchV, 1999) was carried out. For topsoil horizons (0 – 30 cm), precautionary values depending on soil texture and action values for pastures and meadows were specified within the ordnance. Precautionary values

represent thresholds above which hazardous effects can occur in case of continued exposure, whereas action values represent thresholds above which a soil has to be considered as contaminated and remediation measures are required. In accordance with this method, total trace metal concentrations were assessed, while in the abovementioned classification systems the concentrations in the ff20 were used.

4.5.5 Age determination of soil horizons

The pollution history of selected profiles was reconstructed using the chronological development of trace metal input following e.g. Meyercordt (1992), Zwolsman et al. (1993), and Prange (1997). To estimate the deposition period of the investigated soil horizons, the vertical trace metal distribution in soil profiles was compared with the anthropogenic input between 1988 and 2010. A polynomial fit of metal concentrations and ratios in suspended sediments over this period was calculated, to determine the long-term changes in the trace metal load. Threshold values of the Zn/Hg and Hg/Cd ratios could be assigned to specific years when these values were reached. These thresholds could be used as time markers for the comparison with trace metal ratios in soils. Due to the strong difference in metal concentrations at the sampling stations Grauerort and Cuxhaven, no time markers could be determined for the comparison with metal concentrations in soils. However, the anthropogenic influence could be estimated by comparison of trace metal concentrations with geogenic background values according to Gröngröft et al. (1998) and Stachel and Lüschow (1996). The results of the dating approach were compared with accretion rates of the respective estuarine zone according to Butzeck et al. (2015). Additionally, annual storm tide layers were counted where possible, providing an indication of the sedimentation dynamics of the respective profiles.

4.5.6 Up-scaling

The soil organic carbon and trace metal stocks stored in the investigated tidal marshes along the Elbe estuary were calculated by multiplying the SOC pools by the area of the respective marshes. The areal extent of the tidal marshes was calculated based on a soil map of the environmental impact assessment 2006 (Gröngröft et al., 2006). All tidal marshes were separated from diked marshes and upland areas as well as tidal flats (Figure 5) and furthermore divided into different salinity zones (oligo-, meso-, polyhaline) according to Stiller (2009). River islands were excluded

from this estimation, as they consist to a large proportion of deposed dredged sand. Thereafter, the soil organic carbon stock of the tidal marshes was calculated in Tg (1 Tg = 10^{12} g) for the area of each salinity zone separately. Likewise, trace metal stocks were calculated in t (1 t = 10^{6} g). Salinity was chosen as an adequate parameter to split the data set, as soil organic carbon pools and the respective trace metal pools were significantly different between salinity zones (compare chapter 5.3.1 & 5.5.1).

4.5.7 Statistics

To assess the normality of the data set, a Shapiro-Wilk test was carried out. As most parameters were not normally distributed, Spearman's rank correlation coefficient (r_s) was used to determine correlations between different soil parameters. Prior to correlation analysis with elevation above MHW and salinity in the groundwater, soil parameters were pooled by calculating the weighted means for topsoil and subsoil horizons of each profile. Differences in the SOC pools and stocks among salinity zones were determined using one-way analysis of variance (ANOVA) and Tukey (homoscedasticity) or Dunnett-T3 (heteroscedasticity) post-hoc tests, as data in the respective groups were normally distributed. Differences in SOC between the elevation classes were determined using the nonparametric Mann-Whitney-U-Test, as the data were not in line with the assumptions for parametric tests. Nonparametric tests (Mann-Whitney-U-Test for elevation and pair wise Kruskal-Wallis-Test plus Jonckheere-Terpstra-Test for salinity) were also used to determine differences in soil properties (weighted means of bulk density, ff20, TOC, TIC, TN, C/N), trace metal pools, biomass, and SOC turnover in defined groups. These approaches were considered appropriate, when the respective parameters did not show significant differences between sites within each zone. A non-parametric Wilcoxon signed-rank test for related samples was carried out to compare topsoil and subsoil samples as well as aerobic and anaerobic incubations for differences in SOC turnover. Differences between initial and final gas production rates were also tested using the Wilcoxon test. For the evaluation of the trace metal contamination of the investigated marsh soils, a cluster analysis was carried out based on enrichment factors. Enrichment factors were used for normalization of the data to avoid the dominant influence of single elements like Zn that occur in larger quantities than other metals. The cluster analysis was conducted using Ward's method with squared Euclidean distance. The quality of the classification was tested by means of pair wise Kruskal-Wallis-Test. Effects were considered significant when $p < 0.05$. All statistical analyses were conducted using IBM SPSS Statistics 21.0 software package. Graphs were created using Origin Pro 8.1 software package.

Differences in SOC pools, C turnover, and trace metal concentrations across land use types were not analyzed statistically. All five sites have unmanaged plots, but as far as agricultural treatments go, there was little replication. Meadow and pasture with cattle existed at one site each, pasture with sheep at two sites. However, a visual examination of the SOC and trace metal data did not reveal major differences between unmanaged and managed plots. Thus, different land use types were not accounted for as individual factors within the data analysis.

5 Results

5.1 Soil characteristics and properties

5.1.1 Bulk density, texture, and pH

The marsh soils of the Elbe estuary showed an average Bd of 1.08 ± 0.26 g cm^{-3}. The values varied with sites between 0.43 and 1.62 g cm^{-3} (Table A 1). Mean Bd did not differ significantly between salinity zones and elevation classes along the Elbe estuary. However, site 5 in the polyhaline zone had significantly higher Bd than site 1 in the oligohaline zone (Table 8), both in topsoils from $0 - 30$ cm ($p = 0.027$) and over the whole profile depth of 100 cm ($p = 0.046$).

The texture of the studied soil horizons ranged from pure sand to silty clay (Table A 2). The ff20 content showed a high scatter within the investigated marshes, with minima found in pure sand soils in the salt marsh area (3.13 %) and maxima in silty clay soils of the oligohaline zone (89.5 %). The mean ff20 content increased with increasing salinity in topsoils and the whole profile, resulting in significant differences between the oligohaline and polyhaline zone ($p = 0.009$, respectively). ff20 did not differ significantly between sites (Table 8) or elevation classes (Table A 4).

Average pH$_{CaCl2}$ accounted for 7.5 ± 0.3 in the investigated soils. Lowest pH values of 6.8 (neutral) were found in different sites along the course of the estuary, while highest pH values of 8.3 (weakly alkaline) were measured in samples of site 5 (Table A 3). pH values > 8.0 were solely present in soils of the polyhaline zone.

Table 8: Distribution of bulk density and ff20 content. Weighted means ($\pm$ SD) of marsh soils in the different study sites are given for topsoils ($0 - 30$ cm) and the whole profile depth ($0 - 100$ cm).

	Site	Bulk density, g cm^{-3}		ff20, %	
		$0 - 30$ cm	$0 - 100$ cm	$0 - 30$ cm	$0 - 100$ cm
Oligohaline zone	1	0.62 ± 0.14	0.59 ± 0.07	65.03 ± 19.06	49.23 ± 12.31
	2	1.08 ± 0.26	1.20 ± 0.26	48.45 ± 10.72	46.47 ± 12.12
Mesohaline zone	3	1.17 ± 0.09	1.25 ± 0.06	20.44 ± 10.41	15.98 ± 5.23
	4	0.97 ± 0.20	1.01 ± 0.19	40.23 ± 15.30	37.61 ± 17.92
Polyhaline zone	5	1.17 ± 0.11	1.30 ± 0.10	24.73 ± 13.71	19.51 ± 11.92

5.1.2 TOC and TIC concentrations

In the investigated area, the TOC concentrations varied strongly between salinity zones and elevation classes (Table A 3). Lowest concentrations occurred in a sandy subsoil horizon of the polyhaline zone (0.15 %), while highest concentrations occurred in a clay rich topsoil horizon of the oligohaline zone (7.73 %). A significant decrease of TOC was found, in the order: oligohaline > mesohaline > polyhaline zone (p < 0.05, both for 0 – 30 cm and 0 – 100 cm, compare Table A 4). TOC concentrations of low and high marshes did not differ significantly. Regarding the study sites (Table 9), significant differences were found between site 1 and site 5 (0 – 30 cm: p = 0.008; 0 – 100 cm: p = 0.004)

Table 9: Distribution of TOC and TIC concentrations. Weighted means (± SD) of marsh soils in the different study sites are given for topsoils (0 – 30 cm) and the whole profile depth (0 – 100 cm).

	Site	TOC, %		TIC, %	
		0 – 30 cm	0 – 100 cm	0 – 30 cm	0 – 100 cm
Oligohaline zone	1	5.15 ± 1.92	4.95 ± 1.70	0.73 ± 0.27	0.57 ± 0.23
	2	3.36 ± 0.49	2.08 ± 0.56	0.44 ± 0.33	0.41 ± 0.21
Mesohaline zone	3	1.73 ± 0.66	1.20 ± 0.10	0.78 ± 0.10	0.70 ± 0.17
	4	2.43 ± 0.91	2.00 ± 0.86	0.93 ± 0.14	0.86 ± 0.17
Polyhaline zone	5	1.38 ± 0.54	0.83 ± 0.38	0.78 ± 0.08	0.70 ± 0.03

In most profiles TOC concentrations decreased with increasing soil depth (r_s = -0.444, p < 0.001). Major differences appeared between organic rich topsoil horizons (Ah: 3.91 ± 1.72 %) and subsoil horizons showing redoximorphic features (Gro: 1.09 ± 0.81 %, Gor: 1.09 ± 0.73 %). The TOC decrease with soil depth was particularly apparent for high marsh profiles. Furthermore, TOC was negatively correlated with bulk density (r_s = -0.786, p < 0.001) and positively correlated with ff20 (r_s = 0.780, p < 0.001) (Figure 8). The correlation with ff20 was stronger in low marshes (r_s = 0.940, p < 0.001) than in high marshes (r_s = 0.577, p < 0.001).
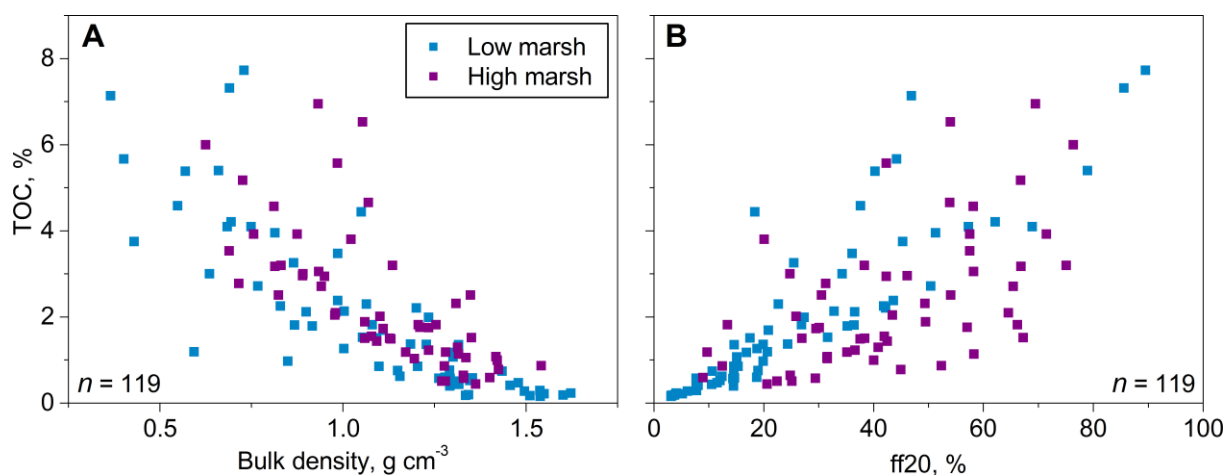
Figure 8: Relation between soil TOC and bulk density (A), as well as ff20 (B) within the different elevation classes.

TIC concentration ranged from 0.14 to 1.21 %, with a mean of 0.71 ± 0.23 % (Table A 3). Maximum values were found in a silty subsoil of site 4 in the mesohaline zone. Consequently, mean TIC concentrations were significantly higher in the mesohaline than in the oligohaline zone ($p = 0.025$). This result was only significant over the whole profile depth. The polyhaline zone did not show significant differences to the other zones. Topsoils of low marshes had significantly higher TIC concentrations than high marshes ($p = 0.014$). Furthermore, site 4 had significantly higher TIC concentrations over the whole profile depth than site 2 ($p = 0.014$, Table 9).

5.1.3 TN concentrations and C/N ratios

TN concentrations showed a strong variation in the investigated sites, with a minimum of 0.01 % in site 3 and a maximum of 0.69 % in site 2 (Table A 3). Similar to TOC, a significant decrease of TN was found in the order: oligohaline > mesohaline > polyhaline zone ($p < 0.05$ both for 0 – 30 cm and 0 – 100 cm). However, differences between sites were only significant between site 1 and 5 (0 – 30 cm: $p = 0.015$; 0 – 100 cm: $p = 0.004$; Table 10). No significant differences were found between low and high marshes.

C/N ratios ranged from 7.25 to 17.60, with a mean of 9.97 ± 1.42 (Table A 3). The sample showing the lowest TN concentration had also the highest C/N ratio, while the lowest C/N ratio was found in site 5. Significant differences in C/N ratios over the whole profile depth were found between study site 1 and 5 ($p = 0.047$, Table 10). Salinity zones did not differ significantly in their C/N ratios. Furthermore, higher C/N ratios were found in topsoils of low compared to high marshes ($p = 0.043$).

49

Table 10: Distribution of TN concentrations and C/N ratios. Weighted means ($\pm$ SD) of marsh soils in the different study sites are given for topsoils (0 – 30 cm) and the whole profile depth (0 – 100 cm).

	Site	TN, %		C/N	
		Mean	SD	Mean	SD
Oligohaline zone	1	0.46 ± 0.13	0.40 ± 0.11	11.15 ± 0.80	12.00 ± 0.81
	2	0.35 ± 0.07	0.22 ± 0.04	9.66 ± 0.45	9.37 ± 0.85
Mesohaline zone	3	0.17 ± 0.08	0.12 ± 0.02	11.05 ± 1.83	10.45 ± 1.11
	4	0.24 ± 0.09	0.20 ± 0.08	10.02 ± 0.43	9.97 ± 0.39
Polyhaline zone	5	0.14 ± 0.06	0.09 ± 0.04	9.77 ± 0.74	9.39 ± 0.73

5.1.4 Trace metal concentrations

The trace metal concentrations of the investigated marsh soils varied strongly between different sites, profiles, and soil depths (Table A 5). Mean Hg concentrations accounted for 0.46 $\pm$ 0.61 mg kg^{-1} in the total sample and 0.73 $\pm$ 0.62 mg kg^{-1} in the ff20. Cd concentrations were in a similar range with 0.51 $\pm$ 0.49 mg kg^{-1} in the total sample and 0.65 $\pm$ 0.39 mg kg^{-1} in the ff20. Pb concentrations ranged in a much higher order of magnitude with 38.3 $\pm$ 23.7 mg kg^{-1} in the total sample and 70.5 $\pm$ 20.2 mg kg^{-1} in the ff20. Mean Zn concentrations were 159.7 $\pm$ 118.3 mg kg^{-1} in the total sample and 304.1 $\pm$ 105.4 mg kg^{-1} in the ff20. As accounted for 28.9 $\pm$ 9.6 mg kg^{-1} in the ff20. All metals had lower average concentrations and higher standard deviations in the total sample than in the ff20.

Minimum trace metal concentrations in the ff20 were found in two profiles of study site 2 in the oligohaline zone. Profile 2b had lowest concentrations of Hg, Cd, Zn, and As and profile 2c had the lowest concentration of Pb in subsoil horizons. Maximum concentrations of all metals were found in the mesohaline zone. Highest concentrations of Hg, Pb, Zn, and As were present in subsoil horizons of profile 4e while the highest concentration of Cd was found in upper part of profile 3b (for a detailed description of these profiles see chapter 5.5.4).

Total concentrations of the investigated trace metals correlated with ff20, SOC, and pH$_{CaCl2}$ (Figure 9). Strongest positive correlations were found between ff20 and Pb as well as Zn. Cd and Hg correlated stronger with SOC than with ff20. pH correlated negatively with the investigated metals, but the correlation coefficients were lower compared to ff20 and SOC. Trace metals

measured in the grain size fraction $< 20\,\mu m$ were not correlated with ff20 and only weakly correlated with SOC (Cd: $r_s = 0.328$; Hg: $r_s = 0.335$; Pb: $r_s = 0.251$; Zn: $r_s = 0.309$; $p < 0.05$ respectively) and pH (Cd: $r_s = -0.370$; Hg: $r_s = -0.238$; Pb: $r_s = -0.210$; Zn: $r_s = -0.315$; $p < 0.05$ respectively). Arsenic, which was not measured in the total sample but only in the ff20, did not correlate significantly with SOC (As: $r_s = -0.005$, $p = 0.960$) and only very weakly with pH (As: $r_s = -0.206$, $p = 0.045$). No significant correlations were found between the respective trace metal concentrations and soil inorganic carbon (SIC) ($p > 0.05$).

Furthermore, negative correlations were found between trace metal concentrations and salinity (Table 11). These correlations were only significant in the topsoil horizons (0 – 30 cm) of the total samples and the ff20. Correlation coefficients were usually higher in the ff20 than in total samples. No significant correlations were found between metal concentrations and salinity in subsoil horizons as well as elevation above MHW in topsoil and subsoil horizons.
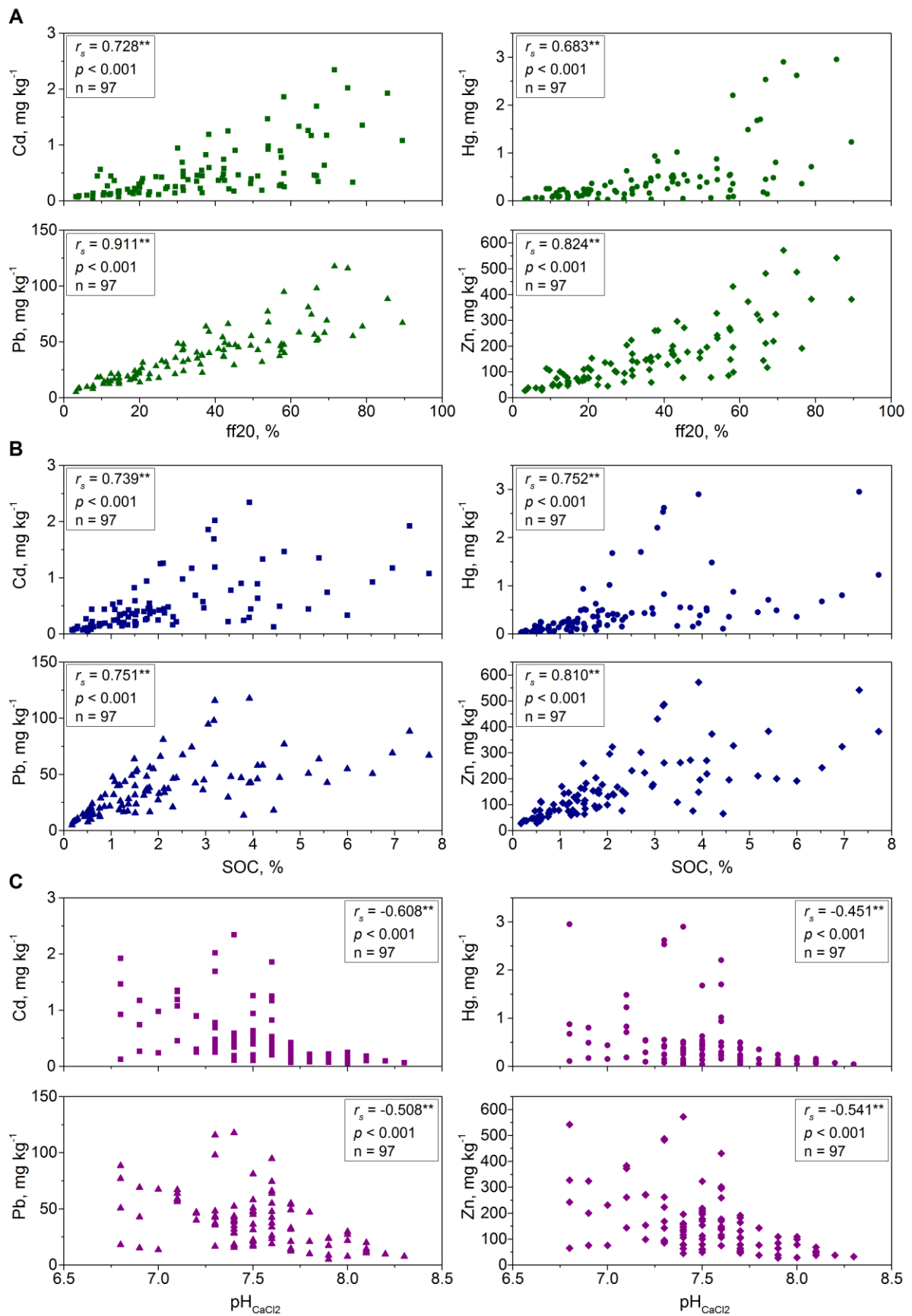
Figure 9: Relation between total trace metal concentrations and selected soil characteristics. Correlations are indicated for the respective metal concentrations and ff20 (A), SOC (B), and pH_{CaCl2} (C). Spearman's rank correlation coefficient (r_s) was considered significant when $p < 0.05$.

Table 11: Correlation between trace metal concentrations and salinity in the groundwater as well as elevation above MHW. Values are given for total metal contents and metal contents in the ff20 of topsoil (0 – 30 cm) and subsoil samples (30 – 100 cm). Spearman's rank correlation coefficient (r_s) was considered significant when $p < 0.05$.

Trace metals, mg kg^{-1}		Salinity		Elevation	
		Topsoil	Subsoil	Topsoil	Subsoil
Cd	r_s	-0.800**	-0.281	0.189	0.449
	p	0.000	0.353	0.400	0.124
	n	22	13	22	13
Cd < 20 µm	r_s	-0.845**	0.121	0.085	-0.121
	p	0.000	0.694	0.708	0.694
	n	22	13	22	13
Hg	r_s	-0.650**	0.041	0.183	0.118
	p	0.001	0.894	0.416	0.700
	n	22	13	22	13
Hg < 20 µm	r_s	-0.636**	0.426	0.108	-0.152
	p	0.001	0.146	0.632	0.621
	n	22	13	22	13
Pb	r_s	-0.479*	-0.264	0.206	0.360
	p	0.024	0.384	0.357	0.226
	n	22	13	22	13
Pb < 20 µm	r_s	-0.638**	0.236	-0.020	-0.289
	p	0.001	0.437	0.928	0.338
	n	22	13	22	13
Zn	r_s	-0.708**	-0.082	0.082	0.223
	p	0.000	0.789	0.715	0.464
	n	22	13	22	13
Zn < 20 µm	r_s	-0.880**	0.236	0.047	-0.088
	p	0.000	0.437	0.836	0.775
	n	22	13	22	13
As < 20 µm	r_s	-0.684**	-0.154	-0.182	0.047
	p	0.000	0.616	0.416	0.879
	n	22	13	22	13

* significant correlation ($p < 0.05$)
** highly significant correlation ($p < 0.01$)

5.2 Above-ground biomass

In summer (September 2010) above-ground biomass ranged between 0.39 kg m^{-2} in the polyhaline zone and 3.26 kg m^{-2} in the oligohaline zone (Figure 10 A). The amount of above-ground biomass decreased with increasing salinity. Significant differences ($p < 0.01$) were found between the polyhaline and the other two zones, respectively. In winter (February 2011) above-ground biomass varied between 0.24 and 3.55 kg m^{-2}. In this period above-ground biomass also

decreased with increasing salinity, but the differences were only significant between the oligo- and polyhaline zone ($p = 0.015$).

Low marshes had significantly higher above-ground biomass in summer than high marshes of the study sites ($p = 0.022$) (Figure 10 B). This difference was not significant in the winter period.
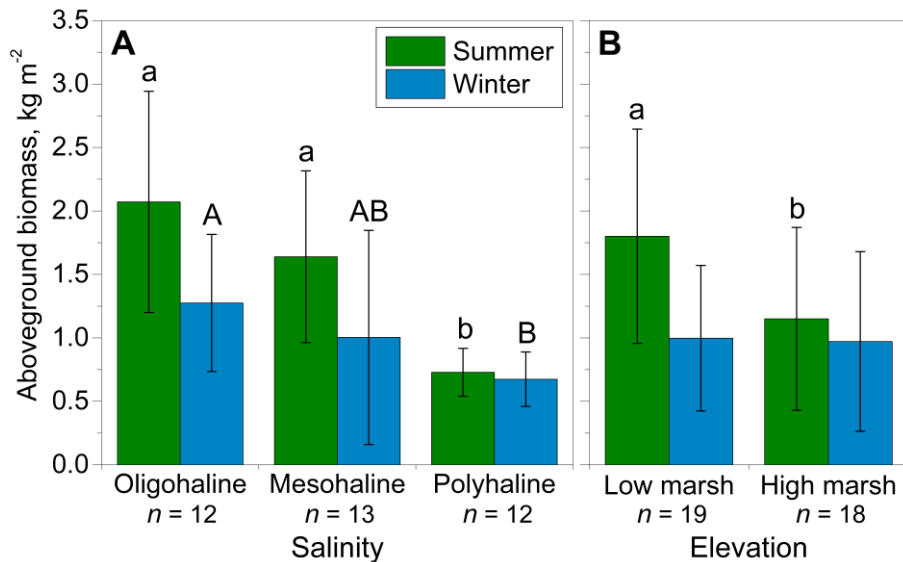
Figure 10: Total above-ground biomass (live & dead biomass) in the different salinity zones (A) and elevation classes (B) of unmanaged marshes of the study sites 1, 4, and 5 (mean $\pm$ SD). Measurements were divided into summer (September 2010) and winter (February 2011). Letters denote statistical differences between salinity zones (Kruskal-Wallis-Test; $p < 0.05$) and between elevation zones (Mann-Whitney-U-Test; $p < 0.05$). Data provided by C. Butzeck.

5.3   Organic carbon

5.3.1   Differentiation of SOC pools

SOC pools (Table 12, Figure 11 A) decreased with increasing salinity in the upper 30 cm soil depth ($r_s = -0.603$, $p = 0.003$) and in 100 cm soil depth ($r_s = -0.637$, $p = 0.001$). The oligohaline zone had an average $SOCP_{30}$ of 10.20 ± 3.54 kg m^{-2}, which was significantly higher than that of the polyhaline zone (4.45 ± 1.27 kg m^{-2}; $p = 0.012$). The mean SOC pool of the mesohaline zone accounted for 6.15 ± 1.88 kg m^{-2} and did not differ significantly from the oligo- and polyhaline zone ($p = 0.066$ and $p = 0.162$, respectively). Regarding 100 cm soil depth, differences between all three zones were significant. The oligohaline zone showed a significantly higher $SOCP_{100}$ of 25.01 ± 5.21 kg m^{-2} than the meso- ($p = 0.006$) and polyhaline zone ($p < 0.001$). The latter salinity zones showed decreasing SOC pools, with 16.64 ± 4.52 kg m^{-2} and 9.72 ± 3.80 kg m^{-2}, respectively. The difference between the meso- and polyhaline zone was significant ($p = 0.022$).

Along an elevational gradient, $SOCP_{30}$ increased with increasing height above mean high water (r_s = -0.462, p = 0.030), while $SOCP_{100}$ did not increase significantly (Figure 11 B). Differences between high and low marsh were significant only in the topsoil (p = 0.012), with a $SOCP_{30}$ of 8.35 $\pm$ 2.55 kg m^{-2} in the high marsh and of 5.69 $\pm$ 3.51 kg m^{-2} in the low marsh. The $SOCP_{100}$ revealed no significant differences between low and high marshes (p = 0.075), with 15.27 $\pm$ 9.30 kg m^{-2} and 19.31 $\pm$ 4.40 kg m^{-2}, respectively. However, the study sites 1, 4, and 5 showed increasing $SOCP_{100}$ with increasing elevation along each transect. This increase appeared on different SOC levels which resulted in a high scatter within the whole dataset.
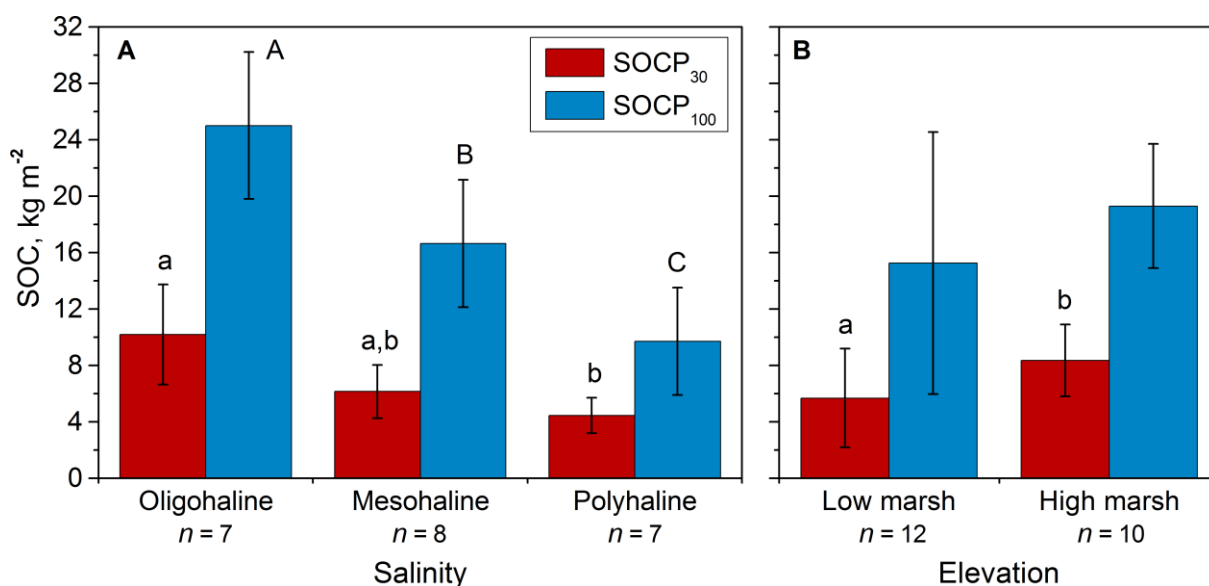
Figure 11: $SOCP_{30}$ and $SOCP_{100}$ of the different salinity zones (A) and elevation classes (B) of the investigated tidal marshes (mean $\pm$ SD). Letters denote statistical differences between salinity zones (one-way ANOVA; p < 0.01) and between elevation classes (Mann-Whitney-U-Test; p = 0.012). No statistical differences were found between low and high marshes within 100 cm soil depth and between managed and unmanaged marshes in both soil depths.

5.3.2 Vertical TOC distribution in soils and their allochthonous proportion

In recent soils of high marshes, positive deviations of SOC in topsoil horizons ($\triangleq$ accumulation) and negative deviations of SOC in subsoil horizons ($\triangleq$ depletion) compared to the initial allochthonous SedOC content were found (e.g. Figure 12 G, N, V). These deviations were more pronounced in the oligo- than in the polyhaline zone. In many low marsh profiles, the recent distribution of SOC followed the initial distribution of SedOC (e.g. Figure 12 A, K, Q). Generally, high OC contents are not restricted to the topsoil horizons, but vary with depth. A strong positive correlation between SOC and SedOC was found in the whole data set (r_s = 0.795, p < 0.001).

Table 12: Soil and sediment organic carbon pools. Organic carbon pools are given in kg m-2 for 0 – 30 cm, 0 – 100 cm, and 30 – 100 cm soil depth. SOCP represents the recent soil organic carbon pool, SedOCP the initial allochthonous proportion, and ΔOCP the change in OC pools since sedimentation.

Name	River km	Profile No.	$SOCP_{30}$, kg m^{-2}	$SOCP_{100}$, kg m^{-2}	$SOCP_{30\text{-}100}$, kg m^{-2}	$SedOCP_{30}$, kg m^{-2}	$SedOCP_{100}$, kg m^{-2}	$SedOCP_{30\text{-}100}$, kg m^{-2}	ΔOCP_{30}, kg m^{-2}	ΔOCP_{100}, kg m^{-2}	$\Delta OCP_{30\text{-}100}$, kg m^{-2}
Haseldorfer Marsch	656	1a	5.42	21.20	15.79	4.04	13.01	8.96	1.37	8.19	6.82
		1b	8.91	28.56	19.65	7.67	17.99	10.32	1.23	10.56	9.33
		1c	15.32	35.02	19.70	10.62	20.34	9.71	4.69	14.67	9.98
Asseler Sand	666	2a	6.51	23.41	16.90	4.82	13.81	8.99	1.68	9.59	7.91
		2b	10.34	19.63	9.28	7.17	29.47	22.31	3.18	-9.85	-13.03
		2c	11.90	23.59	11.68	11.57	44.38	32.81	0.33	-20.80	-21.13
		2d	13.00	23.69	10.69	11.09	38.32	27.24	1.91	-14.64	-16.55
Böschrücken	691	3a	3.10	13.80	10.70	2.61	10.13	7.51	0.49	3.68	3.19
		3b	6.75	13.90	7.15	2.40	6.87	4.47	4.34	7.03	2.68
		3c	6.68	14.64	7.96	4.94	11.94	7.01	1.75	2.70	0.95
Neufelder Vorland	702	4a	4.97	11.47	6.50	4.91	10.96	6.06	0.06	0.51	0.44
		4b	4.12	13.95	9.83	3.25	11.43	8.18	0.86	2.51	1.65
		4c	7.24	20.71	13.47	6.24	18.95	12.71	1.00	1.76	0.76
		4d	8.24	20.26	12.02	5.73	20.68	14.95	2.51	-0.42	-2.94
		4e	8.07	24.38	16.31	7.62	25.46	17.84	0.44	-1.08	-1.52
Dieksanderkoog	725	5a	3.75	6.04	2.29	3.72	6.18	2.46	0.03	-0.14	-0.17
		5b	3.19	5.80	2.60	3.49	6.53	3.04	-0.30	-0.73	-0.43
		5c	3.87	7.75	3.87	2.47	7.05	4.58	1.40	0.70	-0.70
		5d	5.20	10.43	5.23	3.12	9.78	6.66	2.08	0.65	-1.43
		5e	5.61	15.41	9.80	5.81	20.41	14.60	-0.20	-5.00	-4.80
		5f	3.17	8.48	5.32	2.48	10.46	7.98	0.69	-1.97	-2.66
		5g	6.36	14.14	7.78	7.46	22.15	14.69	-1.10	-8.01	-6.91

Figure 12: Vertical distribution of TOC concentrations. The TOC distribution during the initial allochthonous sedimentation is indicated by light blue lines and in recent soils by dark blue lines. The TOC concentrations in recent soils result from a combination of allochthonous and autochthonous OC input minus OC mineralization.
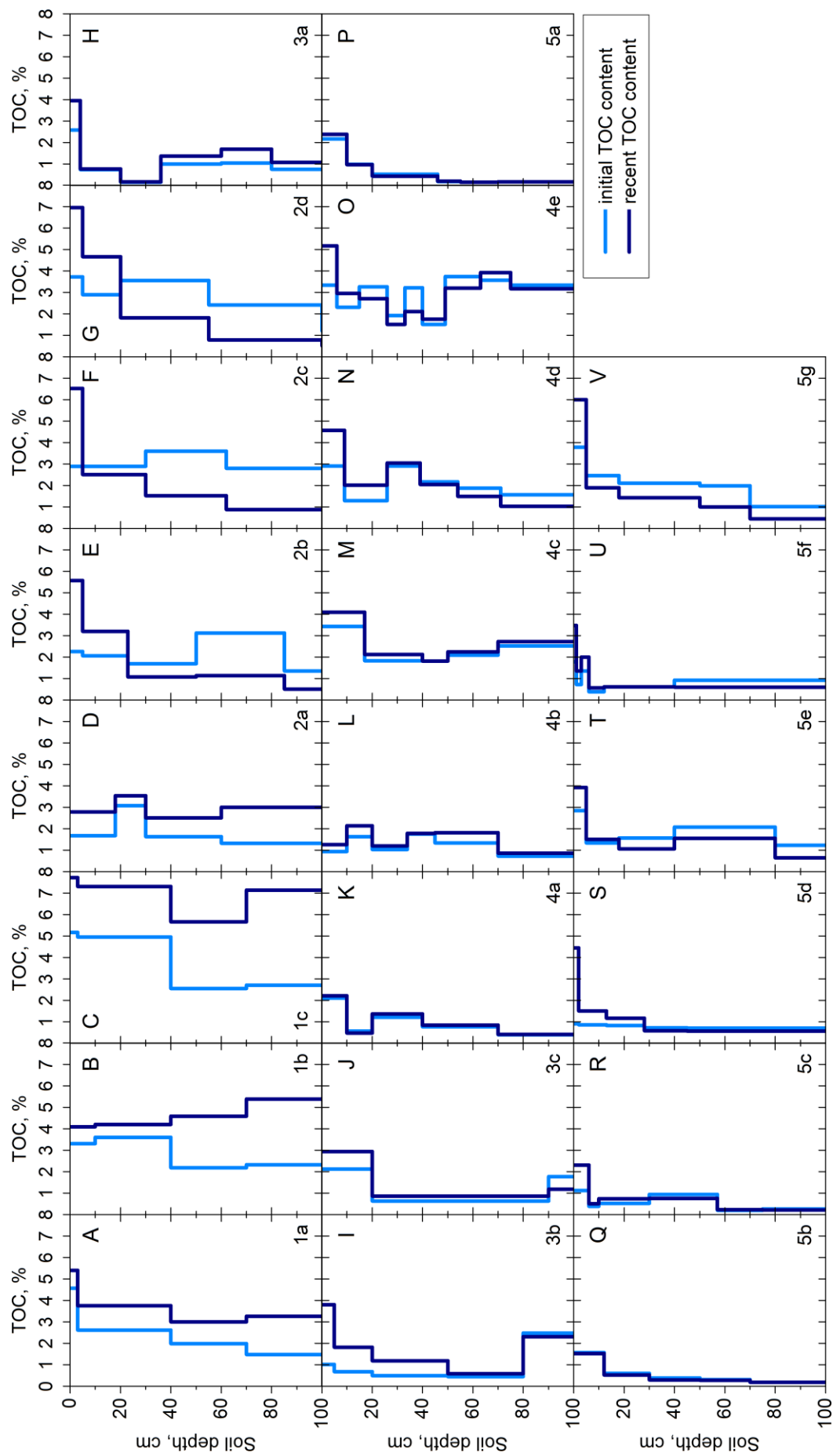
5.3.3 Comparison between initial and recent OC pools

In the upper 30 cm soil depth, 15 marsh profiles showed an OC accumulation between 0.49 and 4.69 kg m^{-2} ($\triangleq$ 16.0 and 180.8 % compared to the initial OC) (Table 12). Only one high marsh profile of the polyhaline zone (profile 5g, see Figure 5 G) showed a net OC depletion of -1.1 kg m^{-2} ($\triangleq$ -14.8 % compared to initial SedOCP). The other six profiles had SedOCP$_{30}$ values close to the SOCP$_{30}$ values ($\pm$ 10 %), which did not indicate a general accumulation or depletion. SOC accumulation in the topsoil significantly decreased with increasing salinity (r_s = -0.611, p = 0.003). No significant differences of ΔOCP$_{30}$ were found along the elevational gradient.

Considering only the subsoil between 30 and 100 cm soil depth, eight profiles of the oligohaline and mesohaline zone exhibited an accumulation of OC between 0.95 and 9.98 kg m^{-2} which represents additional 13.6 to 102.7 % OC compared to the initial OC pools (Table 12). Ten profiles, mainly in the polyhaline but also three profiles of the oligohaline zone (profiles 2b, c, d, see Figure 1 D), showed an OC depletion of -0.43 to -21.13 kg m^{-2} which is a reduction of -14.2 to -64.4 % compared to the initial OC pool. Only four profiles had ΔOCP$_{30-100}$ values around zero. Within the subsoil and over the whole profile depth (0 – 100 cm) a significant decrease of accumulation with increasing elevation was found (r_s = -0.554, p = 0.007 and r_s = -0.465, p = 0.029, respectively). Salinity did not show a significant correlation with ΔOCP$_{30-100}$ or ΔOCP$_{100}$.

5.3.4 Carbon isotope ratios of soils, sediment, and biomass

The δ^{13}C values ranged from -23.5 to -29.3 ‰ in the investigated soil profiles. The mean δ^{13}C values for biomass (-27.8 $\pm$ 0.6 ‰) and fresh sediments (-26.1 $\pm$ 0.9 ‰) were within this range. Horizons showing OC accumulation according to the approach described in chapter 4.5.2 had δ^{13}C values of -28.1 $\pm$ 0.9 ‰ which were similar to the local biomass (Figure 13, Table A 6). Horizons showing OC depletion had higher δ^{13}C values (-26.1 $\pm$ 0.8 ‰) which were similar to the sediments. Horizons with ΔOCP values around zero showed a high scatter in δ^{13}C (-25.1 $\pm$ 1.5 ‰), including horizons with higher δ^{13}C values than sediments and local biomass which cannot be explained by the investigated sources (compare chapter 6.1.1).
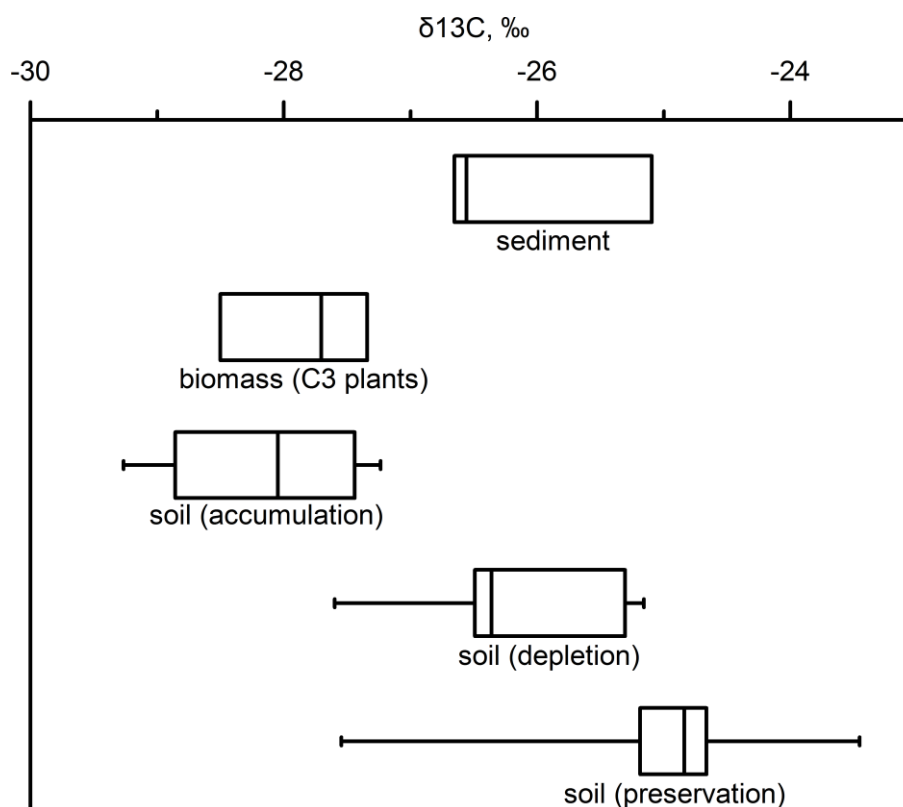
Figure 13: Ranges of $^{13}C/^{12}C$ ratios in fresh sediments, biomass samples, and soil horizons expressed as $\delta^{13}C$ values (‰ VPDB). Soil horizons were grouped in those showing autochthonous OC accumulation, those showing depletion by mineralization, and those showing preservation of allochthonous OC. Each box represents the inter quartile range, the lines within the boxes represent the median, the whiskers represent the top and bottom 25 % of scores.

5.3.5 Spatial distribution of SOC stocks

The considered area of tidal marshes between river kilometer 655 and 727 amounted to 66 km^2 (Table 13). The oligo- and mesohaline zone represented 37 and 35 % of the investigated area, respectively. The smallest proportion of this area was located in the polyhaline zone (28 %).

The organic carbon stored in the upper 30 cm of soil was estimated to be 0.46 ± 0.22 Tg for the total marsh area. The SOC stocks of the oligo- and mesohaline zone accounted for 55.4 ± 39.9 % and 30.8 ± 19.5 % of the stored carbon, respectively. The polyhaline zone stored only 18.0 ± 10.6 % organic carbon within this soil depth. The differences between all three zones were highly significant ($p < 0.001$).

The organic carbon stored within 100 cm soil depth was estimated to be 1.13 ± 0.50 Tg in the investigated marsh zones. The SOC stock of the oligohaline zone accounted for 54.8 ± 25.7 %, that of the mesohaline zone for 33.7 ± 20.6 %, and that of the polyhaline zone for 15.9 ± 14.0 % of the total organic carbon stock. Again, these differences were highly significant ($p < 0.001$).

Table 13: Area and SOC stocks of marsh soils along the Elbe estuary. SOC stocks are given in Tg within 30 cm and 100 cm soil depth (mean ± SD) in the different salinity zones of the estuary.

	Area, km^{-2}	SOC stock in 0 – 30 cm, Tg		SOC stock in 0 – 100 cm, Tg	
		Mean	SD	Mean	SD
Oligohaline zone	25	0.25	0.09	0.62	0.13
Mesohaline zone	23	0.14	0.04	0.38	0.10
Polyhaline zone	18	0.08	0.02	0.18	0.07
Total marsh area	66	0.46	0.22	1.13	0.50

5.4 Aerobic and anaerobic carbon turnover

5.4.1 Soil characteristics of incubated samples

The incubated soil samples were selected topsoil and subsoil samples from the investigated profiles that were sampled a second time in April 2012. Hence, the soil characteristics differed in comparison to values from 2010 (compare Table A 3 & Table A 7). Mean post-incubation pH values ranged from 6.1 to 7.8, indicating a considerable TIC content which ranged from 0.30 to 1.19 %. TIC accounted for 4.5 % of TC in the sample with lowest pH to 67.0 % of TC in the sample with highest pH. Post-incubation TC ranged from 0.87 to 7.76 % and TOC was between 0.29 and 7.27 %. Total N content was between 0.05 and 0.67 %, resulting in C/N ratios of 6.01 to 12.33 after the incubation was finished. The calculated pre-incubation TOC content ranged from 0.31 to 7.59 %.

Significant differences were found between topsoil and subsoil samples (Table 14) in post-incubation TC, TIC, TOC, TN, and pre-incubation TOC ($p < 0.01$). Likewise, ff20 (based on 2010 grain size determination) was significantly higher in topsoil samples than in subsoil samples ($p = 0.006$). No significant differences were found in pH and C/N ratios.

Table 14: Pre and post-incubation soil characteristics. Values are given as mean ± SD of all replicates for topsoil and subsoil samples (n = 12 per group). Statistical differences are indicated by asterisks (Wilcoxon signed-rank test: $*p < 0.01$). Non-significant results are denoted by ns ($p \geq 0.05$).

Parameter	Topsoil		Subsoil		Sig.
	Mean	SD	Mean	SD	
Post-incub. pH	7.5	0.2	7.4	0.5	ns
Post-incub. TC, %	4.72	1.57	2.47	1.52	*
Post-incub. TIC, %	0.83	0.26	0.65	0.22	*
Post-incub. TOC, %	3.89	1.69	1.82	1.57	*
Post-incub. TN, %	0.39	0.15	0.18	0.12	*
Post-incub. C/N	9.75	0.78	9.60	1.58	ns
Pre-incub. TOC, %	4.13	1.76	1.88	1.62	*
Pre-incub. ff20, % [a]	54.32	22.71	31.70	17.71	*

[a] Values from 2010 grain size determination on bulk soils.

5.4.2 Cumulative gas production

Under aerobic conditions all gas produced was in the form of CO_2. Cumulative CO_2 production showed neither a strictly linear nor an exponential increase over the incubation period (Figure 14). In most samples, CO_2 production rates decreased towards the end of the experiment (compare chapter 5.4.3.2). Between day 114 and 153 the incubation bottles could not be flushed with synthetic air due to an alteration in the working procedure. In about half of the cases, the aerobic production slowed down during this period, indicating that high CO_2 concentrations in the headspace led to suppression of further microbial turnover (see chapter 6.2.3.2). In all further data analysis, only the time span of 114 days for aerobic incubations and 118 days for anaerobic incubations will be considered.

Highest respiration was found in profile 5g in the unmanaged, polyhaline zone. Generally, topsoil samples had higher aerobic CO_2 production per gram dry weight than subsoil samples of the respective profiles. One exception to this pattern is the low marsh profile 3a where highest CO_2 production was observed in the subsoil. The gap between subsoil and topsoil CO_2 production even expanded when normalizing to the TOC content of the horizons (see Figure A 1). A systematic error cannot be excluded for the samples of this profile. Therefore, both samples of

profile 3a were excluded from all further statistical analyses. Based on TOC content, topsoil samples of profile 5c showed highest CO_2 production. In profiles 1c and 4c subsoil samples showed equal or higher CO_2 production than the respective topsoil samples.
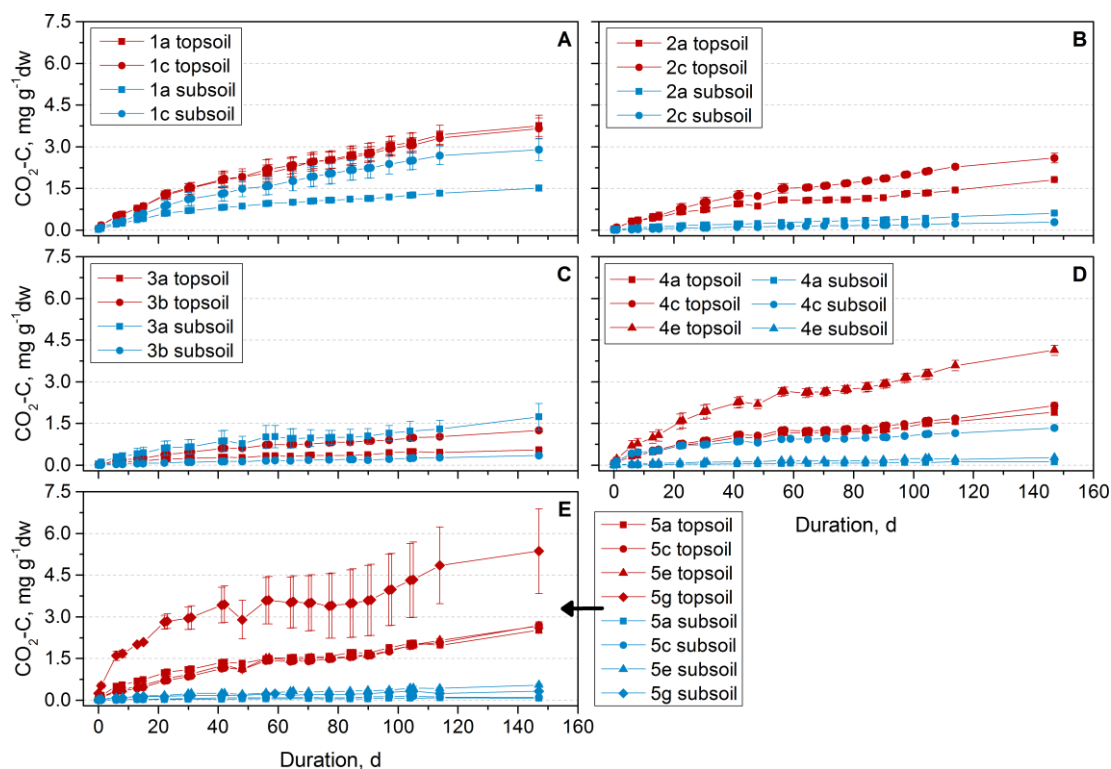
Figure 14: Cumulative CO_2 production for aerobic soil incubation over the incubation period of 147 days. Gas production is shown for the five study sites separately (A=1, B=2, C=3, D=4, E=5). Profiles are denoted by different symbols while horizons are indicated by different colors (red = topsoil, blue = subsoil). Values are given as CO_2-C per gram dry weight (mg CO_2-C g^{-1}dw) including DIC. Error bars indicate standard deviation from the mean (n = 3).

Anaerobic CO_2 production was measured in all incubated samples (Figure 15). In contrast to aerobic incubations, the anaerobic CO_2 production did not slow down towards the end of the incubation experiment. Consequently, the increase of CO_2 production showed a linear curve progression in many samples. Some samples (e.g. 1a), however, showed a second increase after approximately 50 days. Topsoil samples produced more CO_2 than subsoil samples. Highest CO_2 production was found in profiles 1a and 5g. Normalized to TOC content, highest CO_2 production was found in topsoil samples of profile 1a and subsoil samples of profile 5a (see Figure A 2). Apart from these two profiles, the differences between topsoil and subsoil samples decreased when production was calculated based on TOC content.
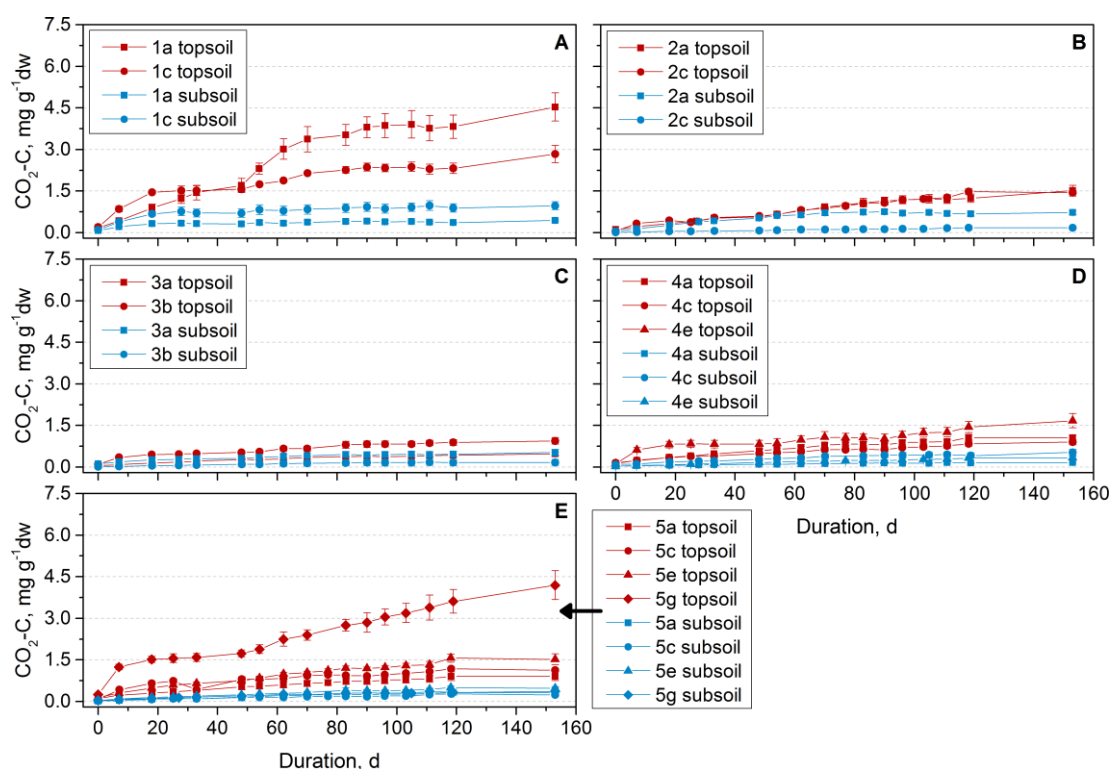
Figure 15: Cumulative CO_2 production for anaerobic soil incubation over the incubation period of 153 days. Gas production is shown for the five study sites separately (A=1, B=2, C=3, D=4, E=5). Profiles are denoted by different symbols while horizons are indicated by different colors (red = topsoil, blue = subsoil). Values are given as CO_2-C per gram dry weight (mg CO_2-C g^{-1}dw) including DIC. Error bars indicate standard deviation from the mean (n = 3).
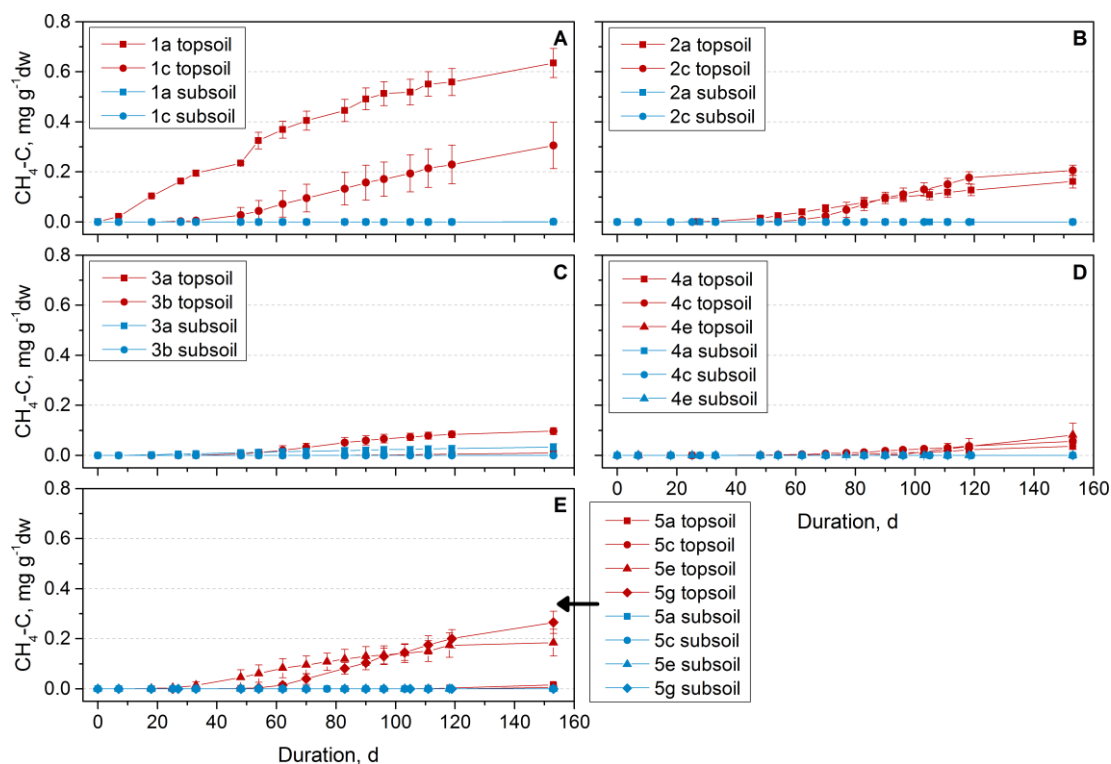
Figure 16: Cumulative CH_4 production for anaerobic soil incubation over the incubation period of 153 days. Gas production is shown for the five study sites separately (A=1, B=2, C=3, D=4, E=5). Profiles are denoted by different symbols while horizons are indicated by different colors (red = topsoil, blue = subsoil). Values are given as CH_4-C per gram dry weight (mg CH_4-C g^{-1}dw) including CH_4(aq). Error bars indicate standard deviation from the mean (n = 3).

CH_4 production was determined in samples from all study sites under anaerobic soil incubation (Figure 16, Figure A 3). Samples with active methanogenesis were predominantly topsoil samples. The onset of CH_4 production in these samples showed a considerable delay of 7 days to 153 days (mean 41 days $\pm$ 31 days). Only topsoil samples of profile 1a in the oligohaline zone showed measureable methanogenesis directly from the start of the incubation without any lag phase. In 36 samples no CH_4 production was observed over the incubation period of 153 days. These samples were almost exclusively subsoil samples. Subsequently, samples were grouped into those with and without CH_4 production. Samples without active methanogenesis had significantly lower SOC contents than samples showing methanogenesis ($p < 0.001$). A significant difference of salinity could not be found between samples with and without CH_4 production. Furthermore, no correlation between lag time and salinity was found in the data set.

As a result of the carbonate - carbonic acid - equilibrium, a considerable part of the produced CO_2 was present in dissolved form as DIC. The majority of DIC was in form of bicarbonate (HCO_3^-) which accounted for 92.4 $\pm$ 10.1 % of DIC. CH_4 solubility was very low. Only 1.5 $\pm$ 0.6 % of CH_4-C was in form of CH_4-C(aq) with a minimum of 0.5 % and a maximum of 2.9 %.

5.4.3 Carbon mineralization rates

5.4.3.1 Maximum mineralization rates

Under aerobic conditions, maximum gas production rates were observed within the first week of incubation for most samples (Table A 8). Only one subsoil sample showed highest rates after 96 days. This sample showed rather constant rates throughout the whole incubation period. Maximum rates ranged between 234.4 and 4750.6 µg CO_2-C g^{-1}TOC d^{-1}. Topsoil samples had significantly higher maximum mineralization rates than subsoil samples (2339.7 $\pm$ 1055.7 and 1209.8 $\pm$ 1200.6 µg CO_2-C g^{-1}TOC d^{-1}, respectively; $p = 0.023$).

Under anaerobic conditions, maximum CO_2 production rates were lower compared to aerobic conditions (Table A 8). Maximum rates ranged from 125.9 to 3143.4 µg CO_2-C g^{-1}TOC d^{-1}. Again topsoil samples had significantly higher rates than subsoil samples (1244.8 $\pm$ 839.7 and 743.0 $\pm$ 704.7 µg CO_2-C g^{-1}TOC d^{-1}, respectively; $p = 0.039$). Even though anaerobic CO_2 production started instantaneously, maximum rates were not always reached at the beginning of the experiment, but partly even towards the end of the incubation period.

In contrast to anaerobic CO_2 production, CH_4 production did not start instantaneously in the majority of samples, but showed a lag time between 18 and 118 days. Thus, no sample reached maximum CH_4 production rates within the first 50 days of incubation (Table A 8). Most samples showed highest rates between day 83 and 118. Maximum production rates ranged from 0.10 to 464.5 µg CH_4-C g^{-1}TOC d^{-1}. Topsoil samples had higher rates than subsoil samples, but also showed a high scatter (79.9 ± 123.6 µg CH_4-C g^{-1}TOC d^{-1}). In subsoils only two samples reached measurable rates at day 111 (compare Table A 8). In these samples rates were very low reaching a maximum of 0.10 to 0.31 µg CH_4-C g^{-1}TOC d^{-1}. Most subsoil samples did not show measurable CH_4 productions during the incubation period.

5.4.3.2   Comparison of initial and final rates

Under aerobic conditions, CO_2 production rates decreased significantly over the course of the experiment in topsoil ($p = 0.002$) as well as subsoil samples ($p = 0.028$). Within the first 30 days of incubation, aerobic CO_2 was produced at a rate of 887.8 ± 330.1 µg CO_2-C g^{-1}TOC d^{-1} in topsoil samples and 399.8 ± 272.2 µg CO_2-C g^{-1}TOC d^{-1} in subsoil samples (Figure 17 A & Table A 9). Final rates within the last 30 days accounted for 488.9 ± 225.2 µg CO_2-C g^{-1}TOC d^{-1} in topsoils and 234.6 ± 85.1 µg CO_2-C g^{-1}TOC d^{-1} in subsoils. Under anaerobic conditions, initial CO_2 production rates (Figure 17 B) were significantly lower than aerobic rates with 306.5 ± 292.5 µg CO_2-C g^{-1}TOC d^{-1} in topsoil samples ($p = 0.002$). In subsoil samples, initial rates (281.2 ± 187.7 µg CO_2-C g^{-1}TOC d^{-1}) did not differ significantly between anaerobic and aerobic conditions. Final rates accounted for 203.1 ± 139.4 µg CO_2-C g^{-1}TOC d^{-1} and 162.3 ± 279.8 µg CO_2-C g^{-1}TOC d^{-1} in topsoils and subsoils, respectively. Final rates differed significantly between aerobic and anaerobic incubations in topsoil samples ($p = 0.002$), but not in subsoil samples. In comparison with initial rates, final rates were lower in topsoil as well as subsoil samples, but this difference was not significant (Figure 17 B).

Mean initial CH_4 production rates were considerably lower than final rates (Figure 17 C & Table A 9). However, this difference was statistically not significant. In topsoils, initial rates averaged 20.3 ± 61.4 µg CH_4-C g^{-1}TOC d^{-1}, showing a high scatter due to instantaneous CH_4 production in profile 1a. Final rates accounted for 34.7 ± 19.8 µg CH_4-C g^{-1}TOC d^{-1}. In most subsoil samples, CH_4 production was below the lowest standard throughout the whole incubation period (compare chapter 5.4.2). For that reason, n was only 2 and no statistical analysis could be carried out for CH_4 rates in subsoil samples.
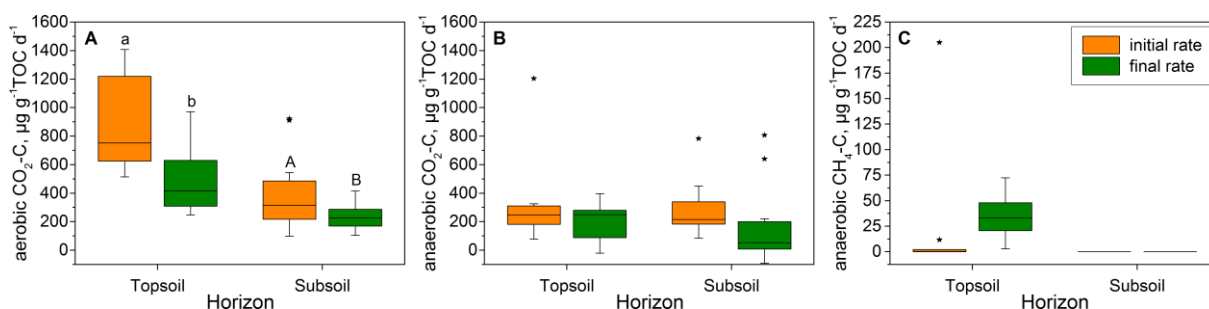
Figure 17: Initial and final CO_2 and CH_4 production rates. Aerobic CO_2 production (A) and anaerobic CO_2 (B) and CH_4 production (C) are given as CO_2-C and CH_4-C per gram organic carbon per day (µg C g^{-1}TOC d^{-1}) for the first and the last 30 days of incubation. Letters denote statistical differences between initial and final rates (Wilcoxon signed-rank test; $p < 0.05$; $n = 12$ per group). Each box represents the inter quartile range, the lines within the boxes represent the median, the whiskers represent the top and bottom 25 % of scores excluding outliers which are represented by asterisks.

5.4.4 Total carbon turnover

The amount of carbon produced within the incubation period of 114 days for aerobic incubations and 118 days for anaerobic incubations was significantly higher in topsoil samples than in subsoil samples ($p < 0.05$, respectively). The total C production accounted for 2.43 ± 1.10 mg C g^{-1}dw in topsoils and 0.62 ± 0.76 mg C g^{-1}dw in subsoils under aerobic conditions (Table A 10). This total production is equivalent to a C turnover of 6.27 ± 2.42 % and 2.84 ± 1.50 % of TOC content, respectively. Under anaerobic conditions, C production accounted for 1.84 ± 1.16 mg C g^{-1}dw in topsoils and 0.38 ± 0.22 mg C g^{-1}dw in subsoils, which is equivalent to 4.68 ± 2.97 % and 2.98 ± 2.73 % of TOC. A reduction of C turnover under anaerobic conditions of 25.3 ± 24.7 % was significant for topsoil samples ($p = 0.023$). No significant reduction in comparison with aerobic conditions was found for subsoil samples, since two profiles in the polyhaline zone showed a considerable increase of C turnover under anaerobic conditions.

C turnover was similar in the different salinity zones of the estuary as well as in the different elevation classes of the marsh, both under aerobic and anaerobic conditions (Figure 18). Only in subsoil samples, significant differences between the oligohaline and polyhaline zone occurred under anaerobic incubations ($p = 0.032$). The difference between these zones was exclusively the result of anaerobic CO_2 production, since no considerable CH_4 production appeared in subsoil samples of both zones. Due to the small number of samples within each zone, the explanatory power of this difference is questionable. However, also salinity in the groundwater correlated with the total anaerobic C turnover in subsoil samples ($r_s = 0.762$, $p = 0.004$).

Total aerobic C production per dry weight was strongly correlated with the pre-incubation TOC content ($r_s = 0.884$, $p < 0.001$) and ff20 of the samples ($r_s = 0.740$, $p < 0.001$) as well as post-incubation TN content ($r_s = 0.884$, $p < 0.001$). Correlations between aerobic C turnover and TOC content ($r_s = 0.523$, $p = 0.009$), ff20 ($r_s = 0.443$, $p = 0.030$), and TN content ($r_s = 0.515$, $p = 0.010$) were also significant, but slightly weaker (Table A 11). Aerobic C turnover correlated most strongly with initial CO_2 production rates, which for their part correlated with TOC, ff20, and TN in a similar magnitude. Total anaerobic C production was significantly correlated with TOC content ($r_s = 0.832$, $p < 0.001$), ff20 ($r_s = 0.639$, $p = 0.001$) and TN content ($r_s = 0.836$, $p < 0.001$). No significant correlations were found between anaerobic C turnover and soil characteristics. Strongest correlations were found between anaerobic C turnover and maximum CO_2 production rates.
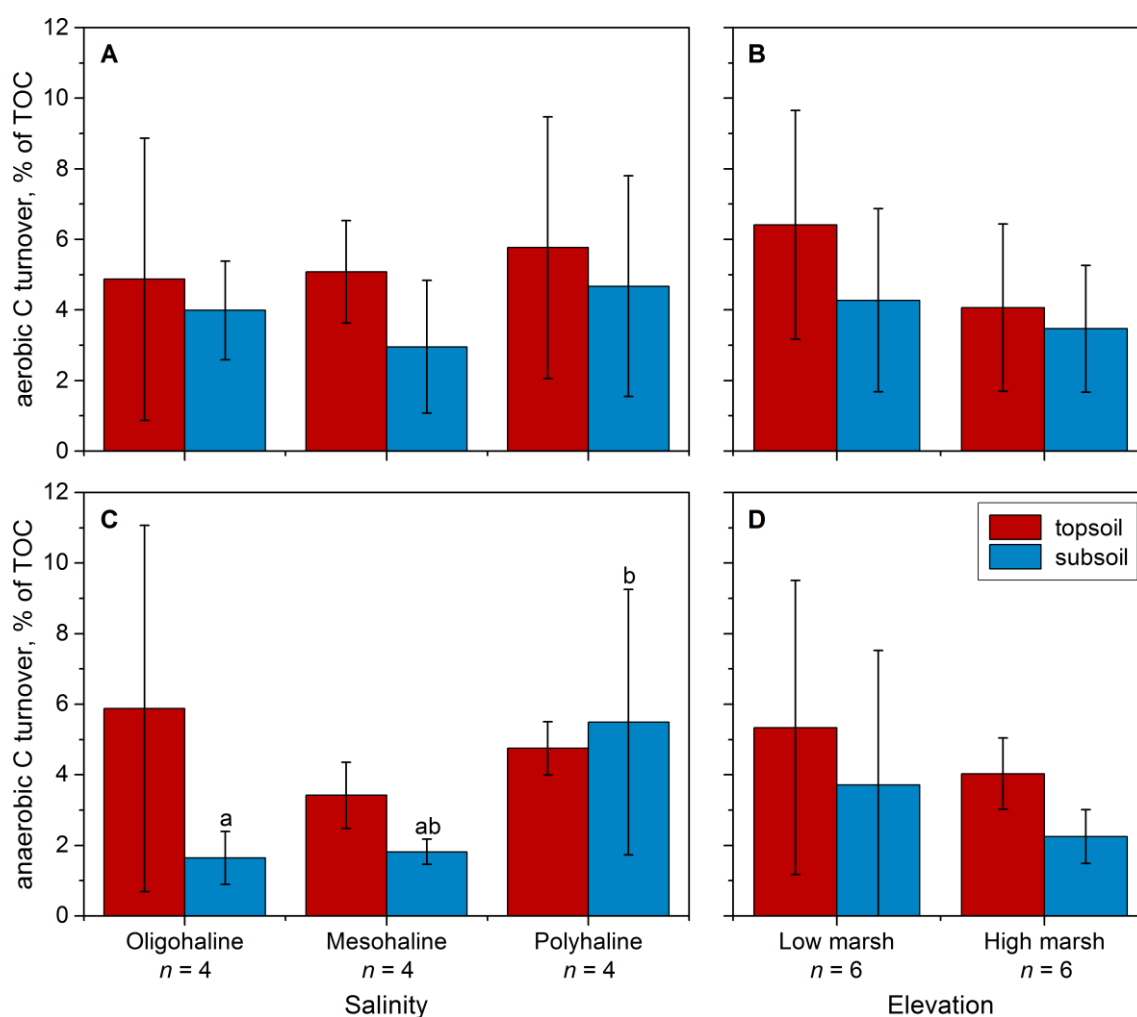
Figure 18: Total C turnover in topsoil and subsoil samples of the different salinity zones and elevation classes of the investigated tidal marshes. The total C turnover refers to the C production after 114 days for the aerobic incubations (A, B) and after 118 days for anaerobic incubations (C, D). Values (mean ± SD) are given in % C mineralization of the organic carbon content of the samples (% of TOC). Lowercase letters denote statistical differences between salinity zones (Kruskal-Wallis-Test; $p = 0.032$).

Although the absence of oxygen reduced the total C production and turnover of most topsoil samples, the GWP was significantly higher under anaerobic than aerobic conditions ($p = 0.034$). The anaerobic CO_2e production accounted for 5.55 ± 5.25 mg CO_2e-C g^{-1}dw in topsoil samples (Table A 10). In contrast, the CO_2e production of subsoil samples was similar to the anaerobic C production and accounted for 0.38 ± 0.22 mg CO_2e-C g^{-1}dw. The differences between aerobic and anaerobic CO_2e production was, therefore, not significant for subsoil samples. No significant difference of CO_2e production was detected between the salinity zones of the estuary. However, a non-significant trend towards highest GWP in topsoils of the oligohaline zone was found (oligohaline: 9.87 ± 6.61 mg g^{-1}dw; mesohaline: 2.32 ± 0.69 mg g^{-1}dw; polyhaline: 4.46 ± 4.06 mg g^{-1}dw). No such trend was visible for subsoil samples (oligohaline: 0.53 ± 0.32 mg g^{-1}dw; mesohaline: 0.26 ± 0.13 mg g^{-1}dw; polyhaline: 0.36 ± 0.10 mg g^{-1}dw). Also, no significant differences were found between low and high marshes in topsoil samples (low: 5.66 ± 7.38 mg g^{-1}dw, high: 5.43 ± 2.46 mg g^{-1}dw) as well as subsoil samples (low: 0.41 ± 0.26 mg g^{-1}dw; high: 0.36 ± 0.20 mg g^{-1}dw).

5.5 Trace metals

5.5.1 Differentiation of trace metal pools and stocks

Total trace metal pools accounted for 0.16 ± 0.11 g Cd m^{-2}, 0.14 ± 0.12 g Hg m^{-2}, 11.28 ± 5.81 g Pb m^{-2}, and 48.61 ± 25.09 g Zn m^{-2} in the upper 30 cm soil depth (Table A 12). Within 100 cm soil depth, trace metal pools accounted for 0.50 ± 0.31 g Cd m^{-2}, 0.40 ± 0.38 g Hg m^{-2}, 40.45 ± 20.01 g Pb m^{-2}, and 155.44 ± 70.94 g Zn m^{-2}. Due to missing data in the total sample, no pool could be calculated for As.

Trace metal pools did not differ significantly between sites within each zone and could, therefore, be evaluated statistically by zone. Trace metal pools decreased significantly from the oligohaline to the polyhaline zone in the topsoil (Cd, Hg, Pb, and Zn: $p < 0.05$) and the total soil depth (Cd, Pb, and Zn: $p < 0.05$, Hg: n.s.; see Figure 19 and Table A2). In contrast to trace metal concentrations in relation to elevation, trace metal pools differed between low and high marshes. Trace metal pools were significantly higher in high marshes both in topsoils and the total profile depth (Cd, Hg, Pb, and Zn: $p < 0.05$; see Figure 20 and Table A2). Furthermore, all trace metal pools correlated negatively with SIC pools and positively with SOC pools and ff20 in the respective soil depths (Table A 13).
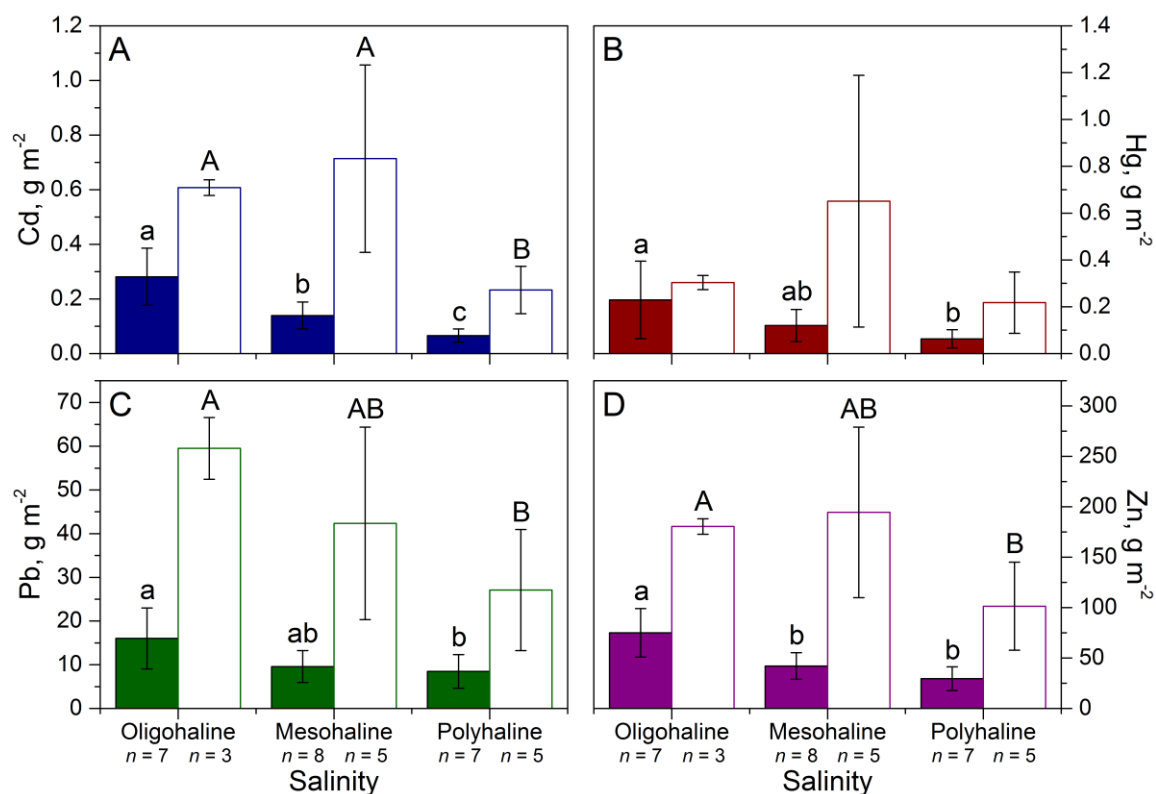
Figure 19: Trace metal pools in the different salinity zones of the Elbe estuary. Metal pools ((A) = Cd, (B) = Hg, (C) = Pb, (D) = Zn) are given in g m^{-2} for 0 – 30 cm (solid bars) and 0 – 100 cm soil depth (open bars), respectively. Letters denote statistical differences between salinity zones based on Jonckheere-Terpstra-Test (p < 0.05).
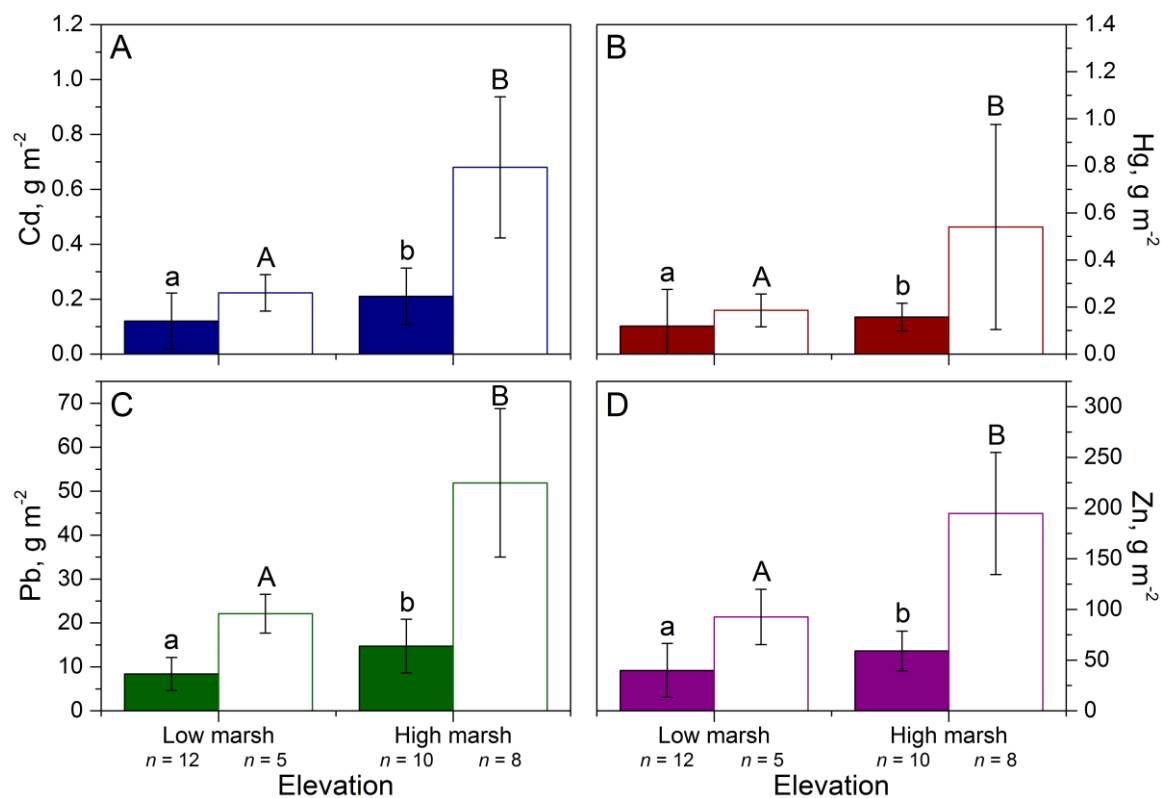
Figure 20: Trace metal pools in the different elevation classes of the Elbe estuary. Metal pools ((A) = Cd, (B) = Hg, (C) = Pb, (D) = Zn) are given in g m^{-2} for 0 – 30 cm (solid bars) and 0 – 100 cm soil depth (open bars), respectively. Lowercases letters denote statistical differences between elevation classes based on Mann-Whitney-U-Test (p < 0.05).

The trace metal stocks within 30 cm soil depth were estimated at 10.6 ± 7.27 t Cd, 9.0 ± 7.98 t Hg, 745.1 ± 383.9 t Pb, and 3210.8 ± 1657.5 t Zn in the investigated stretch of the Elbe estuary (Table 15). For all metals, the oligohaline zone differed significantly from the polyhaline zone ($p < 0.05$). Trace metal stocks of the oligohaline zone accounted for 51 to 61 % of the total metal stocks of the estuary. The mesohaline zone stored 28 to 29 % of the total trace metal stocks whereas the polyhaline zone stored only 11 to 20 %. Within 100 cm soil depth, total trace metal stocks were estimated at 33.3 ± 20.2 t Cd, 26.7 ± 25.1 t Hg, 2671.7 ± 1321.7 t Pb, and 10267.5 ± 4686.3 t Zn. Differences between salinity zones were only significant for Cd and Pb ($p < 0.05$). Differences in Hg and Zn stocks between salinity zones were not significant. The trace metal storage accounted for 12 to 17 % in the polyhaline zone, 33 to 56 % in the mesohaline zone, and another 28 to 50 % in the oligohaline zone.

Table 15: Trace metal stocks in marsh soils of the Elbe estuary. The respective stocks are given in t (mean $\pm$ SD) within 30 cm and 100 cm soil depth for each salinity zone separately and for the total investigated marsh area. The surface areas of the respective zones are presented in Table 13.

	Cd stock (0 - 30 cm), t		Cd stock (0 - 100 cm), t	
	Mean	SD	Mean	SD
Oligohaline zone	6.96	2.59	15.04	0.71
Mesohaline zone	3.19	1.13	16.31	7.84
Polyhaline zone	1.21	0.45	4.30	1.61
Total marsh area	10.64	7.27	33.32	20.20

	Hg stock (0 - 30 cm), t		Hg stock (0 - 100 cm), t	
	Mean	SD	Mean	SD
Oligohaline zone	5.67	4.09	7.50	0.75
Mesohaline zone	2.74	1.57	14.88	12.28
Polyhaline zone	1.16	0.72	4.01	2.41
Total marsh area	9.02	7.98	26.68	25.12

	Pb stock (0 - 30 cm), t		Pb stock (0 - 100 cm), t	
	Mean	SD	Mean	SD
Oligohaline zone	396.63	172.49	1472.62	174.31
Mesohaline zone	218.96	83.36	967.75	503.18
Polyhaline zone	156.37	70.90	500.30	255.71
Total marsh area	745.09	383.89	2671.66	1321.68

	Zn stock (0 - 30 cm), t		Zn stock (0 - 100 cm), t	
	Mean	SD	Mean	SD
Oligohaline zone	1856.37	593.81	4465.10	189.60
Mesohaline zone	962.86	298.97	4444.26	1932.20
Polyhaline zone	546.29	216.01	1871.64	804.56
Total marsh area	3210.82	1657.48	10267.55	4686.27

5.5.2 Estimation of contamination level

To estimate the contamination level of the investigated soils, a cluster analysis based on enrichment factors was combined with a classification of pollution and ecotoxicological levels (compare chapter 4.5.4). Since tidal marsh soils developed from fluvial and marine sediments, and are in constant exchange with the river due to regular inundation, these classification systems were chosen, to account for the potential threat coming from erosion and redistribution of these soils. For the cluster analysis, a minimum of two and a maximum of six cluster groups were chosen (Figure 21). The quality control by a Mann-Whitney-U-Test revealed an optimal partitioning of the dataset in three groups. Significant differences between all three clusters were found for Hg ($p < 0.05$). The other trace metals had significant differences between cluster 1 and 2 ($p < 0.05$) as well as 1 and 3 ($p < 0.01$). In accordance to differences in trace metal concentrations, a significant decrease of ff20 and SOC from cluster 3 to 1 was found ($p < 0.05$). A further partitioning in four to six groups resulted in decreasing significances between the respective groups that became progressively fragmented.

Cluster 1 is representative for horizons with a low pollution level (Table 16). Lowest concentrations of all trace metals were found in the subsoil horizons of profiles in study site 2 (compare Figure 21 and Table A 5). Furthermore, almost all horizons of study site 5 belong to this cluster. Mean enrichment factors vary between 1.30 and 2.52, with lowest pollution for Hg and As and highest pollution for Zn and Pb (Table A 14). A classification according to Stachel and Lüschow (1996) resulted in ARGE classes I-II (very low pollution) to II-III (considerable pollution). Furthermore, cluster 1 comprises samples with the ecotoxicological value classes C (medium value) and D (high value) according to BfG (2004).

Horizons in cluster 2 were moderately polluted with mean enrichment factors from 1.51 to 3.83 (Table 16). Lowest enrichment factors were found for As and highest for Cd and Zn. Cluster 2 is evenly spread over all study sites and soil depth except for site 5. Medium trace metal concentrations were found in this cluster. The ARGE classes II (moderate pollution) and II-III (considerable pollution) and the BfG classes C and D (medium to high value) were dominant in cluster 2.

Cluster 3 consists of samples with a comparably high pollution level (Table 16). Highest concentrations of Zn, Hg, Pb, and As were found in subsoil horizons of profile 4e which belongs to this cluster. Mean enrichment factors reached from 1.95 for As to 7.42 for Hg. Comparable to cluster 2, in cluster 3 the ARGE classes II (moderate pollution) and II-III (considerable

pollution) were prevailing. Regarding the ecotoxicological value, cluster 3 had a wide range from class D (high value) for Cd and Pb to class B (low value) for Zn and Hg.

In order to account also for risk coming from soils under agricultural use, an evaluation according to the German Ordnance on soil protection and contaminated sites (BBodSchV, 1999) was carried out. Various topsoil samples of all study sites and different textures outreached the precautionary values according to BBodSchV (1999). These samples belong to all three clusters showing no distinct accumulation in cluster 3. However, none of the investigated samples reached the so-called action values for the pathway soil - crops in meadows and pastures according to BBodSchV (1999).

Table 16: Trace metal composition in three groups based on cluster analysis. For each element in the ff20 minimum, maximum, and mean concentrations, standard deviations, mean enrichment factors (in comparison to background concentrations according to Gröngröft et al. (1998)), mean ARGE classes (according to Stachel and Lüschow (1996)), and mean ecotoxicological values (according to BfG (2004)) are given.

Cluster 1	Cd (<20µm)	Zn (<20µm)	Hg (<20µm)	Pb (<20µm)	As (<20µm)
Min, mg kg^{-1}	0.07	124.89	0.06	37.33	11.91
Max, mg kg^{-1}	0.70	361.85	0.82	92.33	45.33
Mean, mg kg^{-1}	0.38	236.56	0.40	60.82	25.97
SD, mg kg^{-1}	0.16	53.11	0.18	13.53	7.75
Enrichment factor	1.58	2.52	1.33	2.43	1.30
ARGE class	I-II	II-III	I-II	II	II-III
Ecotox value	D	C	D	D	C

Cluster 2	Cd (<20µm)	Zn (<20µm)	Hg (<20µm)	Pb (<20µm)	As (<20µm)
Min, mg kg^{-1}	0.69	283.79	0.44	57.67	14.66
Max, mg kg^{-1}	1.83	434.19	0.99	114.00	46.67
Mean, mg kg^{-1}	0.92	352.04	0.74	76.93	30.21
SD, mg kg^{-1}	0.23	43.02	0.15	13.47	7.51
Enrichment factor	3.83	3.75	2.48	3.08	1.51
ARGE class	II	II-III	II	II	II-III
Ecotox value	D	C	D	D	C

Cluster 3	Cd (<20µm)	Zn (<20µm)	Hg (<20µm)	Pb (<20µm)	As (<20µm)
Min, mg kg^{-1}	0.65	390.19	1.73	67.17	22.45
Max, mg kg^{-1}	1.79	638.52	2.67	148.00	71.67
Mean, mg kg^{-1}	1.20	498.03	2.23	99.93	39.06
SD, mg kg^{-1}	0.40	86.08	0.30	25.15	13.87
Enrichment factor	5.02	5.30	7.42	4.00	1.95
ARGE class	II	II-III	II-III	II	II-III
Ecotox value	D	B	B	D	C
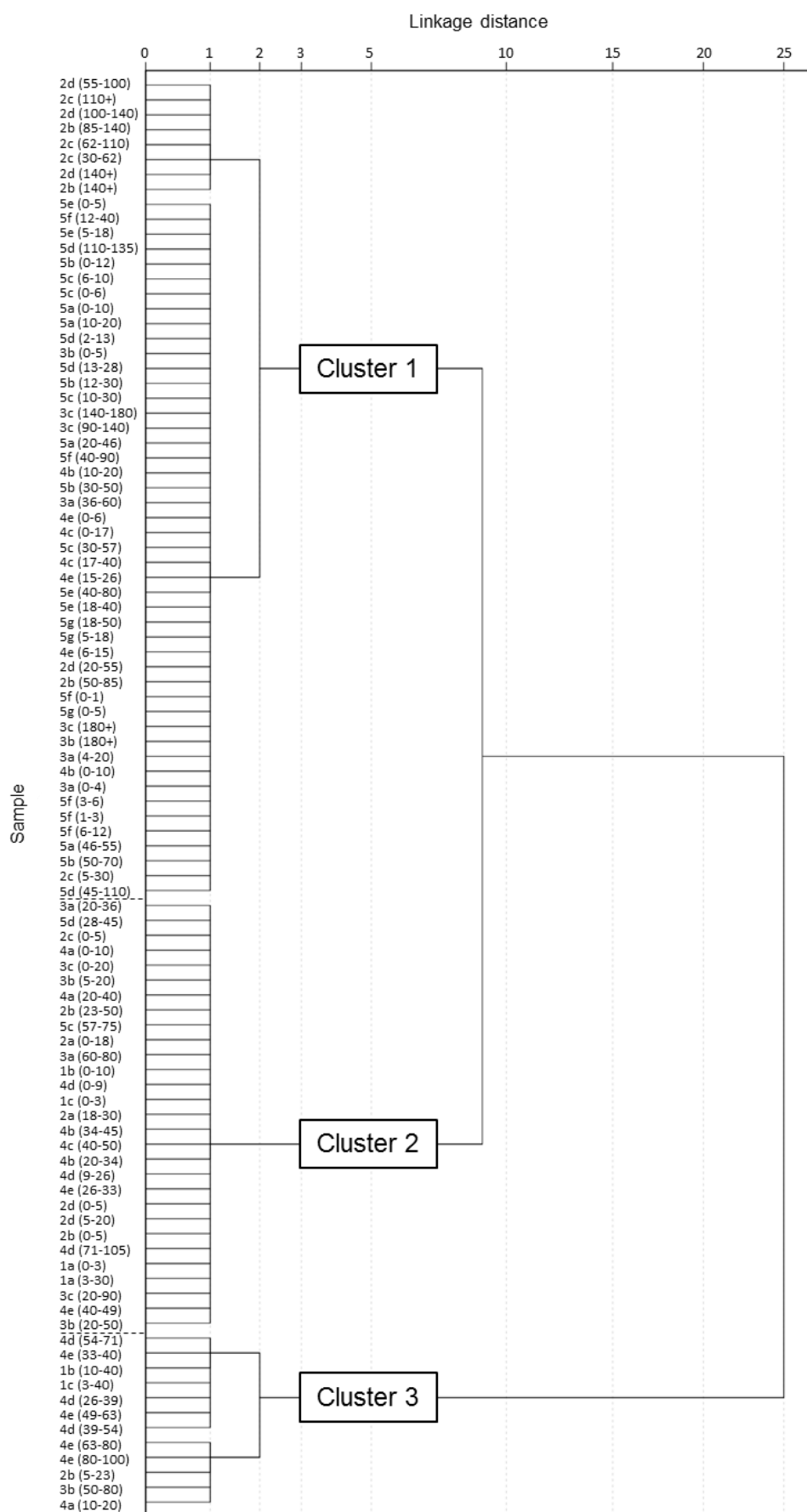
Figure 21: Dendrogram of cluster analysis for all soil horizons based on enrichment factors. Cluster 1 represents a low pollution level, cluster 2 represents moderate pollution, and cluster 3 represents considerable pollution. The cluster analysis was carried out using Ward's method with squared Euclidean distance. Note non-linear scaling of the x-axis.

5.5.3 Trace metals in suspended sediments

Trace metal concentrations of suspended sediments at the automated sampling stations Grauerort in the oligohaline zone and Cuxhaven in the polyhaline zone were compared to account for spatiotemporal alterations in trace metal input to the tidal marshes. Trace metal concentrations in the ff20 of the suspended sediments varied strongly with river discharge and, accordingly, with season (Figure A 4 & Table A 15). These fluctuations were more pronounced at the sampling station Grauerort in the oligohaline zone than at Cuxhaven in the polyhaline zone, with strongest correlations for Zn and Cd (r_s = 0.624 and 0.547, respectively, p < 0.001, n = 264). For further data analysis, mean metal concentrations over the winter season were used (Figure 22). However, even the seasonal concentrations showed inter-annual variations that impeded clear interpretation of trends in the chronological development of the investigated metals. Hg concentrations showed the strongest decrease over time while Pb appeared to increase slightly. Zn and Cd concentrations were highest in the first measurement years (1988-89) and fluctuated continuously afterwards. The trace metal As showed a striking increase in the year 1993 which is probably due to a change in the extraction technique (Gröngröft, pers. comm.) and not to actual changes in the As concentrations in the suspended sediments (Figure A 4). Due to the inexplicable As distribution, it is not considered in further data analyses.
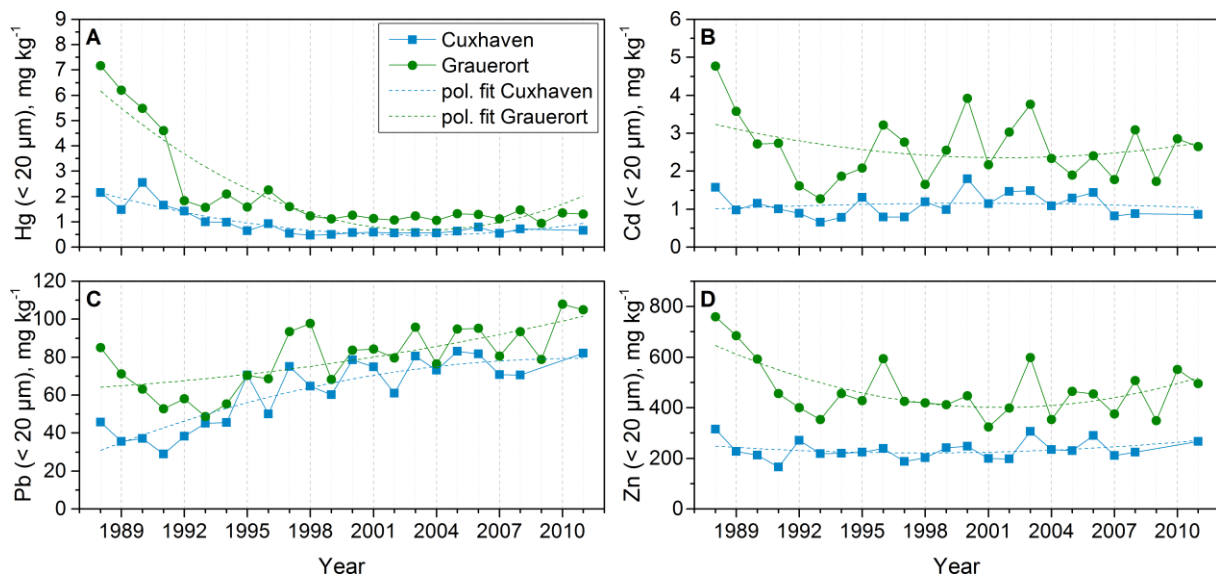
Figure 22: Temporal alterations in mean winter trace metal concentrations in the ff20 of suspended sediments between 1988 and 2011. Metal concentrations in mg kg-1 are indicated by green lines for the automated sampling station Grauerort and blue lines for Cuxhaven. Dashed lines represent the polynomial fit of the development of concentrations at the respective stations. Data were kindly provided by FGG Elbe (2014).

Since some trace metals fluctuated around an intermediate value (Cd & Zn), while others decreased (Hg) or increased (Pb) in the considered period of time, the temporal alterations of the respective trace metal ratios were also evaluated. The ratios of the investigated trace metals fluctuated strongly (Figure 23). The trend curve of the two sampling stations (polynomial fit of metal ratios over time) shows an increase for Zn/Hg, Pb/Hg, and Pb/Cd, and a decrease for Zn/Pb and Hg/Cd. The Zn/Cd ratio stayed at approximately the same level over the measuring period. The respective ratios of Zn/Hg and Hg/Cd were similar for the stations Grauerort and Cuxhaven at the two extremities of the brackish zone, indicating that these ratios are valid for all study sites along the estuary. Therefore, these ratios seemed convenient for the use as time markers.
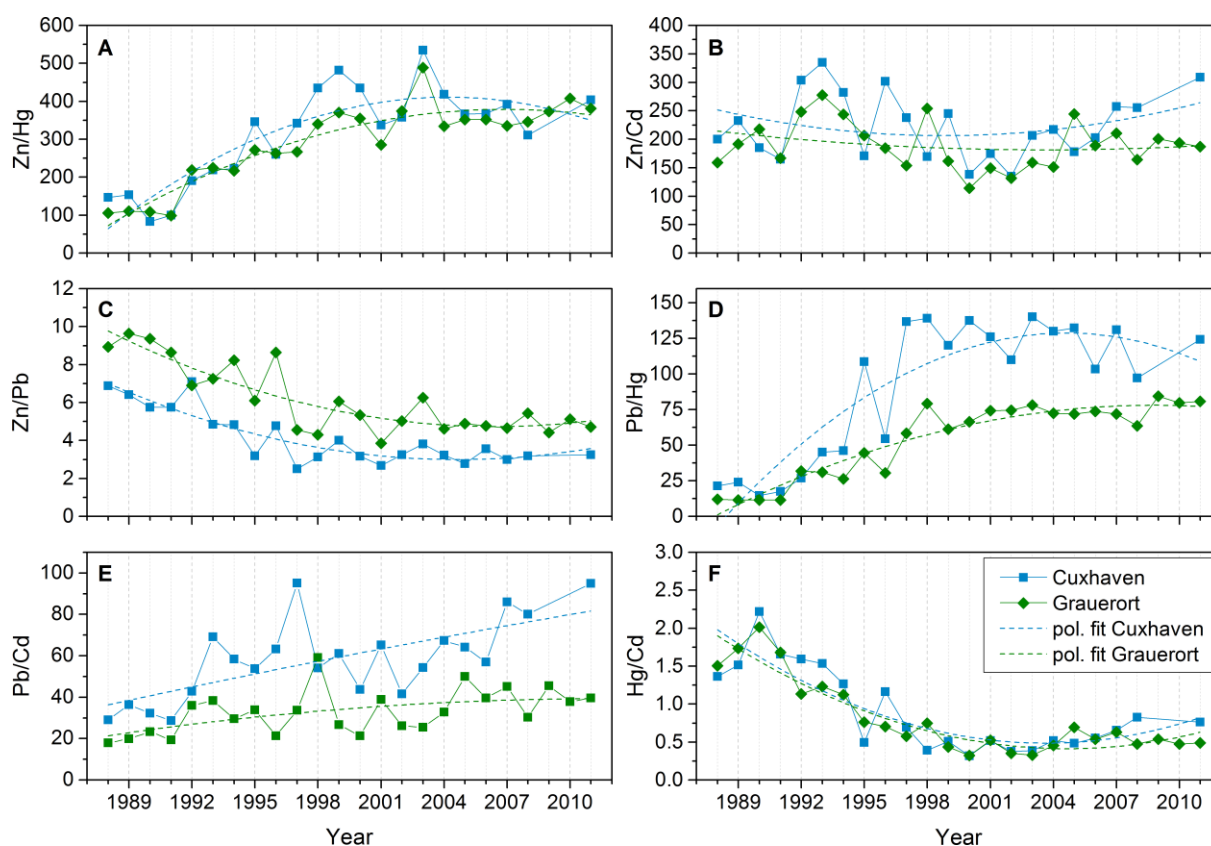
Figure 23: Temporal alterations in mean winter trace metal ratios in the ff20 of suspended sediments between 1988 and 2011. Metal ratios are indicated by green lines for the automated sampling station Grauerort and blue lines for Cuxhaven. Dashed lines represent the polynomial fit of the development of ratios at the respective stations. Data were kindly provided by FGG Elbe (2014).

5.5.4   Comparison between suspended sediments and soils

To evaluate the period in which different soil horizons were deposited, the chronological development of trace metal concentrations in suspended sediments, background values for the area, and vertical metal distributions in soils showing distinct metal peaks were compared. In profile 4e, a distinct increase in trace metal concentrations with soil depth was visible (Figure 24). Highest concentrations of all investigated metals were found in subsoil horizons below 63 cm depth. Lowest concentrations were usually found in the two topsoil horizons (0 – 15 cm) of this profile. For As and Cd these low concentrations in the most recent horizons were close to geogenic background levels calculated by Gröngröft et al. (1998). The vertical distribution of trace metals in profile 2b and 2c differed from the pattern in profile 4e. Highest concentrations were found in the upper part of the profiles (0 – 30 cm). Profile 2b had a distinct metal peak in the Go-Ah horizon from 5 to 23 cm soil depth, especially for Hg, Cd, and Zn. The adjacent profile 2c had lower concentrations of most trace metals than 2b and showed a more uniform decrease of concentrations with depth. Metal concentrations decreased strongly with increasing soil depth and partly fell below background concentrations (Cd, Hg) in the deepest horizons of both profiles. Profile 3b showed an intermediate pattern with increasing metal concentrations between 0 and 80 cm and decreasing concentrations in the lower part of the profile. This decrease is not very pronounced for Pb and As. In all profiles, Pb and As distributions did not show such distinct peaks as Hg, Cd, and Zn, but a rather "smoothed" vertical distribution. Not one of the investigated profiles reached values as high as maximum Hg, Cd, or Zn concentrations in the suspended sediments at the sampling station Grauerort of the year 1988 (Figure 22). Concentrations of all metals at the sampling station Cuxhaven were comparable to the measured concentrations in the soil profiles, but could not be assigned to a specific year within the time span of 1988 to 2010. Furthermore, no horizon reached the geogenic background values of Pb and Zn.
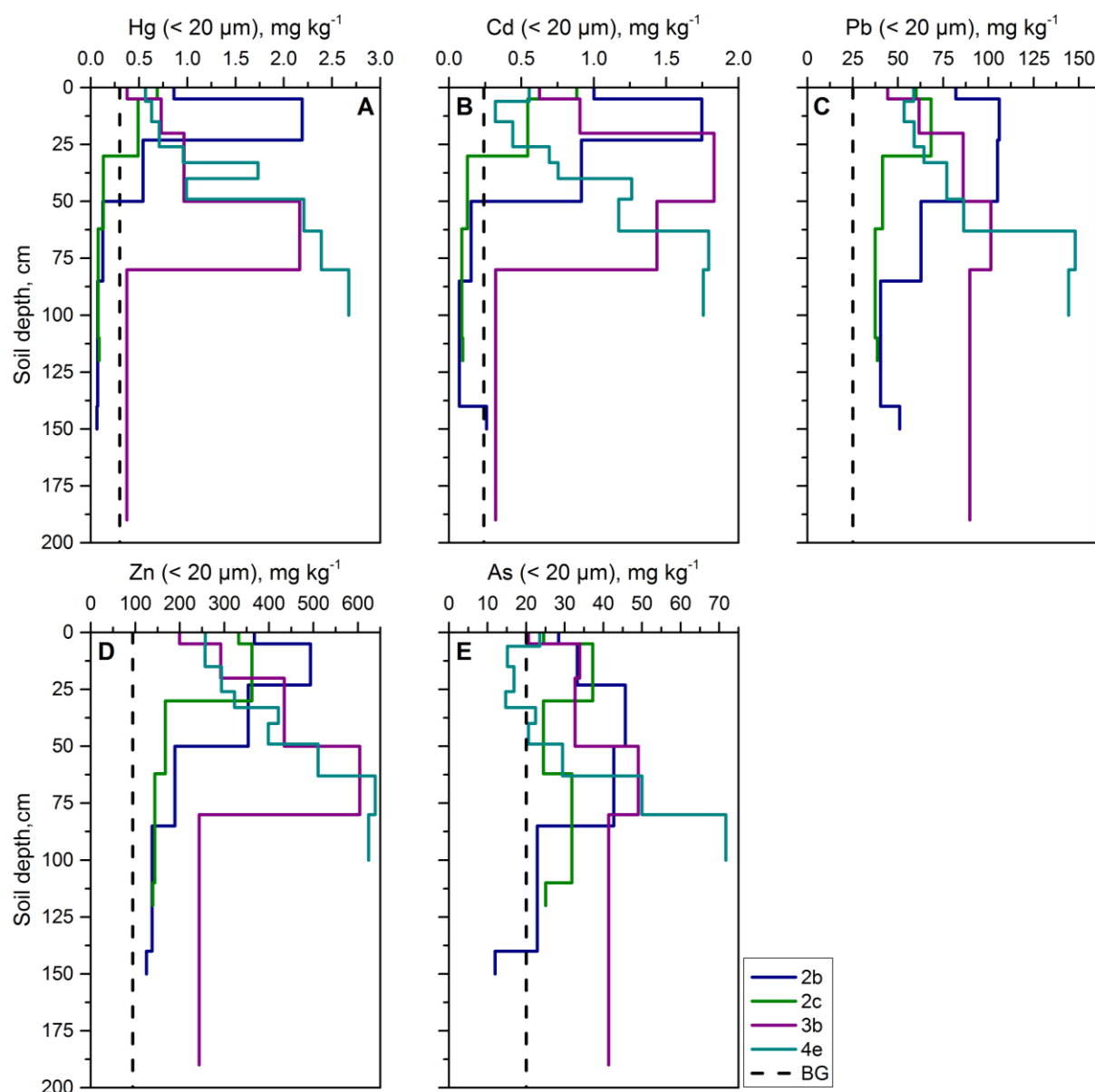
Figure 24: Vertical distribution of the trace metal concentrations. Concentrations of the investigated metals in the ff20 in four selected profiles are given in mg kg⁻¹. Dashed lines indicate the background values of Cd, Hg, As, and Zn according to Gröngröft et al. (1998) and of Pb according to Stachel and Lüschow (1996) in the study region.

Additionally, specific threshold values of the Zn/Hg and Hg/Cd ratios in suspended sediments were assigned to specific years when these thresholds were reached (Figure 23 & Figure 25). The Zn/Hg ratio increased to 100 in 1988 and reached 230 around 1992/93 (slight delay between Cuxhaven and Grauerort). The Hg/Cd ratio decreased below 1 in 1994 and below 0.6 around 1998/99. As all ratios tend to level off after 1999, the time period between 1999 and 2011 could not be distinguished further. Furthermore, no comparable data were available from suspended sediments older than 1988.

The Zn/Hg ratios fluctuated around an intermediate level in the profiles 3b and 4e (Figure 25 A). This intermediate level was equivalent to the geogenic background in sediments of the Elbe estuary. The profiles 2b and 2c showed increasing Zn/Hg ratios with increasing soil depth. None of the investigated profiles met the 1988 time marker. Only two profiles reached the 1992/93 time marker (2b: 5 - 23 cm, 4e: > 50 cm). The Hg/Cd rations of all profiles showed a fluctuation around an intermediate value, which was the background ratio in profile 4e and the 1994 time marker in the profiles 2b, 2c, and 3b (Figure 25 B). The 1998/99 time marker was outreached in the upper part of profile 3b (< 50 cm) and by two horizons in profile 2b (23 - 50 cm and > 140 cm). The metal ratios of background concentrations (BG) and the different time markers were close to each other and not necessarily in a chronological sequence (e.g. Zn/Hg: 1988 < 1992/93 < BG).
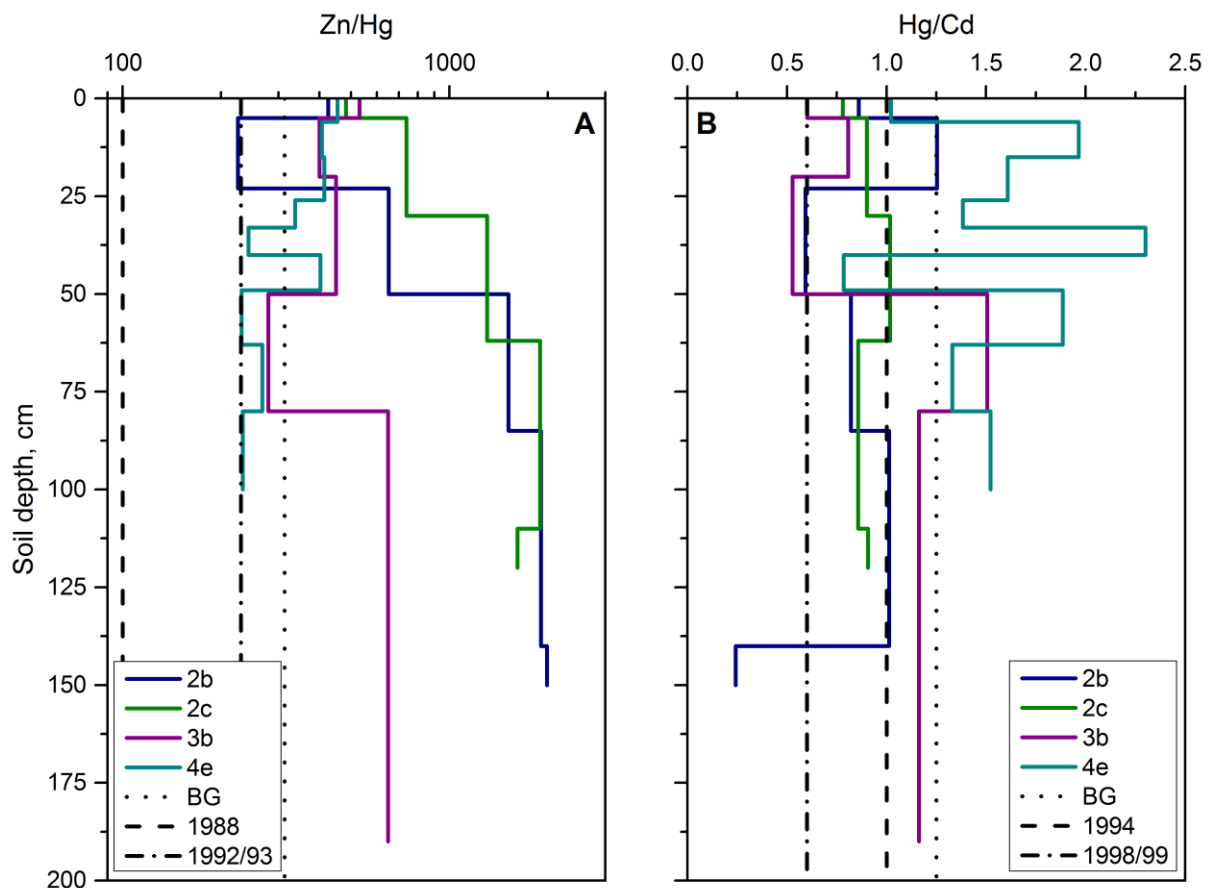
Figure 25: Vertical distribution of trace metal ratios. Zn/Hg (A) and Hg/Cd ratios (B) in the ff20 are indicated for four selected soil profiles (2b, 2c, 3b, and 4e). Dashed lines represent time markers derived from the chronological development of metal ratios in the ff20 of suspended sediments at the automated sampling stations Grauerort and Cuxhaven and the ratios of background concentrations according to Gröngröft et al. (1998).

In contrast to the aforementioned ratios, the Zn/Cd ratios were not shifting over time, but stayed rather constant. At both samplings stations, Zn/Cd ratios fluctuated around an intermediate value. Hence, deviations of Zn/Cd ratios in soils from those in suspended sediments could not be attributed to the anthropogenic input, but could be an indicator of mobilization of the different metal species. Strong deviations of Zn/Cd were found in all selected profiles (Figure 26). Only few horizons (2b: 5 - 23 cm, 3b: 0 – 50 cm, 4e: 40 - 49 cm) had Zn/Cd ratios between minimum and maximum ratios in suspended sediments. Profile 4e had decreasing Zn/Cd ratios with increasing soil depth, whereas all other profile had increasing ratios.
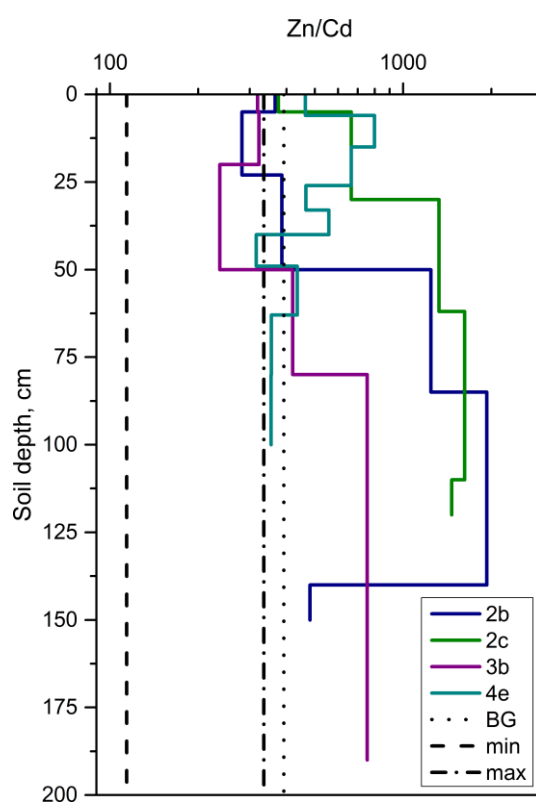
Figure 26: Vertical distribution of Zn/Cd ratios. The Zn/Cd ratios in the ff20 are indicated for four selected soil profiles (2b, 2c, 3b, and 4e). Dashed lines represent minimum and maximum Zn/Cd ratios in the ff20 of suspended sediments at the automated sampling stations Grauerort and Cuxhaven and the ratios of background concentrations according to Gröngröft et al. (1998).

6 Discussion

6.1 Organic carbon in tidal marsh soils and suspended sediments

6.1.1 Impact of allochthonous and autochthonous OC deposition

In this study, a new method to quantify the proportions of allochthonous and autochthonous OC in different soil depths of tidal marshes, based on a comparison between initial and recent OC pools, has been introduced. $\delta^{13}C$ values of soils, vegetation, and fresh sediments were used to validate this new approach. The investigated sediment samples had $\delta^{13}C$ values of -26.1 ± 0.9 ‰ which are typical for sediments of the Elbe estuary (Schoer, 1990). Horizons showing OC accumulation had lower $\delta^{13}C$ values of -28.1 ± 0.9 ‰ which were comparable to those of biomass samples of the local vegetation. These values were in the range of most terrestrial C3 plants (Hedges et al., 1997). Horizons showing mineralization and those showing preservation of allochthonous OC had higher $\delta^{13}C$ values of -26.1 ± 0.8 ‰ and -25.1 ± 1.5 ‰, respectively, which were comparable to the sediments. These groups of horizons could not be distinguished by carbon isotope ratios, as they showed a high standard deviation (Figure 13). Potential additional OC sources with higher $\delta^{13}C$ values, like C4 plants or marine plankton, make an interpretation of carbon isotope ratios in terms of decomposition processes difficult.

The vertical distribution of TOC differed between low and high marsh soils of the Elbe estuary. In low marshes, the TOC distribution seems to be predominantly controlled by the allochthonous OC input, caused by high sedimentation rates (Butzeck et al., 2015). This OC source is indicated by the TOC distribution in the recent soils which followed the calculated initial TOC distribution (Figure 12). Also, the correlation of TOC and ff20 was strongest in these young Fluvisols (Figure 8 B) and $\delta^{13}C$ values were highest, both indicating a mainly allochthonous OC source. The high importance of allochthonous organic matter in low marshes is in accordance with several other authors (e.g. Ember et al., 1987; Middelburg et al., 1997; Spohn et al., 2013), who found higher $\delta^{13}C$ in low marshes near creeks compared to back marshes and interpreted this distribution as an indicator for a higher allochthonous OC input by inundation.

Along the course of the Elbe estuary a shift in the TOC to ff20 ratio was apparent (Figure 7). This decrease of TOC might be a result of the quick mineralization of particulate organic carbon (POC) in the oligohaline zone of the estuary (see Amann et al., 2012). Additionally, increasing quantities of marine sediments, which contain only low amounts of OC (Salomons and Mook, 1981), might dilute the TOC concentrations in the sediments at higher salinities. Especially in the

low marshes a decrease of TOC content in the suspended sediments could lead to a decrease of SOC.

Additional OC accumulation was determined over the whole depths in low marsh profiles of the oligo- and mesohaline zone (Table 12). As highest above-ground biomass was found in the low marshes of the oligohaline zone (Figure 10), the autochthonous OC deposition seems to have a stronger influence on the OC distribution of these marshes compared to the low, polyhaline marshes (Figure 12). This accumulation was most likely due to a combination of continuous allochthonous OC input from sedimentation during inundation, autochthonous OC input from the local vegetation, and steady carbon burial by sediment deposition which decreases mineralization (e.g. Elsey-Quirk et al., 2011; Lal, 2003).

For high marshes, which are inundated only occasionally the TOC content seems to be less influenced by allochthonous OC input. For most high marsh soil profiles, a topsoil enrichment of OC, compared to the calculated level during sedimentation, was found (Table 12 & Figure 12). Furthermore, topsoil $\delta^{13}C$ values were comparable with those of the local vegetation. Even though high marshes have significantly lower above-ground biomass than low marshes (Figure 10 B), the longer time for autochthonous OC accumulation during soil development could yield these higher OC values. This conclusion is in accordance with Spohn and Giani (2012) who used monosaccharides as biomarkers in marsh soils of the German North Sea coast. Higher OC stocks and lower hexose to pentose ratios with increasing elevation were associated with organic matter that was mostly from plant-origin of the local vegetation.

6.1.2 Factors influencing SOC pools of tidal marshes

6.1.2.1 Biomass production and litter redistribution

SOC of tidal marshes considerably decreased with increasing salinity (Figure 11 A). The results from the minerogenic marshes of the Elbe estuary correspond with findings from several other authors for organogenic marshes (Craft, 2007; Loomis and Craft, 2010; Więski et al., 2010). One reason for less SOC contents in salt marshes is a lower concentration of OC in the fresh sediments, as discussed above. Additionally, a decrease of plant biomass with increasing salinity (see Figure 10 A) probably results in less litter input and, therefore, less SOC accumulation. The study sites in the oligo- and mesohaline zone are mainly covered by *Phragmites australis*. This species has been described to have approximately three times greater above-ground biomass production than salt marsh species (Windham, 2001). Więski et al. (2010) found significantly

higher SOC and standing crop biomass in fresh and brackish marshes compared to salt marshes and associated the latter with salinity stress.

In the investigated marsh soils, significantly higher TOC concentrations and $SOCP_{30}$ in the high marsh compared to the low marsh zone were found (Figure 11 B). These results are confirmed by findings from several other marshes where SOC concentrations and densities increased with elevation due to soil development under less frequent tidal flooding and suspended sediment supply (Chmura et al., 2003; Spohn et al., 2013). A stimulation of biomass production by moving water, input of nutrients, and export of toxins has been reported for tidal marshes (see compilation of Mitsch and Gosselink, 1993) and could be a possible explanation for higher summer biomass in low marshes of the Elbe estuary (Figure 10 B). However, the difference in summer biomass between low and high marshes seems not to have a positive influence on the SOC pools of the sites.

Although tidal inundation is considered to be important for OC deposition, it can also lead to a depletion of the SOC pools in the regularly flooded low marshes, where litter is swept away by the tides (Bouchard and Lefeuvre, 2000). Missing litter layers in most of the low marshes along the Elbe estuary support this conclusion. The abundant litter layers in most high marshes provide organic matter input to the soils and may additionally protect them from erosion. Equal amounts of above-ground biomass in low and in high marshes in winter (Figure 10 B) may, therefore, indicate an export of litter to the river or a redistribution of litter within the marshes from the low to the high marsh zone. This translocation of litter may have a stronger influence on the SOC pools of tidal marshes than the maximum biomass production in summer.

6.1.2.2   Decomposition

Comparable to the results of the recent study, a negative correlation of SOC and salinity was also reported for tidal marshes in North America (Craft, 2007). However, Craft (2007) did not identify a relation of SOC and plant biomass, but a negative correlation between SOC and decomposition rate to be the major driving factor. Higher decomposition rates in salt marshes might be caused by higher bioturbation or by the availability of sulfate for anaerobic decomposition (compare chapter 6.2.1 and (Craft, 2007; Sutton-Grier et al., 2011)). In the marsh soils of the Elbe estuary, the grain size distribution could be an additional factor influencing SOC decomposition along the salinity gradient. Positive correlations between SOC and ff20 (Figure 8) and low SOC pools in study site 5 (Table 12), which had also a low ff20 contents (Table 8), indicate a relation between

SOC decomposition and grain size in the study sites. Aggregation of OC with fine grained particles and the formation of organo-mineral complexes are important processes, leading to SOM stabilization against decomposition (Chenu and Plante, 2006; Kögel-Knabner et al., 2008; Von Lützow et al., 2008). Therefore, higher amounts of physically protected OC can be found in fine textured soils (e.g. Hassink, 1997; Six et al., 2002).

The influence of elevation on SOC pools by autochthonous OC accumulation was only significant in $0 - 30$ cm soil depth, as mineralization seems to be an important process in the subsoils of most high marsh profiles. The mineralization of OC was indicated by negative ΔOCP values beneath 30 cm soil depth (Table 12). Significant differences in ΔOCP_{30-100} occurred between low and high marshes. Compared to the low marsh profiles, the high marshes had lower ground water table depths and deep oxidized horizons, in which mineralization processes can take place more quickly than in anoxic soil horizons (Hemminga and Buth, 1991). However, the interpretation of ΔOCP_{30-100} of the highest marsh profiles (e.g. 2b, 2c, 3b) is difficult, as these plots are assumed to have the longest soil development. As the sediment samples used for the calculation of SedOCP were collected in the 1990s, large differences between initial and recent SOCP in the subsoils could result from a different OC to ff20 ratio at the time of deposition and, therefore, a false estimation of the initial OC pool.

6.1.3 SOC storage in tidal marshes

The low SOC storage of the Elbe estuary (Table 13) is mainly due to the small area covered by the investigated tidal marshes. A SOC stock of 1.13 Tg may appear negligible on a global scale (430 Tg in 50 cm soil depth globally according to Chmura et al. (2003)), but these marsh soils are of particular importance on the regional scale of Northern Germany and these systems do constantly accumulate further SOC, as sedimentation of fresh sediments is larger than erosion along the shore lines.

The oligohaline zone contributed most (ca. 55 %) to the SOC storage of the study area, although the extent of this zone was similar to the mesohaline zone. This inequality between the two salinity zones emphasizes the importance of the oligohaline zone for the carbon budget of the Elbe estuary. The contribution of the polyhaline zone was smallest, even though its area was only slightly smaller compared to the oligo- and mesohaline zone (Table 13). The predicted sea level rise (e.g. IPCC, 2013) could lead to an upstream shift of salinity zones in estuaries (e.g. Grabemann et al., 2005) and a transition of tidal freshwater marshes to brackish and saline

marshes (Reed, 2002). Since the Elbe estuary is bounded by an upstream weir, a spread of the polyhaline zone could result in a reduction of the other zones and a decrease of the total carbon storage of the estuary.

In this study SOC pools and storage were calculated for 1 m soil depth, however, soils of the estuarine ecosystems are much deeper. Holocene tidal sediments have been found as deep as 11 m to 24 m below ground surface in the marsh area of the Elbe estuary (Sindowski, 1979; Streif, 2004). Even if a part of the initial SOC has been mineralized over the last millennia, a considerable part of the SOC could be preserved in the deep, water-saturated soil layers. Hence, C burial by mineral sediments can be considered as a significant process for C accumulation in the marshes of the Elbe estuary.

6.2   Organic carbon turnover in tidal marsh soils

6.2.1   Potential decomposability of soil carbon

In addition to the characterization of SOC pools, another central aim of this study was to characterize the degradability of SOM in the study sites. The conducted incubation experiment shall give further information on the potential turnover of the marsh soils, to improve the understanding of their capacity to act as a source or sink for carbon in the face of climate change and anthropogenic interference.

Direct comparison of the measured mineralization rates with other incubation studies of tidal marsh soils is difficult, because soils of the study sites differ considerably in their SOC contents and experimental designs differ with regard to sampling techniques, treatments, incubation temperature and time (e.g. Chambers et al., 2013; Neubauer et al., 2013; Sutton-Grier et al., 2011; Weston et al., 2011). However, mineralization rates of marsh soils of the Elbe estuary were in a similar range with the few studies stating comparable measurement unites (Neubauer et al., 2013; Sutton-Grier et al., 2011).

6.2.1.1   Influence of oxygen availability

The availability of oxygen influences the potential decomposability of the investigated samples. Under aerobic conditions organic substances are completely oxidized to CO_2. A significantly higher total C turnover was determined in aerobic than in anaerobic incubations for topsoil

samples. In subsoil samples which have lower production rates, this difference was not significant (Figure 18). However, higher aerobic turnover is a well-known phenomenon which is commonly explained by a higher energy yield when oxygen is the TEA (Megonigal et al., 2004). Anaerobic decomposition is generally slower than aerobic respiration (Kristensen and Holmer, 2001), resulting in significantly lower topsoil mineralization rates (Figure 17). Given that low marshes are predominantly anaerobic throughout most of the year, which is indicated by high inundation frequencies and durations (Table A 17) as well as visible reductive features in shallow soil depths, they may mineralize less organic matter than high marshes. In comparison, high marshes can have deep oxidized horizons even in winter, which might lead to higher in-situ mineralization. Although, the potential decomposability of the investigated samples did not show significant differences between low and high marsh soils (Figure 18 B & D), the stronger anaerobic conditions in the low marshes might cause a difference in greenhouse gas emissions.

During the course of the experiment, anaerobic CO_2 production was neither strictly linear nor exponential (Figure 15). High rates at the beginning of the experiment might be a consequence of alternative pathways of microbial respiration than methanogenesis. Using other TEAs like NO_3^-, Mn^{4+}, Fe^{3+}, or SO_4^{2-} is thermodynamically more favorable and generates a higher energy yield (Megonigal et al., 2004). Denitrification could be an important process, especially in marsh soils of the oligohaline zone where the nitrogen content is comparatively high (Table A 3). Sulfate reduction could be more abundant in the polyhaline zone where sea water is constantly supplying the marshes with a mixture of salts including sulfate (Poffenbarger et al., 2011; Weston et al., 2014).

Other indicators for the dominance of non-methanogenic metabolic pathways under anaerobic conditions are the lag time of methanogenesis and the ratio between CO_2 and CH_4 production. Methanogenesis commonly yields 1 mol CH_4 and 1 mol CO_2 when acetate is used as a substrate, which is the most important methanogenic pathway in tidal marshes (Weston et al., 2014; Weston et al., 2011). In the incubated samples showing active methanogenesis, CH_4-C production reached a maximum of 13 % of total anaerobic C production. Thus, anaerobic C mineralization cannot be explained by methanogenesis alone. A considerable amount of the measured anaerobic C production has to be the result of other respiration pathways.

The lag time of CH_4 production could additionally be favored by insufficient anaerobic conditions at the beginning of the experiment. Methanogenesis is the last reaction that occurs after oxygen is depleted, typically starting at redox potentials lower than -250 mv (Mitsch and Gosselink, 1993). At higher redox potentials the abovementioned alternative TEAs are used for

decomposition of SOM. Usually, active methanogenesis takes place not before those TEAs are depleted, which seems to be the case after approximately 50 days in the incubated samples. Due to the changing water table in the field, most profiles will not establish redox potential low enough for methanogenesis within the investigated soil depth. Only some low marsh profiles might be able to actively produce CH_4. Above all, site 1 featuring low marshes with high inundation frequencies and long inundation periods (Table A 17), might have the potential to emit considerable amounts of CH_4. When regarding the CO_2e, the difference between aerobic and anaerobic incubations diminished and site 1 had even up to 5-fold higher GWP under anaerobic conditions, implying a higher potential of this site to contribute to climate change as a response to increasing inundation. However, further supply with alternative TEAs by inundation might reduce or even suppress CH_4 emissions of the soils (Giani and Gebhardt, 1984; Pfeiffer, 1994; Poffenbarger et al., 2011), even though coexistence of different metabolic pathways, because of a surplus of available organic substrates or spatial variation in the abundance of TEAs, is possible (Giani et al., 1996; Holmer and Kristensen, 1994; King and Wiebe, 1980; Megonigal et al., 2004; Weston et al., 2011).

CH_4 produced in subsoil horizons might, nevertheless, be of minor importance in most investigated marshes, as these horizons are covered by oxidized topsoil horizons. While passing through the overlying soil, CH_4 can be oxidized to a great extent by methanotrophs (75 % according to Pfeiffer (1994), 60 – 90 % according to Le Mer and Roger (2001)). Pfeiffer (1994) found a CH_4 production of 40 mg m^{-2} d^{-1} and emissions of 12 mg m^{-2} d^{-1} in the reed zone of study site 2, whereas only 0.49 mg m^{-2} d^{-1} was produced and 0.07 mg m^{-2} d^{-1} was emitted in the higher elevated pasture of the same study site. The lower production and high oxidation of CH_4 in high marshes of the Elbe estuary suggests that the actual CH_4 emissions of these sites will be comparably small. Again, an exception could be the low marshes in study site 1, where reduction features are almost reaching the soil surface. In the uppermost few centimeters that are oxic, only minor amounts of CH_4 can be oxidized and emissions might, therefore, be higher.

6.2.1.2   Influence of C quantity and quality

The results of the incubation experiment showed significantly higher total C production in topsoils compared to subsoils, both under aerobic and anaerobic conditions (Figure 18). Furthermore, CH_4 production appeared almost exclusively in topsoil samples (Figure 16). However, not soil depth itself seems to be the factor mainly influencing C decomposition, but the availability of organic substances. Topsoil and subsoil samples differed strongly in their C

content, with significantly higher SOC contents in topsoils. This relation is further supported by a strong correlation between total C production and SOC content. SOC content and, consequently, the quantity of electron donors have been shown to affect microbial activity, supporting higher mineralization rates (Giani et al., 1996; Groffman et al., 1996; Sutton-Grier et al., 2011).

Additionally, a positive correlation between C production and ff20 was found. This result seems to be contradictory to the results discussed in chapter 6.1.2.2 and to other studies reporting stabilization processes related to aggregation of OC with fine grained particles and the formation of organo-mineral complexes (Chenu and Plante, 2006; Kögel-Knabner et al., 2008; Von Lützow et al., 2008). This stabilization is mainly influencing the longevity of the intermediate and stable carbon pool (Von Lützow et al., 2008). During the incubation period, mainly C turnover of the labile organic carbon pool was detected (see below). As discussed in chapter 6.1.1, ff20 is strongly correlated with OC content due to the deposition of allochthonous OC in tidal marshes. Consequently, ff20 is significantly higher in topsoil than subsoil samples. This suggests that ff20 acts primarily as a measure for C quantity in the incubated samples. The influence of the fine fraction on C quality could not be determined within the limited incubation period.

Nevertheless, the quality of SOC seems to have influenced the C turnover of the investigated marsh soils. When C production was normalized to SOC content of the soil samples, significantly higher total C turnover and mineralization rates were found in topsoil samples under aerobic conditions. An equalization or even inversion of the results that has been found in other studies (Knoblauch et al., 2013; Sutton-Grier et al., 2011) could only be found for single samples of the Elbe estuary, indicating that most samples with higher SOC content also provide bigger amounts of easily degradable organic substances. Consequently, the C quality decreased with increasing soil depth, most probably due to accumulation of labile OC from fresh litter in the topsoil and aggregation of older, recalcitrant OC in the subsoil. These results are in accordance with the calculated accumulation of autochthonous OC in topsoils and mineralization in subsoils which was primarily found in high marshes (Figure 12). As the potential decomposability did not considerably differ between high and low marshes (Figure 18), total C production and ΔOCP (in % of SOCP) were only moderately correlated (aerobic: $r_s = 0.507$, $p = 0.011$; anaerobic: $r_s = 0.433$, $p = 0.035$).

Microbial decomposition usually proceeds in several phases representing the different decomposable C pools, as known from other studies on carbon mineralization (Dutta et al., 2006; Knoblauch et al., 2013). During the course of the experiment the C production did not follow a common curve progression in all samples. Some samples could be fitted best by a linear approach

while others were better described by an exponential decay model. To assure a good quality of the model, the variances of the residues and the regression coefficient R^2 were compared with those of the linear model. Since several samples showed equal or better results for the linear approach, the output parameters of the exponential model did not always appear reliable. Furthermore, the test for normality of the residues failed in about half of the investigated samples, so that they had to be discarded. For that reason, it was not possible to use exponential decay models for all samples and calculate parameters like turnover times or the total amount of degradable carbon. Generally, turnover times of 24 to 175 days were modeled, for labile pools of different soils incubated under different temperatures and oxygen availabilities (Schädel et al., 2014; Zou et al., 2005). With a total incubation time of 118 days, a considerable part of the labile C is presumably decomposed until the end of the experiment. Lower final than initial mineralization rates (Figure 17) in many samples indicate the consumption of the easily decomposable SOM, resulting in a decrease of rates when only the slow and recalcitrant SOM fractions remain (Kristensen and Holmer, 2001). Especially under anaerobic incubation, the labile pool seems not to be totally depleted as differences between initial and final CO_2 production rates were smaller and CH_4 production was just starting in most profiles. Despite the lack of significance, each profile with active methanogenesis showed higher final than initial rates, except for profile 1a. As C turnover is slower under anaerobic conditions (Kristensen and Holmer, 2001), the labile carbon pool takes longer to be completely decomposed.

Annual mean temperature in the study area (DWD, 2013) is much lower than the incubation temperature, resulting in lower in-situ soil temperatures. Consequently, decomposition rates will be below the measured values under laboratory conditions, as temperature is one of the major parameters affecting greenhouse gas production (Mitsch and Gosselink, 1993; Wang et al., 2013). Hence, refill of labile carbon by allochthonous and autochthonous input might be quicker than decomposition in the investigated soils.

Along the salinity and elevation gradient, no clear pattern in SOC turnover could be found (Figure 18). The potential decomposability seems not to vary considerably between sites of the different salinity zones or elevation classes. As a result, the incubation experiment did not reproduce or inverse the pattern determined for SOC pools of the study area which significantly differed between salinity and elevation zones (Figure 11). Only anaerobic subsoil samples showed a tendency towards higher decomposition in the polyhaline zone which could be related to an increased sulfate reduction (compare chapter 6.1.2.2 and Sutton-Grier et al. (2011). It follows that differences in SOC pools are not only due to the potential decomposability of soil caused by different C quality, but mainly result from in-situ processes at the respective sites, including

subsequent supply of allochthonous and autochthonous OC (chapter 6.1.1), varying inundation frequencies and durations (Table A 17), or alternative metabolic pathways and CH_4 suppression in salt marshes (chapter 6.2.1.1). However, some uncertainty exists regarding differences between salinity zones and elevation classes since SOC turnover shows a high scatter in the different sites. Specific soil properties like SOC content, N content, and ff20 seem to have a stronger influence on the decomposability of organic matter than differences in salinity or elevation (Table A 11).

6.2.2 Dissolution of soil carbon

When estimating C turnover, the amount of carbon being dissolved in the soil solution at the respective partial pressure within each incubation bottle has to be accounted for. The incubated marsh soils are calcareous (Table 14), resulting in solution of respired CO_2 and dissociation to HCO_3^- and CO_3^{2-} (Kalff, 2001). As the amount of DIC and the proportions of the different carbon species in the soil solution exist within equilibrium, these amounts could be calculated by the law of mass action using soil pH as an indicator for DIC composition. At the measured soil pH of 5.5 to 7.9, the biggest part of the produced CO_2 was present in the soil solution as HCO_3^- ions. Therefore, the calculation of $CO_2(aq)$ (Conrads et al., 2011) without accounting for the different carbon species is insufficient for the investigated samples and would result in an underestimation of the total produced C.

Moreover, CO_2 production from microbial respiration or organic acid originating from SOM decomposition can result in dissolution of carbonates and release of carbonate-derived CO_2 (Ramnarine et al., 2012). CO_2 produced by incubated silt loam samples with a similar pH to the investigated marsh samples, originated to a high extent (up to 80 %) of SIC dissolution (Ramnarine et al., 2012). This process could not be accounted for with the data at hand, but should not be neglected in future studies.

CH_4 solution is not affected by the carbonate equilibrium, but mainly by partial pressure of CH_4, temperature, and to a minor extent by salinity (Yamamoto et al., 1976). The solubility of CH_4 in the investigated samples was very low. Of the relatively small CH_4 production, only 1.5 % was soluble. In contrast to CO_2, the CH_4 solubility did not have a big impact on the total C turnover.

6.2.3 Methodological limitations

6.2.3.1 Experimental bias due to sample preparation

Taking bulk samples for an incubation experiment represents a major disturbance and might cause an alteration of the biological processes within the soil sample (Subke et al., 2009). By removing roots, an artificial increase of dead biomass was avoided. Homogenizing the samples helped to ensure that replicates were comparable. However, both preparation procedures might have caused a physical disturbance, mainly by loosening the soil matrix (Subke et al., 2009). The sample preparation was carried out very cautiously to avoid destruction of aggregates preserving OC from rapid decomposition. Nevertheless, maximum mineralization rates within the first days of incubation (especially under aerobic conditions, Table A 8) indicate a disturbance by sample preparation, which was also described for similar incubation experiments (e.g. Knoblauch et al., 2013). For the interpretation of the results, only data after this period was used, to avoid over-interpretation of the mineralization rates.

Despite careful homogenization of the soil, some samples show a high standard deviation between the respective replicates. Another uncertainty resulting from insufficient homogenization is a discrepancy between pre and post-incubation values of pH, TOC, and TIC, as pre-incubation soil characteristics were determined on the bulk sample, while post-incubation values were determined on each replicate. Therefore, post-incubation values were considered more reliable and used for normalizing the values and calculating correlation analyzes (compare chapter 4.5.3).

6.2.3.2 Experimental bias due to flushing

When concentrations of CO_2 in the headspace of incubation bottles reach a certain level, aerobic respiration of microorganisms will be suppressed due to CO_2 stress (Knoblauch, pers. comm.). This suppression was observed in about half of the samples during the last month of incubation, when no flushing was carried out, so that the time span between day 114 and 153 could not be considered in the data analysis (Figure 14). Therefore, it was necessary to exchange the headspace and flush it with CO_2-free air when concentrations reached 3 % CO_2 (Knoblauch et al., 2013). This procedure led to negative post-flushing mineralization rates which do not represent a change of microbial activity, but are a methodological artifact. The CO_2 measured directly after the flushing procedure (within 1 to 6 hours) was only to a minor extent due to new respiration. The major extent is most probably a result of CO_2 efflux from the soil solution. By flushing, CO_2 was

completely removed from the headspace, but the dissolved proportion was assumed to stay constant. Due to the change in partial pressure of CO_2 in the headspace, a new equilibrium between gaseous and aqueous phase had to be established after flushing. Therefore, the first post-flushing value cannot be trusted and was replaced by the mean of the previous and subsequent mineralization rates. By calculating the cumulative C production from these rates might have led to a slight underestimation of total C turnover in aerobic incubations. Consequently, the difference between aerobic and anaerobic C turnover could in fact be more distinct. Especially in subsoil samples, where aerobic and anaerobic turnover were not significantly different, the accurate determination of CO_2 dissolution processes could provide a better approximation of C turnover, when flushing of the headspace is necessary. However, the general processes can be adequately estimated by the results from this experiment.

6.2.3.3   Transferability of results to field conditions

The conducted incubation experiment had the advantage of controlled laboratory conditions which allowed a direct comparison of the mineralization potential of the investigated samples in relation to oxygen availability as well as C quantity and quality. However, the results of the experiment are not directly transferable to field conditions, where a range of abiotic and biotic parameters might affect C turnover (Subke et al., 2009). For example, the microbial growth conditions might be altered from those in the field, due to artificial changes in available pore space or the limited carbon and nutrient availability (Subke et al., 2009; Zou et al., 2005). The actual greenhouse gas emissions are modified by the production and oxidation potential of the soil (Le Mer and Roger, 2001; Pfeiffer, 1994), in combination with various other processes in the field, e.g. the formation of microenvironments or aggregates (Chenu and Plante, 2006; King and Wiebe, 1980), transport of gases through cracks, plant tissue, or ebullition (Chanton and Whiting, 1995; Sutton-Grier and Megonigal, 2011; Van der Nat and Middelburg, 2000), advection of gases during tides (Morris and Whiting, 1985), and additional supply of labile carbon by vegetation, algae, and sediments (Tobias and Neubauer, 2009). Because those processes cannot be quantified with the data available, all interpretations and conclusions drawn from the experiment regarding implications for field conditions should be treated with caution.

An additional limitation of the laboratory conditions is reflected in the lack of significance between SOC turnover in different elevation classes. Due to the implementation of the experiment, all samples have either been kept aerobic or anaerobic during the time of incubation. Under field conditions, different inundation frequencies and durations cause differences in redox

potentials between low and high marshes (Andresen, 1996). In the study sites 2 and 3, Andresen (1996) found a strong decrease of redox potentials in the upper soil horizons (below 10 cm soil depth) of the low marshes. In the drained high marshes reduced conditions appeared only in deep subsoil horizons below 150 cm soil depth. A similar pattern was visible from redoximorphic features in the profiles of the present study (e.g. Table 2 - Table 4). Consequently, in low marshes the anaerobic turnover (Figure 18 D) might be dominant while aerobic turnover (Figure 18 B) might be more important in high marshes, which could lead to significant differences of in-situ C turnover. Furthermore, CH_4 was only detected in topsoil samples, because of their high SOC content. In the field however, topsoil horizons are mostly aerobic, not producing but oxidizing CH_4 (Pfeiffer, 1994). Methane can only be produced in anaerobic subsoil samples where the SOC content is usually lower, probably resulting in overall low or negligible CH_4 production rates.

Since the investigated calcareous samples showed a considerable CO_2 dissolution, another problem arises when results shall be transferred to field conditions. The temperature is substantially higher in the laboratory, causing a lower CO_2 solubility. Then again, the partial pressure in the incubation bottles might differ from that in the soil pores under undisturbed field conditions. In soils influenced by tidal dynamics, the CO_2 pressure can fluctuate due to flooding which decreases the diffusion of gases through pore water (Du Laing et al., 2007). The actual efflux of DIC in the marshes is impossible to estimate from the incubation data, as leaching might be enhanced due to regular inundations in tidal marshes (Du Laing et al., 2007). Duve (1999) suggested that dissolution and export of carbonates into the river is an important process in the marshes of the Elbe estuary.

6.3 Trace metals in tidal marsh soils and suspended sediments

Soils act as a natural cleaning system removing pollutants from biogeochemical cycles within the ecosystem. This filter and buffer function of tidal marsh soils is of vital importance at the Elbe, due the strong pollution of the river in the past (e.g. Netzband et al., 2002).

6.3.1 Factors influencing trace metal concentrations

6.3.1.1 Determination of metal distribution along estuarine gradients

Trace metals are mainly transported attached to suspended sediments with the river runoff from upstream areas to the estuary (Förstner et al., 2004). On their way downstream, these sediments are deposited on the river banks and marshes and are mixed with marine sediments (e.g. Förstner et al., 1990; Gröngröft et al., 1998), resulting in decreasing trace metal concentrations with increasing salinity (Table 11). This effect was most pronounced for trace metal concentrations in the ff20, resulting in negative correlations with salinity in topsoils. Also, decreasing trace metal pools along the salinity gradient were clearly visible (Figure 19). Background concentrations for Hg and Cd in topsoil samples of study site 5 confirm the strong marine influence at this lower end of the estuarine salinity gradient. Within the investigated estuarine stretch, Gröngröft et al. (1998) found 83 to 94 % of fine grained sediments to be of marine origin. Since the year 2000, the proportion of marine sediments further increased due to hydrodynamic changes caused by the conducted channel deepening in 1999 (BfG, 2008). Moreover, the decrease of organic matter in sediments and marsh soils along the course of the estuary (see chapter 6.1.1) might have reduced the fixation and deposition of attached trace metals. In subsoil horizons, decreasing trace metal concentration could not be found (Table 11). These horizons were formed in previous deposition periods and do not represent recent pollution loads. Differences of subsoil pollution along the salinity gradient might, therefore, be caused by different ages of horizons (compare chapter 6.3.3.2). Also, mobilization processes due to salinity cannot be excluded along the salinity gradient (e.g. Du Laing et al., 2008b). The role of retention and mobilization processes on metal distribution will be discussed in detail in chapter 6.3.1.2.

In addition to large-scale trace metal variability related to the sediment source, local influences related to the geomorphic structure of marshes have to be accounted for (Chen and Torres, 2012). Trace metal pools were significantly higher in high compared to low marshes (Figure 20). These results are in contrast to findings of Chen and Torres (2012) and Rinklebe et al. (2007)

who found decreasing trace metal pollution with increasing elevation due to the grain size effect in salt marsh and floodplain soils. In their studies, the amount of coarse particles increased with elevation due to short inundation and deposition times at higher elevated sites. At most investigated marshes of the Elbe estuary, no significant difference in ff20 was found between low and high marshes (Table A 4). However, a non-significant trend toward lower ff20 content in low marshes might be a result of higher flow velocities at low elevations in this macrotidal estuary. Consequently, only fine-grained sediments with higher trace metal contents might be able to reach the high marshes while low contaminated coarse sediments are deposited already in the low marshes. Similar sedimentation successions are common in tidal marshes at the North Sea coast (Kuntze, 1965). Site 1, representing a low marsh with high amounts of ff20, SOC, and trace metals, constitutes an exception at the Elbe estuary. This site is situated at a tidal branch with attenuated current velocities (WSD-Nord, 2013) that promote sedimentation of fine-grained sediments.

In contrast to trace metal pools, no explicit relations were found between trace metal concentrations and elevation (Table 11). Site specific differences in deposition patterns could explain the missing correlations. However, not only differences in grain size distribution are responsible for the lack of relations, but also differences in the pollution load, since total trace metal concentrations and those normalized to ff20 show equally weak relations with elevation. Furthermore, differences in sedimentation dynamics, which were found to be highly variable along elevation and salinity gradients (Butzeck et al., 2015), could have an influence on trace metal concentrations. This finding is in accordance with Chen and Torres (2012), who suggested that morphodynamic processes and marsh age are strongly influencing the variability in trace metal abundance along marsh transects. At the Elbe estuary, highly polluted horizons from past deposition might appear in deeper soil depth in low marshes, due to higher sedimentation and accretion rates at theses elevations (Butzeck et al., 2015). However, the strong influence of position along the salinity gradient of the estuary seems to decrease the explanatory power of elevation as an indicator for the pollution load.

6.3.1.2 Role of retention and mobilization processes

As metals are predominately bound to fine-grained soil particles and SOM (Christiansen et al., 2002; Kabata-Pendias, 2011), trace metal concentrations can vary strongly between sites with different sedimentation dynamics and organic content (Rinklebe et al., 2007). Fine-grained soil layers are usually stronger polluted than sandy layers, even if the local metal loads at the site of

deposition are similar (Stachel and Lüschow, 1996). The high variation of grain size distribution in the investigated soils (Table 8) suggests accounting for the grain size effect when interpreting trace metal concentrations (Ackermann et al., 1983). Strong correlations of all investigated metals with ff20 and SOC (Figure 6) confirm the major importance of grain size distribution and SOM content for trace metal concentrations in the marsh soils of the Elbe estuary. The individual contribution of the mineral and organic soil components could not be distinguished due to a strong collinearity between ff20 and SOC. A weaker correlation between normalized trace metal concentrations and ff20 as well as SOC can be expected due to the strong relation between these parameters explained in chapter 6.1.1. The results of this study go in line with findings of several other studies on trace metal retention in fluvial and estuarine systems and can be explained by sorption and complexation processes (see compilation of Du Laing et al., 2009c). Due to their high surface area and cation exchange capacity, fine-grained and organic rich soils play an important role in the sorption of trace metals (Kabata-Pendias, 2011). Such soils were mainly abundant in the oligohaline zone, especially in study site 1 (Table 8 & Table 9), suggesting its importance for metal retention along the estuary.

The influence of Fe/Mn (hydr)oxides or sulfides in trace metal retention could not be quantified within the scope of this study. Nevertheless, redoximorphic features were visible in all studied soils (Table 2 – Table 4 & Table A 1) indicating aerobic conditions in the upper parts and anaerobic conditions in the lower parts of the studied profiles, depending on the water table. Under aerobic conditions, an increased affinity between Fe/Mn oxides and trace metals was found in estuarine sediments (Guo et al., 1997). Even though the amount of (hydr)oxides was not determined, it can be assumed that they primarily exist in the fine fraction (Kabata-Pendias, 2011). Thus, the strong correlation between ff20 and trace metal concentrations most likely includes the effect of co-precipitation with oxides in topsoil and aerobic subsoil horizons. In anaerobic subsoil horizons the formation of metal sulfide precipitates can strongly reduce trace metal mobility (Du Laing et al., 2008a; Du Laing et al., 2009a; Spencer et al., 2003). Typical sulfate concentrations of the Elbe water ranging from 114 to 189 mg l^{-1} (Andresen, 1996) are sufficient to form considerable amounts of sulfide precipitates under reductive conditions (Lovley and Klug, 1986). Consequently, Andresen (1996) found very low trace metal concentrations in pore water and groundwater of study sites 2 and 3. In the current study, grey or black colors and a characteristic smell indicated sulfide formation in Gr horizons of the investigated profiles. Therefore, a strong retention of trace metals can be assumed in these horizons.

A distinct relation between trace metal and SIC concentrations was not found, indicating that co-precipitation with carbonates is not one of the major processes for metal retention at the Elbe estuary. For all investigated elements, however, precipitation as carbonates was described to be a possible retention process (Kabata-Pendias, 2011). Especially for Cd and Pb, high carbonate concentrations were reported to be a major factor promoting immobilization due to the formation of precipitates (Guo et al., 1997; Kabata-Pendias, 2011). A possible explanation could be that carbonates do not represent a limiting factor due to their abundance in all investigated samples (Table A 3). In this context, however, it appears counterintuitive that trace metal pools correlated negatively with SIC pools. A similar contradiction appears with pH, which is another major factor controlling trace metal retention and mobilization in soils (e.g. Du Laing et al., 2009c; Kabata-Pendias, 2011). The pH range of the investigated samples reached from neutral to weakly alkaline (Table 8), indicating a low mobilization capacity, since threshold values for trace metal mobilization were not reached (e.g. Cd < 6, Zn < 5.5, Pb, and Hg < 4, see Blume and Brümmer (1991)). Hence, the correlation of trace metals and pH is weak, both in the total samples and especially in the ff20. Slightly lower metal concentrations were found at higher pH values (Figure 9). This result seems contradictory, since trace metal mobility and availability has been found to decrease with increasing pH (e.g. Gröngröft et al., 2005; Overesch et al., 2007). Highest pH values and SIC pools appeared in samples of study site 5 in the polyhaline zone. Since soils of this study site contained lower amounts of ff20 and SOC, the adsorption capacity was lower compared to the other sites. The negative correlation of trace metals with pH and SIC pools might actually be biased due to the abovementioned effect of grain size and SOM. Generally, no major translocation and leaching due to pH or carbonate dissolution can be expected.

Although the mobilization capacity of the studied soils can be considered low, due to grain size, SOC content, pH, and possibly co-precipitation with (hydr)oxides, sulfides, and carbonates, a part of the trace metals that were originally deposited on the marsh was likely mobilized. Indicators for mobilization were lower trace metal concentrations in the marsh soils in comparison to suspended sediments at nearby sampling stations (compare chapter 5.5.4). Due to the fluctuating level of the water table in frequently flooded soils, an oxic-anoxic interface established which was visible as Gro and Gor horizons in the studied soils, showing both oxic as well as reductive features (Table 2 – Table 4 & Table A 1). This interface is subject to change, resulting in mobilization of trace metals (Du Laing et al., 2009c). Reduction of (hydr)oxides or oxidation of sulfides, can lead to dissolution and leaching of attached trace metals (Du Laing et al., 2008a; Du Laing et al., 2009a; Guo et al., 1997). Leaching from the oxic horizons can be followed by downward transport and accumulation of metals in the anoxic horizons, referred to

as "oxidative pumping" (Förstner et al., 1990). As a result of an increased tidal amplitude since the last deepening of the Elbe estuaries shipping channel in 1999 (Kerner, 2007), a stronger variation of the groundwater table could further increase this mobilization.

A second possible process related to changes in tidal amplitude and sea level rise is an upstream shift of the brackish zone (Bergemann, 2004a). Increased salinity was found to increase metal mobility, due to the formation of soluble chloro-complexes and competition of cations for sorption sites (Millward and Liu, 2003; Paalman et al., 1994). Especially Cd was found to be easily mobilizable with increasing salinity, whereas Zn mobility is less affected by salinity (Du Laing et al., 2008b; Gerringa et al., 2001; Salomons, 1980). Gerth et al. (1981) found high Cl⁻ concentrations to reduce the adsorption of Hg, Cd, and Pb, and suggested increased availability of these metals in soils exposed to elevated salinities. Due to different binding strengths of the investigated metals, a shift in the trace metal ratios could be expected. In the selected soil profiles, such a shift towards higher Zn/Hg ratios in soils compared to sediments was observed (Figure 25 A). Also, Zn/Cd ratios were higher than the respective ratio in suspended sediments, indicating depletion of Cd in relation to Zn (Figure 26). Furthermore, different shifts in the Zn/Cd ratios with soil depth were determined in the respective profiles. The decreasing Zn/Cd ratios in profile 4e, could be due to a combination of oxidation and high salinities in the topsoil of this profile, resulting in increased mobilization of Cd as described by Gerringa et al. (2001) and Du Laing et al. (2008a). Cd leached from the topsoil could be accumulated in the subsoil as sulphide precipitates (Du Laing et al., 2008a). Increasing Zn/Cd ratios with soil depth in the profiles 2b, 2c, and 3b could be due to relatively quick dissolution kinetics of Zn compare to Cd when salinity is low (Gerringa et al., 2001), resulting in increased leaching of Zn from oxidized topsoils.

6.3.2 Evaluation of contamination levels

The cluster analysis revealed considerable variations in contamination levels between samples of different profiles and soil depths (Figure 21). The analysis is based on enrichment factors in comparison to geogenic background values according to Gröngröft et al. (1998), which were specifically determined for sediments of the Elbe estuary. Therefore, these background levels are best suited to estimate the amount of anthropogenic contamination at the study sites. A comparison of trace metal concentrations in the total sample with background values of marsh soils in Schleswig-Holstein, including geogenic and nonpoint sources (LLUR, 2011), showed similar enrichment factors for Cd, Pb, and Zn. However, enrichment factors for Hg were higher

in the total sample than in the ff20, most probably because low background values for Hg were determined at the whole coastline of Schleswig-Holstein, which mainly represents marine sources, and might not be most suitable for the marsh soils at the Elbe estuary. Because of differing methods for Pb determination between Gröngröft et al. (1998) and the present study, Pb background levels of Stachel and Lüschow (1996) were used for the calculation of enrichment factors. Furthermore, background levels of Stachel and Lüschow (1996) are within the same range for Hg, Cd, and Zn and were used for a classification of pollution classes. The ARGE ELBE classification gave a good overview of the pollution level (Table 16), but gave no indication about the ecotoxicological value of the soils. To estimate the environmental risk coming from polluted soils, a second classification system according to BfG (2004) was used. This classification is based on natural background values of coastal sediments and target values for the protection of surface water bodies defined by the German Working Group on Water Issues of the Federal States and the Federal Government (BfG, 2004). The differences in contamination levels between the analyzed cluster groups will be discussed subsequently.

Generally, enrichment factors significantly increased from cluster 1 to 3. Soil samples of cluster 1 showed a low contamination level. The dominance of unpolluted and very low polluted samples from study site 5 (Figure 21) confirms this conclusion. Also, subsoil horizons of site 2 having minimum trace metal concentrations were classified into this cluster. Several samples of sites 5 and 2 even had Cd and Hg concentrations below background values (compare Table A 5). It follows that soils influenced by tidal mixing (compare chapter 6.3.1.1) and horizons deposited in pre-industrial times (compare chapter 6.3.3.2) can be considered most valuable. Samples of cluster 1 had predominantly low enrichment factors, low pollution classes, and high ecotoxicological values (Table A 14). Especially, Cd, Hg, and Pb remained below so-called target values (ARGE class II and BfG class D), indicating no risk due to pollution or toxicity of these soils (BfG, 2004; Stachel and Lüschow, 1996). However, ff20 and SOC concentrations were lowest in cluster 1, implying a lower retention capacity for trace metals in comparison with samples from cluster 2 and 3.

Soils of cluster 2 can be evaluated as of intermediate contamination level. In comparison to cluster 1, trace metal concentrations and enrichments factors of all elements increased (Table 16). This increase was most evident for Cd that had 2.4-times the concentrations of cluster 1. However, mean ARGE classes changed only slightly for Cd and Hg, and mean BfG classes did not change at all in this cluster. Regarding the individual samples, it appears that cluster 2 consists of a wide variety of different sites, profiles, and soil depths (Figure 21). Therefore, this cluster represents a transition between cluster 1 and 3, without particular features.

Cluster 3 is the smallest cluster, consisting of only twelve samples (Figure 21). These samples had highest trace metal concentrations and enrichment factors. Especially Hg increased strongly, being 3-times that of cluster 2 (Table 16). On average, Hg concentrations were 7.4-times the geogenic background, confirming its role as one of the main problematic substance for the river Elbe (compare Stachel and Lüschow, 1996). Consequently, soil samples in cluster 3 were evaluated as highly toxic with regard to Hg, but also Zn. The classification for Cd, Pb, and As did not differ between cluster 2 and 3, and enrichment factors increased only slightly (ca. 1.3-fold). Nevertheless, the hazardous nature of Hg, being one of the priority substances according to EU Water Framework Directive (EU WFD, 2008), represents a major environmental threat in case of erosion and re-suspension of sediments. In the face of sea level rise and changing tidal currents due to anthropogenic interference (Gönnert et al., 2009; Roberz, 2003), this process cannot be excluded, especially for topsoil horizons of low marshes (1b, 1c, 4a). However, the risk of erosion is small due to high sedimentation rates at the low marshes of the Elbe estuary (Butzeck et al., 2015). Subsoil horizons of the high marsh profiles belonging to cluster 3 (3b, 4d, 4e) are most likely well protected against erosion, being covered by low polluted horizons of clusters 2 and 1.

For As, the considerable pollution according to Stachel and Lüschow (1996) and the intermediate value according to BfG (2004) seem to be a misjudgment, as enrichment factors were low in all clusters. In contrast to the other investigated metals, background values of As differed strongly between Gröngröft et al. (1998), Stachel and Lüschow (1996), and BfG (2004). Since background values of Gröngröft et al. (1998) were specifically estimated for the Elbe estuary, they appear to be most appropriate for the comparison with the investigated marsh soils. On the other hand, ecotoxicological values of BfG (2004) are not only indicating the anthropogenic pollution in comparison to background concentrations, but also the degree of toxicity. The intermediate and low BfG classes of many samples (Table A 14) in all clusters suggest a certain threat by As for the environment.

In total, only a minority of soil horizons had a high contamination level and can be considered as a potential threat for the environment. None of the investigated elements had very low ecotoxicological values in the different cluster groups, implying a very high degree of toxicity (Table 16). Also action values for grasslands of the BBodSchV (1999) were not exceeded in the studied topsoils, but a number of profiles from all managed sites exceeded precautionary values. However, these thresholds have the character of a value for orientation rather than implying an inevitable damage of the ecosystem. Furthermore, plants dominating the tidal marshes of the Elbe estuary have rather low transfer coefficients for trace metals (Du Laing et al., 2009d; Teuchies et al., 2013), and might, therefore, represent no substantial threat for the human food

chain. In combination with the low mobilization potential of the soils (chapter 6.3.1.2), a low phytoavailability can be assumed. SOC and ff20 concentrations, which are supposed to strongly affect the retention capacity of the tidal marsh soils, were highest in samples with highest trace metal concentrations. Hence, the retention function of the investigated soils was reciprocal to the contamination level.

In comparison with floodplain soils of the upper reach of the river Elbe, mean trace metal concentrations of the tidal marsh soils were low (Krüger and Gröngröft, 2003; Krüger et al., 2005; Overesch et al., 2007; Rennert et al., 2010; Rennert and Rinklebe, 2010; Rinklebe et al., 2010; Rupp et al., 2010). This decrease has already been described for suspended and freshly deposited sediments in the past and can be explained by dilution due to tidal mixing (BfG, 2008; Gröngröft et al., 1998; Heise et al., 2007). The quality evaluation of the investigated marsh soils was similar to the assessment of sediment quality by Stachel and Lüschow (1996), even though the range of variation was higher in sediments of 1994. This deviation might be due to mobilization processes described in chapter 6.3.1.2. The similarity between today's soils and former sediments suggests, however, that marsh soils of the Elbe estuary still retain big amounts of pollutants from the past. Also, the estimated trace metal stocks (Table 15) suggest that the investigated marsh soils contribute significantly to the purification of the river water. The respective stocks, both in the uppermost 30 cm soil depth and the whole profile depth of 100 cm, exceed the current trace metal loads by far (e.g. 361 to 7072 % in 2008, compare Table A 16 and (ARGE ELBE, 1997, 2001; Bergemann, 2004b; Bergemann and Gaumert, 2006, 2008a, b, 2010; Bergemann et al., 2005; Bergemann and Stachel, 2004)). When considering the total trace metal loads from the available years, the tidal marsh soils store a considerable proportion of the trace metals discharged since 1985 (Cd: 26 %, Hg: 21 %, Pb: 177 %, Zn: 92 %). Even though this estimation has to be considered with some degree of uncertainty, since data of annual loads published in the analyzed quality assessment reports were incomplete, it highlights the importance of the retention function of tidal marsh soils and the potential threat resulting from re-suspension.

6.3.3 Estimation of sedimentation period from vertical trace metal distributions

6.3.3.1 Temporal variations of trace metal concentrations in suspended sediments

In suspended sediments of the Elbe estuary short-term and long-term temporal variations of trace metal concentrations were observed (Figure 22 & Figure A 4). Short-term variations were

strongly related to river discharge which in turn varied with season (Figure A 4). These seasonal variations were even stronger at sampling stations further upstream between Wedel and Geesthacht (BfG, 2008). The investigated sampling stations showed higher correlation coefficients of trace metal concentrations with river discharge at Grauerort in comparison to Cuxhaven (Table A 15). Cuxhaven, which is situated at the estuarine mouth where the tidal influence is more intense, might be less affected by river discharge. The interpretation of long-term variations can be substantially complicated by seasonal variations or single extreme events (compare chapter 6.3.3.3). As sedimentation was found to be strongest in the Elbe marshes during the winter season (Butzeck et al., 2015), mean winter concentrations were interpreted below.

A long-term shift in trace metal concentrations is mainly due to a change in the anthropogenic input of pollutants in the catchment area (BSU and HPA, 2011; IKSE, 2010). The structural changes in the course of the German reunification, led to a strong decrease of trace metal loads in the Elbe (Heise et al., 2005; Stachel and Lüschow, 1996). This decrease was most pronounced for Hg at the station Grauerort (Figure 10 & Stachel and Lüschow (1996)). At the station Cuxhaven, concentrations of all investigated metals were lower and did not show such a distinct trend as concentrations at Grauerort, due to the abovementioned marine influence. For some trace metals (Hg, Pb, and As), values close to the geogenic background were observed at Cuxhaven. However, these values appeared at different time periods. Hg had lowest concentrations in the most recent years, while lowest Pb and As concentrations were measured in the early to mid-1990s. Increasing Pb and As concentrations at both sampling stations since 1991 are in accordance with Stachel and Lüschow (1996). As strongest pollution of the Elbe appeared in the 1970s and 1980s (Müller, 1996), the highest trace metal peak might only be truncated by the dataset starting in 1988 (Figure 22). Heise et al. (2005) found strongest Hg loads between 1983 and 1986. Trace metal concentrations of fresh sediments from the early 1970s showed a considerable pollution (Lichtfuß, 1977), comparable to values from the late 1980s.

6.3.3.2   Age determination of soil horizons

Soils represent an archive of the landscape development and can give a glimpse into the history of the respective sites. The investigation of the vertical distribution of trace metal concentrations can give an inside into the anthropogenic impact in the past (Zwolsman et al., 1993). Due to the abovementioned long-term shift of trace metal concentrations in suspended sediments, trace metal peaks in marsh soils can be used as a proxy for the deposition period of the respective

horizons. As a result of different sedimentation dynamics at the respective sites, peaks were determined in different soil depths of the investigated profiles (Figure 24). A decrease of metal loads accompanied by an improvement of the water quality since the early 1990s, was reported by various authors (e.g. BfG, 2008; BSU and HPA, 2011; Heise et al., 2005; Stachel and Lüschow, 1996). Consequently, low contamination of horizons covering high contaminated horizons, indicate younger sedimentation. In contrast, trace metal concentrations around the geogenic background in underlying horizons could indicate pre-industrial deposition.

Similar dating approaches have been used with some degree of success (Ackermann and Stammerjohann, 1997; Meyercordt, 1992; Prange, 1997). Ackermann and Stammerjohann (1997) used sediment cores from the site "Mühlenberger Loch" near Hamburg and assigned different contamination levels and grain size distributions to specific time marks or events. As they used an artificially constructed basin which was later filled with highly contaminated dredged material from the Hamburg harbor (e.g. max Hg = 30 mg kg^{-1} or Zn = 3700 mg kg^{-1}), the published trace metal concentrations cannot be compared directly. In the natural marsh areas, metal concentrations are mainly influenced by river discharge and tidal mixing and have never reached such high values. In contrast, Prange (1997) investigated subaqueous sediments with natural sedimentation dynamics in the upper reach of the Elbe. He could reconstruct the development of contamination in the Elbe catchment during the 20th century. Strongest pollution by most trace metals reached the Elbe from industrial and mining areas at the Saale and Mulde rivers in the 1970s and 1980s. An improvement of the water quality since the early 1990s was related to decreasing metal concentrations in the uppermost sediment layers (Prange, 1997). Meyercordt (1992) used salt marsh soils from the south-eastern North Sea to reconstruct the contamination history of this region. In his study, he could clearly distinguish uncontaminated pre-industrial sediments from contaminated sediments of the 20th century. A decrease of trace metal concentrations in the uppermost horizon was assumed to be caused by mobilization processes rather than decrease of anthropogenic input which did not yet have a substantial effect on metal concentrations in marsh soils at the time of sampling in 1989. This mobilization decreased the absolute amounts of metals in the horizons, but did not change the vertical distribution and the position of trace metal peaks in the profiles, so that a dating of the investigated profiles was possible (Meyercordt, 1992).

All three studies used ^{210}Pb and ^{137}Cs dating to assure an accurate chronology of metal inputs to the sediments (Ackermann and Stammerjohann, 1997; Meyercordt, 1992; Prange, 1997). The current study is based upon their successful dating approaches and aims to simplify this method

by estimating the deposition period with the help of trace metal distributions only. This dating method will be discussed by means of four selected profiles introduced in chapter 5.1.4 and 5.5.4.

Minimum trace metal concentrations close to background concentrations in subsoil horizons of profiles 2b and 2c in the oligohaline zone (Figure 24) seem to contradict with decreasing trace metal concentrations along the salinity gradient. However, these minimum concentrations were present in subsoil horizons and could be an indicator for sedimentation of these horizons during times when pollution was low. According to Meyercordt (1992), sediments deposited earlier than 1840 can be considered as pre-industrial. In North Sea sediments, the first increase above background concentrations was determined for Pb between ca 1860 to 1884, while other trace metal concentrations (including Hg, Cd, and Zn) increased since the beginning of the 20th century (Meyercordt, 1992). The high marsh profiles in study site 2 might, therefore, be among the oldest investigated profiles at the Elbe estuary. The vertical trace metal distributions with highest concentrations in the upper part of the profiles confirm this assumption. These horizons were probably deposited during times of strongest pollution (ca. 1970-1991 (IKSE, 2010; Müller, 1996; Prange, 1997)). A decrease of concentrations in the shallow topsoil horizons might indicate the deposition of recent sediments with lower pollution levels. The shallowness of the uppermost horizon further indicates low sedimentation at these high marsh sites in recent times, which is in accordance with low accretion rates of high marsh soils in the oligohaline zone determined by Butzeck et al. (2015). Similar trace metal distributions were found in profiles 2d and 5f (Table A 5), indicating sedimentation at a comparable period.

Profile 3b had highest concentrations of the investigated metals slightly deeper than profiles 2b and 2c, indicating higher recent sedimentation at this site. Low trace metal concentrations in the deepest part of the profile indicate oldest deposition. The profiles 3c, 4d, and 5d had comparable vertical distributions to 3b (Table A 5). Most dynamic sedimentation seems to be present at site 4e. This profile had increasing trace metal concentrations over the total investigated soil depth. Highest contamination was measured in the deepest horizons (63 - 80 cm and > 80 cm), but even higher concentration could be abundant in deeper horizons which were not sampled. High sedimentation dynamics and comparatively young age of this profile are supported by accretion rates of the mesohaline zone (Butzeck et al., 2015) and the number of seasonal layers in this profile, suggesting a sedimentation period between 1979 and 1991 in 63 cm soil depth. The trace metal distribution of profiles 3a and 5c were comparable to 4e (Table A 5). In total, the parent material of the investigated profiles can be sorted chronologically. The profiles 2b, 2c, 2d, and 5f are considered to be of oldest age, profiles 3b, 3c, 4d, and 5d of intermediate age, and profiles 3a, 4e, and 5c of youngest age. However, the results of profiles of study site 5 have to be handled

with care, since low trace metal concentrations and less pronounced peaks impeded a clear assignment to a specific sedimentation period. Furthermore, not all profiles were equally suitable to be classified chronologically (compare chapter 6.3.3.3).

The Zn/Hg and Hg/Cd ratios were more difficult to interpret and partly gave ambiguous results (Figure 25). Profile 2b had lowest Zn/Hg ratios in the Go-Ah horizon (5 - 23 cm) indicating a deposited period around 1992/93 for this horizon. But highest Hg/Cd ratios in the same horizon were comparable to background concentrations indicating this horizon to be pre-industrial. The Gr horizon in 140 cm soil depth appears to be the youngest, as it had the lowest Hg/Cd ratio of the whole profile. Similar problems occurred concerning the distribution of trace metal ratios in the profiles 3b and 4e (Figure 25). The fluctuating ratios around an intermediate value in both profiles did not allow a clear interpretation of the deposition period of the different horizons. For profile 3b, the Hg/Cd ratios might indicate younger horizons in the upper part (0 - 50 cm) and background ratios in the deepest horizon (> 80 cm). In all cases, the distribution of actual concentrations gave a better inside into the history of the respective profiles. Comparable to the Zn/Cd ratio discussed in chapter 6.3.1.2, biogeochemical processes like chloro-complexation (Gerth et al., 1981) or methylation (Frohne et al., 2012; Wilken and Hintelmann, 1991), favoring mobilization of one metal over another (e.g. Hg over Zn) could explain the exceptional vertical distribution of trace metal ratios.

6.3.3.3   Evaluation of the dating method

Due to the processes discussed in chapter 6.3.1, the age determination of specific horizons from its trace metal contents is not straightforward. The discussion of the vertical distribution of trace metal concentrations and ratios revealed difficulties concerning the comparison with suspended sediments and interpretation of the period of deposition. One problem is related to the unknown trace metal input into the study sites. Even though, the concentrations of trace metals in suspended sediments at the sampling stations Grauerort and Cuxhaven are known from 1988 onwards, it remains unclear how much of these sediments are effectively deposited on the marsh soils. Storm tides are key processes in sedimentation and accretion of high marsh soils (Butzeck et al., 2015), which are visible as sandy layers in most high marsh profiles (e.g. Table 4). These extreme events might provide the marsh soils with a higher amount of marine sediments which can delude the trace metal concentrations in the soils. No soil horizon had comparable concentration to the pollution measured in suspended sediments at the station Grauerort, but

concentrations ranged in a comparable level to those at the station Cuxhaven. This could be an indicator for the higher influence of sedimentation of marine particles at the study sites.

However, the high marsh profiles of site 2 did not show storm tide layers. At this study site, which is situated in the immediate vicinity of Grauerort, a higher influence of fluvial sediment in the soils and comparable concentrations to the adjacent sampling station could be expected. The deviation between trace metal concentrations in soils and sediments could also be due to mobilization processes. Mobilization can be considered a minor process, because of favorable soil characteristics for metal fixation like ff20, SOC, and pH (see chapter 5.1). Still, a certain proportion of the incorporated trace metals could be mobilized and leached out of the horizons since deposition, modifying the vertical metal distribution (Du Laing et al., 2008a; Spencer et al., 2003). Mobile metal species could be relocated in the profile e.g. due to advective transport during flooding and re-precipitation in the anoxic horizons (Meyercordt, 1992). Consequently, a downward shift of the trace metal peaks could be assumed. Furthermore, bioturbation could modify the vertical trace metal distribution, so that no clear peaks are detectable (Sharma et al., 1987; Spencer et al., 2003). Conversely, the highest peaks have been found in the upper part of both profiles that exhibit oxic conditions, while lowest concentrations where found in the lower, anoxic parts (Figure 24). Apparently, the metal peaks resulting from maximum anthropogenic input before 1990 have not been relocated completely and can be used for the estimation of sedimentation dynamics. This result confirms the suitability of vertical trace metal distributions for the assessment of the pollution chronology. Lower metal concentrations in soils compared to suspended sediment might be due to sampling of total horizons representing sedimentation spanning over several decades with differing pollution loads. Hence, horizons combining low and high polluted layers might feature intermediate trace metal concentrations.

The investigated trace metals had different suitability for the use as indicator of the marsh age. Pb and As showed a smoothed vertical distribution without distinct peaks in specific horizons (Figure 24), which made a clear interpretation difficult. For As, the relatively high background concentration at the Elbe estuary (Gröngröft et al., 1998) further impeded the differentiation between pre-industrial and recent horizons. In contrast, Hg, Cd, and Zn had greater variations between horizons in different soil depths. Hg and Cd did even show background concentrations in subsoil horizons. These metals were mainly discharged by industrial activities in the former GDR and Czechoslovakia (Prange, 1997) and seem to be good indicators for the recent anthropogenic influence at the Elbe.

A main problem, concerning the interpretation of trace metal ratios, is the proximity of the background ratios and those of the time markers (Figure 25). Fluctuations of metal ratios in soils lead to party unreasonable results, like horizons indicating recent sedimentations covered by horizons indicating older sedimentation. Therefore, the chronological classification is difficult and ratios cannot be recommended for this issue.

Generally, dating based on metal distributions is difficult for low marsh profiles, where environmental conditions are dynamic and accretion rates are high (Butzeck et al., 2015). Deep soil cores of more than 1.2 m soil depth (if accretion rates of 2.03 cm given by Butzeck et al. (2015) are assumed) are probably necessary to reach soil depths in which metal peaks could be present. In low marshes without stable vegetated surfaces, reworking of the sediment could prevent a reliable reconstruction of discrete contamination inputs (Spencer et al., 2003). Furthermore, soils having low trace metal concentrations in all soil depth, like those of study site 5, are not particularly suitable for the assessment of the pollution chronology. In this case, spatial influences like tidal mixing superimposed temporal differences due to anthropogenic influences. When no distinct peak is visible in specific horizons, the analysis of the pollution history is almost impossible.

In total, the vertical distribution of trace metal concentrations in marsh soils can be used as an indicator for the sedimentation dynamics and marsh age at the investigated sites. The comparison of high marsh profiles allows a qualitative classification relative to each other as younger or older. For a determination of the absolute marsh age, this dating approach should be combined with a more universal method, e.g. radionuclide dating with ^{137}Cs and ^{210}Pb (e.g. Meyercordt, 1992). Such dating approaches are very laborious, expensive, and time consuming, so that for this study a simple approach was required. An estimation of marsh age based on trace metal distribution seems to be possible when socioeconomic changes resulting in variation of metal loads are known and peaks resulting from these variations are detectible.

7 Conclusions

The overall aim of this study was to characterize the ecosystem functions of estuarine tidal marsh soils from a regional perspective. In this context, two soil functions were investigated in detail: the influence of these soils on carbon storage and dynamics as well as their effect on trace metal retention of the sites. These soil functions are of particular interest at the Elbe estuary and may be altered due to climate change and anthropogenic interference.

This study presents a method to distinguish between the proportions of allochthonous, autochthonous, and mineralized OC in tidal marsh soils based on a comparison between soils and fresh sediments (Hypothesis 1). This approach provides reasonable results for most profiles. These results were partly supported by carbon isotope ratios. Horizons characterized by autochthonous OC accumulation, had also similar $\delta^{13}C$ values of biomass and soil samples. Horizons showing mineralization or preservation of allochthonous OC could not be distinguished by carbon isotope ratios, since the latter group showed a high scatter. Furthermore, an interpretation of accumulation and depletion in older high marsh profiles is difficult and results for such sites have to be handled with care, since investigated sediment samples were of comparatively recent times. Nevertheless, some general conclusions can be drawn from the results of the investigated marshes. The low marshes were provided to a greater extent with allochthonous OC by inundation (Hypothesis 2). Still they can contain high amounts of autochthonous OC when covered by dense *Phragmites* vegetation. Autochthonous OC accumulation was also dominant in the upper 30 cm of the high marsh soils, whereas in the subsoils mineralization took place under aerobic conditions, which was most likely caused by a longer soil development of these older marshes. Since most labile OC was already mineralized in the investigated subsoils before sampling, significantly lower microbial carbon turnover was found in subsoil samples. Topsoil samples showed higher SOC turnover, indicating a higher amount of labile substrates (Hypothesis 6). Consequently, not only the quantity of substrates, but also the quality of the available carbon is of importance for the potential turnover in these soils.

Furthermore, the results of this study support the hypothesis that salinity and elevation are major indirect drivers affecting SOC pools by their influence on OC accumulation and decomposition (Hypothesis 3). A decreasing SOC pool with increasing salinity was mainly attributed to a decreasing biomass production and a shift in the ratio of TOC to ff20 in the estuarine sediments. The hypothesized decrease of SOC pools with increasing elevation was not supported by the results of this study. Increasing topsoil SOC pools with increasing elevation suggest that

accumulation of autochthonous OC was considerably affecting the SOC pools. However, elevation had no significant influence on SOC pools over the total profile depth, further implying the importance of other processes than just accumulation of autochthonous OC in tidal marshes. In the low marshes, carbon burial seems to be a substantial process and SOC might have been preserved under anaerobic conditions. This conclusion is supported by the results of the incubation experiment, where significantly lower microbial carbon turnover took place under anaerobic conditions (Hypothesis 4). The hypothesis that environmental factors like salinity and elevation determine C decomposability by their influence on SOC quantity and quality could not be supported (Hypothesis 5). Similar carbon turnover in the different salinity zones and elevation classes highlight the importance of in-situ processes for turnover of SOC in the estuarine marshes which could not be reproduced under laboratory conditions. It remains questionable whether the starting CH_4 production in many samples under anaerobic conditions would take place under in-situ conditions, because tidal marshes are regularly supplied with substances suppressing methanogenesis like sulfate by inundation. Moreover, significantly lower turnover rates under anaerobic in comparison to aerobic conditions and in subsoil in comparison to topsoil samples indicate that increased carbon burial due to enhanced sea level rise could decrease the carbon turnover in the marsh soils.

The SOC storage in the marsh soils of the Elbe estuary appears comparably small, when looking at global carbon stocks of tidal wetland soils (Chmura et al., 2003). This is due to the small extent of the marsh area at the estuary. As the holocene sediments are of high depth, the calculated carbon stock only represents the uppermost part of the marshes and does not characterize the total carbon storage of these sites, which may be considerably larger. However, the spatial distribution of the carbon stocks reveals the importance of the tidal marsh soils, especially of the oligohaline zone, in the face of climate change and sea level rise. The SOC storage of the mineral marshes of the Elbe estuary might be small, especially in comparison with organogenic marsh soil common in North America, but due to steady sedimentation and low carbon turnover, the investigated soils can be regarded as potential carbon sinks.

The third part of this study addresses the anthropogenic input and the retention of trace metals in tidal marsh soils. The hypothesis that trace metal pools are decreasing with increasing salinity could be supported by the results of this study (Hypothesis 7). These results may be mainly attributed to the process of tidal mixing, since the retention capacity of the investigated soils can be considered high. High ff20 as well as SOC contents in soils of the study sites 1 and 2 in the oligohaline zone and high pH values in all sites support this conclusion (Hypothesis 8). Site 5 in the polyhaline zone may be affected to a higher extent by mobilization processes, due to its lower

concentrations in ff20 and SOC. However, only small amounts of trace metals are expected to be leached from the marsh soils due to chloro-complexation or competition for sorption sites under high salinity conditions, since mobilized metals are likely to be re-precipitated as insoluble metal sulfides in the anoxic parts of the soils (Du Laing et al., 2008a). Thus, sulfide concentration is presumably an important factor influencing the trace metal concentrations of the investigated marsh soil, in addition to the hypothesized factors grain size distribution, SOM content, and pH.

The hypothesis that trace metal concentrations and pools are decreasing with increasing elevation was not supported by the results of this study (Hypothesis 7). Higher metal pools in high marshes are likely related to the different age of the sampled horizons. In the younger low marshes the highly contaminated horizons might not have been reached within the investigated soil depth, due to high sedimentation and accretion rates in this elevation class (Butzeck et al., 2015). Differences in ff20 and SOM content between low and high marshes are probably not high enough to cause differences in metal retention with elevation.

In total, the investigated marsh soils can be considered as of low contamination level, since trace metal concentrations below target values are predominant in the studied marshes. Horizons with higher trace metal enrichments are usually providing a high retention capacity, inhibiting substantial mobilization and leaching from the soils. Consequently, this contamination represents a legacy from the past (Hypothesis 9). However, erosion and re-suspension of stronger contaminated horizons as a result of sea level rise or further river-engineering measures represent potential threats for the estuarine ecosystem in the future.

Finally, the examination of vertical trace metal distributions could be used as a method for the determination of sedimentation dynamics in the estuarine marshes (Hypothesis 10). The dating approach worked well in the selected profiles, but it was reaching its limits in the polyhaline zone, where concentrations were low, and in low marshes due to the shallow sampling depths. Trace metal concentrations in the suspended sediments could not be compared directly with concentrations in the soils. The knowledge of socioeconomic changes in the catchment area and background values of estuarine sediments were, however, useful indicators for the assessment of the marsh age.

The presented study stresses the importance of the investigated soil functions of tidal marsh ecosystems. These functions can be considered as valuable benefits for society (Barbier et al., 2011). Nevertheless, the overall value of estuarine marshes is based on the variety of ecosystem functions provided, not just single ones. Since soils form the basis of this important ecosystem, they are in need of special protection. Further loss of tidal marshes would lead to the degradation

of the Elbe estuary to a channel without much ecological value. Despite their relatively small extent, the Elbe marshes are representative for many mineral marshes around the world that provide valuable ecosystem functions and suffer under similar threats (Gedan et al., 2009). This study can, therefore, be considered a case study just around the corner where further investigations are necessary to get a complete picture of the important processes in these soils.

8 Outlook

The results of this study show the contribution of tidal marsh soils in geochemical processes like carbon cycling and trace metal retention. The study provides a quantification of carbon pools and a basis for the differentiation between allochthonous and autochthonous carbon input. $\delta^{13}C$ ratios can provide further information about the carbon input, but also about decomposition processes in soils. Since $\delta^{13}C$ was only measured on few samples, the results did not allow a distinct determination of mineralization processes. Therefore, carbon isotope ratios should be determined from a broader variety of samples, to distinguish different autochthonous (C3 and C4 plants) and allochthonous carbon sources (marine algae, fluvial algae, and suspended organic matter) from mineralization.

Although, the results of this study suggest that the investigated tidal marsh soils seem to have the potential to act as a carbon sink, an uncertainty remains. Future studies should, therefore, aim at calculating carbon budgets for tidal marshes. Such an attempt requires further data, including above- and below-ground biomass from the very same plots of soil sampling, the amount of litter effectively incorporated in the soil, up to date measurements of allochthonous OC in fresh sediments, DIC and DOC concentrations, and in-situ CO_2 and CH_4 fluxes. In order to understand the underlying processes further measurements are required. Even though a low CH_4 production was found in the incubation experiment, the actual emissions could be of interest especially in low marshes of the oligohaline zone (e.g. site 1). Whether these marshes are effective carbon sinks, due to lower turnover under anaerobic conditions, or carbon sources, due to a low CH_4 oxidation capacity in the reduced soils, should be investigated using in-situ measurement techniques, e.g. chamber measurements or eddy covariance systems.

Additionally, long-term incubation experiments could be conducted to differentiate between labile and stable carbon pool fractions. The experiments should include soil samples as well as fresh sediments and biomass to account for the decomposability of the different C sources (allochthonous and autochthonous). The effect of climate change and predicted sea level rise could be taken into consideration by exposing the samples to different temperatures, soil moisture contents, and salinities. Furthermore, the contribution of microbial respiration and carbonate dissolution to total CO_2 production should be identified. This distinction could be made by measuring the $\delta^{13}C$ of the emitted CO_2 according to Ramnarine et al. (2012). Such an extensive data set could be used to predict carbon turnover of tidal marshes in the future by applying a carbon decomposition model (Andrén and Kätterer, 1997; Knoblauch et al., 2013).

While land use is usually regarded as an important factor for carbon dynamics of marsh soils (e.g. Ford et al., 2012; Vanselow-Algan, 2008), it did not have a distinct effect on the SOC pools of the investigated marshes. However, due to different land use treatments in the different study sites an effect of agricultural management could not be taken into account. A high scatter in the SOC pools within the different study sites may have prevented a significant difference between managed and unmanaged marshes. Therefore, a higher number of replicates (sites, plots, and treatments) should be considered in future studies. The effects of grazing or drainage on C turnover and sequestration should be taken into account and sustainable management plans should be developed for these vulnerable ecosystems.

The determination of trace metal pools and distributions is a beginning towards the characterization of the metal retention function of local marsh soils. Future studies should focus on the underlying processes of mobilization by measuring trace metal concentrations in different fractions using a sequential extraction technique (compare Guo et al., 1997). In order to assess the influence of redox processes on the behavior of metals in the investigated soils, an additional laboratory experiment could be conducted to compare the extractable fractions under aerobic and anaerobic conditions. To differentiate whether trace metal concentrations in these soils are mainly controlled by mobilization or input, suspended sediments in the flooding water above the respective marsh surface should be sampled (according to Temmerman et al. (2003) or Butzeck et al. (2015)) and analyzed for its metal fractions. This will allow for the determination of spatial differences between the tidal marsh area and the river, and of temporal differences related to seasons or single events like storm tides.

The long-term shift in trace metal input, due to measures taken up to improve the water quality of the river Elbe, was related to the vertical trace metal distribution in the marsh soils. The presented dating method constitutes a good estimate of the approximate marsh age of the investigated profiles. Future studies, aiming at the precise determination of the soil age and the calculation of carbon sequestration rates, should be supplemented with an additional dating approach, e.g. radionuclide dating. Also, the distribution of organic pollutants in soils could be tested for its suitability as a dating method, since these substances are man-made and do not have natural background concentrations. Therefore, parent material deposited before the start of production of a specific pollutant in the Elbe catchment, should be free of the respective substance. In this context, organotin compounds could be of interest, which were introduced to the marine environment as a component of antifouling paints in the early 1960s (Kuballa, 1994). However, all of these dating methods require an estimation of mobilization and decomposition processes to avoid misinterpretation of the results.

The profound knowledge of the underlying processes of carbon cycling and trace metal retention is of vital importance in the face of predicted sea level rise and future human impacts. In order to develop sustainable management strategies for the vulnerable tidal marsh ecosystems along the Elbe estuary, these ecosystem functions should be taken into account.

References

Abril, G., Nogueira, M., Etcheber, H., Cabeçadas, G., Lemaire, E., Brogueira, M.J., 2002. Behaviour of Organic Carbon in Nine Contrasting European Estuaries. Estuarine, Coastal and Shelf Science 54, 241-262.

Ackermann, F., Bergmann, H., Schleichert, U., 1983. Monitoring of heavy metals in coastal and estuarine sediments - a question of grain-size: <20 μm versus <60 μm. Environmental Technology Letters 4, 317-328.

Ackermann, F., Stammerjohann, D., 1997. Heavy metal contamination in the sediment of the Mühlenberger Loch: (an artificial embayment in the tidal River Elbe). Temporal development ("annual Layers") and overall balance; sediment core annalysis (Report), BfG-1017e. Bundesanstalt für Gewässerkunde, Koblenz, Germany.

Acosta, J.A., Jansen, B., Kalbitz, K., Faz, A., Martínez-Martínez, S., 2011. Salinity increases mobility of heavy metals in soils. Chemosphere 85, 1318-1324.

Ad-hoc-AG Boden, 2005. Bodenkundliche Kartieranleitung, 5. ed, Hannover, Germany.

Alvim Ferraz, M.C.M., Lourenço, J.C.N., 2000. The Influence of Organic Matter Content of Contaminated Soils on the Leaching Rate of Heavy Metals. Environmental Progress 19, 53-58.

Amann, T., Weiss, A., Hartmann, J., 2012. Carbon dynamics in the freshwater part of the Elbe estuary, Germany: Implications of improving water quality. Estuarine, Coastal and Shelf Science 107, 112-121.

Andrén, O., Kätterer, T., 1997. ICBM: The introductory carbon balance model for exploration of soil carbon balances. Ecological Applications 7, 1226-1236.

Andresen, J., 1996. Eigenschaften der Feststoff- und Lösungsphase von Aussendeichsböden der Unterelbe. Hamburger Bodenkundliche Arbeiten, Hamburg, Germany.

ARGE ELBE, 1997. Die Wassergüte der Elbe im Jahre 1997 (Report). Arbeitsgemeinschaft für die Reinhaltung der Elbe, Hamburg, Germany.

ARGE ELBE, 2001. Die Wassergüte der Elbe im Jahre 2001 (Report). Arbeitsgemeinschaft für die Reinhaltung der Elbe, Hamburg, Germany.

Bahadir, M., Parlar, H., Spiteller, M., 2000. Springer Umweltlexikon. Springer Verlag, Berlin & Heidelberg, Germany.

Barbier, E.B., Hacker, S.D., Kennedy, C., Koch, E.W., Stier, A., Silliman, B.R., 2011. The value of estuarine and coastal ecosystem services. Ecological Monographs 81, 169-193.

Bartlett, K.B., Bartlett, D.S., Harriss, R.C., Sebacher, D.I., 1987. Methane emissions along a salt marsh salinity gradient. Biogeochemistry 4, 183-202.

Batjes, N.H., 1996. Total carbon and nitrogen in the soils of the world. European Journal of Soil Science 47, 151-163.

References

Bazelmans, J., Meier, D., Nieuwhof, A., Spek, T., Vos, P., 2012. Understanding the cultural historical value of the Wadden Sea region. The co-evolution of environment and society in the Wadden Sea area in the Holocene up until early modern times (11,700 BC - 1800 AD): An outline. Ocean & Coastal Management 68, 114-126.

BBodSchV, 1999. Bundes-Bodenschutz- und Altlastenverordnung vom 12. Juli 1999 (BGBl. I S. 1554), die zuletzt durch Artikel 5 Absatz 31 des Gesetzes vom 24. Februar 2012 (BGBl. I S. 212) geändert worden ist.

Beaumont, N.J., Jones, L., Garbutt, A., Hansom, J.D., Toberman, M., 2014. The value of carbon sequestration and storage in coastal habitats. Estuarine, Coastal and Shelf Science 137, 32-40.

Bennett, E.M., Peterson, G.D., Gordon, L.J., 2009. Understanding relationships among multiple ecosystem services. Ecology Letters 12, 1394-1404.

Bergemann, M., 2004a. Die Trübungszone in der Tideelbe - Beschreibung der räumlichen und zeitlichen Entwicklung (Report). Wassergütestelle Elbe, Hamburg, Germany.

Bergemann, M., 2004b. Gewässergütebericht der Elbe 2003 (Report). Arbeitsgemeinschaft für die Reinhaltung der Elbe, Hamburg, Germany.

Bergemann, M., 2005. Berechnung des Salzgehaltes der Elbe (Report). Wassergütestelle Elbe, Hamburg, Germany.

Bergemann, M., pers. comm. Email of Michael Bergemann, Behörde für Stadtentwicklung und Umwelt, 12.11.2014.

Bergemann, M., Gaumert, T., 2006. Gewässergütebericht der Elbe 2005 (Report). Arbeitsgemeinschaft für die Reinhaltung der Elbe, Hamburg, Germany.

Bergemann, M., Gaumert, T., 2008a. Gewässergütebericht der Elbe 2006 (Report). Arbeitsgemeinschaft für die Reinhaltung der Elbe, Hamburg, Germany.

Bergemann, M., Gaumert, T., 2008b. Gewässergütebericht der Elbe 2007. Ergebnisse der überblicksweisen Überwachung (Report). Arbeitsgemeinschaft für die Reinhaltung der Elbe, Hamburg, Germany.

Bergemann, M., Gaumert, T., 2010. Elbebericht 2008. Ergebnisse des nationalen Überwachungsprogramms Elbe der Bundesländer über den ökologischen und chemischen Zustand der Elbe nach EG-WRRL sowie der Trendentwicklung von Stoffen und Schadstoffgruppen (Report). Flussgebietsgemeinschaft Elbe, Hamburg, Germany.

Bergemann, M., Gaumert, T., Stachel, B., 2005. Gewässergütebericht der Elbe 2004 (Report). Arbeitsgemeinschaft für die Reinhaltung der Elbe, Hamburg, Germany.

Bergemann, M., Stachel, B., 2004. Gewässergütebericht der Elbe 2002 (Report). Arbeitsgemeinschaft für die Reinhaltung der Elbe, Hamburg, Germany.

BfG, 2004. Methode der Umweltrisikoeinschätzung und FFH-Verträglichkeitseinschätzung für Projekte an Bundeswasserstraßen - Ein Beitrag zur Bundesverkehrswegeplanung (Report), BfG Mitteilungen Nr. 26. Bundesanstalt für Gewässerkunde, Koblenz, Germany.

BfG, 2008. WSV-Sedimentmanagement Tideelbe - Strategien und Potenziale - eine Systemstudie. Ökologische Auswirkungen der Umlagerung von Wedeler Baggergut. Untersuchung im Auftrag des Wasser- und Schifffahrtsamtes Cuxhaven (Report), BfG-1584. Bundesanstalt für Gewässerkunde, Koblenz, Germany.

Blum, L.K., 1993. *Spartina alterniflora* root dynamics in a Virginia marsh. Marine Ecology Progress Series 102, 169-178.

Blume, H.-P., Brümmer, G., 1991. Prediction of Heavy Metal Behavior in Soil by Means of Simple Field Tests. Ecotoxicology and Environmental Safety 22, 164-174.

Blume, H.-P., Stahr, K., Leinweber, P., 2011. Bodenkundliches Praktikum - Eine Einführung in pedologisches Arbeiten für Ökologen, insbesondere Land- und Forstwirte, und für Geowissenschaftler. Spektrum Akademischer Verlag, Heidelberg, Germany.

Boehlich, M.J., Strotmann, T., 2008. The Elbe Estuary. Die Küste 74, 288-306.

Bouchard, V., Lefeuvre, J.-C., 2000. Primary production and macro-detritus dynamics in a European salt marsh: carbon and nitrogen budgets. Aquatic Botany 67, 23-42.

Bridgham, S.D., Megonigal, J.P., Keller, J.K., Bliss, N.B., Trettin, C., 2006. The carbon balance of North American wetlands. Wetlands 26, 889-916.

BSH, 2009. Gezeitenkalender 2010. Hoch- und Niedrigwasserzeiten für die Deutsche Bucht und deren Flussgebiete. Bundesamt für Seeschifffahrt und Hydrographie, Hamburg, Germany.

BSU, HPA, 2011. Projekt "ELSA" Schadstoffsanierung Elbsedimente. Jahresbericht 2010 (Report). Behörde für Stadtentwicklung und Umwelt; Hamburg Port Authority, Hamburg, Germany.

Burden, A., Garbutt, R.A., Evans, C.D., Jones, D.L., Cooper, D.M., 2013. Carbon sequestration and biogeochemical cycling in a saltmarsh subject to coastal managed realignment. Estuarine, Coastal and Shelf Science 120, 12-20.

Butzeck, C., Eschenbach, A., Gröngröft, A., Hansen, K., Nolte, S., Jensen, K., 2015. Sediment deposition and accretion rates in tidal marshes are highly variable along estuarine salinity and flooding gradients. Estuaries and Coasts 38, 434-450.

Butzeck, C.E.G., 2014. Tidal marshes of the Elbe estuary: spatial and temporal dynamics of sedimentation and vegetation, Dissertation im Fachbereich Biologie der Fakultät für Mathematik, Informatik und Naturwissenschaften. Universität Hamburg, Hamburg, Germany.

Callaway, J.C., DeLaune, R.D., Patrick Jr., W.H., 1996. Chernobyl 137Cs used to determine sediment accretion rates at selected northern European coastal wetlands. Limnology and Oceanography 41, 444-450.

Chambers, L.G., Osborne, T.Z., Reddy, K.R., 2013. Effects of salinity-altering pulsing events on soil organic carbon loss along an intertidal wetland gradient: a laboratory experiment. Biogeochemistry 115, 363-383.

References

Chanton, J.P., Whiting, G.J., 1995. Trace gas exchange in freshwater and coastal marine ecosystems: ebullition and transport by plants, in: Matson, P.A., Harriss, R.C. (Eds.), Biogenic Trace Gases: Measuring Emissions from Soil and Water. Blackwell Science Ltd., Cambridge, UK.

Chen, S., Torres, R., 2012. Effects of Geomorphology on the Distribution of Metal Abundance in Salt Marsh Sediment. Estuaries and Coasts 35, 1018-1027.

Chenu, C., Plante, A.F., 2006. Clay-sized organo-mineral complexes in a cultivation chronosequence: revisiting the concept of the'primary organo-mineral complex'. European Journal of Soil Science 57, 596-607.

Chmura, G.L., Anisfeld, S.C., Cahoon, D.R., Lynch, J.C., 2003. Global carbon sequestration in tidal, saline wetland soils. Global Biogeochemical Cycles 17, 1111.

Chmura, G.L., Kellman, L., Guntenspergen, G.R., 2011. The greenhouse gas flux and potential global warming feedbacks of a northern macrotidal and microtidal salt marsh. Environmental Research Letters 6.

Christensen, T.H., 1984. Cadmium soil sorption at low concentrations: I. Effect of time, cadmium load, pH, and calcium. Water, Air, & Soil Pollution 21, 105-114.

Christiansen, C., Bartholdy, J., Kunzendorf, H., 2002. Effects of morphological changes on metal accumulation in a salt marsh sediment of the Skallingen peninsula, Denmark. Wetlands Ecology and Management 10, 11-23.

Conrads, H., Bisharat, R., Ingwersen, J., Streck, T., 2011. Anpassung der Barometrischen Prozess-Separation (BaPS) für die Anwendung in kalkhaltigen Böden. Berichte der DBG.

Craft, C., 2007. Freshwater input structures soil properties, vertical accretion, and nutrient accumulation of Georgia and U.S. tidal marshes. Limnology and Oceanography 52, 1220-1230.

Craig, J.K., Crowder, L.B., 2000. Factors influencing habitat selection in fishes with a review of marsh ecosystems, in: Weinstein, M.P., Kreeger, D.A. (Eds.), Concepts and Controversies in Tidal Marsh Ecology. Kluwer Academic Publishers, Dordrecht, The Netherlands, pp. 241-266.

De Groot, R.S., Wilson, M.A., Boumans, R.M.J., 2002. A typology for the classification, description and valuation of ecosystem functions, goods and services. Ecological Economics 41, 393-408.

Dijkema, K.S., 1990. Salt and Brackish Marshes Around the Baltic Sea and Adjacent Parts of the North Sea: Their Vegetation and Management. Biological Conservation 51, 191-209.

DIN ISO 10694, 1996. Bodenbeschaffenheit - Bestimmung von organischem Kohlenstoff und Gesamtkohlenstoff nach trockener Verbrennung (Elementaranalyse) (ISO 10694:1995).

DIN ISO 11277, 2002. Bodenbeschaffenheit - Bestimmung der Partikelgrößenverteilung in Mineralböden - Verfahren mittels Siebung und Sedimentation (ISO 11277:1998 + ISO 11277: 1998 Corrigendum 1:2002.

DIN ISO 11466, 1997. Bodenbeschaffenheit - Extraktion in Königswasser löslicher Spurenelemente (ISO 11466:1995).

Du Laing, G., De Meyer, B., Meers, E., Lesage, E., Van de Moortel, A., Tack, F.M.G., Verloo, M.G., 2008a. Metal accumulation in intertidal marshes: Role of sulphide precipitation. Wetlands 28, 735-746.

Du Laing, G., De Vos, P., Vandecasteele, B., Lesage, E., Tack, F.M.G., Verloo, M.G., 2008b. Effect of salinity on heavy metal mobility and availability in intertidal sediments of the Scheldt estuary. Estuarine, Coastal and Shelf Science 77, 589-602.

Du Laing, G., Meers, E., Dewispelaere, M., Rinklebe, J., Vandecasteele, B., Verloo, M.G., Tack, F.M.G., 2009a. Effect of Water Table Level on Metal Mobility at Different Depths in Wetland Soils of the Scheldt Estuary (Belgium). Water, Air, & Soil Pollution 202, 353-367.

Du Laing, G., Meers, E., Dewispelaere, M., Vandecasteele, B., Rinklebe, J., Tack, F.M.G., Verloo, M.G., 2009b. Heavy metal mobility in intertidal sediments of the Scheldt estuary: Field monitoring. Science of the Total Environment 407, 2919-2930.

Du Laing, G., Rinklebe, J., Vandecasteele, B., Meers, E., Tack, F.M.G., 2009c. Trace metal behaviour in estuarine and riverine floodplain soils and sediments: A review. Science of the Total Environment 407, 3972-3985.

Du Laing, G., Van de Moortel, A., Moors, W., De Grauwe, P., Meers, E., Tack, F.M.G., Verloo, M.G., 2009d. Factors affecting metal concentrations in reed plants (Phragmites australis) of intertidal marshes in the Scheldt estuary. Ecological Engineering 35, 310-318.

Du Laing, G., Van Ryckegem, G., Tack, F.M.G., Verloo, M.G., 2006. Metal accumulation in intertidal litter through decomposing leaf blades, sheaths and stems of *Phragmites australis*. Chemosphere 63, 1815-1823.

Du Laing, G., Vanthuyne, D.R.J., Vandecasteele, B., Tack, F.M.G., Verloo, M.G., 2007. Influence of hydrological regime on pore water metal concentrations in a contaminated sediment-derived soil. Environmental Pollution 147, 615-625.

Duffus, J.H., 2002. "Heavy metals" - a meaningless term? Pure and Applied Chemistry 74, 793-807.

Dutta, K., Schuur, E.A.G., Neff, J.C., Zimov, S.A., 2006. Potential carbon release from permafrost soils of Northeastern Siberia. Global Change Biology 12, 2336-2351.

Duve, J., 1999. Bilanzierung des Stoffaustausches zwischen Elbe und Deichvorland am Beispiel zweier tidebeeinflusster Untersuchungsgebiete. Hamburger Bodenkundliche Arbeiten, Hamburg, Germany.

DWD, 2013. Deutscher Wetterdienst, http://www.dwd.de (access date: 27.03.2013).

Elsey-Quirk, T., Seliskar, D.M., Sommersfield, C.K., Gallagher, J.L., 2011. Salt Marsh Carbon Pool Distribution in a Mid-Atlantic Lagoon, USA: Sea Level Rise Implications. Wetlands 31, 87-99.

Ember, L.M., Williams, D.F., Morris, J.T., 1987. Processes that influence carbon isotope variations in salt marsh sediments. Marine Ecology Progress Series 36, 33-42.

Engels, J.G., Jensen, K., 2009. Patterns of wetland plant diversity along estuarine stress gradients of the Elbe (Germany) and Connecticut (USA) Rivers. Plant Ecology & Diversity 2, 301-311.

References

Eswaran, H., Van den Berg, E., Reich, P., 1993. Organic carbon in soils of the world. Soil Science Society of America Journal 57, 192-194.

EU WFD, 2000. RICHTLINIE 2000/60/EG DES EUROPÄISCHEN PARLAMENTS UND DES RATES vom 23. Oktober 2000 zur Schaffung eines Ordnungsrahmens für Maßnahmen der Gemeinschaft im Bereich der Wasserpolitik, Amtsblatt der Europäischen Union L 327.

EU WFD, 2008. RICHTLINIE 2008/105/EG DES EUROPÄISCHEN PARLAMENTS UND DES RATES vom 16. Dezember 2008 über Umweltqualitätsnormen im Bereich der Wasserpolitik und zur Änderung und anschließenden Aufhebung der Richtlinien des Rates 82/176/EWG, 83/513/EWG, 84/156/EWG, 84/491/EWG und 86/280/EWG sowie zur Änderung der Richtlinie 2000/60/EG, Amtsblatt der Europäischen Union L 348/84.

Evans, L.J., 1989. Chemistry of metal retention by soils. Environmental Science & Technology 23, 1046-1056.

FAO, 2006. World reference base for soil resources 2006. A framework for international classification, correlation and communication. World Soil Resources Reports 103, Rome, Italy.

FGG Elbe, 2014. Flussgebietsgemeinschaft Elbe, http://www.fgg-elbe.de (access date: 12.11.2014).

Figge, K., 1980. Das Elbe-Urstromtal im Bereich der Deutschen Bucht (Nordee). Eiszeitalter und Gegenwart 30, 203-211.

Ford, H., Garbutt, A., Jones, L., Jones, D.L., 2012. Methane, carbon dioxide and nitrous oxide fluxes from a temperate salt marsh: Grazing management does not alter Global Warming Potential. Estuarine, Coastal and Shelf Science 113, 182-191.

Förstner, U., Heise, S., Schwartz, R., Westrich, B., Ahlf, W., 2004. Historical Contaminated Sediments and Soils at the River Basin Scale. Examples from the Elbe River Catchment Area. Journal of Soils and Sediment 4, 247-260.

Förstner, U., Schoer, J., Knauth, H.-D., 1990. Metal Pollution in the Tidal Elbe River. The Science of the Total Environment 97/98, 347-368.

Frohne, T., Rinklebe, J., Diaz-Bone, R.A., Du Laing, G., 2011. Controlled variation of redox conditions in a floodplain soil: Impact on metal mobilization and biomethylation of arsenic and antimony. Geoderma 160, 414-424.

Frohne, T., Rinklebe, J., Langer, U., Du Laing, G., Mothes, S., Wennrich, R., 2012. Biogeochemical factors affecting mercury methylation rate in two contaminated floodplain soils. Biogeoscience 9, 493-507.

Garcia, J.-L., Patel, B.K.C., Ollivier, B., 2000. Taxonomic, Phylogenetic, and Ecological Diversity of Methanogenic Archaea. Anaerobe 6, 205-226.

Gedan, K.B., Silliman, B.R., Bertness, M.D., 2009. Centuries of Human-Driven Change in Salt Marsh Ecosystems. Annual Review of Marine Science 1, 117-141.

Gerringa, L.J.A., De Baar, H.J.W., Nolting, R.F., Paucot, H., 2001. The influence of salinity on the solubility of Zn and Cd sulphides in the Scheldt estuary. Journal of Sea Research 46, 201-211.

Gerth, J., Schimming, C.G., Brümmer, G., 1981. Einfluß der Chloro-Komplexbildung auf Löslichkeit und Adsorption von Nickel, Zink und Cadmium. Mitteilungen der Deutschen Bodenkundlichen Gesellschaft 30, 19-30.

Giani, L., Dittrich, K., Martsfeld-Hartmann, A., Peters, G., 1996. Methanogenesis in saltmarsh soils of the North Sea coast of Germany. European Journal of Soil Science 47, 175-182.

Giani, L., Gebhardt, H., 1984. Zur Pedogenese und Klassifikation von Marschböden des Unterweserraumes II. Die Bedeutung von Schwefelmetabolismus, Methanproduktion und Ca/Mg-Verhältnis für die Marschen-Klassifikation. Zeitschrift für Pflanzenernährung und Bodenkunde 147, 704-715.

Giani, L., Landt, A., 2000. Initiale Marschbodenentwicklung aus brackigen Sedimenten des Dollarts an der südwestlichen Nordseeküste. Journal of Plant Nutrition and Soil Science 163, 549-553.

Gibbard, P.L., Rose, J., Bridgland, D.R., 1988. The History of the Great Northwest European Rivers During the Past Three Million Years. Philosophical Transactions of the Royal Society of London. Series B, Biological Science 318, 559-602.

Gönnert, G., Jensen, J., Von Storch, H., Thumm, S., Wahl, T., Wiese, R., 2009. Der Meeresspiegelanstieg. Ursachen, Tendenzen und Risikobewertung. Die Küste 76, 225-256.

Grabemann, H.-J., Grabemann, I., Müller, A., 2005. Die Auswirkungen eines Klimawandels auf Hydrografie und Gewässergüte der Unterweser, in: Schuchardt, B., Schirmer, M. (Eds.), Klimawandel und Küste. Die Zukunft der Unterweserregion, Berlin and Heidelberg, Germany, pp. 59-77.

Gren, I.-M., Folke, C., Turner, K., Batemen, I., 1994. Primary and Secondary Values of Wetland Ecosystems. Environmental and Resource Economics 4, 55-74.

Groffman, P.M., Hanson, G.C., Kiviat, E., Stevens, G., 1996. Variation in Microbial Biomass and Activity in Four Different Wetland Types. Soil Science Society of America Journal 60, 622-629.

Gröngröft, A., pers. comm. Personal conversation with Dr. Alexander Gröngröft, Institute of Soil Science, Universität Hamburg, 06.03.2015.

Gröngröft, A., Grabowsky, K., Schwank, S., 2006. Anpassung der Fahrrinne der Unter- und Außenelbe an die Containerschifffahrt. Planfeststellungsunterlage nach Bundeswasserstraßengesetzt, Umweltverträglichkeitsuntersuchung, Teilgutachten zum Schutzgut Wasser, Teilbereich Sedimente (Schadstoffgehalte und -freisetzung). (Report). Projektbüro Fahrrinnenanpassung von Unter- und Außenelbe für Wasser- und Schiffahrtsverwaltung des Bundes, Wasser- und Schiffahrtsamt Hamburg; Freie und Hansestadt Hamburg, Hamburg Port Authority, Hamburg, Germany.

Gröngröft, A., Jähnig, U., Miehlich, G., Lüschow, R., Maass, V., Stachel, B., 1998. Distribution of Metals in Sediments of the Elbe Estuary in 1994. Water Science and Technology 37, 109-116.

Gröngröft, A., Krüger, F., Grunewald, K., Meißner, R., Miehlich, G., 2005. Plant and Soil Contamination with Trace Metals in the Elbe Floodplains: A Case Study after the Flood in August 2002. Acta hydrochimica et hydrobiologica 33, 466-474.

Großkopf, G., 1992. Küstenschutz und Binnenentwässerung zwischen Weser und Elbe, in: Kramer, J., Rohde, H. (Eds.), Historischer Küstenschutz – Deichbau, Inselschutz und Binnenentwässerung an Nord-

und Ostsee. Deutscher Verband für Wasserwirtschaft und Kulturbau e.V., Verlag Konrad Wittwer, Stuttgart, Germany.

Grüttner, H., 1992. Deichschutz und Binnenentwässerung der schleswig-holsteinischen Elbmarschen, in: Kramer, J., Rohde, H. (Eds.), Historischer Küstenschutz - Deichbau, Inselschutz und Binnenentwässerung an Nord- und Ostsee. Deutscher Verband für Wasserwirtschaft und Kulturbau e.V., Verlag Konrad Wittwer, Stuttgart, Germany.

Guo, T., DeLaune, R.D., Patrick Jr., W.H., 1997. The Influence of Sediment Redox Chemistry on Chemically Active Forms of Arsenic, Cadmium, Chromium, and Zink in Estuarine Sediment. Environment International 23, 305-316.

Hansen, K., Butzeck, C., Eschenbach, A., Gröngröft, A., Jensen, K., Pfeiffer, E.-M., in prep. Factors influencing the organic carbon pools in tidal marsh soils of the Elbe estuary (Germany).

Hassink, J., 1997. The capacity of soils to preserve organic C and N by their association with clay and silt particles. Plant and Soil 191, 77-87.

Hedges, J.I., Keil, R.G., Benner, R., 1997. What happens to terrestrial organic matter in the ocean? Organic Geochemistry 27, 195-212.

Heise, S., Claus, E., Heininger, P., Krämer, T., Krüger, F., Schwartz, R., Förstner, U., 2005. Studie zur Schadstoffbelastung der Sedimente im Elbeeinzugsgebiet. Ursachen und Trends. (Report). Hamburg Port Authority, Hamburg, Germany.

Heise, S., Krüger, F., Barborowski, M., Stachel, B., Götz, R., Förstner, U., 2007. Bewertung der Risiken durch Feststoffgebundene Schadstoffe im Elbeeinzugsgebiet. Im Auftrag der Flussgebietsgemeinschaft Elbe und Hamburg Port Authority (Report). Beratungszentrum für integriertes Sedimentmanagement (BIS/TuTech) an der TU Hamburg-Harburg, Hamburg, Germany.

Hemminga, M.A., Buth, G.J.C., 1991. Decomposition in salt marsh ecosystems of the S.W. Netherlands: the effects of biotic and abiotic factors. Vegetatio 92, 73-83.

Hoffmann, D., 1992. Erdgeschichtliche Entwicklung der Küstengebiete an Nord- und Ostsee, in: Kramer, J., Rohde, H. (Eds.), Historischer Küstenschutz - Deichbau, Inselschutz und Binnenentwässerung an Nord- und Ostsee. Deutscher Verband für Wasserwirtschaft und Kulturbau e.V., Verlag Konrad Wittwer, Stuttgart, Germany, pp. 1-16.

Hoffmann, D., 2004. Holocene landscape development in the marshes of the West Coast of Schleswig-Holstein, Germany. Quarternary International 112, 29-36.

Holmer, M., Kristensen, E., 1994. Coexistence of sulfate reduction and methane production in an organic-rich sediment. Marine Ecology Progress Series 107, 177-184.

Hulisz, P., Gonet, S.S., Giani, L., Markiewicz, M., 2013. Chronosequential alterations in soil organic matter during initial development of coastal salt marsh soils at the southern North Sea. Zeitschrift für Geomorphologie 57, 515-529.

IKSE, 2005. Die Elbe und ihr Einzugsgebiet. Ein geographisch-hydrologischer und wasserwirtschaftlicher Überblick (Report). Internationale Kommission zum Schutz der Elbe, Magdeburg, Germany.

IKSE, 2010. Die Elbe ist wieder ein lebendiger Fluss. Abschlussbericht Aktionsprogramm Elbe 1996-2010 (Report). Internationale Kommission zum Schutz der Elbe, Magdeburg, Germany.

IPCC, 2013. Climate Change 2013: The Physical Science Basis. Contirbution of Working Group I to the Fifth Assesment Report of the Intergovernmental Panel on Climate Change, in: Stocker, T.F., Qin, D., Plattner, G.-K., Tigor, M., Allen, S.K., Boschung, J., Nauels, A., Xia, Y., Bex, V., Midgley, P.M. (Eds.). Intergovernmental Panel on Climate Change, Cambridge, UK and New York, USA.

Janetzko, P., 1977. Das Entwässerungssystem von Stör und Kremperau in der jüngeren Nacheiszeit im Bereich der Krempermarsch (Schleswig-Holstein). Schriften des Naturwissenschaftlichen Vereins für Schlewig-Holstein 47, 63-70.

Jobbágy, E.G., Jackson, R.B., 2000. The vertical distribution of soil organic carbon and its relation to climate and vegetation. Ecological Applications 10, 423-436.

Kabata-Pendias, A., 2011. Trace Elements in Soils and Plants. CRC Press, Boca Raton, USA.

Kalff, J., 2001. Limnology: Inland Water Ecosystems. Prentice Hall, Upper Saddle River, USA.

Kausch, H., 1996. Die Elbe- ein immer wieder veränderter Fluß, in: Lozán, J.L., Kausch, H. (Eds.), Warnsignale aus Flüssen und Ästuaren. Wissenschaftliche Fakten. Parey Buchverlag, Berlin, Germany, pp. 43-52.

Kerner, M., 2007. Effects of deepening the Elbe Estuary on sediment regime and water quality. Estuarine, Coastal and Shelf Science 75, 492-500.

King, G.M., Wiebe, W.J., 1980. Regulation of Sulfate Concentrations and Methanogenesis in Salt Marsh Soils. Estuarine and Coastal Marine Science 10, 215-223.

Kirwan, M.L., Megonigal, J.P., 2013. Tidal wetland stability in the face of human impacts and sea-level rise. Nature 504, 53-60.

Knoblauch, C., pers. comm. Personal conversation with Dr. Christian Knoblauch, Institute of Soil Science, Universität Hamburg, 04.03.2015.

Knoblauch, C., Beer, C., Sosnin, A., Wagner, D., Pfeiffer, E.-M., 2013. Predicting long-term carbon mineralization and trace gas production from thawing permafrost of Northeast Siberia. Global Change Biology 19, 1160-1172.

Kögel-Knabner, I., Guggenberger, G., Kleber, M., Kandeler, E., Kalbitz, K., Scheu, S., Eusterhues, K., Leinweber, P., 2008. Organo-mineral associations in temperate soils: Integrating biology, mineralogy, and organic matter chemistry. Journal of Plant Nutrition and Soil Science 171, 61-82.

Kowalik, C., Kraft, J., Einax, J.W., 2003. The Situation of the German Elbe Tributaries - Development of the Loads in the Last 10 Years. Acta hydrochimica et hydrobiologica 31, 334-345.

Kristensen, E., Holmer, M., 2001. Decomposition of plant materials in marine sediment exposed to different electron acceptors (O_2, NO_3^-, and SO_4^{2-}), with emphasis on substrate origin, degradation kinetics, and the role of bioturbation. Geochimica et Cosmochimica Acta 65, 419-433.

Krüger, F., Gröngröft, A., 2003. The Difficult Assessment of Heavy Metal Contamination of Soils and Plants in Elbe River Floodplains. Acta hydrochimica et hydrobiologica 31, 436-443.

Krüger, F., Meißner, R., Gröngröft, A., Grunewald, K., 2005. Flood Induced Heavy Metal and Arsenic Contamination of Elbe River Floodplain Soils. Acta hydrochimica et hydrobiologica 33, 455-465.

Kuballa, J., 1994. Einträge und Anwendungen von toxischen Organozinnverbindungen, in: Lozán, J.L., Rachor, E., Reise, K., V. Westernhagen, H., Lenz, W. (Eds.), Warnsignale aus dem Wattenmeer. Wissenschaftliche Fakten. Blackwell Wissenschafts-Verlag, Berlin, Germany, pp. 42-45.

Kuntze, H., 1965. Die Marschen - Schwere Böden in der landwirtschaftlichen Evolution. Nutzungs- und Verbesserungsmöglichkeiten schwieriger Standorte. Verlag Paul Parey, Hamburg and Berlin, Germany.

Lai, D.Y.F., 2009. Methane Dynamics in Northern Peatlands: A Review. Pedosphere 19, 409-421.

Lal, R., 2003. Soil erosion and the global carbon budget. Environment International 29, 437-450.

Laxen, D.P.H., 1985. Trace metal adsorption/coprecipitation on hydrous ferric oxide under realistic conditions. Water Research 19, 1229-1236.

Le Mer, J., Roger, P., 2001. Production, oxidation, emission and consumption of methane by soils: A review. European Journal of Soil Biology 37, 25-50.

Lichtfuß, R., 1977. Schwermetalle in den Sedimenten Schleswig-Holsteinischer Fliessgewässer - Untersuchungen zu Gesamtgehalten und Bindungsformen, Dissertation im Fachbereich Agrarwissenschaften. Christian-Albrecht-Universität zu Kiel, Kiel, Germany.

LLUR, 2011. Hintergrundwerte stofflich gering beeinflusster Böden Schleswig-Holsteins. (Report). Landesamt für Landwirtschaft, Umwelt und ländliche Räume des Landes Schleswig-Holstein, Flintbek, Germany.

Loomis, M.J., Craft, C.B., 2010. Carbon Sequestration and Nutrient (Nitrogen, Phosphorus) Accumulation in River-Dominated Tidal Marshes, Georgia, USA. Soil Science Society of America Journal 74, 1028-1036.

Lovley, D.R., Klug, M.J., 1986. Model for the distribution of sulfate reduction and methanogenesis in freshwater sediments. Geochimica et Cosmochimica Acta 50, 11-18.

Ludwig, J., pers. comm. Email of Jürgen Ludwig, Niedersächsischer Landesbetrieb für Wasserwirtschaft, Küsten- und Naturschutz, 11.06.2013.

MEA, 2003. Ecosystems and human well-being: a framework for assessment (Report). Conceptual Framework Working Group of the Millenium Ecosystem Assessment, Washington, USA.

Megonigal, J.P., Hines, M.E., Visscher, P.T., 2004. Anaerobic Metabolism: Linkages to Trace Gases and Aerobic Processes, in: Schlesinger, W.H. (Ed.), Biogeochemistry. Elsevier-Pergamon, Oxford, UK, pp. 317-424.

Meier, D., 1996. Besiedlungsgeschichte in den Flußmündungsgebieten am Beispiel der Eider und Elbe, in: Lozán, J.L., Kausch, H. (Eds.), Warnsignale aus Flüssen und Ästuaren. Wissenschaftliche Fakten. Parey Buchverlag, Berlin, Germany, pp. 19-23.

Meyercordt, J., 1992. Untersuchungen zum langjährigen Verlauf von Schwermetalldepositionen in ausgewählten schleswig-holsteinischen Salzmarschen auf der Basis von Radionuklidmessungen, Dissertation im Fachbereich Biologie der Fakultät für Mathematik, Informatik und Naturwissenschaften. Universität Hamburg, Geesthacht, Germany.

Middelburg, J.J., Herman, P.M.J., 2007. Organic matter processing in tidal estuaries. Marine Chemistry 106, 127-147.

Middelburg, J.J., Nieuwenhuize, J., Lubberts, R.K., van de Plassche, O., 1997. Organic Carbon Isotope Systematics of Coastal Marshes. Estuarine, Coastal and Shelf Science 45, 681-687.

Miehlich, G., Kiene, A., Gröngröft, A., Neuschmidt, O., Franke, S., Graack, G., 1997. Umweltverträglichkeitsuntersuchung zur Anpassung der Fahrrinne der Unter- und Außenelbe an die Containerschiffahrt; Marterialband V; Fachgutachten Schutzgut Boden. (Report). Planungsgruppe Ökologie + Umwelt Nord für Wasser- und Schiffahrtsverwaltung des Bundes, Wasser- und Schiffahrtsamt Hamburg; Freie und Hansestadt Hamburg, Amt Strom- und Hafenbau, Hamburg, Germany.

Millward, G.E., Liu, Y.P., 2003. Modelling metal desorption kinetics in estuaries. The Science of the Total Environment 314-316, 613-623.

Mitsch, W.J., Gosselink, J.G., 1993. Wetlands, 2nd ed, New York, USA.

Morris, J.T., Whiting, G.J., 1985. Gas advection in sediments of a South Carolina salt marsh. Marine Ecology Progress Series 27, 187-194.

Morrissey, E.M., Gillespie, J.L., Morina, J.C., Franklin, R.B., 2014. Salinity affects microbial activity and soil organic matter content in tidal wetlands. Global Change Biology 20.

Müller, F., 2013. Management effects on ecosystem functions of salt marshes: silica cycling and sedimentation processes, Dissertation im Fachbereich Biologie der Fakultät für Mathematik, Informatik und Naturwissenschaften. Universität Hamburg, Hamburg, Germany.

Müller, G., 1996. Schwermetalle und organische Schadstoffe in den Flußsedimenten, in: Lozán, J.L., Kausch, H. (Eds.), Warnsignale aus Flüssen und Ästuaren. Wissenschaftliche Fakten. Parey Buchverlag, Berlin, Germany, pp. 113-124.

Müller, G., Förstner, U., 1975. Heavy Metals in Sediments of the Rhine and Elbe Estuaries: Mobilization or Mixing Effects? Environmental Geology 1, 33-39.

Netzband, A., Reincke, H., Bergemann, M., 2002. The River Elbe: A Case Study for the Ecological and Economical Chain of Sediments. Journal of Soils and Sediment 2, 112-116.

Neubauer, S.C., 2008. Contribution of mineral and organic components to tidal freshwater marsh accretion. Estuarine, Coastal and Shelf Science 78, 78-88.

References

Neubauer, S.C., 2013. Ecosystem Responses of a Tidal Freshwater Marsh Experiencing Saltwater Intrusion and Altered Hydrology. Estuaries and Coasts 36.

Neubauer, S.C., Franklin, R.B., Berrier, D.J., 2013. Saltwater intrusion into tidal freshwater marshes alters the biogeochemical processing of organic carbon. Biogeosciences 10, 8171-8183.

Nyman, J.A., Walters, R.J., DeLaune, R.D., Patrick Jr., W.H., 2006. Marsh vertical accretion via vegetative growth. Estuarine, Coastal and Shelf Science 69, 370-380.

Odum, E.P., 2000. Tidal marshes as outwelling/pulsing systems, in: Weinstein, M.P., Kreeger, D.A. (Eds.), Concepts and Controversies in Tidal Marsh Ecology. Kluwer Academic Publishers, Dordrecht, The Netherlands, pp. 3-7.

Odum, W.E., 1988. Comparative Ecology of Tidal Freshwater and Salt Marshes. Annual Review of Ecology and Systematics 19, 147-176.

Olsen, Y.S., Dausse, A., Garbutt, A., Ford, H., Thomas, D.N., Jones, D.L., 2011. Cattle grazing drives nitrogen and carbon cycling in a temperate salt marsh. Soil Biology & Biochemistry 43, 531-541.

Oremland, R.S., Polcin, S., 1982. Methanogenesis and Sulfate Reduction: Competitive and Noncompetitive Substrates in Estuarine Sediments. Applied and Environmental Microbiology 44, 1270-1276.

Overesch, M., Rinklebe, J., Broll, G., Neue, H.-U., 2007. Metals and arsenic in soils and corresponding vegetation at Central Elbe river floodplains (Germany). Environmental Pollution 145, 800-812.

Paalman, M.A.A., Van der Weijden, C.H., Loch, J.P.G., 1994. Sorption of cadmium on suspended matter under estuarine conditions; competition and complexation with major sea-water ions. Water, Air, & Soil Pollution 73, 49-60.

Pfeiffer, E.-M., 1994. Methane Fluxes in Natural Wetlands (Marsh and Moor) in Northern Germany. Current Topics in Wetland Biogeochemistry 1, 36-47.

Pfeiffer, E.-M., 1998. Methanfreisetzung aus hydromorphen Böden verschiedener naturnaher und genutzter Feuchtgebiete (Marsch, Moor, Tundra, Reisanbau). Hamburger Bodenkundliche Arbeiten, Hamburg, Germany.

Plummer, L.N., Busenberg, E., 1982. The solubilities of calcite, aragonite and vaterite in CO_2-H_2O solutions between 0 and 90°C, and an evaluation of the aqueous model for the system $CaCO_3$-CO_2-H_2O. Geochimica et Cosmochimica Acta 46, 1011-1040.

Poffenbarger, H.J., Needelman, B.A., Megonigal, J.P., 2011. Salinity Influence on Methane Emissions from Tidal Marshes. Wetlands 31, 831-842.

Post, W.M., Emanuel, W.R., Zinke, P.J., Stangenberger, A.G., 1982. Soil carbon and world life zones. Nature 298, 156-159.

Prange, A., 1997. Geogene Hintergrundwerte und zeitliche Belastungsentwicklung. Abschlußbericht für den Zeitraum vom 1.9.1993 bis 30.9.1997 (Report). GKSS Forschungszentrum Geesthacht GmbH, Geesthacht, Germany.

Rainbow, P.S., 2006. Biomonitoring of trace metals in estuarine and marine environments. Australasian Journal of Ecotoxicology 12, 107-122.

Ramnarine, R., Wagner-Riddle, C., Dunfield, K.E., Voroney, R.P., 2012. Contributions of carbonates to soil CO_2 emissions. Canadian Journal of Soil Science 92, 599-607.

Reed, D.J., 2002. Sea-level rise and coastal marsh sustainability: geological and ecological factors in the Mississippi delta plain. Geomorphology 48, 233-243.

Reise, K., 2005. Coast of change: habitat loss and transformations in the Wadden Sea. Helgoland Marine Research 59, 9-21.

Rennert, T., Meißner, S., Rinklebe, J., Totsche, K.U., 2010. Dissolved Inorganic Contaminants in a Floodplain Soil: Comparison of In Situ Soil Solutions and Laboratory Methods. Water, Air, & Soil Pollution 209.

Rennert, T., Rinklebe, J., 2010. Release of Ni and Zn from Contaminated Floodplain Soils Under Saturated Flow Conditions. Water, Air, & Soil Pollution 205, 93-105.

Rinklebe, J., During, A., Overesch, M., Du Laing, G., Wennrich, R., Stärk, H.-J., Mothes, S., 2010. Dynamics of mercury fluxes and their controlling factors in large Hg-polluted floodplain areas. Environmental Pollution 158, 308-318.

Rinklebe, J., Franke, C., Neue, H.-U., 2007. Aggregation of floodplain soils based on classification principles to predict concentrations of nutrients and pollutants. Geoderma 141, 210-223.

Roberz, P., 2003. Flussvertiefungen contra Hochwasserschutz. Auswirkungen der Flussvertiefungen auf die Höhe der Wasserstände in den Unterläufen von Elbe, Weser und Ems (Report). WWF Deutschland, Frankfurt am Main, Germany.

Rupp, H., Rinklebe, J., Bolze, S., Meißner, R., 2010. A scale-dependent approach to study pollution control processes in wetland soils using three different techniques. Ecological Engineering 36, 1439-1447.

Ryan, M.G., Law, B.E., 2005. Interpreting, measuring, and modeling soil respiration. Biogeochemistry 73, 3-27.

Salomons, W., 1980. Adsorption processes and hydrodynamic conditions in estuaries. Environmental Technology Letters 1, 356-365.

Salomons, W., Mook, W.G., 1977. Trace metal concentrations in estuarine sediments: mobilization, mixing or precipitation. Netherlands Journal of Sea Research 11, 119-129.

Salomons, W., Mook, W.G., 1981. Field Observations of the Isotopic Composition of Particulate Organic Carbon in the Southern North Sea and Adjacent Estuaries. Marine Ecology 41, M11-M20.

Schädel, C., Schuur, E.A.G., Bracho, R., Elberling, B., Knoblauch, C., Lee, H., Lou, Y., Shaver, G.R., Turetsky, M.R., 2014. Circumpolar assessment of permafrost C quality and its vulnerability over time using long-term incubation data. Global Change Biology 20, 641-652.

Schaefer, M., 2003. Wörterbuch der Ökologie. Spektrum Akademischer Verlag, Heidelberg & Berlin, Germany.

Schirmer, M., 1994. Ökologische Konsequenzen des Ausbaus der Ästuare von Elbe und Weser, in: Lozán, J.L., Rachor, E., Reise, K., V. Westernhagen, H., Lenz, W. (Eds.), Warnsignale aus dem Wattenmeer. Wissenschaftliche Fakten. Blackwell Wissenschafts-Verlag GmbH, Berlin, Germany, pp. 164-175.

Schirmer, M., 1996. Das Klima und seine Bedeutung für Fluß-Ökosysteme, in: Lozán, J.L., Kausch, H. (Eds.), Warnsignale aus Flüssen und Ästuaren. Wissenschaftliche Fakten. Parey Buchverlag, Berlin, Germany, pp. 23-27.

Schirmer, M., Schuchardt, B., 1993. Klimaänderungen und ihre Folgen für den Küstenraum: Impaktfeld Ästuar, in: Schellnhuber, H.-J., Sterr, H. (Eds.), Klimaveränderung und Küste. Springer, Berlin, Germany, pp. 244-259.

Schoer, J.H., 1990. Determination of the Origin of Suspended Matter and Sediments in the Elbe Estuary Using Natural Tracers. Estuaries 13, 161-172.

Shaheen, S.M., Rinklebe, J., Rupp, H., Meissner, R., 2014. Lysimeter trials to assess the impact of different flood–dry-cycles on the dynamics of pore water concentrations of As, Cr, Mo and V in a contaminated floodplain soil. Geoderma 228-229, 5-13.

Sharma, P., Gardner, L.R., Moore, W.S., Bollinger, M.S., 1987. Sedimentation and bioturbation in a salt marsh as revealed by ^{210}Pb, ^{137}Cs, and ^{7}Be studies. Limnology and Oceanography 32, 313-326.

Sindowski, K.-H., 1979. Zwischen Jadebusen und Unterelbe. Sammlung Geologischer Führer. Gebrüder Borntraeger, Berlin and Stuttgart, Germany.

Six, J., Conant, R.T., Paul, E.A., Paustian, K., 2002. Stabilization mechanisms of soil organic matter: Implications for C-saturation of soils. Plant and Soil 241, 155-176.

Spencer, K.L., Cundy, A.B., Croudace, I.W., 2003. Heavy metal distribution and early-diagenesis in salt marsh sediments from the Medway Estuary, Kent, UK. Estuarine, Coastal and Shelf Science 57, 43-54.

Spohn, M., Babka, B., Giani, L., 2013. Changes in soil organic matter quality during sea-influenced marsh soil development at the North Sea coast. Catena 107, 110-117.

Spohn, M., Giani, L., 2012. Carbohydrates, carbon and nitrogen in soils of a marine and a brackish marsh as influenced by inundation frequency. Estuarine, Coastal and Shelf Science 107, 89-96.

Stachel, B., Lüschow, R., 1996. Entwicklung der Metallgehalte in Sedimenten der Tideelbe 1979 - 1994 (Report). Arbeitsgemeinschaft für die Reinhaltung der Elbe, Hamburg, Germany.

Stiller, G., 2009. Untersuchungen zur Ermittlung von Ursachen für die Variabilität von Makrophytenbeständen im Bearbeitungsgebiet der Tideelbe (Report), Hamburg, Germany.

Stock, M., Gettner, S., Hagge, H., Heinzel, K., Kohlus, J., Stumpe, H., 2005. Salzwiesen an der Westküste von Schleswig-Holstein 1988-2011 (Report), Schriftenreihe des Nationalparks Schleswig-Holsteinisches Wattenmeer. Landesamt für den Nationalpark Schleswig-Holsteinisches Wattenmeer, Heide, Germany.

Streif, H., 1993. Geologische Aspekte der Klimawirkungsforschung im Küstenraum der südlichen Nordsee, in: Schellnhuber, H.-J., Sterr, H. (Eds.), Klimaveränderung und Küste. Springer, Berlin, Germany, pp. 77-96.

Streif, H., 1996. Die Entwicklung der Küstenlandschaft und Ästuare im Eiszeitalter und in der Nacheiszeit, in: Lozán, J.L., Kausch, H. (Eds.), Warnsignale aus Flüssen und Ästuaren. Wissenschaftliche Fakten. Parey Buchverlag, Berlin, Germany, pp. 11-19.

Streif, H., 2004. Sedimentary record of Pleistocene and Holocene marine inundations along the North Sea coast of Lower Saxony, Germany. Quarternary International 112, 3-28.

Subke, J.-A., Heinemeyer, A., Reichstein, M., 2009. Experimental design: scaling up in time and space, and its statistical considerations, in: Kutsch, W.L., Bahn, M., Heinemeyer, A. (Eds.), Soil Carbon Dynamics: An Integrated Methodology. Cambridge University Press, Cambridge, UK.

Sutton-Grier, A.E., Keller, J.K., Koch, R., Gilmour, C., Megonigal, J.P., 2011. Electron donors and acceptors influence anaerobic soil organic matter mineralization in tidal marshes. Soil Biology & Biochemistry 43, 1576-1583.

Sutton-Grier, A.E., Megonigal, J.P., 2011. Plant species traits regulate methane production in freshwater wetland soils. Soil Biology & Biochemistry 43, 413-420.

Temmerman, S., Govers, G., Wartel, S., Meire, P., 2003. Spatial and temporal factors controlling short-term sedimentation in a salt and freshwater tidal marsh, Scheldt estuary, Belgium, SW Netherlands. Earth Surface Processes and Landforms 28, 739-755.

Temmerman, S., Meire, P., Bouma, T.J., Herman, P.M.J., Ysebaert, T., De Vriend, H., 2013. Ecosystem-based coastal defence in the face of global change. Nature 504, 79-83.

Teuchies, J., Jacobs, S., Oosterlee, L., Bervoets, L., Meire, P., 2013. Role of plants in metal cycling in a tidal wetland: Implications for phytoremidiation. Science of the Total Environment 445-446, 146-154.

Tobias, C., Neubauer, S.C., 2009. Salt Marsh Biogeochemistry - An Overview, in: Perillo, G.M.E., Wolanski, E., Cahoon, D.R., Brinson, M.M. (Eds.), Coastal Wetlands: An Integrated Ecosystem Approach. Elsevier B.V., pp. 445-492.

Valéry, L., Bouchard, V., Lefeuvre, J.-C., 2004. Impact of the Invasive Native Species *Elymus athericus* on Carbon Pools in a Salt Marsh. Wetlands 24, 268-276.

Valiela, I., Cole, M.L., McClelland, J., Hauxwell, J., Cebrian, J., Joye, S.B., 2000. Role of salt marshes as part of coastal landscapes, in: Weinstein, M.P., Kreeger, D.A. (Eds.), Concepts and Controversies in Tidal Marsh Ecology. Kluwer Academic Publishers, Dordrecht, The Netherlands, pp. 23-38.

Van der Nat, F.-J., Middelburg, J.J., 2000. Methane emissions from tidal freshwater marshes. Biogeochemistry 49, 103-121.

Vanselow-Algan, M.B., 2008. Auswirkung der Beweidung auf Vegetation, Bodeneigenschaften und mikrobiellen Kohlenstoffumsatz in einer Vordeichsfläche im Nationalpark Schleswig-Holsteinisches Wattenmeer, Diplomarbeit im Fachbereich Biologie der Fakultät für Mathematik, Informatik und Naturwissenschaften. Universität Hamburg.

References

Von Lützow, M., Kögel-Knabner, I., Ludwig, B., Matzner, E., Flessa, H., Ekschmitt, K., Guggenberger, G., Marschner, B., Kalbitz, K., 2008. Stabilization mechanisms of organic matter in four temperate soils: Development and application of a conceptual model. Journal of Plant Nutrition and Soil Science 171, 111-124.

Wang, G., Zhou, Y., Xu, X., Ruan, H.H., Wang, J., 2013. Temperature Sensitivity of Soil Organic Carbon Mineralization along an Elevation Gradient in the Wuyi Mountains, China. PLoS ONE 8.

Weiss, A., 2013. The silica and inorganic carbon system in tidal marshes of the Elbe estuary, Germany: Fluxes and spatio-temporal patterns, Dissertation im Fachbereich Geowissenschaften der Fakultät für Mathematik, Informatik und Naturwissenschaften. Universität Hamburg, Hamburg, Germany.

Weston, N.B., Neubauer, S.C., Velinsky, D.J., Vile, M.A., 2014. Net ecosystem carbon exchange and the greenhouse gas balance of tidal marshes along an estuarine salinity gradient. Biogeochemistry 120, 163-189.

Weston, N.B., Vile, M.A., Neubauer, S.C., Velinsky, D.J., 2011. Accelerated micobial organic matter mineralization following salt-water intrusion into tidal freshwater marsh soils. Biogeochemistry 102, 135-151.

Whalen, S.C., 2005. Biogeochemistry of Methane Exchange between Natural Wetlands and the Atmosphere. Environmental Engineering Science 22, 73-94.

Więski, K., Guo, H., Craft, C.B., Pennings, S.C., 2010. Ecosystem Functions of Tidal Fresh, Brackish, and Salt Marshes on the Georgia Coast. Estuaries and Coasts 33, 161-169.

Wilken, R.-D., Hintelmann, H., 1991. Mercury and methylmercury in sediments and suspended particles from the river Elbe, North Germany. Water, Air, & Soil Pollution 56, 427-437.

Windham, L., 2001. Comparison of Biomass Production and Decomposition between *Phragmites Australis* (Common Reed) and *Spartina Patens* (Salt Hay Grass) in Brackish Tidal Marshes of New Jersey, USA. Wetlands 21, 179-188.

WSD-Nord, 2013. Wasser- und Schifffahrtsdirektion Nord, http://www.portal-tideelbe.de (access date: 13.06.2013).

Yamamoto, S., Alcauskas, J.B., Crozier, T.E., 1976. Solubility of Methane in Distilled Water and Seawater. Journal of Chemical and Engineering Data 21, 78-80.

Yao, H., Conrad, R., 1999. Thermodynamics of methane production in different rice paddy soils from China, the Philippines and Italy. Soil Biology & Biochemistry 31, 463-473.

Zou, X.M., Ruan, H.H., Fu, Y., Yang, X.D., Sha, L.Q., 2005. Estimating soil labile organic carbon and potential turnover rates using a sequential fumigation–incubation procedure. Soil Biology & Biochemistry 37, 1923-1928.

Zwolsman, J.J.G., Berger, G.W., Van Eck, G.T.M., 1993. Sediment accumulation rates, historical input, postdepositional mobility and retention of major elements and trace metals in salt marsh sediments of the Scheldt estuary, SW Netherlands. Marine Chemistry 44, 73-94.

Appendix

List of Figures in Appendix

List of Tables in Appendix

Figures

Figure A 1: Cumulative CO_2 production for aerobic soil incubation over the incubation period of 147 days. Gas production is shown for the five study sites separately (A=1, B=2, C=3, D=4, E=5). Profiles are denoted by different symbols while horizons are indicated by different colors. Values are given as CO_2-C per gram SOC (mg CO_2-C g^{-1}TOC) including DIC. Error bars indicate standard deviation from the mean ($n = 3$).

Figure A 2: Cumulative CO_2 production for anaerobic soil incubation over the incubation period of 153 days. Gas production is shown for the five study sites separately (A=1, B=2, C=3, D=4, E=5). Profiles are denoted by different symbols while horizons are indicated by different colors. Values are given as CO_2-C per gram SOC (mg CO_2-C g^{-1}TOC) including DIC. Error bars indicate standard deviation from the mean ($n = 3$).
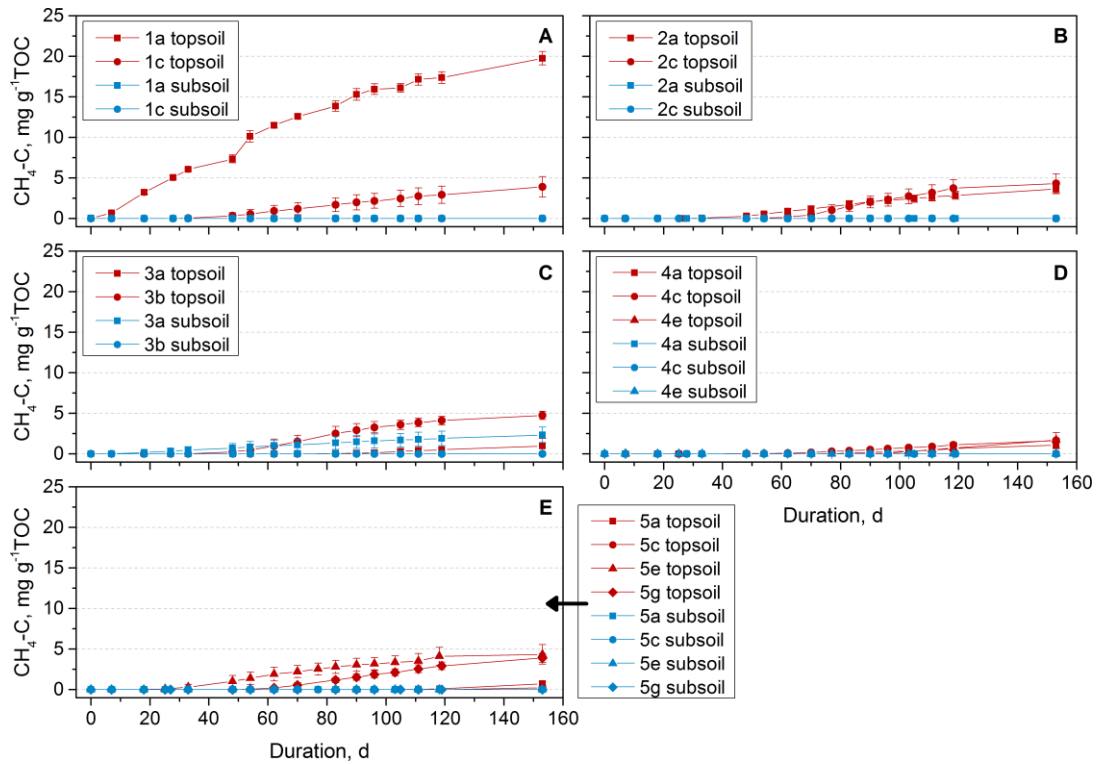
Figure A 3: Cumulative CH$_4$ production for anaerobic soil incubation over the incubation period of 153 days. Gas production is shown for the five study sites separately (A=1, B=2, C=3, D=4, E=5). Profiles are denoted by different symbols while horizons are indicated by different colors. Values are given as CH$_4$-C per gram SOC (mg CH$_4$-C g^{-1}TOC) including CH$_{4(aq)}$. Error bars indicate standard deviation from the mean (n = 3).
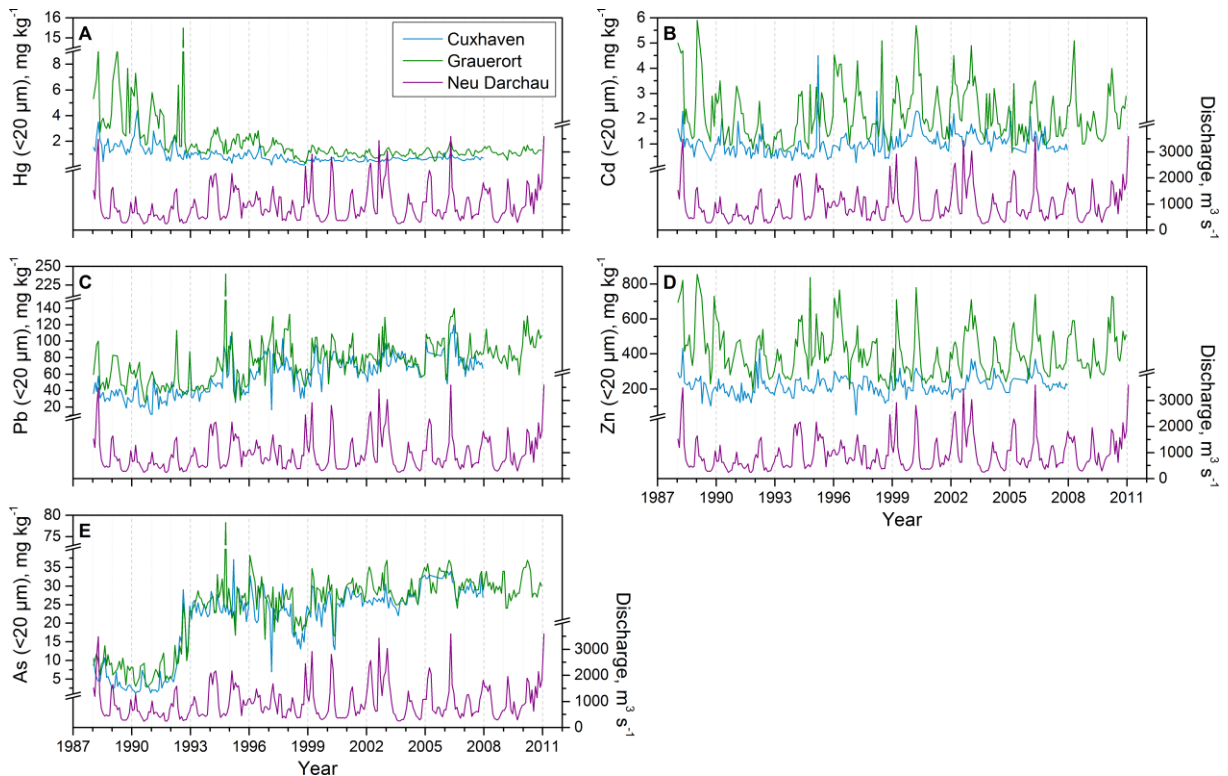
Figure A 4: Chronological development of trace metals in the ff20 of suspended sediments as well as river discharge. Mean monthly metal concentrations in mg kg^{-1} are indicated by green lines for the automated sampling station Grauerort and blue lines for Cuxhaven. The monthly discharge in m^3 s^{-1} at the hydrological station Neu Darchau is indicated by purple lines. Data were kindly provided by FGG Elbe (2014).

Tables

Table A 1: Characteristics of the investigated soil samples.

Profile	Lab No.	Upper edge cm	Lower edge cm	Horizon	Color	Soil moisture vol %	Bulk density g cm⁻³
1a	16021	0	3	Go	bn	*nd*	0.66
1a	16022	3	40	Gr	sw	85.44	0.43
1a	17251	40	70	Gr	sw	*nd*	0.64
1a	17252	70	100	Gr	sw	*nd*	0.87
1b	16023	0	10	Go	bn	72.86	0.75
1b	16024	10	40	Gr	sw	69.82	0.69
1b	17253	40	70	Gr	sw	*nd*	0.55
1b	17254	70	100	Gr	sw	*nd*	0.57
1c	16025	0	3	Go	bn	*nd*	0.73
1c	16026	3	40	Gr	sw	*nd*	0.69
1c	17255	40	70	Gr	sw	*nd*	0.40
1c	17256	70	100	Gr	sw	*nd*	0.37
2a	16019	0	18	Go	bn	70.45	0.72
2a	16020	18	30	Gro	bn gr	66.94	0.69
2a	17242	30	60	Gor	gr bn	*nd*	0.82
2a	17243	60	100	Gor	gr	*nd*	0.89
2b	15971	0	5	Ah	bn	23.65	0.98
2b	15972	5	23	Go-Ah	bn gr	28.33	1.14
2b	15973	23	50	Go	bn	24.70	1.42
2b	15974	50	85	Gro	bn gr	37.82	1.32
2b	15975	85	140	Gor	gr oc	*nd*	1.28
2b	15976	140	150	Gr	gr sw	*nd*	1.23
2c	15966	0	5	Ah	bn	22.90	1.05
2c	15967	5	30	Go-Ah	bn gr	24.95	1.35
2c	15968	30	62	Go	bn	31.17	1.35
2c	15969	62	110	Gro	gr bn	36.48	1.54
2c	15970	110	120	Gor	gr oc	*nd*	1.33
2d	15960	0	5	Ah	bn	26.21	0.93
2d	15961	5	20	Go-Ah	oc bn	26.90	1.07
2d	15962	20	55	Go	oc	30.01	1.25
2d	15963	55	100	Gro	gr oc	40.21	1.43
2d	15964	100	140	Gor	oc gr	*nd*	1.27
2d	15965	140	150	Gr	gr sw	*nd*	1.21
3a	16014	0	4	Ah	bn	*nd*	0.81
3a	16015	4	20	Go	oc bn	39.81	1.29
3a	16016	20	36	Gro	gr oc bn	38.02	1.34
3a	16017	36	60	G(o)r	sw gr	48.15	1.23
3a	16018	60	80	Gr	sw	*nd*	1.11
3a	17241	80	100	Gr	sw	*nd*	1.30
3b	16009	0	5	Ah-Go	bn	27.14	1.02
3b	16010	5	20	fAh°Go	bn	23.23	1.21
3b	16011	20	50	I Gro	oc bn	24.38	1.28
3b	16012	50	100	II Gro	gr oc bn	28.91	1.40
3b	16013	180	190	Gr	sw	*nd*	1.31
3c	16004	0	20	Ah-Go	bn	33.74	0.95
3c	16005	20	90	fAh°Go	bn + gr oc	32.71	1.28
3c	16006	90	140	Gro	gr oc	44.44	1.17
3c	16007	140	180	Gor	gr oc	*nd*	1.31
3c	16008	180	190	Gr	sw	*nd*	1.11

Continuation of Table A 1

Profile	Lab No.	Upper edge cm	Lower edge cm	Horizon	Color	Soil moisture vol %	Bulk density g cm⁻³
4a	15934	0	10	Fo	gr bn	59.44	1.20
4a	15935	10	20	For	bn gr	41.55	1.48
4a	15936	20	40	Fr	sw	50.64	1.18
4a	17235	40	70	Fr	sw	nd	1.20
4a	17236	70	100	Fr	sw	nd	1.46
4b	15937	0	10	Go-Ah	oc bn	58.03	1.00
4b	15938	10	20	Go	oc bn	54.94	1.00
4b	15939	20	34	Gor	gr	45.88	0.59
4b	15940	34	45	Gr	sw	54.48	0.92
4b	17237	45	70	Gr	sw	nd	1.08
4b	17238	70	100	Gr	sw	nd	1.10
4c	15941	0	17	Go-Ah	bn	71.62	0.68
4c	15942	17	40	Gor	bn gr	62.95	0.90
4c	15943	40	50	Gr	gr sw	77.78	0.87
4c	17239	50	70	Gr	sw	nd	0.83
4c	17240	70	100	Gr	sw	nd	0.77
4d	15944	0	9	Ah	bn	34.60	0.81
4d	15945	9	26	Go	gr bn	47.65	1.10
4d	15946	26	39	fAh°Go	bn	51.21	0.93
4d	15947	39	54	Go	gr bn	53.91	0.98
4d	15948	54	71	Gor	gr	53.02	1.13
4d	15949	71	105	Gor	gr	49.76	1.20
4e	15951	0	6	Go-Ah	bn	45.50	0.73
4e	15952	6	15	Go	oc bn	47.07	0.89
4e	15953	15	26	fAh°Go	bn	54.05	0.94
4e	15954	26	33	Go	oc	55.39	1.06
4e	15955	33	40	fAh°Go	bn	57.70	0.98
4e	15956	40	49	Go	gr oc	nd	1.23
4e	15957	49	63	fAh°Gor	oc gr	66.56	0.83
4e	15958	63	80	Gr	gr sw	69.54	0.76
4e	15959	80	100	Gr	sw	nd	0.81
5a	15915	0	10	Go-Ah	bn	nd	0.99
5a	15916	10	20	Gro	bn gr	65.49	0.85
5a	15917	20	46	Gor	gr bn	51.44	1.32
5a	15918	46	55	Gr	gr	43.33	1.34
5a	17244	55	70	Gr	gr	nd	1.54
5a	17245	70	100	Gr	sw	nd	1.51
5b	15919	0	12	Go-Ah	bn	55.53	1.05
5b	15920	12	30	Gro	bn gr	49.06	1.35
5b	15921	30	50	Gor	gr	46.02	1.54
5b	15922	50	70	Gr	gr sw	nd	1.50
5b	17246	70	100	Gr	sw	nd	1.60
5c	15923	0	6	Go-Ah	gr bn	54.81	1.06
5c	15924	6	10	Go	gr oc bn	41.91	1.30
5c	15925	10	30	Go	gr oc	42.09	1.44
5c	15926	30	57	Gro	h gr	46.88	1.15
5c	15927	57	75	Gr	gr sw	44.55	1.62
5c	17247	75	100	Gr	sw	nd	1.55
5d	15928	0	2	Ai	bn	nd	1.05
5d	15929	2	13	Go-Ah	d bn + gr oc	25.69	1.09
5d	15930	13	28	Go°fAh	d bn + gr oc	25.40	1.30
5d	15931	28	45	Go	gr bn	37.13	1.35
5d	15932	45	110	Gor	bn gr	44.85	1.29
5d	15933	110	135	Gr	gr sw	nd	1.29

Continuation of Table A 1

Profile	Lab No.	Upper edge cm	Lower edge cm	Horizon	Color	Soil moisture vol %	Bulk density g cm⁻³
5e	15991	0	5	Ah-Go	bn	55.04	0.87
5e	15992	5	18	Go	gr bn	47.41	1.13
5e	15993	18	40	Gro	gr oc bn	41.98	1.34
5e	15994	40	80	Gor	oc gr	54.11	1.08
5e	17248	80	100	Gor	oc gr	*nd*	1.33
5f	15995	0	1	Ai	bn	*nd*	0.99
5f	15996	1	3	Go	gr bn	*nd*	1.32
5f	15997	3	6	fAh	bn	*nd*	1.23
5f	15998	6	12	Go	gr bn	34.63	1.26
5f	15999	12	40	Gro	gr oc bn	45.09	1.16
5f	16000	40	100	Gor	oc gr	46.84	1.28
5g	16001	0	5	Ah	bn	45.27	0.63
5g	16002	5	18	Gro	gr oc bn	51.23	1.06
5g	16003	18	50	Gor	oc gr	52.76	1.09
5g	17249	50	70	Gor	oc gr	*nd*	1.42
5g	17250	70	100	Gor	oc gr	*nd*	1.36

nd = not determined

Table A 2: Grain size distribution of all investigated soil samples. Texture classes are given according to Ad-hoc-AG Boden (2005).

Profile	Lab No.	Clay	Fine silt	Medium silt	Coarse silt	Silt	Fine sand	Medium sand	Coarse sand	Sand	ff20	Texture
		%	%	%	%	%	%	%	%	%	%	
1a	16021	33.53	17.83	27.55	17.24	62.62	3.81	0.03	0.03	3.87	78.91	Tu3
1a	16022	14.82	10.55	19.91	44.28	74.74	10.21	0.21	0.03	10.45	45.28	Ut3
1a	17251	9.99	7.88	16.43	42.12	66.43	21.78	1.74	0.07	23.59	34.30	Ut2
1a	17252	7.96	5.82	11.68	43.82	61.32	27.87	2.78	0.03	30.68	25.46	Us
1b	16023	29.77	9.36	18.14	38.05	65.55	4.58	0.07	0.00	4.65	57.27	Lu
1b	16024	31.10	10.83	20.20	34.88	65.91	2.95	0.03	0.00	2.98	62.13	Tu3
1b	17253	8.91	9.18	19.55	42.47	71.20	17.12	2.77	0.03	19.92	37.64	Us
1b	17254	11.38	9.39	19.51	34.04	62.94	21.29	4.30	0.11	25.70	40.28	Uls
1c	16025	44.66	20.14	24.69	8.99	53.82	1.50	0.03	0.00	1.53	89.49	Tu3
1c	16026	46.19	0.00	39.36	13.42	52.78	0.97	0.07	0.00	1.04	85.55	Tu2
1c	17255	11.22	10.15	22.81	21.33	54.29	26.24	8.13	0.10	34.47	44.18	Uls
1c	17256	8.17	12.45	26.28	22.84	61.57	20.34	9.78	0.14	30.26	46.90	Us
2a	16019	17.87	5.22	8.21	53.34	66.77	15.25	0.07	0.00	15.32	31.30	Ut3
2a	16020	29.74	9.12	18.63	31.49	59.24	10.94	0.03	0.00	10.97	57.49	Lu
2a	17242	9.07	6.88	14.57	29.42	50.87	36.57	3.46	0.03	40.06	30.52	Slu
2a	17243	7.40	6.23	11.13	32.61	49.97	39.84	2.71	0.07	42.62	24.76	Su4
2b	15971	21.50	7.27	13.52	40.38	61.17	17.10	0.21	0.00	17.31	42.29	Lu
2b	15972	19.95	7.06	11.31	41.51	59.88	20.18	0.00	0.00	20.18	38.32	Lu
2b	15973	11.98	9.20	10.41	25.33	44.94	42.86	0.25	0.00	43.11	31.59	Slu
2b	15974	30.19	10.40	17.67	21.72	49.79	19.72	0.24	0.00	19.96	58.26	Lt2
2b	15975	11.77	3.29	10.05	34.78	48.12	38.42	1.72	0.00	40.14	25.11	Slu
2b	15976	16.74	5.25	14.61	38.01	57.87	25.32	0.03	0.00	25.35	36.60	Uls
2c	15966	28.39	10.10	15.51	33.13	58.74	12.14	0.71	0.04	12.89	54.00	Lu
2c	15967	31.84	8.17	14.03	29.09	51.29	16.45	0.34	0.03	16.82	54.04	Tu3
2c	15968	41.12	10.35	15.78	21.97	48.10	10.76	0.03	0.00	10.79	67.25	Lt3
2c	15969	29.70	7.56	15.08	24.11	46.75	23.18	0.36	0.00	23.54	52.34	Lt2
2c	15970	15.36	3.96	10.07	35.04	49.07	35.25	0.25	0.03	35.53	29.39	Slu
2d	15960	37.33	13.28	18.87	20.24	52.39	9.63	0.58	0.04	10.25	69.48	Tu3
2d	15961	30.34	8.28	15.24	26.50	50.02	17.06	2.48	0.08	19.62	53.86	Lt2
2d	15962	40.46	10.24	15.51	19.50	45.25	13.52	0.50	0.27	14.29	66.21	Lt3
2d	15963	25.10	6.81	13.05	29.04	48.90	25.83	0.14	0.00	25.97	44.96	Ls2
2d	15964	10.98	3.01	8.44	38.92	50.37	38.42	0.21	0.00	38.63	22.43	Slu
2d	15965	30.53	7.22	19.29	32.77	59.28	10.11	0.10	0.03	10.24	57.04	Lu
3a	16014	27.47	8.37	15.45	42.99	66.81	5.66	0.07	0.00	5.73	51.29	Tu4
3a	16015	6.55	1.80	6.20	63.16	71.16	21.87	0.42	0.03	22.32	14.55	Us
3a	16016	2.03	0.29	0.87	24.88	26.04	71.85	0.03	0.00	71.88	3.19	Su3
3a	16017	9.72	2.50	7.66	48.11	58.27	31.55	0.40	0.03	31.98	19.88	Uls
3a	16018	9.94	3.56	7.36	32.88	43.80	46.18	0.10	0.00	46.28	20.86	Slu
3a	17241	4.30	2.68	8.08	37.85	48.61	46.43	0.63	0.03	47.09	15.06	Su4
3b	16009	7.43	4.09	8.55	57.58	70.22	22.35	0.03	0.00	22.38	20.07	Us
3b	16010	6.05	1.78	5.56	56.23	63.57	30.35	0.03	0.00	30.38	13.39	Us
3b	16011	3.87	1.36	4.46	41.36	47.18	48.75	0.18	0.00	48.93	9.69	Su4
3b	16012	5.60	0.88	2.43	25.23	28.54	65.65	0.14	0.03	65.82	8.91	Su3
3b	16013	29.14	7.62	12.61	22.80	43.03	27.82	0.03	0.00	27.85	49.37	Lt2
3c	16004	18.35	6.65	17.34	48.74	72.73	8.87	0.03	0.00	8.90	42.34	Ut4
3c	16005	5.16	3.46	3.85	39.14	46.45	46.84	1.41	0.10	48.35	12.47	Su4
3c	16006	16.42	6.69	12.03	41.50	60.22	22.97	0.38	0.00	23.35	35.14	Uls
3c	16007	19.84	8.14	12.87	29.69	50.70	29.20	0.24	0.00	29.44	40.85	Ls2
3c	16008	15.13	6.49	7.89	34.29	48.67	35.79	0.37	0.00	36.16	29.51	Slu

Continuation of Table A 2

Profile	Lab No.	Clay %	Fine silt %	Medium silt %	Coarse silt %	Silt %	Fine sand %	Medium sand %	Coarse sand %	Sand %	ff20 %	Texture
4a	15934	23.04	7.93	11.22	25.76	44.91	31.18	0.84	0.04	32.06	42.19	Ls2
4a	15935	5.67	2.20	3.65	18.29	24.14	69.32	0.81	0.03	70.16	11.52	Su2
4a	15936	12.66	3.83	7.88	36.28	47.99	33.91	4.52	0.91	39.34	24.37	Slu
4a	17235	5.33	3.30	6.66	27.00	36.96	57.11	0.61	0.03	57.75	15.29	Su3
4a	17236	3.44	1.42	3.16	21.97	26.55	69.98	0.03	0.03	70.04	8.02	Su3
4b	15937	10.19	2.45	6.15	75.61	84.21	5.51	0.10	0.00	5.61	18.79	Ut2
4b	15938	16.12	4.80	11.90	59.77	76.47	6.14	1.22	0.08	7.44	32.82	Ut3
4b	15939	11.04	3.27	6.33	71.80	81.40	7.20	0.30	0.04	7.54	20.64	Ut2
4b	15940	18.72	6.06	10.45	56.94	73.45	7.67	0.14	0.03	7.84	35.23	Ut4
4b	17237	7.90	6.54	12.43	41.47	60.44	28.29	3.22	0.21	31.72	26.87	Us
4b	17238	4.48	2.80	7.28	19.08	29.16	65.18	1.20	0.03	66.41	14.56	Su3
4c	15941	38.58	10.21	20.08	28.54	58.83	1.67	0.68	0.21	2.56	68.87	Tu3
4c	15942	19.04	7.21	10.33	56.32	73.86	7.04	0.07	0.03	7.14	36.58	Ut4
4c	15943	19.45	5.77	11.24	54.72	71.73	8.45	0.27	0.07	8.79	36.46	Ut4
4c	17239	13.91	10.39	17.52	39.24	67.15	16.29	2.45	0.16	18.90	41.82	Ut3
4c	17240	14.39	13.19	22.86	35.08	71.13	12.25	2.09	0.07	14.41	50.44	Ut3
4d	15944	30.93	7.82	19.42	38.21	65.45	3.55	0.03	0.00	3.58	58.17	Lu
4d	15945	13.02	3.08	9.76	49.64	62.48	20.27	4.15	0.09	24.51	25.86	Uls
4d	15946	32.92	8.26	17.01	33.76	59.03	7.88	0.08	0.04	8.00	58.19	Tu3
4d	15947	21.58	7.23	14.59	44.52	66.34	11.64	0.31	0.17	12.12	43.40	Ut4
4d	15948	20.82	4.86	11.87	37.79	54.52	21.39	3.27	0.04	24.70	37.55	Lu
4d	15949	17.16	5.67	8.74	40.72	55.13	27.43	0.28	0.00	27.71	31.57	Uls
4e	15951	37.41	10.24	19.16	29.71	59.11	2.50	0.94	0.04	3.48	66.81	Tu3
4e	15952	24.78	6.54	14.80	46.86	68.20	6.91	0.14	0.00	7.05	46.12	Ut4
4e	15953	37.22	9.59	18.63	25.62	53.84	8.31	0.56	0.07	8.94	65.44	Tu3
4e	15954	20.90	6.05	11.44	45.85	63.34	15.64	0.07	0.00	15.71	38.39	Lu
4e	15955	36.26	9.80	18.51	27.80	56.11	7.01	0.61	0.00	7.62	64.57	Tu3
4e	15956	14.97	4.90	10.24	49.42	64.56	17.86	2.42	0.20	20.48	30.11	Uls
4e	15957	41.79	12.17	21.09	19.71	52.97	5.01	0.18	0.04	5.23	75.05	Tu3
4e	15958	39.64	11.41	20.45	22.24	54.10	5.99	0.24	0.03	6.26	71.50	Tu3
4e	15959	34.25	10.20	22.38	22.35	54.93	10.33	0.45	0.00	10.78	66.83	Tu3
5a	15915	26.15	6.53	10.95	45.12	62.60	9.68	1.42	0.14	11.24	43.63	Lu
5a	15916	10.96	2.86	6.09	38.45	47.40	38.35	3.25	0.03	41.63	19.91	Slu
5a	15917	6.46	1.27	2.75	22.28	26.30	67.05	0.11	0.03	67.19	10.48	Su3
5a	15918	2.51	0.42	0.84	12.05	13.31	83.95	0.24	0.00	84.19	3.77	Su2
5a	17244	1.99	0.52	0.62	6.29	7.43	90.44	0.10	0.00	90.54	3.13	Ss
5a	17245	2.10	0.51	0.66	8.77	9.94	87.81	0.13	0.03	87.97	3.27	Ss
5b	15919	17.01	4.65	9.97	34.34	48.96	32.47	1.39	0.14	34.00	31.63	Slu
5b	15920	6.57	1.90	3.58	25.64	31.12	61.75	0.53	0.00	62.28	12.05	Su3
5b	15921	4.80	0.96	1.99	14.35	17.30	77.78	0.07	0.00	77.85	7.75	Su2
5b	15922	3.74	0.78	1.60	19.85	22.23	73.88	0.11	0.03	74.02	6.12	Su2
5b	17246	2.40	0.45	0.89	8.34	9.68	87.69	0.17	0.03	87.89	3.74	Ss
5c	15923	11.56	3.90	7.19	38.85	49.94	36.48	2.00	0.03	38.51	22.65	Slu
5c	15924	4.43	1.07	2.18	27.02	30.27	64.44	0.64	0.18	65.26	7.68	Su3
5c	15925	6.07	1.65	2.91	24.40	28.96	64.42	0.46	0.07	64.95	10.63	Su3
5c	15926	10.27	3.03	5.68	27.71	36.42	52.68	0.52	0.07	53.27	18.98	Sl3
5c	15927	2.96	0.45	0.62	9.97	11.04	85.93	0.07	0.03	86.03	4.03	Su2
5c	17247	3.48	0.48	1.19	7.42	9.09	87.25	0.13	0.03	87.41	5.15	Ss
5d	15928	11.25	2.90	4.23	29.68	36.81	51.16	0.66	0.07	51.89	18.38	Sl3
5d	15929	10.12	2.13	5.22	42.14	49.49	40.25	0.10	0.03	40.38	17.47	Slu
5d	15930	9.05	1.90	5.91	47.74	55.55	35.20	0.14	0.07	35.41	16.86	Uls
5d	15931	7.78	2.03	4.85	42.62	49.50	42.51	0.25	0.00	42.76	14.66	Su4
5d	15932	7.44	2.25	4.67	41.01	47.93	44.37	0.18	0.03	44.58	14.36	Su4
5d	15933	8.67	2.31	3.54	22.49	28.34	62.90	0.11	0.00	63.01	14.52	Su3

Continuation of Table A 2

Profile	Lab No.	Clay	Fine silt	Medium silt	Coarse silt	Silt	Fine sand	Medium sand	Coarse sand	Sand	ff20	Texture
		%	%	%	%	%	%	%	%	%	%	
5e	15991	33.06	9.26	15.17	35.00	59.43	7.51	0.03	0.00	7.54	57.49	Tu3
5e	15992	13.06	4.06	9.82	55.39	69.27	16.89	0.79	0.00	17.68	26.94	Ut3
5e	15993	16.33	5.60	9.56	40.75	55.91	27.73	0.07	0.00	27.80	31.49	Uls
5e	15994	23.30	7.09	11.55	43.37	62.01	14.23	0.51	0.00	14.74	41.94	Lu
5e	17248	13.84	3.87	7.11	22.90	33.88	52.03	0.20	0.00	52.23	24.82	Sl4
5f	15995	20.69	5.78	9.62	41.71	57.11	22.04	0.15	0.00	22.19	36.09	Lu
5f	15996	7.84	2.25	4.54	39.18	45.97	46.00	0.18	0.00	46.18	14.63	Su4
5f	15997	14.21	3.89	9.27	41.44	54.60	30.97	0.25	0.00	31.22	27.37	Uls
5f	15998	4.32	1.24	2.10	28.73	32.07	62.79	0.83	0.00	63.62	7.66	Su3
5f	15999	6.03	2.48	3.89	50.18	56.55	36.36	0.98	0.03	37.37	12.40	Us
5f	16000	10.51	2.33	5.88	45.89	54.10	34.70	0.70	0.03	35.43	18.72	Uls
5g	16001	43.59	13.52	19.26	19.61	52.39	4.02	0.03	0.00	4.05	76.37	Tu3
5g	16002	29.60	7.36	12.54	37.10	57.00	13.27	0.10	0.00	13.37	49.50	Lu
5g	16003	22.35	5.94	14.20	42.75	62.89	14.77	0.03	0.00	14.80	42.49	Lu
5g	17249	21.03	7.06	11.92	29.47	48.45	30.38	0.10	0.00	30.48	40.01	Ls2
5g	17250	11.18	2.89	6.53	30.33	39.75	49.07	0.03	0.00	49.10	20.60	Sl3

Clay:	< 2.0 µm
Fine silt:	2.0 to < 6.3 µm
Medium silt:	6.3 to < 20 µm
Coarse silt:	20 to < 63 µm
Fine sand:	63 to < 200 µm
Medium sand:	200 to < 630 µm
Coarse sand:	630 to < 2000 µm

Table A 3: pH values, carbon contents, nitrogen contents, and C/N ratios of all investigated soil samples.

Profile	Lab No.	pH H$_2$O	pH CaCl$_2$	TC %	TC kg m^{-2}	TIC %	TIC kg m^{-2}	TOC %	TOC kg m^{-2}	TN %	C/N ratio
1a	16021	7.1	7.1	6.20	1.23	0.80	0.16	5.40	1.07	0.51	10.58
1a	16022	7.2	7.2	4.73	5.49	0.98	1.14	3.75	4.35	0.36	10.41
1a	17251	nd	nd	3.71	7.07	0.71	1.35	3.00	5.73	0.25	11.91
1a	17252	nd	nd	3.88	10.06	0.62	1.61	3.26	8.45	0.25	12.81
1b	16023	7.4	7.2	4.97	3.72	0.88	0.66	4.09	3.07	0.38	10.77
1b	16024	7.2	7.1	4.97	12.08	0.77	1.86	4.21	10.22	0.38	11.07
1b	17253	nd	nd	5.09	6.98	0.51	0.70	4.58	6.28	0.41	11.20
1b	17254	nd	nd	5.78	9.88	0.40	0.68	5.38	9.20	0.40	13.55
1c	16025	7.2	7.1	8.38	1.84	0.66	0.14	7.73	1.69	0.65	11.88
1c	16026	6.9	6.8	7.72	19.70	0.40	1.02	7.32	18.68	0.60	12.19
1c	17255	nd	nd	5.88	7.08	0.21	0.25	5.67	6.83	0.41	13.69
1c	17256	nd	nd	7.45	8.17	0.32	0.35	7.13	7.82	0.51	13.93
2a	16019	7.7	7.3	3.75	4.83	0.97	1.25	2.78	3.58	0.28	9.93
2a	16020	7.6	7.3	4.36	3.60	0.83	0.68	3.53	2.92	0.34	10.39
2a	17242	nd	nd	3.28	8.11	0.78	1.92	2.51	6.20	0.25	10.24
2a	17243	nd	nd	3.53	12.57	0.52	1.87	3.00	10.70	0.25	11.96
2b	15971	7.3	6.9	6.14	3.02	0.57	0.28	5.57	2.74	0.54	10.31
2b	15972	7.6	7.1	3.59	7.34	0.40	0.81	3.20	6.53	0.34	9.40
2b	15973	8.0	7.3	1.40	5.36	0.32	1.23	1.08	4.14	0.13	8.31
2b	15974	7.8	7.2	1.34	6.17	0.20	0.93	1.14	5.24	0.14	8.13
2b	15975	8.1	7.4	0.98	6.90	0.47	3.32	0.51	3.58	0.06	8.47
2b	15976	7.9	7.5	1.81	2.23	0.58	0.72	1.23	1.52	0.12	10.25
2c	15966	7.1	6.8	6.94	3.66	0.41	0.22	6.53	3.44	0.62	10.53
2c	15967	7.5	7.0	2.65	8.94	0.14	0.47	2.51	8.46	0.27	9.30
2c	15968	7.9	7.4	1.85	8.00	0.33	1.43	1.52	6.57	0.18	8.44
2c	15969	7.9	7.4	1.28	9.47	0.41	3.02	0.87	6.45	0.11	7.93
2c	15970	8.3	7.5	1.08	1.44	0.50	0.67	0.58	0.77	0.07	8.26
2d	15960	7.2	6.9	7.38	3.44	0.43	0.20	6.95	3.24	0.69	10.07
2d	15961	7.3	6.8	4.87	7.82	0.21	0.34	4.66	7.48	0.52	8.96
2d	15962	7.6	7.1	1.99	8.74	0.17	0.75	1.82	7.99	0.21	8.66
2d	15963	7.8	7.4	1.14	7.31	0.36	2.33	0.78	4.98	0.10	7.77
2d	15964	8.0	7.5	1.02	5.18	0.51	2.60	0.51	2.58	0.06	8.47
2d	15965	7.6	7.3	2.19	2.65	0.43	0.52	1.76	2.13	0.17	10.36
3a	16014	7.6	7.4	5.07	1.65	1.12	0.36	3.95	1.29	0.37	10.69
3a	16015	8.2	7.7	1.78	3.68	1.02	2.10	0.76	1.58	0.07	10.91
3a	16016	8.5	7.9	0.77	1.65	0.59	1.27	0.18	0.38	0.01	17.60
3a	16017	7.8	7.6	2.39	7.04	1.03	3.03	1.36	4.02	0.13	10.48
3a	16018	7.5	7.5	2.59	5.75	0.90	1.99	1.69	3.76	0.17	9.96
3a	17241	nd	nd	1.93	5.02	0.86	2.24	1.07	2.78	0.11	9.91
3b	16009	7.5	7.0	4.54	2.32	0.74	0.38	3.80	1.94	0.37	10.28
3b	16010	8.4	7.3	2.59	4.68	0.77	1.39	1.82	3.29	0.17	10.71
3b	16011	8.2	7.4	1.82	6.99	0.64	2.46	1.18	4.53	0.11	10.73
3b	16012	8.0	7.5	1.12	4.71	0.53	2.23	0.59	2.48	0.06	9.83
3b	16013	7.3	7.2	2.98	3.90	0.67	0.87	2.31	3.03	0.21	11.01
3c	16004	8.3	7.5	3.76	7.14	0.82	1.55	2.94	5.59	0.31	9.49
3c	16005	8.1	7.5	1.39	12.43	0.53	4.76	0.86	7.67	0.09	9.53
3c	16006	7.9	7.4	1.73	10.13	0.55	3.22	1.18	6.91	0.13	9.08
3c	16007	8.0	7.4	1.92	10.08	0.63	3.29	1.29	6.80	0.14	9.24
3c	16008	7.4	7.3	2.59	2.88	0.86	0.96	1.73	1.92	0.17	10.17

Continuation of Table A 3

Profile	Lab No.	pH H$_2$O	pH CaCl$_2$	TC %	TC kg m^{-2}	TIC %	TIC kg m^{-2}	TOC %	TOC kg m^{-2}	TN %	C/N ratio
4a	15934	7.6	7.3	3.09	3.71	0.88	1.06	2.21	2.65	0.24	9.20
4a	15935	7.0	6.9	1.12	1.66	0.65	0.96	0.47	0.70	0.05	9.40
4a	15936	7.7	7.4	2.39	5.66	1.02	2.41	1.37	3.25	0.14	9.80
4a	17235	nd	nd	1.57	5.68	0.72	2.60	0.85	3.07	0.10	8.95
4a	17236	nd	nd	1.01	4.43	0.60	2.63	0.41	1.80	0.05	9.16
4b	15937	8.0	7.5	2.30	2.31	1.03	1.03	1.27	1.27	0.12	10.57
4b	15938	8.1	7.6	3.22	3.23	1.09	1.09	2.13	2.14	0.19	11.22
4b	15939	nd	nd	2.37	1.97	1.18	0.98	1.19	0.99	0.12	9.94
4b	15940	7.6	7.4	2.89	2.91	1.10	1.11	1.79	1.80	0.17	10.51
4b	17237	nd	nd	2.83	7.64	1.01	2.72	1.82	4.92	0.18	10.35
4b	17238	nd	nd	1.55	5.10	0.69	2.27	0.86	2.82	0.10	8.74
4c	15941	7.7	7.5	5.13	5.96	1.03	1.20	4.10	4.76	0.41	9.99
4c	15942	8.0	7.6	3.19	6.60	1.07	2.22	2.12	4.38	0.20	10.59
4c	15943	7.6	7.4	3.01	2.61	1.20	1.04	1.81	1.57	0.18	9.95
4c	17239	7.3	7.1	3.46	8.61	1.21	3.00	2.25	5.60	0.24	9.26
4c	17240	nd	nd	3.79	8.73	1.07	2.47	2.72	6.26	0.26	10.41
4d	15944	8.1	7.5	5.62	4.10	1.05	0.77	4.56	3.33	0.47	9.71
4d	15945	8.8	7.7	2.65	4.96	0.64	1.20	2.01	3.77	0.21	9.58
4d	15946	8.4	7.6	3.73	4.53	0.68	0.82	3.05	3.71	0.30	10.17
4d	15947	8.3	7.6	2.74	4.02	0.70	1.02	2.04	3.00	0.20	10.22
4d	15948	8.2	7.6	2.19	4.21	0.70	1.35	1.49	2.87	0.15	9.93
4d	15949	8.3	7.6	1.81	7.36	0.78	3.15	1.04	4.21	0.10	10.35
4e	15951	8.9	7.5	6.06	2.64	0.88	0.38	5.18	2.25	0.49	10.56
4e	15952	8.2	7.5	3.82	3.06	0.86	0.69	2.96	2.37	0.30	9.87
4e	15953	8.3	7.6	3.56	3.68	0.85	0.88	2.71	2.80	0.29	9.33
4e	15954	7.7	7.4	2.36	1.75	0.86	0.63	1.51	1.12	0.15	10.03
4e	15955	7.9	7.5	3.00	2.06	0.90	0.62	2.10	1.44	0.21	10.00
4e	15956	7.9	7.5	2.50	2.78	0.75	0.83	1.75	1.95	0.16	10.96
4e	15957	7.5	7.3	3.83	4.46	0.64	0.74	3.19	3.72	0.31	10.30
4e	15958	7.5	7.4	4.37	5.62	0.45	0.57	3.92	5.05	0.36	10.90
4e	15959	7.6	7.3	4.10	6.67	0.93	1.51	3.18	5.17	0.30	10.58
5a	15915	8.0	7.8	3.58	3.53	1.20	1.18	2.38	2.35	0.28	8.50
5a	15916	8.3	8.0	1.89	1.61	0.92	0.78	0.97	0.83	0.11	8.85
5a	15917	8.5	8.1	1.12	3.83	0.68	2.34	0.44	1.50	0.05	8.76
5a	15918	8.7	8.3	0.75	0.91	0.56	0.67	0.20	0.24	0.02	9.75
5a	17244	nd	nd	0.63	1.44	0.47	1.09	0.15	0.36	0.02	7.33
5a	17245	nd	nd	0.70	3.15	0.53	2.38	0.17	0.78	0.02	7.43
5b	15919	8.1	7.9	2.44	3.08	0.91	1.15	1.53	1.93	0.16	9.54
5b	15920	8.4	8.1	1.25	3.03	0.73	1.77	0.52	1.26	0.05	10.42
5b	15921	8.6	8.1	0.95	2.92	0.66	2.03	0.29	0.89	0.04	7.25
5b	15922	8.6	8.2	0.97	2.90	0.69	2.07	0.28	0.83	0.03	9.23
5b	17246	nd	nd	0.72	3.44	0.53	2.56	0.18	0.88	0.02	9.20
5c	15923	7.9	7.8	3.11	1.99	0.81	0.52	2.30	1.47	0.22	10.46
5c	15924	8.3	8.0	1.12	0.58	0.61	0.32	0.51	0.26	0.05	10.14
5c	15925	8.5	8.1	1.53	4.39	0.79	2.25	0.75	2.14	0.08	9.31
5c	15926	8.5	8.1	1.55	4.81	0.79	2.46	0.76	2.35	0.08	9.46
5c	15927	8.1	7.9	0.77	2.25	0.54	1.57	0.23	0.68	0.02	11.70
5c	17247	nd	nd	0.74	2.86	0.52	2.02	0.22	0.84	0.03	7.48
5d	15928	7.3	6.8	5.04	1.06	0.60	0.12	4.44	0.93	0.36	12.33
5d	15929	8.4	7.4	2.22	2.67	0.71	0.85	1.51	1.81	0.13	11.62
5d	15930	8.5	7.6	2.06	4.03	0.88	1.73	1.18	2.30	0.11	10.69
5d	15931	8.5	7.7	1.27	2.92	0.69	1.58	0.58	1.34	0.06	9.72
5d	15932	8.3	7.7	1.32	11.09	0.75	6.31	0.57	4.78	0.06	9.48
5d	15933	8.4	7.7	1.02	3.30	0.62	2.00	0.40	1.29	0.04	10.00

Continuation of Table A 3

Profile	Lab No.	pH H$_2$O	pH CaCl$_2$	TC %	TC kg m^{-2}	TIC %	TIC kg m^{-2}	TOC %	TOC kg m^{-2}	TN %	C/N ratio
5e	15991	8.0	7.6	4.62	2.02	0.70	0.31	3.92	1.71	0.42	9.34
5e	15992	7.9	7.7	2.31	3.39	0.81	1.18	1.50	2.20	0.17	8.85
5e	15993	7.8	7.7	1.84	5.41	0.79	2.31	1.05	3.10	0.11	9.58
5e	15994	7.6	7.7	2.26	9.75	0.71	3.08	1.55	6.67	0.17	9.10
5e	17248	*nd*	*nd*	1.30	3.44	0.65	1.73	0.64	1.71	0.08	8.15
5f	15995	8.9	8.0	4.34	0.43	0.87	0.09	3.48	0.34	0.35	9.93
5f	15996	9.0	7.9	2.17	0.57	0.82	0.22	1.35	0.36	0.14	9.66
5f	15997	8.8	8.0	2.92	1.08	0.93	0.34	1.99	0.74	0.21	9.49
5f	15998	9.2	7.8	1.18	0.89	0.60	0.46	0.58	0.44	0.06	9.60
5f	15999	8.9	7.7	1.38	4.46	0.76	2.45	0.62	2.02	0.07	8.90
5f	16000	8.6	7.9	1.31	8.38	0.71	4.55	0.60	3.83	0.07	8.56
5g	16001	8.3	7.7	6.57	2.05	0.57	0.18	5.99	1.87	0.57	10.52
5g	16002	8.0	7.6	2.61	3.60	0.72	0.99	1.89	2.60	0.20	9.45
5g	16003	8.1	7.7	2.08	7.27	0.64	2.25	1.44	5.02	0.15	9.58
5g	17249	*nd*	*nd*	1.74	4.93	0.74	2.11	0.99	2.83	0.12	8.64
5g	17250	*nd*	*nd*	1.16	4.74	0.72	2.93	0.44	1.81	0.05	8.20

nd = not determined

Table A 4: Weighted means of TOC and ff20 concentration in the salinity zones and elevation classes along the Elbe estuary. TOC and ff20 in % is given for topsoils (0 – 30 cm) and the whole profile depth (0 – 100 cm). Letters denote statistical differences between salinity zones (Jonckheere-Terpstra-Test; p < 0.05). No significant difference was found between elevation classes (*ns*).

	TOC 0 - 30 cm, %		TOC 0 - 100 cm, %		ff20 0 – 30 cm, %		ff20 0 – 100 cm, %	
Salinity zone	Mean ± SD	Sig.	Mean ± SD	Sig.	Mean ± SD	Sig.	Mean ± SD	Sig.
oligohaline	4.13 ± 1.50	a	3.31 ± 1.87	a	55.56 ± 16.03	a	47.65 ± 11.23	a
mesohaline	2.17 ± 0.86	b	1.70 ± 0.77	b	32.81 ± 16.42	b	29.50 ± 17.80	ab
polyhaline	1.38 ± 0.54	b	0.83 ± 0.38	c	24.73 ± 13.71	b	19.51 ± 11.92	b
Elevation class								
low marsh	2.34 ± 1.98	*ns*	2.01 ± 2.00	*ns*	33.66 ± 23.32	*ns*	26.29 ± 17.74	*ns*
high marsh	2.78 ± 0.70	*ns*	1.85 ± 0.66	*ns*	42.06 ± 14.10	*ns*	39.06 ± 16.10	*ns*

Table A 5: Concentrations of the investigated trace metals Cd, Hg, Pb, Zn, and As in all investigated samples.

Profile	Lab No.	Cd mg kg⁻¹	Cd (<20µm) mg kg⁻¹	Hg mg kg⁻¹	Hg (<20µm) mg kg⁻¹	Pb mg kg⁻¹	Pb (<20µm) mg kg⁻¹	Zn mg kg⁻¹	Zn (<20µm) mg kg⁻¹	As (<20µm) mg kg⁻¹
1a	16021	1.35	1.23	0.71	0.71	63.71	86.33	382.85	419.52	31.36
1a	16022	0.90	1.07	0.55	0.65	47.04	87.67	271.79	381.85	33.70
1a	17251	nd	nd	nd	nd	nd	nd	nd	nd	nd
1a	17252	nd	nd	nd	nd	nd	nd	nd	nd	nd
1b	16023	0.89	0.84	0.53	0.68	46.04	77.67	270.42	352.85	28.82
1b	16024	1.33	0.90	1.49	2.24	58.38	111.67	372.85	425.19	33.00
1b	17253	nd	nd	nd	nd	nd	nd	nd	nd	nd
1b	17254	nd	nd	nd	nd	nd	nd	nd	nd	nd
1c	16025	1.08	0.76	1.23	0.59	67.04	75.33	382.19	330.15	24.11
1c	16026	1.93	0.93	2.96	2.32	88.38	100.33	542.52	390.19	36.87
1c	17255	nd	nd	nd	nd	nd	nd	nd	nd	nd
1c	17256	nd	nd	nd	nd	nd	nd	nd	nd	nd
2a	16019	0.69	0.76	0.43	0.62	42.38	84.50	223.65	376.69	33.06
2a	16020	0.78	0.73	0.55	0.78	48.04	78.00	262.05	379.52	27.35
2a	17242	nd	nd	nd	nd	nd	nd	nd	nd	nd
2a	17243	nd	nd	nd	nd	nd	nd	nd	nd	nd
2b	15971	0.74	1.00	0.49	0.86	42.71	82.00	200.59	366.85	28.41
2b	15972	1.19	1.75	0.83	2.19	59.04	106.00	261.12	493.19	33.23
2b	15973	0.43	0.91	0.25	0.54	43.71	105.00	143.49	353.19	45.67
2b	15974	0.25	0.15	0.09	0.12	40.04	62.67	99.05	188.85	42.67
2b	15975	0.11	0.07	0.03	0.07	17.71	40.33	45.02	137.52	22.86
2b	15976	0.14	0.26	0.03	0.06	22.38	51.00	59.59	124.89	11.91
2c	15966	0.92	0.88	0.68	0.69	50.71	60.00	242.72	331.85	24.53
2c	15967	0.98	0.54	0.44	0.49	67.38	68.33	231.22	361.85	37.23
2c	15968	0.34	0.13	0.15	0.13	52.38	41.50	116.85	167.49	24.46
2c	15969	0.19	0.09	0.06	0.08	32.04	37.33	79.32	143.55	31.80
2c	15970	0.14	0.09	0.04	0.09	21.04	38.67	60.92	139.09	25.01
2d	15960	1.17	0.90	0.80	0.85	69.04	65.33	323.89	377.85	20.96
2d	15961	1.47	1.06	0.87	0.87	77.04	57.67	327.59	378.85	22.84
2d	15962	0.46	0.23	0.18	0.20	56.38	68.33	144.39	215.35	42.20
2d	15963	0.17	0.11	0.05	0.09	29.04	38.50	77.99	139.04	25.58
2d	15964	0.11	0.09	0.03	0.07	16.71	39.00	49.47	129.49	26.47
2d	15965	0.27	0.35	0.08	0.08	37.38	63.67	85.82	148.79	13.58
3a	16014	0.44	0.62	0.39	0.44	42.71	73.50	196.15	282.74	30.36
3a	16015	0.18	0.70	0.12	0.39	12.38	63.33	64.72	257.99	32.89
3a	16016	0.07	0.93	0.03	0.44	5.04	67.33	27.21	283.79	33.00
3a	16017	0.30	0.57	0.24	0.51	23.71	69.33	116.09	278.95	21.82
3a	16018	0.40	0.72	0.36	0.66	31.38	94.67	153.59	354.52	35.00
3a	17241	nd	nd	nd	nd	nd	nd	nd	nd	nd
3b	16009	0.24	0.62	0.15	0.38	13.71	44.33	76.02	199.15	20.60
3b	16010	0.36	0.90	0.24	0.73	16.71	61.67	91.45	291.95	33.87
3b	16011	0.56	1.83	0.25	0.96	18.38	86.00	106.32	434.19	32.67
3b	16012	0.44	1.44	0.25	2.16	18.04	101.33	113.24	603.85	49.00
3b	16013	0.31	0.32	0.29	0.37	46.54	89.67	153.57	243.02	41.33
3c	16004	0.58	0.82	0.54	0.75	36.38	60.33	170.19	306.89	19.52
3c	16005	0.44	1.17	0.22	0.66	21.38	69.00	100.85	418.52	23.85
3c	16006	0.35	0.37	0.31	0.39	40.38	47.50	146.55	307.59	17.29
3c	16007	0.36	0.40	0.25	0.32	43.71	55.83	129.15	235.65	17.46
3c	16008	0.25	0.45	0.14	0.26	35.71	83.33	95.39	188.39	45.33

Continuation of Table A 5

Profile	Lab No.	Cd mg kg⁻¹	Cd (<20µm) mg kg⁻¹	Hg mg kg⁻¹	Hg (<20µm) mg kg⁻¹	Pb mg kg⁻¹	Pb (<20µm) mg kg⁻¹	Zn mg kg⁻¹	Zn (<20µm) mg kg⁻¹	As (<20µm) mg kg⁻¹
4a	15934	0.48	0.79	0.40	0.71	37.38	62.67	168.95	331.85	28.48
4a	15935	0.27	1.28	0.17	1.73	15.38	87.33	75.92	403.85	43.67
4a	15936	0.43	0.95	0.32	0.72	28.38	70.00	136.82	347.85	39.00
4a	17235	nd	nd	nd	nd	nd	nd	nd	nd	nd
4a	17236	nd	nd	nd	nd	nd	nd	nd	nd	nd
4b	15937	0.20	0.56	0.14	0.47	16.71	57.00	79.49	291.45	32.00
4b	15938	0.38	0.40	0.29	0.54	33.88	56.67	137.40	288.92	31.33
4b	15939	0.33	0.73	0.23	0.75	26.38	79.00	107.09	306.89	33.33
4b	15940	0.46	0.75	0.36	0.89	35.04	86.67	147.15	312.55	36.67
4b	17237	nd	nd	nd	nd	nd	nd	nd	nd	nd
4b	17238	nd	nd	nd	nd	nd	nd	nd	nd	nd
4c	15941	0.64	0.49	0.48	0.60	58.04	67.33	219.22	277.22	21.66
4c	15942	0.45	0.53	0.42	0.66	37.54	72.00	140.90	278.95	27.64
4c	15943	0.55	0.73	0.47	0.89	38.38	81.00	157.62	291.65	36.27
4c	17239	nd	nd	nd	nd	nd	nd	nd	nd	nd
4c	17240	nd	nd	nd	nd	nd	nd	nd	nd	nd
4d	15944	0.49	0.83	0.36	0.70	47.38	84.00	196.05	331.52	35.60
4d	15945	0.42	0.86	0.39	0.93	33.04	77.67	131.89	325.05	34.67
4d	15946	1.86	1.12	2.20	2.42	94.71	92.00	431.19	502.85	46.33
4d	15947	1.25	0.89	1.02	2.65	66.04	77.67	296.15	516.52	27.23
4d	15948	0.82	0.65	0.93	2.00	63.71	67.17	260.02	447.69	25.82
4d	15949	0.53	0.93	0.22	0.59	47.71	72.33	170.19	418.85	21.96
4e	15951	0.45	0.55	0.45	0.57	51.04	58.67	211.10	257.09	23.47
4e	15952	0.46	0.32	0.42	0.63	45.04	53.33	177.99	256.32	15.11
4e	15953	1.17	0.44	1.70	0.71	74.38	59.00	301.82	293.32	16.85
4e	15954	0.59	0.69	0.51	0.96	40.04	64.33	160.62	322.69	14.66
4e	15955	1.26	0.75	1.68	1.73	81.04	77.00	323.29	420.85	22.45
4e	15956	0.94	1.26	0.63	0.99	48.38	77.00	204.15	398.52	20.55
4e	15957	2.02	1.17	2.62	2.21	115.71	86.33	487.85	510.19	29.39
4e	15958	2.34	1.79	2.90	2.39	117.71	148.00	572.19	638.52	50.00
4e	15959	1.69	1.76	2.53	2.67	98.04	144.33	482.19	623.52	71.67
5a	15915	0.21	0.32	0.35	0.43	47.04	57.67	142.82	222.97	26.14
5a	15916	0.14	0.29	0.14	0.42	21.71	52.67	78.39	215.42	25.96
5a	15917	0.10	0.48	0.08	0.45	12.38	59.00	47.32	250.29	26.11
5a	15918	0.07	0.52	0.04	0.68	7.71	92.33	32.69	307.05	30.76
5a	17244	nd	nd	nd	nd	nd	nd	nd	nd	nd
5a	17245	nd	nd	nd	nd	nd	nd	nd	nd	nd
5b	15919	0.18	0.30	0.14	0.36	23.71	51.00	85.22	214.29	20.66
5b	15920	0.11	0.37	0.08	0.43	12.38	55.33	46.59	238.22	19.55
5b	15921	0.14	0.43	0.06	0.49	10.71	60.33	38.12	263.49	34.37
5b	15922	0.10	0.45	0.07	0.63	9.71	87.67	37.92	303.45	36.57
5b	17246	nd	nd	nd	nd	nd	nd	nd	nd	nd
5c	15923	0.16	0.32	0.15	0.31	21.04	46.00	77.22	195.85	21.55
5c	15924	0.05	0.33	0.05	0.33	7.71	52.00	29.47	211.75	21.97
5c	15925	0.14	0.42	0.10	0.39	14.38	55.00	53.72	257.42	20.72
5c	15926	0.18	0.42	0.16	0.57	20.04	64.00	69.32	253.72	22.32
5c	15927	0.09	0.72	0.05	0.94	8.71	114.00	38.87	388.85	46.67
5c	17247	nd	nd	nd	nd	nd	nd	nd	nd	nd
5d	15928	0.13	nd	0.11	nd	18.04	nd	65.55	nd	nd
5d	15929	0.15	0.38	0.10	0.39	15.71	50.67	63.32	223.22	25.55
5d	15930	0.21	0.52	0.16	0.40	19.04	48.33	75.35	238.19	21.20
5d	15931	0.16	0.93	0.09	0.45	14.04	63.67	56.15	293.82	29.62
5d	15932	0.16	0.45	0.17	0.71	21.04	66.33	78.35	330.79	32.67
5d	15933	0.07	0.25	0.05	0.30	14.71	58.50	47.15	247.09	25.42

Continuation of Table A 5

Profile	Lab No.	Cd mg kg⁻¹	Cd (<20µm) mg kg⁻¹	Hg mg kg⁻¹	Hg (<20µm) mg kg⁻¹	Pb mg kg⁻¹	Pb (<20µm) mg kg⁻¹	Zn mg kg⁻¹	Zn (<20µm) mg kg⁻¹	As (<20µm) mg kg⁻¹
5e	15991	0.29	0.27	0.23	0.38	42.38	60.00	148.65	209.82	21.70
5e	15992	0.22	0.24	0.22	0.40	31.71	54.67	104.09	207.19	19.42
5e	15993	0.25	0.28	0.24	0.50	32.04	60.67	107.12	236.19	18.34
5e	15994	0.41	0.32	0.50	0.82	54.04	59.67	183.05	303.59	19.64
5e	17248	*nd*	*nd*	*nd*	*nd*	*nd*	*nd*	*nd*	*nd*	*nd*
5f	15995	0.22	0.42	0.16	0.36	29.71	77.67	109.42	236.19	25.83
5f	15996	0.16	0.54	0.10	0.39	17.38	77.67	64.32	250.65	27.41
5f	15997	0.25	0.63	0.18	0.39	27.38	81.00	99.72	252.99	34.13
5f	15998	0.08	0.70	0.05	0.38	10.04	86.67	38.25	273.49	39.67
5f	15999	0.13	0.31	0.10	0.40	14.71	61.67	51.55	215.29	23.23
5f	16000	0.22	0.45	0.24	0.50	24.04	61.67	109.79	262.75	25.54
5g	16001	0.33	0.38	0.36	0.38	55.04	76.67	191.85	243.22	27.70
5g	16002	0.39	0.26	0.50	0.61	55.04	67.67	177.59	259.62	20.97
5g	16003	0.36	0.27	0.49	0.53	49.04	62.67	164.32	253.79	14.24
5g	17249	*nd*	*nd*	*nd*	*nd*	*nd*	*nd*	*nd*	*nd*	*nd*
5g	17250	*nd*	*nd*	*nd*	*nd*	*nd*	*nd*	*nd*	*nd*	*nd*

nd = not determined

Table A 6: δ^{13}C values of selected sediment, soil, and biomass samples ($n = 2$). Values are given in ‰ of VPDB.

Profile	Lab No.	δ^{13}C ‰	Range ‰	Material
*	4533	-26.6	0.0	sediment
*	4536	-25.1	0.0	sediment
*	4550	-26.7	0.1	sediment
5a	15915	-23.5	0.0	soil
5a	15916	-24.8	0.3	soil
5a	15917	-25.2	0.1	soil
5a	15918	-27.5	0.2	soil
5a	17244	-24.7	0.0	soil
5a	17245	-25.2	0.0	soil
5d	15928	-29.3	0.2	soil
5d	15929	-28.4	0.1	soil
5d	15930	-27.2	0.1	soil
5d	15931	-27.6	0.1	soil
5d	15932	-26.5	0.2	soil
5g	16001	-27.6	0.0	soil
5g	16002	-26.4	0.0	soil
5g	16003	-26.4	0.2	soil
5g	17249	-25.6	0.3	soil
5g	17250	-25.3	0.3	soil
5d	16154	-28.5	0.2	biomass
5g	16158	-27.7	0.2	biomass
5g	16159	-27.3	0.0	litter

*fresh sediments from a mudflat near Cuxhaven (compare chapter 4.1)

Table A 7: Pre and post-incubation soil characteristics. Post-incubation pH values, carbon and nitrogen contents were measured in each replicate ($n = 6$). Pre-incubation TOC concentrations were calculated by adding the total carbon turnover to the post-incubation TOC content.

Sample No.	Lab No.	Post-incub. pH CaCl$_2$		Post-incub. TC, %		Post-incub. TIC, %		Post-incub. TOC, %		Post-incub. TN, %		Post-incub. C/N		Pre-incub. TOC, %	
		Mean	SD	Mean	SD	Mean	SD	Mean	SD	Mean	SD	Mean	SD	Mean	SD
1a topsoil	16021	7.3	0.1	3.80	0.22	1.02	0.07	2.79	0.21	0.26	0.03	10.75	0.49	3.23	0.18
1c topsoil	16025	7.2	0.1	7.76	0.33	0.49	0.14	7.27	0.34	0.67	0.01	10.84	0.36	7.59	0.31
2a topsoil	16019	7.4	0.1	5.13	0.24	1.01	0.16	4.13	0.21	0.42	0.01	9.86	0.27	4.30	0.20
2c topsoil	15966	7.1	0.2	5.47	0.80	0.38	0.06	5.09	0.81	0.52	0.11	9.90	0.94	5.30	0.84
3a topsoil	16014	7.6	0.1	2.25	0.17	1.08	0.27	1.16	0.36	0.12	0.02	9.80	2.00	1.22	0.36
3b topsoil	16009	7.4	0.1	2.67	0.08	0.64	0.09	2.03	0.16	0.21	0.01	9.76	0.39	2.15	0.17
4a topsoil	15934	7.5	0.1	4.31	0.09	1.11	0.07	3.20	0.09	0.37	0.01	8.74	0.34	3.35	0.06
4c topsoil	15941	7.5	0.1	4.50	0.16	1.13	0.07	3.37	0.15	0.36	0.02	9.28	0.19	3.52	0.21
4e topsoil	15951	7.5	0.0	5.61	0.15	0.84	0.04	4.77	0.18	0.46	0.02	10.48	0.19	5.07	0.29
5a topsoil	15915	7.6	0.1	3.35	0.12	1.19	0.10	2.15	0.17	0.26	0.02	8.19	0.50	2.33	0.19
5c topsoil	15923	7.7	0.0	2.78	0.27	0.83	0.13	1.96	0.28	0.21	0.02	9.44	0.75	2.15	0.21
5e topsoil	15991	7.5	0.0	4.27	0.54	0.64	0.06	3.62	0.49	0.38	0.04	9.56	0.28	3.84	0.44
5g topsoil	16001	7.8	0.0	6.99	0.24	0.73	0.16	6.26	0.22	0.61	0.02	10.19	0.22	6.75	0.30
1a subsoil	17251	7.1	0.1	3.07	0.12	0.78	0.07	2.29	0.15	0.20	0.01	11.56	0.72	2.39	0.18
1c subsoil	17255	6.1	0.5	6.63	0.23	0.30	0.10	6.33	0.16	0.51	0.01	12.33	0.29	6.53	0.08
2a subsoil	17242	7.4	0.0	3.23	0.14	0.85	0.10	2.39	0.17	0.24	0.02	9.80	0.46	2.45	0.18
2c subsoil	15968	7.2	0.1	2.06	0.04	0.27	0.01	1.79	0.04	0.21	0.00	8.43	0.10	1.81	0.04
3a subsoil	16017	7.6	0.1	2.32	0.07	1.01	0.13	1.32	0.11	0.13	0.01	9.89	1.08	1.43	0.09
3b subsoil	16011	7.5	0.1	1.40	0.03	0.59	0.05	0.81	0.07	0.09	0.00	9.24	0.72	0.83	0.06
4a subsoil	17235	7.4	0.1	1.91	0.20	0.79	0.07	1.12	0.13	0.12	0.02	9.75	0.62	1.14	0.13
4c subsoil	17239	7.5	0.1	3.09	0.26	1.05	0.14	2.04	0.12	0.21	0.02	9.74	0.49	2.13	0.08
4e subsoil	15956	7.5	0.1	2.28	0.14	0.80	0.03	1.48	0.13	0.14	0.01	10.50	0.30	1.51	0.14
5a subsoil	15918	7.8	0.1	0.87	0.04	0.58	0.07	0.29	0.06	0.05	0.00	6.01	1.51	0.31	0.06
5c subsoil	15926	7.7	0.0	1.14	0.05	0.58	0.08	0.56	0.10	0.06	0.00	9.12	1.03	0.58	0.09
5e subsoil	15994	7.7	0.1	2.33	0.05	0.62	0.07	1.71	0.07	0.17	0.00	9.85	0.36	1.76	0.07
5g subsoil	16003	7.7	0.1	1.68	0.07	0.64	0.07	1.04	0.11	0.12	0.01	8.86	0.60	1.08	0.11

Table A 8: Maximum production rates (in µg g^{-1}TOC d^{-1}) under aerobic and anaerobic conditions.

Sample No.	Aerobic incubation			Anaerobic incubation					
	Duration, d	CO$_2$-C, µg g^{-1}TOC d^{-1}		Duration, d	CO$_2$-C, µg g^{-1}TOC d^{-1}		Duration, d	CH$_4$-C, µg g^{-1}TOC d^{-1}	
		Mean	SD		Mean	SD		Mean	SD
1a topsoil	1	3766.05	130.36	54	3143.41	528.28	54	464.49	124.29
1c topsoil	1	1692.00	204.72	7	1191.02	195.76	90	44.93	10.65
2a topsoil	1	1487.39	45.34	33	402.70	271.97	90	48.89	6.92
2c topsoil	1	1115.91	641.52	7	780.47	275.80	118	76.68	15.18
3a topsoil	1	1179.60	175.40	33	647.20	269.24	111	16.76	14.51
3b topsoil	1	1309.79	302.06	7	1824.53	332.58	83	74.74	11.00
4a topsoil	1	1740.07	301.33	118	611.89	122.06	118	23.24	8.76
4c topsoil	1	2294.85	344.14	7	407.46	107.74	118	28.34	0.56
4e topsoil	1	2320.89	404.43	7	1445.36	241.06	103	31.70	27.50
5a topsoil	1	3800.16	504.80	7	698.10	133.95	*nd*	*nd*	*nd*
5c topsoil	1	2298.88	121.82	7	2180.79	190.46	*nd*	*nd*	*nd*
5e topsoil	1	1944.24	252.36	118	771.17	118.43	118	80.08	25.74
5g topsoil	1	4306.09	1025.90	7	2077.72	243.35	96	61.49	8.35
1a subsoil	1	1622.29	52.90	7	898.43	80.01	111	0.10	0.03
1c subsoil	1	1146.92	119.92	7	629.88	55.87	111	0.18	0.02
2a subsoil	1	623.55	254.95	54	669.59	91.63	*nd*	*nd*	*nd*
2c subsoil	1	328.69	78.50	62	125.91	15.07	*nd*	*nd*	*nd*
3a subsoil	1	4334.36	1505.00	7	664.54	209.97	54	26.55	19.22
3b subsoil	1	679.48	175.29	111	429.03	135.39	*nd*	*nd*	*nd*
4a subsoil	97	234.36	39.00	111	252.37	8.49	*nd*	*nd*	*nd*
4c subsoil	1	4750.58	579.77	70	305.14	52.34	*nd*	*nd*	*nd*
4e subsoil	6	404.99	11.89	96	415.09	259.73	*nd*	*nd*	*nd*
5a subsoil	6	869.20	439.00	54	2904.28	4202.81	*nd*	*nd*	*nd*
5c subsoil	1	1199.80	334.54	111	1014.99	310.40	*nd*	*nd*	*nd*
5e subsoil	1	1314.19	310.90	118	412.76	153.81	*nd*	*nd*	*nd*
5g subsoil	1	1343.08	657.92	111	936.47	158.56	*nd*	*nd*	*nd*

nd = not determined, below limit of determination

Table A 9: Initial and final production rates (in µg g⁻¹TOC d⁻¹) under aerobic and anaerobic conditions.

Sample No.	Aerobic incubation				Anaerobic incubation							
	Initial rate, µg CO₂-C g⁻¹TOC d⁻¹		Final rate, µg CO₂-C g⁻¹TOC d⁻¹		Initial rate, µg CO₂-C g⁻¹TOC d⁻¹		Final rate, g CO₂-C g⁻¹TOC d⁻¹		Initial rate, µg CH₄-C g⁻¹TOC d⁻¹		Final rate, µg CH₄-C g⁻¹TOC d⁻¹	
	Mean	SD	Mean	SD	Mean	SD	Mean	SD	Mean	SD	Mean	SD
1a topsoil	1408.86	275.60	765.61	38.96	1204.25	232.92	-20.78	48.45	205.03	4.39	72.54	6.05
1c topsoil	636.59	99.58	307.55	10.52	319.91	132.79	-19.20	23.00	2.23	3.38	33.14	5.01
2a topsoil	515.51	37.67	248.89	4.69	255.76	32.91	68.13	7.42	2.22	1.27	27.18	2.35
2c topsoil	534.19	65.01	306.04	14.97	136.33	12.55	263.96	87.85	0.30	0.32	59.11	14.89
3a topsoil	559.27	183.47	315.61	69.37	461.85	51.80	145.10	4.40	0.24	0.21	15.52	14.48
3b topsoil	614.91	42.01	311.89	29.76	235.72	42.61	107.72	51.25	0.89	1.34	40.81	10.57
4a topsoil	714.12	71.96	350.41	55.43	262.15	25.64	236.08	28.18	0.27	0.25	15.87	6.74
4c topsoil	637.31	33.13	332.12	16.61	190.94	15.99	205.63	39.25	0.32	0.44	20.68	2.19
4e topsoil	1062.69	109.10	481.36	32.28	173.06	46.35	282.20	86.63	0.01	0.01	26.64	23.03
5a topsoil	1298.39	79.00	531.69	63.67	300.86	90.51	265.37	80.62	0.15	0.18	2.94	4.07
5c topsoil	1260.25	118.91	971.32	71.83	78.23	235.17	395.22	68.25	nd	nd	nd	nd
5e topsoil	790.03	37.97	567.13	34.97	327.00	21.77	277.56	84.63	11.61	11.51	34.66	16.96
5g topsoil	1180.40	213.69	692.70	42.18	193.86	45.53	374.87	72.36	0.11	0.07	48.06	2.76
1a subsoil	911.26	25.90	305.41	56.81	185.30	116.15	-66.43	41.33	0.03	0.02	0.06	0.02
1c subsoil	546.08	125.13	275.73	24.27	196.68	77.82	8.49	15.98	0.02	0.01	0.11	0.03
2a subsoil	218.59	6.67	193.73	3.14	449.71	19.57	-92.29	13.59	nd	nd	nd	nd
2c subsoil	147.64	6.64	105.34	10.31	85.28	8.66	80.97	7.89	nd	nd	nd	nd
3a subsoil	1353.17	659.97	738.63	242.07	309.01	73.29	26.52	31.80	18.05	15.21	14.64	3.16
3b subsoil	417.94	78.74	289.39	23.51	259.00	191.04	12.40	18.06	nd	nd	nd	nd
4a subsoil	98.78	9.67	160.27	14.64	123.15	19.72	23.80	36.05	nd	nd	nd	nd
4c subsoil	921.68	31.16	285.08	45.45	183.61	50.26	7.70	7.31	nd	nd	nd	nd
4e subsoil	215.46	22.25	150.31	9.92	194.52	31.59	182.03	38.17	nd	nd	nd	nd
5a subsoil	265.34	82.90	416.81	236.25	782.75	139.98	806.09	312.50	nd	nd	nd	nd
5c subsoil	263.05	43.80	180.49	82.38	368.17	43.61	640.23	73.95	nd	nd	nd	nd
5e subsoil	367.08	25.94	220.15	90.94	236.40	26.71	220.30	40.42	nd	nd	nd	nd
5g subsoil	424.88	35.59	231.90	30.42	309.92	46.91	124.49	52.64	nd	nd	nd	nd

nd = not determined, below limit of determination

Table A 10: Total C production (in mg g^{-1}dw) and turnover (in % of TOC) under aerobic and anaerobic conditions.

Sample No.	Aerobic incubation				Anaerobic incubation					
	Total C production, mg g^{-1}dw		Total C turnover, % of TOC		Total C production, mg g^{-1}dw		Total CO$_2$e-C production, mg g^{-1}dw		Total C turnover, % of TOC	
	Mean	SD	Mean	SD	Mean	SD	Mean	SD	Mean	SD
1a topsoil	3.43	0.34	10.59	1.48	4.38	0.41	19.47	1.94	13.65	1.34
1c topsoil	3.06	0.27	4.52	0.42	2.55	0.26	8.76	2.35	3.26	0.41
2a topsoil	1.44	0.02	3.46	0.09	1.37	0.17	4.81	0.79	3.09	0.44
2c topsoil	2.29	0.08	4.04	0.10	1.66	0.13	6.42	0.80	3.51	1.08
3a topsoil	0.46	0.02	3.50	1.14	0.43	0.03	0.57	0.17	4.20	0.14
3b topsoil	1.03	0.07	4.58	0.42	0.97	0.12	3.23	0.49	4.77	0.38
4a topsoil	1.57	0.07	4.70	0.25	1.09	0.10	1.68	0.43	3.23	0.32
4c topsoil	1.68	0.06	4.58	0.13	0.88	0.10	1.90	0.32	2.62	0.25
4e topsoil	3.58	0.19	6.75	0.24	1.48	0.23	2.46	1.08	3.06	0.39
5a topsoil	1.99	0.03	8.31	0.55	0.91	0.15	0.97	0.23	4.10	1.07
5c topsoil	2.07	0.08	10.35	0.74	1.18	0.06	1.18	0.06	5.19	0.51
5e topsoil	2.15	0.06	6.23	0.25	1.74	0.20	6.46	1.53	4.11	0.42
5g topsoil	4.85	1.38	7.17	1.54	3.81	0.44	9.21	1.43	5.61	0.55
1a subsoil	1.33	0.06	5.34	0.05	0.36	0.02	0.37	0.02	1.58	0.15
1c subsoil	2.68	0.33	4.13	0.50	0.89	0.15	0.90	0.15	1.36	0.24
2a subsoil	0.49	0.01	2.05	0.07	0.67	0.07	0.67	0.07	2.70	0.25
2c subsoil	0.23	0.01	1.30	0.04	0.17	0.01	0.17	0.01	0.95	0.06
3a subsoil	1.30	0.32	9.05	2.99	0.49	0.11	1.22	0.48	3.47	0.69
3b subsoil	0.27	0.01	3.31	0.31	0.16	0.11	0.16	0.11	2.02	1.61
4a subsoil	0.13	0.00	1.14	0.10	0.15	0.02	0.15	0.02	1.29	0.22
4c subsoil	1.15	0.05	5.57	0.16	0.42	0.10	0.42	0.10	1.92	0.46
4e subsoil	0.22	0.00	1.52	0.02	0.32	0.06	0.32	0.06	2.04	0.46
5a subsoil	0.09	0.02	3.12	1.27	0.33	0.05	0.33	0.05	10.87	3.92
5c subsoil	0.11	0.01	1.76	0.27	0.27	0.01	0.27	0.01	5.26	0.68
5e subsoil	0.43	0.03	2.42	0.14	0.50	0.06	0.50	0.06	2.83	0.31
5g subsoil	0.25	0.00	2.40	0.23	0.33	0.10	0.33	0.10	3.00	0.60

Table A 11: Correlation between total C production as well as total C turnover and soil properties (pH, TC, TIC, TOC, TN, C/N, ff20), site characteristics (salinity and elevation), as well as maximum, initial, and final production rates.

		Aerobic incubation		Anaerobic incubation	
		Total C production	Total C turnover	Total C production	Total C turnover
		mg g^{-1}dw	% of TOC	mg g^{-1}dw	% of TOC
Post-incub. pH	r_s	-0.206	0.128	-0.192	0.427*
	p	0.333	0.552	0.369	0.038
	n	24	24	24	24
Post-incub.TC, %	r_s	0.894**	0.543**	0.824**	0.119
	p	0.000	0.006	0.000	0.579
	n	24	24	24	24
Post-incub. TIC, %	r_s	0.170	0.430*	0.278	0.135
	p	0.427	0.036	0.188	0.530
	n	24	24	24	24
Post-incub. TOC, %	r_s	0.868**	0.487*	0.817**	0.098
	p	0.000	0.016	0.000	0.648
	n	24	24	24	24
Post-incub. TN, %	r_s	0.885**	0.515**	0.836**	0.155
	p	0.000	0.010	0.000	0.470
	n	24	24	24	24
Post-incub. C/N	r_s	0.514*	0.180	0.421*	-0.124
	p	0.010	0.400	0.041	0.563
	n	24	24	24	24
Pre-incub. TOC, %	r_s	0.884**	0.523**	0.832**	0.124
	p	0.000	0.009	0.000	0.562
	n	24	24	24	24
Pre-incub. ff20, %	r_s	0.740**	0.443*	0.639**	0.078
	p	0.000	0.030	0.001	0.716
	n	24	24	24	24
Salinity in groundwater	r_s	-0.150	0.082	-0.068	0.323
	p	0.484	0.703	0.752	0.124
	n	24	24	24	24
Height above MHW, m	r_s	-0.085	-0.258	-0.036	-0.065
	p	0.691	0.223	0.868	0.765
	n	24	24	24	24
Maximum production rate, µg g^{-1}TOC d^{-1}	r_s	0.685**	0.893**	0.498*	0.795**
	p	0.000	0.000	0.013	0.000
	n	24	24	24	24
Initial production rate, µg g^{-1}TOC d^{-1}	r_s	0.791**	0.989**	0.130	0.483*
	p	0.000	0.000	0.545	0.017
	n	24	24	24	24
Final production rate, µg g^{-1}TOC d^{-1}	r_s	0.690**	0.898**	0.115	0.558**
	p	0.000	0.000	0.593	0.005
	n	24	24	24	24

* significant correlation ($p < 0.05$)

** highly significant correlation ($p < 0.01$)

Table A 12: Trace metal pools in g m^{-2} for topsoils (0 – 30 cm) and the whole profile depth (0 – 100 cm).

Profile	0 - 30 cm				0 - 100 cm			
	Cd, g m^{-2}	Hg, g m^{-2}	Pb, g m^{-2}	Zn, g m^{-2}	Cd, g m^{-2}	Hg, g m^{-2}	Pb, g m^{-2}	Zn, g m^{-2}
1a	0.13	0.08	6.72	39.11	nd	nd	nd	nd
1b	0.25	0.25	11.56	72.05	nd	nd	nd	nd
1c	0.38	0.58	17.93	109.44	nd	nd	nd	nd
2a	0.15	0.10	9.43	50.49	nd	nd	nd	nd
2b	0.32	0.22	18.51	77.50	0.58	0.34	52.76	172.47
2c	0.38	0.18	25.39	90.75	0.64	0.28	66.81	187.76
2d	0.35	0.20	22.66	85.79	0.60	0.29	58.96	181.08
3a	0.06	0.04	4.62	23.39	0.33	0.27	25.95	128.00
3b	0.15	0.08	6.07	34.04	0.60	0.32	23.42	140.58
3c	0.17	0.13	9.64	45.20	0.54	0.34	30.75	139.64
4a	0.15	0.11	10.12	47.73	nd	nd	nd	nd
4b	0.08	0.06	6.64	28.11	nd	nd	nd	nd
4c	0.13	0.11	11.14	41.96	nd	nd	nd	nd
4d	0.18	0.18	13.19	55.13	0.87	0.77	59.63	243.83
4e	0.20	0.25	15.22	61.49	1.22	1.54	71.99	320.28
5a	0.05	0.06	8.11	26.97	nd	nd	nd	nd
5b	0.05	0.04	6.00	22.07	0.17	0.11	16.55	62.15
5c	0.05	0.04	5.87	21.89	0.17	0.12	18.17	70.53
5d	0.07	0.05	6.37	25.24	0.21	0.19	24.18	92.36
5e	0.08	0.08	11.64	38.94	0.38	0.43	50.90	171.73
5f	0.05	0.04	5.58	20.08	0.23	0.23	25.73	110.28
5g	0.11	0.14	15.73	52.00	nd	nd	nd	nd

Table A 13: Correlation between trace metal pools and soil properties (SIC, SOC, ff20) and site characteristics (salinity and elevation).

		Cd (0-30cm), g m^{-2}	Cd (0-100cm), g m^{-2}	Hg (0-30cm), g m^{-2}	Hg (0-100cm), g m^{-2}	Pb (0-30cm), g m^{-2}	Pb (0-100cm), g m^{-2}	Zn (0-30cm), g m^{-2}	Zn (0-100cm), g m^{-2}
SIC (0-30cm), kg m^{-2}	r_s	-0.804**	-0.753**	-0.731**	-0.533	-0.746**	-0.742**	-0.817**	-0.769**
	p	0.000	0.003	0.000	0.061	0.000	0.004	0.000	0.002
	n	22	13	22	13	22	13	22	13
SIC (0-100cm), kg m^{-2}	r_s	-0.811**	-0.736**	-0.770**	-0.593*	-0.703**	-0.731**	-0.802**	-0.775**
	p	0.000	0.004	0.000	0.033	0.000	0.005	0.000	0.002
	n	22	13	22	13	22	13	22	13
SOC (0-30cm), kg m^{-2}	r_s	0.940**	0.775**	0.915**	0.555*	0.853**	0.720**	0.916**	0.802**
	p	0.000	0.002	0.000	0.049	0.000	0.006	0.000	0.001
	n	22	13	22	13	22	13	22	13
SOC (0-100cm), kg m^{-2}	r_s	0.864**	0.901**	0.833**	0.786**	0.730**	0.945**	0.855**	0.967**
	p	0.000	0.000	0.000	0.001	0.000	0.000	0.000	0.000
	n	22	13	22	13	22	13	22	13
ff20 (0-30cm), %	r_s	0.748**	0.665*	0.831**	0.582*	0.833**	0.868**	0.867**	0.802**
	p	0.000	0.013	0.000	0.037	0.000	0.000	0.000	0.001
	n	22	13	22	13	22	13	22	13
ff20 (0-100cm), %	r_s	0.807**	0.753**	0.854**	0.670*	0.848**	0.978**	0.875**	0.885**
	p	0.000	0.003	0.000	0.012	0.000	0.000	0.000	0.000
	n	22	13	22	13	22	13	22	13
Salinity in groundwater	r_s	-0.753**	-0.566*	-0.530*	-0.280	-0.367	-0.462	-0.615**	-0.505
	p	0.000	0.044	0.011	0.354	0.093	0.112	0.002	0.078
	n	22	13	22	13	22	13	22	13
Elevation above MHW, m	r_s	0.395	0.646*	0.316	0.569*	0.397	0.476	0.320	0.602*
	p	0.069	0.017	0.152	0.042	0.067	0.100	0.147	0.029
	n	22	13	22	13	22	13	22	13

* significant correlation (*p* < 0.05)

** highly significant correlation (*p* < 0.01)

Table A 14: Evaluation of contamination levels. Enrichment factors of the investigated trace metal concentrations in comparison to geogenic background values (colors denote the respective ARGE classes according to Stachel and Lüschow (1996)[a] and ecotoxicological values according to BfG (2004)[b].

Profile	Lab No.	Cd (<20μm)		Hg (<20μm)		Pb (<20μm)		Zn (<20μm)		As (<20μm)	
		Enrichm. factor	Ecotox. value	Enrichm. factor	Ecotox. value	Enrichm. factor	Ecotox. value	Enrichm. factor	Ecotox. value	Enrichm. factor	Ecotox. value
1a	16021	5.13	C	2.36	D	3.45	D	4.46	B	1.57	C
1a	16022	4.44	D	2.17	D	3.51	D	4.06	C	1.69	C
1a	17251	nd	nd	nd	nd	nd	nd	nd	nd	nd	nd
1a	17252	nd	nd	nd	nd	nd	nd	nd	nd	nd	nd
1b	16023	3.52	D	2.25	D	3.11	D	3.75	C	1.44	C
1b	16024	3.77	D	7.47	B	4.47	C	4.52	B	1.65	C
1b	17253	nd	nd	nd	nd	nd	nd	nd	nd	nd	nd
1b	17254	nd	nd	nd	nd	nd	nd	nd	nd	nd	nd
1c	16025	3.16	D	1.96	D	3.01	D	3.51	C	1.21	C
1c	16026	3.89	D	7.73	B	4.01	C	4.15	C	1.84	C
1c	17255	nd	nd	nd	nd	nd	nd	nd	nd	nd	nd
1c	17256	nd	nd	nd	nd	nd	nd	nd	nd	nd	nd
2a	16019	3.16	D	2.06	D	3.38	D	4.01	C	1.65	C
2a	16020	3.05	D	2.60	D	3.12	D	4.04	C	1.37	C
2a	17242	nd	nd	nd	nd	nd	nd	nd	nd	nd	nd
2a	17243	nd	nd	nd	nd	nd	nd	nd	nd	nd	nd
2b	15971	4.17	D	2.87	C	3.28	D	3.90	C	1.42	C
2b	15972	7.28	C	7.29	B	4.24	C	5.25	B	1.66	C
2b	15973	3.81	D	1.80	D	4.20	C	3.76	C	2.28	B
2b	15974	0.63	E	0.41	E	2.51	D	2.01	D	2.13	B
2b	15975	0.30	E	0.24	E	1.61	D	1.46	D	1.14	C
2b	15976	1.08	E	0.21	E	2.04	D	1.33	D	0.60	D
2c	15966	3.68	D	2.29	D	2.40	D	3.53	C	1.23	C
2c	15967	2.27	D	1.63	D	2.73	D	3.85	C	1.86	C
2c	15968	0.53	E	0.43	E	1.66	D	1.78	D	1.22	C
2c	15969	0.37	E	0.25	E	1.49	D	1.53	D	1.59	C
2c	15970	0.40	E	0.29	E	1.55	D	1.48	D	1.25	C
2d	15960	3.75	D	2.83	C	2.61	D	4.02	C	1.05	C
2d	15961	4.40	D	2.91	C	2.31	D	4.03	C	1.14	C
2d	15962	0.95	E	0.66	E	2.73	D	2.29	C	2.11	B
2d	15963	0.44	E	0.30	E	1.54	D	1.48	D	1.28	C
2d	15964	0.40	E	0.23	E	1.56	D	1.38	D	1.32	C
2d	15965	1.44	D	0.26	E	2.55	D	1.58	D	0.68	D
3a	16014	2.57	D	1.47	D	2.94	D	3.01	C	1.52	C
3a	16015	2.90	D	1.31	D	2.53	D	2.74	C	1.64	C
3a	16016	3.85	D	1.48	D	2.69	D	3.02	C	1.65	C
3a	16017	2.39	D	1.69	D	2.77	D	2.97	C	1.09	C
3a	16018	3.02	D	2.21	D	3.79	D	3.77	C	1.75	C
3a	17241	nd	nd	nd	nd	nd	nd	nd	nd	nd	nd
3b	16009	2.60	D	1.25	D	1.77	D	2.12	D	1.03	C
3b	16010	3.77	D	2.43	D	2.47	D	3.11	C	1.69	C
3b	16011	7.63	C	3.22	C	3.44	D	4.62	B	1.63	C
3b	16012	5.99	C	7.21	B	4.05	C	6.42	B	2.45	B
3b	16013	1.34	D	1.25	D	3.59	D	2.59	C	2.07	B
3c	16004	3.41	D	2.50	D	2.41	D	3.26	C	0.98	D
3c	16005	4.86	D	2.19	D	2.76	D	4.45	B	1.19	C
3c	16006	1.56	D	1.31	D	1.90	D	3.27	C	0.86	D
3c	16007	1.69	D	1.05	D	2.23	D	2.51	C	0.87	D
3c	16008	1.86	D	0.88	D	3.33	D	2.00	D	2.27	B

Continuation Table A 14

Profile	Lab No.	Cd (<20μm)		Hg (<20μm)		Pb (<20μm)		Zn (<20μm)		As (<20μm)	
		Enrichm. factor	Ecotox. value	Enrichm. factor	Ecotox. value	Enrichm. factor	Ecotox. value	Enrichm. factor	Ecotox. value	Enrichm. factor	Ecotox. value
4a	15934	3.28	D	2.35	D	2.51	D	3.53	C	1.42	C
4a	15935	5.35	C	5.76	B	3.49	D	4.30	B	2.18	B
4a	15936	3.95	D	2.41	D	2.80	D	3.70	C	1.95	C
4a	17235	nd	nd	nd	nd	nd	nd	nd	nd	nd	nd
4a	17236	nd	nd	nd	nd	nd	nd	nd	nd	nd	nd
4b	15937	2.34	D	1.58	D	2.28	D	3.10	C	1.60	C
4b	15938	1.66	D	1.80	D	2.27	D	3.07	C	1.57	C
4b	15939	3.03	D	2.51	D	3.16	D	3.26	C	1.67	C
4b	15940	3.12	D	2.97	C	3.47	D	3.33	C	1.83	C
4b	17237	nd	nd	nd	nd	nd	nd	nd	nd	nd	nd
4b	17238	nd	nd	nd	nd	nd	nd	nd	nd	nd	nd
4c	15941	2.03	D	2.01	D	2.69	D	2.95	C	1.08	C
4c	15942	2.23	D	2.19	D	2.88	D	2.97	C	1.38	C
4c	15943	3.03	D	2.98	C	3.24	D	3.10	C	1.81	C
4c	17239	nd	nd	nd	nd	nd	nd	nd	nd	nd	nd
4c	17240	nd	nd	nd	nd	nd	nd	nd	nd	nd	nd
4d	15944	3.48	D	2.33	D	3.36	D	3.53	C	1.78	C
4d	15945	3.60	D	3.10	C	3.11	D	3.46	C	1.73	C
4d	15946	4.66	D	8.06	B	3.68	D	5.35	B	2.32	B
4d	15947	3.70	D	8.82	B	3.11	D	5.49	B	1.36	C
4d	15948	2.72	D	6.68	B	2.69	D	4.76	B	1.29	C
4d	15949	3.85	D	1.97	D	2.89	D	4.46	B	1.10	C
4e	15951	2.31	D	1.88	D	2.35	D	2.73	C	1.17	C
4e	15952	1.34	D	2.10	D	2.13	D	2.73	C	0.76	D
4e	15953	1.84	D	2.36	D	2.36	D	3.12	C	0.84	D
4e	15954	2.88	D	3.19	C	2.57	D	3.43	C	0.73	D
4e	15955	3.14	D	5.78	B	3.08	D	4.48	B	1.12	C
4e	15956	5.26	C	3.30	C	3.08	D	4.24	C	1.03	C
4e	15957	4.88	D	7.36	B	3.45	D	5.43	B	1.47	C
4e	15958	7.48	C	7.96	B	5.92	C	6.79	B	2.50	B
4e	15959	7.32	C	8.91	B	5.77	C	6.63	B	3.58	B
5a	15915	1.32	D	1.42	D	2.31	D	2.37	C	1.31	C
5a	15916	1.22	E	1.39	D	2.11	D	2.29	C	1.30	C
5a	15917	2.00	D	1.49	D	2.36	D	2.66	C	1.31	C
5a	15918	2.17	D	2.26	D	3.69	D	3.27	C	1.54	C
5a	17244	nd	nd	nd	nd	nd	nd	nd	nd	nd	nd
5a	17245	nd	nd	nd	nd	nd	nd	nd	nd	nd	nd
5b	15919	1.25	E	1.19	D	2.04	D	2.28	C	1.03	C
5b	15920	1.54	D	1.42	D	2.21	D	2.53	C	0.98	D
5b	15921	1.78	D	1.64	D	2.41	D	2.80	C	1.72	C
5b	15922	1.85	D	2.11	D	3.51	D	3.23	C	1.83	C
5b	17246	nd	nd	nd	nd	nd	nd	nd	nd	nd	nd
5c	15923	1.34	D	1.04	D	1.84	D	2.08	D	1.08	C
5c	15924	1.38	D	1.10	D	2.08	D	2.25	C	1.10	C
5c	15925	1.74	D	1.30	D	2.20	D	2.74	C	1.04	C
5c	15926	1.76	D	1.91	D	2.56	D	2.70	C	1.12	C
5c	15927	2.99	D	3.12	C	4.56	C	4.14	C	2.33	B
5c	17247	nd	nd	nd	nd	nd	nd	nd	nd	nd	nd
5d	15928	nd	nd	nd	nd	nd	nd	nd	nd	nd	nd
5d	15929	1.60	D	1.30	D	2.03	D	2.37	C	1.28	C
5d	15930	2.16	D	1.32	D	1.93	D	2.53	C	1.06	C
5d	15931	3.86	D	1.50	D	2.55	D	3.13	C	1.48	C
5d	15932	1.89	D	2.36	D	2.65	D	3.52	C	1.63	C
5d	15933	1.05	E	0.99	D	2.34	D	2.63	C	1.27	C

Continuation Table A 14

Profile	Lab No.	Cd (<20µm)		Hg (<20µm)		Pb (<20µm)		Zn (<20µm)		As (<20µm)	
		Enrichm. factor	Ecotox. value	Enrichm. factor	Ecotox. value	Enrichm. factor	Ecotox. value	Enrichm. factor	Ecotox. value	Enrichm. factor	Ecotox. value
5e	15991	1.13	E	1.27	D	2.40	D	2.23	C	1.09	C
5e	15992	1.02	E	1.33	D	2.19	D	2.20	C	0.97	D
5e	15993	1.18	E	1.66	D	2.43	D	2.51	C	0.92	D
5e	15994	1.34	D	2.73	C	2.39	D	3.23	C	0.98	D
5e	17248	nd	nd	nd	nd	nd	nd	nd	nd	nd	nd
5f	15995	1.76	D	1.20	D	3.11	D	2.51	C	1.29	C
5f	15996	2.26	D	1.29	D	3.11	D	2.67	C	1.37	C
5f	15997	2.61	D	1.31	D	3.24	D	2.69	C	1.71	C
5f	15998	2.93	D	1.27	D	3.47	D	2.91	C	1.98	C
5f	15999	1.30	D	1.35	D	2.47	D	2.29	C	1.16	C
5f	16000	1.87	D	1.67	D	2.47	D	2.80	C	1.28	C
5g	16001	1.59	D	1.26	D	3.07	D	2.59	C	1.39	C
5g	16002	1.10	E	2.03	D	2.71	D	2.76	C	1.05	C
5g	16003	1.12	E	1.77	D	2.51	D	2.70	C	0.71	D
5g	17249	nd	nd	nd	nd	nd	nd	nd	nd	nd	nd
5g	17250	nd	nd	nd	nd	nd	nd	nd	nd	nd	nd
Geogenic BG*		0.24±0.09		<0.3		25-30		94±19		20±6	

*Geogenic background (in mg kg^{-1}) of Cd, Hg, Zn, and As according to Gröngröft et al. (1998) and of Pb according to Stachel and Lüschow (1996).

[a]Color code for classification according to Stachel and Lüschow (1996):

ARGE class	Cd, mg kg^{-1}	Hg, mg kg^{-1}	Pb, mg kg^{-1}	Zn, mg kg^{-1}	As, mg kg^{-1}	
I	0.2-0.4	0.2-0.4	25-30	90-110	3-5	Geogenic background
I-II	<0.5	<0.5	<50	<150	<10	Very low pollution
II (TV§)	<1.2	<0.8	<100	<200	<20	Moderate pollution
II-III	<5	<5	<150	<500	<40	Considerable pollution
III	<10	<10	<250	<1000	<70	Increased pollution
III-IV	≤25	≤25	≤500	≤2000	≤100	High pollution
IV	>25	>25	>500	>2000	>100	Very high pollution

[b]Color code for classification according to BfG (2004):

Ecotox. values	Cd, mg kg^{-1}	Hg, mg kg^{-1}	Pb, mg kg^{-1}	Zn, mg kg^{-1}	As, mg kg^{-1}	
E	≤0.3	≤0.2	≤25	≤100	≤10	Natural background
D	≤1.2	≤0.8	≤100	≤200	≤20	Target value (TV§)
C	≤2.4	≤1.6	≤200	≤400	≤40	2*TV§
B	≤4.8	≤3.2	≤400	≤800	≤80	4*TV§
A	>4.8	>3.2	>400	>800	>80	>4*TV§

§TV = Target value according to the respective classification

Table A 15: Correlation between maximum as well as minimum river discharge at Neu Darchau and trace metal concentrations at the sampling stations Grauerort and Cuxhaven. Data were kindly provided by FGG Elbe (2014).

		Maximum river discharge	Minimum river discharge
		$m^3 s^{-1}$	$m^3 s^{-1}$
Grauerort: Cd, mg kg^{-1}	r_s	0.547**	0.611**
	p	0.000	0.000
	n	264	264
Cuxhaven: Cd, mg kg^{-1}	r_s	0.210**	0.252**
	p	0.001	0.000
	n	229	229
Grauerort: Hg, mg kg^{-1}	r_s	0.196**	0.207**
	p	0.001	0.001
	n	264	264
Cuxhaven: Hg, mg kg^{-1}	r_s	0.066	0.046
	p	0.320	0.489
	n	229	229
Grauerort: Pb, mg kg^{-1}	r_s	0.341**	0.352**
	p	0.000	0.000
	n	264	264
Cuxhaven: Pb, mg kg^{-1}	r_s	0.162*	0.197**
	p	0.014	0.003
	n	229	229
Grauerort: Zn, mg kg^{-1}	r_s	0.624**	0.620**
	p	0.000	0.000
	n	264	264
Cuxhaven: Zn, mg kg^{-1}	r_s	0.410**	0.377**
	p	0.000	0.000
	n	229	229
Grauerort: As, mg kg^{-1}	r_s	0.253**	0.264**
	p	0.000	0.000
	n	264	264
Cuxhaven: As, mg kg^{-1}	r_s	0.185**	0.175**
	p	0.005	0.008
	n	229	229

* significant correlation ($p < 0.05$)
** highly significant correlation ($p < 0.01$)

Table A 16: Annual trace metal loads at the sampling station Schnackenburg. Trace metal loads in t a⁻¹ were available for most years since 1985 (ARGE ELBE, 1997, 2001; Bergemann, 2004b; Bergemann and Gaumert, 2006, 2008a, b, 2010; Bergemann et al., 2005; Bergemann and Stachel, 2004). The total load in t was calculated as the sum of all available years.

	Hg	Cd	Pb	Zn	As
Year	t a⁻¹	t a⁻¹	t a⁻¹	t a⁻¹	t a⁻¹
1985	28.0	13.0	110	*nd*	*nd*
1986	22.0	13.0	120	2400	110
1987	25.0	15.0	130	3800	100
1988	*nd*	*nd*	*nd*	*nd*	*nd*
1989	12.0	6.4	110	*nd*	*nd*
1990	6.5	6.0	73	*nd*	*nd*
1991	6.9	4.9	70	*nd*	*nd*
1992	4.2	5.3	76	*nd*	*nd*
1993	1.9	5.0	75	*nd*	*nd*
1994	*nd*	*nd*	*nd*	*nd*	*nd*
1995	*nd*	*nd*	*nd*	*nd*	*nd*
1996	1.7	5.6	100	*nd*	*nd*
1997	1.4	5.6	100	*nd*	*nd*
1998	1.6	5.1	73	*nd*	*nd*
1999	1.4	6.5	57	*nd*	*nd*
2000	1.3	5.6	63	*nd*	*nd*
2001	1.2	5.9	59	*nd*	*nd*
2002	1.9	9.5	98	1200	99
2003	1.3	5.9	66	740	45
2004	1.0	5.2	59	700	45
2005	1.4	6.2	64	670	61
2006	1.7	4.0	63	730	56
2007	1.2	2.6	56	790	65
2008	1.4	2.4	41	730	56
2009	*nd*	*nd*	*nd*	*nd*	*nd*
Total load	t	t	t	t	t
	125.0	138.7	1663	11760	637
	n = 21	*n* = 21	*n* = 21	*n* = 9	*n* = 9

nd = not determined

Table A 17: Inundation frequency (i.e. inundation events per year) and inundation duration (i.e. total inundation time) in the year 2010. Inundation data was only available for the sites 1, 4, and 5 (compare chapter 4.4).

Profile	Elevation above MHW, m	Inundation frequency, a^{-1}	Inundation duration, d
1a	-0.29	597	72.05
1b	0.13	309	26.83
1c	0.10	337	29.58
2a	0.49	*nd*	*nd*
2b	1.18	*nd*	*nd*
2c	1.08	*nd*	*nd*
2d	0.75	*nd*	*nd*
3a	0.14	*nd*	*nd*
3b	1.11	*nd*	*nd*
3c	0.86	*nd*	*nd*
4a	-0.04	415	44.31
4b	0.14	258	22.36
4c	0.31	127	11.32
4d	0.45	66	5.75
4e	0.37	111	8.64
5a	0.04	254	30.99
5b	0.12	194	22.39
5c	0.24	116	13.48
5d	0.34	82	8.62
5e	0.56	28	3.14
5f	0.34	82	8.62
5g	0.63	18	2.39

nd = not determined

Acknowledgements

My journey with the research vessel "Buddelschiff" is coming to an end. I would like to take this opportunity to thank all travel companions, supporting me on my way.

I am very grateful to my doctoral advisor Prof. Dr. Eva-Maria Pfeiffer for entrusting me with this research project. Eva welcomed my at the Institute, supported me throughout this challenging time, and gave me the necessary independence to work on this topic. I would further like to thank my co-advisor Prof. Dr. Annette Eschenbach for constructive advice, helpful guidance, and positive criticism. Special thanks go to Dr. Alexander Gröngröft for active support, fruitful discussions, and his contagious enthusiasm.

Many colleagues from the Institute of Soil Science were involved in this research project. I would like to thank Dr. Christian Knoblauch and Prof. Dr. Lars Kutzbach for helpful discussions on the incubation experiment. Besides, Lars did a very good job as panel chair, for which I am very grateful. Further thanks are due to all Hiwi-students for assistance in field and laboratory work, especially Fabian Beermann, Maren Reese, and Hedda Straehler-Pohl, to name but a few. The active support of a team of qualified technicians, including Angela Meier, Monika Voß, Susanne Kopelke, and Birgit Schwinge, is deeply appreciated. Last but not least, all colleagues from office #428 are thanked for creating a pleasant and productive working atmosphere.

Moreover, my research project was part of the "Estuary and Wetland Research Graduate School Hamburg" (ESTRADE). I acknowledge the work of the coordinators Dr. Andrea Staudler and Dr. Tobias Gebauer as well as the speakers Prof. Dr. Kai Jensen, Prof. Dr. Eva-Maria Pfeiffer, and Prof. Dr. Annette Eschenbach who supported all participants and made short communication channels possible. All ESTRADE PhD students are thanked for mutual exchange of ideas and experiences. I am especially grateful to Christian Butzeck for productive cooperation and encouragement.

For proofreading parts of this thesis, I would like to thank the Saenger family and Carla Bockermann. My family and friends are thanked for moral support. Most of all, I thank Oliver Witter for common solving of brainteasers, bringing me back on track, and enduring me on darker and brighter days.

I would like to express gratitude to Schleswig-Holstein's Government-Owned Company for Coastal Protection, National Parks and Ocean Protection, and the nature protection authorities of the administrative districts Pinneberg and Stade for providing research permissions.